UNIVERSITY OF SHEFFIELD

Department of Civil and Structural Engineering

BEHAVIOUR OF COLUMNS IN SUB-FRAMES WITH SEMI-RIGID JOINTS

By

ABDUSSALAM MAHMUD RIFAI

(B.Sc.,M.Sc.)

A thesis submitted to the University of Sheffield

for the Degree of Doctor of Philosophy

June, 1987

SUMMARY

The behaviour of limited subassemblages with flexible beams and semi-rigid beam to column connections was studied using a computer program in which the finite element method was employed in a non-linear analysis which accounts for the presence of semi-rigid connections and the inelastic behaviour of frames. The program accounts for many other factors such as initial imperfections and residual stresses. The theoretical background to the present computer program has been presented along with the program layout.

The program was used to simulate some of the experimental results obtained from tests on rigidly and flexibly connected frames with different combinations of beam and column loads. The analytical results were found to compare reasonably well with the experimental results.

The program was also used to simulate a series of I-shaped subassemblages that were tested at the University of Sheffield. Comparisons were made between the analytical and experimental results characterized by the maximum loads, load-deflection curves and load-moment curves. Good agreement was obtained between the analytical and the experimental load-deflection curves for all of the cases considered. The general trends of the measured and calculated load-moment curves for most cases were found to be comparable. The recommendations given in BS5950 for the design of columns in simple construction were applied to all cases in the last series and were found unconservative in the cases of balanced loading and conservative in the cases of unbalanced loads.

A limited parametric study was conducted to study the effects of semi-rigid joints, beam flexibility and type of loading. In this

study, an I-shaped subassemblage was analysed for different load types and different types of beam to column connections. A substantial effect was recognized due to the presence of semi-rigid connections whether or not a beam load was applied. Beam flexibility was also seen to affect the carrying capacity of the subassemblage under the action of column load only although this effect was less noticeable than that of the connection flexibility. The presence of beam load was found to result in an unexpected interaction curve which relates the total force in the column to the moment that is transmitted to the column's end. An almost linear relationship with negative gradient seems to exist between the column and beam loads.

It is pointed out that all the findings of the present study are based on the range of cases considered in the parametric study but it is suggested that they serve as indicators to the behaviour of any the subassemblage under axial load only or axial load combined with beam loads. A few recommendations for future work are presented.

ACKNOWLEDGEMENTS

The author would like to thank Dr. D.A. Nethercot, Reader, and Dr. P.A. Kirby, Lecturer in the Department of Civil and Structural Engineering for their excellent supervision throughout this program of study. Appreciations are also due to all academic and secretarial staff in the Department of Civil and Structural Engineering.

The patience and support of the author's wife during the last years is greatly appreciated.

The grant given to the author by the Ministry of Education, Tripoli, Libya made it possible for the author to conduct the present work.

CONTENTS

	Page
SUMMARY	i
ACKNOWLEDGEMENTS	iii
LIST OF FIGURES	vi
LIST OF TABLES	xi
NOTATIONS	xii
1. INTRODUCTION	
1.1 Considerations in Design of Frames with Semi-Rigid Joints	1
1.2 Objectives of the Present Investigation	2
1.3 Limitations of the Present Investigation	6
2. REVIEW OF LITERATURE OF STRUCTURES WITH SEMI-RIGID CONNECTIONS	
2.1 The Column Problem	8
2.1.1 Pin-Ended Columns	8
2.1.2 Restrained Columns	11
2.2 Columns as Part of Frames	16
2.2.1 Types of Analyses of Rigidly Connected Frames	16
2.2.1.1 Slope Deflection Methods	16
2.2.1.2 Moment Distribution Methods	18
2.2.1.3 Matrix Methods	18
2.2.1.4 Finite Element Method	19
2.2.2 Inclusion of Semi-Rigid Joints in the Analysis of Frames	20
2.3 Review of Tests on Frames with Rigid and Semi-Rigid Connections	28
2.4 Review of Semi-Rigid Beam-to-Column Connections	32
2.4.1 Experimental Studies	32
2.4.2 Modelling of the Moment-Rotation Data	33
3. ANALYSIS OF FRAMES WITH SEMI-RIGID JOINTS : FORMULATION	
3.1 Introduction	34
3.2 Shape Functions	35
3.3 Strains and Stresses	39
3.4 Stiffness Matrix	41
3.5 Connection Modelling	48
3.5.1 Numerical Representation of Moment-Rotation Curves	48
3.5.2 Joint Behaviour in Unloading and Reloading	52
3.5.3 Offset of Connection	52
3.6 Section Properties	55
3.6.1 Evaluation of Section Properties for a General Elastic Section	55
3.6.2 Spread of Yield	57
3.6.3 Stress-Strain Relationship	60
3.7 Internal Stresses and Forces	62
3.8 Inclusion of Initial Imperfections	63
3.8.1 Residual Stresses	63
3.8.2 Initial Out-of-Straightness	67

3.8.3 Axial Load Eccentricity 70

4. COMPUTER PROGRAM
4.1 Program Layout 72
4.2 Reading Input Data 76
4.3 Calculation of Element Stiffness Matrix and the Vector of Element End Forces 78
4.3.1 The Element Stiffness Matrix 78
4.3.2 Element Fixed End Forces 80
4.3.3 Transformation 82
4.4 Assembly of Global Stiffness Matrix and Load Vector 85
4.5 Solution of Simultaneous Equations 86
4.5.1 Boundary Conditions 86
4.5.2 Cholesky's Method of Solving Simultaneous Equations 87
4.6 Updating the Strains 88
4.7 Calculating Section Properties and Internal Forces 88
4.8 Load Iteration Procedure 89
4.8.1 Newton-Raphson Iterative Procedure 89
4.8.2 Modified Newton-Raphson Iterative Procedure 91
4.8.3 Calculation of Out-of-Balance Forces 92
4.8.4 Convergence Criterion 97
4.9 Printing Out Results 97
4.10 Incrementation of the Applied Loads 98
4.11 Special Facilities 101
4.11.1 Restart Facility 101
4.11.2 Step-Back Facility 101

5. PROGRAM VERIFICATION: PART I COMPARISONS WITH TESTS ON RIGIDLY AND FLEXIBLY CONNECTED FRAMES
5.1 Introduction 103
5.2 Rigidly Connected Frames with Eccentrically Applied Column Loads 103
5.2.1 Description of Experimental Tests 103
5.2.2 Comparisons Between Analytical and Experimental Results 107
5.2.3 Calculation of Maximum Loads for the Cases of Concentric Axial Load Using Effective Lengths 113
5.2.4 Calculation of the Maximum Loads for the Subassemblages Under the Action of Eccentrically Applied Loads 123
5.3 Rigidly Connected Frames Under the Action of Combined Axial and Lateral Column Loads 127
5.3.1 Description of Test Program 127
5.3.2 Analytical Results 130
5.3.3 Discussion of Results 132
5.4 Flexibly Connected Frames Under the Action of Axial Column Loads 132
5.4.1 Description of Experimental Program 132
5.4.2 Comparisons of Analytical and Experimental Results 138
5.4.3 Discussion of Results 142
5.4.4 Effect of Beam Flexibility 145
5.5 Conclusions 147

6. PROGRAM VERIFICATION: PART II COMPARISONS WITH TESTS ON SUBASSEMBLAGES WITH SEMI-RIGID JOINTS
6.1 Introduction 148

6.2 Experimental Data 149
6.2.1 Joint Tests 149
6.2.2 Smoothing of the Moment-Rotation Data 152
6.2.3 Subassemblage Tests 163
6.3 Comparisons of Analysis with Experimental Results 168
6.3.1 Load-Deflection Curves 168
6.3.2 Column Axial Load-Column Moment (P-M) Curves 188
6.4 Conclusions 201

7. PARAMETRIC STUDY
7.1 Introduction 203
7.2 Description of Parametric Study 204
7.3 Discussion of Results 210
7.3.1 Column Strength Due to Axial Load Only 210
7.3.1.1 Column Strength Curves 210
7.3.1.2 Effective Length Factor 218
7.3.2 Subassemblage Strength Due to Combined Column and Beam Loads 232
7.3.2.1 Interaction Curves 232
7.3.2.2 Effect of Beam-to-Column Connections on the Failure Load 243
7.3.2.3 Effect of Beam Load on Column Load 245
7.3.2.4 Maximum moment at Column End 247
7.3.2.5 A Remark on the Recommendations of BS5950 for Designing Columns with Flexible Connections 250
7.4 Conclusions 252

8. CONCLUSIONS
8.1 Summary 254
8.2 Recommendations for Future Work 256

APPENDICES
Appendix-A Derivation of the Combined Beam and Beam-to-Column Connection Stiffness 259
Appendix-B Calculation of the Effective Length Factor for a Restrained Column Using Column Strength Curves 262

REFERENCES 265

LIST OF FIGURES

		Page
1.1	Typical Moment-Rotation Relationship for a Semi-Rigid Connection	3
1.2	Effect of Semi-Rigid Joints on the Bending Moments in Beams	4
2.1	Behaviour of Perfect and Imperfect Columns Under Axially Applied Loads	9
2.2	Typical Column Strength Curve	9
2.3	A Column with Semi-Rigid End Supports: Effective Length	12
2.4	A Beam Element in Its Original and Deflected Positions	12
2.5	Frame Analysed by Simitses and Vlahinos	25
2.6	Model Used by Chen and Lui for a beam-Column Element with Semi-Rigid Joints	27
2.7	Model Used by Cosenza et al for a beam-Column Element with Semi-Rigid Joints	27
3.1	A Beam-Column with Semi-Rigid Joints	36
3.2	Mode Shapes for an Element with Semi-Rigid Joints (Unit Displacements)	38
3.3	Mode Shapes for an Element with Rigid Joints (Unit Displacements)	38
3.4	Different Types of Moment-Rotation Representations	49
3.5	Comparison of Moment-Rotation Idealization	51
3.6	Typical Momeny-Rotation Relationship Including Unloading	51
3.7	Idealization of Practical Connections	54
3.8	Subassemblage Analysed for Joint Offset	54
3.9	Load-Deflection Curves for the Subassemblage of Fig-3.8	56
3.10	Load-Moment Curves for the Subassemblage of Fig-3.8; Web Cleats	56
3.11	A General Cross-Section	58
3.12	A General I-Shaped Cross-Section: Subdivision for Approximate Calculation of Section Properties and Internal Forces	58
3.13	Idealized Stress-Strain Relationship	61
3.14	An Approximate Pattern for Residual Stresses: Parabolic Distribution (Young)	61
3.15	An Approximate Pattern for Residual Stresses: Linear Distribution (Lehigh)	66
3.16	An Approximate Pattern for Residual Stresses: Rectangular Distribution (Welded)	66
3.17	An Approximate Shape for Initial Deflections in a Column	69
3.18	Initial and Updated Deflection Shapes	69
3.19	Inclusion of Load Eccentricity	71
4.1	A General Type of Subassemblage	73
4.2	Analysis Flow Chart	74
4.3	A Beam-Column Element: Local Co-ordinate Axes, Degrees of Freedom and End Forces	79
4.4	Types of Acceptable Applied Loads	81
4.5	Local and Global Axes	83
4.6	Axes Transformation	83
4.7	Prediction of Load-Deflection Curve Using Incremental Analysis	90
4.8	Prediction of Load-Deflection Curve Using Incremental-Iterative Analysis	90
4.9	Free Body Diagram for the Calculation of Out-of-Balance Force	

	Due to the Column Load	93
4.10	Free Body Diagram for a Frame Member for the Calculation of Out-of-Balance Force Due to a Lateral Load Q	95
4.11	An Example of Load Patterns	100
5.1	Subassemblage Tested by Aoki and Fukumoto	105
5.2	Residual Stresses in Column Section of Fig-5.1	106
5.3	Load-Deflection Curves for Case A1 (L/r=40)	109
5.4	Load-Deflection Curves for Case B3 (L/r=70)	110
5.5	Load-Deflection Curves for Case C3 (L/r=100)	111
5.6	Variation of Moments at Top End of Column	112
5.7	Interaction Plot for the Subassemblage of Fig-5.1	114
5.8	Column Strength Curves for a Pin-Ended Column	116
5.9	Models for Determining Effective Length	117
5.10	Subassemblage Tested by English and Adams	128
5.11	Residual Stresses in W5x16 section	131
5.12	Load-Deflection Curves for a Rigid jointed Frame (English and Adams)	133
5.13	Load-Deflection Curves for a Rigid jointed Frame (English and Adams)	134
5.14	Subassemblage Tested by Bergquist	135
5.15a	Moment-Rotation Curves from Joint Tests (Bergquist)	137
5.15b	Moment-Rotation Curves as Inferred from Bergquist Subassemblage Tests	137
5.16	Load-Deflection Curves for Bergquist Subassemblage	139
5.17	Moment-Rotation Curves Assumed for the Bergquist Subassemblage	140
5.18	Variation of Moments at Top End of Column (Bergquist Subassemblage)	144
6.1	Joint Test Apparatus (Reproduced from Ref 53)	151
6.2	Moment-Rotation Curves for Web Cleat Connection to Column Web	153
6.3	Moment-Rotation Curves for Web Cleat Connection to Column Flanges	153
6.4	Moment-Rotation Curves for Flange Cleat Connection to Column Web	154
6.5	Moment-Rotation Curves for Flange Cleat Connection to Column Flanges	154
6.6	Moment-Rotation Curves for Web and Seat Cleat Connection to Column Web	155
6.7	Moment-Rotation Curves for Web and Seat Cleat Connection to Column Flanges	155
6.8	Moment-Rotation Curves for Flush End Plate Connection to Column Web	156
6.9	Moment-Rotation Curves for Flush End Plate Connection to Column Flanges	156
6.10	Moment-Rotation Curves for Extended End Plate Connection to Column Flanges	157
6.11	Smoothed Moment-Rotation Curves for the Range of Tested Connections (Major Axis)	159
6.12	Smoothed Moment-Rotation Curves for the Range of Tested Connections (Minor Axis)	160
6.13	Moment-Rotation Curves (Major Axis): Enlargement of the Early Parts	161
6.14	Moment-Rotation Curves (Minor Axis): Enlargement of the Early Parts	162
6.15	The Test Subassemblage	164
6.16a	Load Patterns for Cases ST2, ST3, ST4 and ST6	171

6.16b Load Patterns for Cases ST7, ST8, ST9 and ST10 172
6.17 Load-Deflection Curves for Case ST2 173
6.18 Load-Deflection Curves for Case ST3 174
6.19 Load-Deflection Curves for Case ST4 175
6.20 Load-Deflection Curves for Case ST6 176
6.21 Load-Deflection Curves for Case ST7 177
6.22 Load-Deflection Curves for Case ST8 178
6.23 Load-Deflection Curves for Case ST9 179
6.24 Load-Deflection Curves for Case ST10 180
6.25 Bridging Effect on Transfer of the Beam Load to the Column 182
6.26 Load-Deflection Curves for Case ST6 (ReRun: Extra Parameters: A Lateral Column Load) 184
6.27 Moment-Rotation Curves for a Flange Cleat Connection (Curves 1 and 2 Inferred from Test ST6) 186
6.28 Load-Deflection Curves for Case ST6 (ReRun): Extra Parameters (1) A Parabolic Residual Stress Pattern (2) Two Different Moment-Rotation Curves for Left and Right Connections 187
6.29 Load-Deflection Curves for Case ST7 (ReRun): Extra Parameters: A Lateral Column Load 189
6.30 Variation of Moments at Top End of Column: ST4 190
6.31 Variation of Moments at Top End of Column: ST8 191
6.32 Variation of Moments at Top End of Column: ST9 192
6.33 Variation of Moments at Top End of Column: ST6 194
6.34 Variation of Moments at Top End of Column: ST7 195
6.35 Variation of Moments at Top End of Column: ST7 (ReRun) 197
6.36 Interaction Plot for Subassemblage Series 200
7.1 Standard Subassemblage 205
7.2a Idealized Stress-Strain Curve 206
7.2b Residual Stress Pattern Adopted for the Parametric Study 206
7.3 Model for the Isolated Column with Four Semi-Rigid Connections 209
7.4 Load Pattern Used in the Parametric Study 209
7.5 Column Strength Curves for an Isolated Column 211
7.6 Column Strength Curves for a Subassemblage with 1.5m Beams 211
7.7 Column Strength Curves for a Subassemblage with 3.0m Beams 213
7.8 Column Strength Curves for a Subassemblage with 4.5m Beams 213
7.9 Column Strength Curves for a Rigid Jointed Subassemblage 214
7.10 Column Strength Curves for a Flexibly Connected Subassemblage 214
7.11 Column Strength Curves for a Flexible Connected Subassemblage 215
7.12 Column Strength Curves for a Flexible Connected Subassemblage 215
7.13 Comparison Between Estimated and Calculated Ultimate Loads 226
7.14 Comparison Between Estimated and Calculated Ultimate Loads 226
7.15 Comparison Between Estimated and Calculated Ultimate Loads 227
7.16 Comparison Between Estimated and Calculated Ultimate Loads 227
7.17 Variation of Estimated Effective Length Factors k with Combined Beam and Connection Stiffness C^* 229
7.18 Effective Length Factors Vs. C_j/C^* 230
7.19 Correlation Between Effective Length Factors 230
7.20 Interaction Curves for the Subassemblage of Fig-7.1 233
7.21 Behaviour of Subassemblage Under Beam Load Only 235
7.22 Behaviour of Subassemblage Under Column Load Only 237
7.23 Behaviour of Subassemblage Under Combined Beam and Column Loads 238
7.24 Force-Moment Curves for Different Beam Loads (Rigid Joints) 240
7.25 Force-Moment Curves for Different Beam Loads (Web Cleats) 240
7.26 Spread of Yield (Rigid Joints) 241

7.27	Spread of Yield (Web Cleat Connections)	241
7.28	Column Load vs. Connection Stiffness	244
7.29	Interaction Curves (P vs. Q)	246
7.30	Effect of Connection Type on Maximum Moment at the Column's End	248
7.31	Effect of Connection Type on Maximum Moment at the Column's End	249
7.32	Interaction Curves	251
A.1	Deflected Shape for a Subassemblage Under the Action of Column Load	260
B.1	Ultimate Strength Curves for an Isolated Column	263

LIST OF TABLES

		Page
2.1	Coefficients for Slope Deflection Method: Effect of Semi-Rigid Connections Included	22
2.2	Semi-Fixed Moments, Carry Over Factors and Rotational Stiffness: Effect of Semi-Rigid Joints Included	23
5.1	Geometrical Dimensions and Maximum Initial Out of Straightness Assumed in the Analytical Simulations of the Subassemblage of Fig-5.1	108
5.2	Analytical Maximum Loads for the Subassemblage of Fig-5.1	108
5.3	Maximum Loads in kN: Comparison of Different Approaches for Predicting the Carrying Capacity of the Column of Fig-5.1: Concentric Loads	122
5.4	Maximum Loads in kN: Comparison of Different Approaches for Predicting the Carrying Capacity of the Column of Fig-5.1: Concentric Loads	122
5.5	Euler and Critical Loads in kN Used in the AISC Interaction Formulae Relating to the Column of Fig-5.1	125
5.6	Maximum Load in kN Calculated by AISC and BS5950 Specifications for the Column of Fig-5.1: Eccentric Loads	125
5.7	Geometrical Dimensions and Locations of Lateral Loads for the Subassemblage of Fig-5.10	129
5.8	Comparisons of Maximum Loads in kN for the Subassemblage of Fig-5.10	129
6.1	Joint Tests	150
6.2	Initial Joint Stiffness	150
6.3	Cross-Sectional Dimensions and Tensile Strength of Test Specimens	165
6.4	Subassemblage Test Series	165
6.5	Beam Load Lever arms and Locations of Beam-to-Column Connections	169
6.6	Results of Subassemblage Analyses	169
6.7	Total Column Loads and Column Moments at Maximum Load	198
7.1	Main Parameters in the Parametric Study	208
7.2	Initial and Combined Stiffnesses for the Connections Used the Parametric Study	218
7.3	Comparison of Effective Length Factors Calculated by Different Methods	225
B.1	Calculation of Effective Length Factor Using Column Strength Curves	264

NOTATIONS

a_o	central initial deflection
A	area of cross section
A_f	flange area
A_w	web area
$A', B'_{AA}, B'_{AB}, B'_{AC}, B'_{BA}$ $B'_{BB}, B'_{BC}, C'_{AA}, C'_{AB}, C'_{BA}$ C'_{BB}	coefficients of generalized slope deflection equation
b_{AB}, b_{BA}	width of connections at ends A and B of a beam with semi-rigid joints
B, D, t_f, t_w	various cross sectional dimensions
c, s	stability functions
C_j	connection stiffness
C^*	combined connection and beam stiffness
e	load eccentricity
E	modulus of elasticity
E_{eff}	effective modulus of elasticity
E_{sh}	modulus of elasticity in the strain hardening range
E_t	tangent modulus
EI	flexural rigidity
$\overline{EI}$	reduced flexural rigidity
F, F_i	axial forces at a section
F_{bal}	unbalanced axial force
G	distribution factor (AISC Specifications)
G_{inel}	distribution factor including effect of instability
h	number of B-Spline knots
I	moment of inertia of cross section

I_b, I_c	moment of inertia of beam and column cross sections
k	effec tive length factor
k_{bs}	B-Spline knot
k_{rigid}	effective length factor for a column in a subassemblage with rigid jointts
$\bar{k}_i$	distribution factor at the top column's end (i=1) and lower column end (i=2)
l_b	clear beam span
L	element length
L_b,L_c	beam and column lengths
L/r	slenderness ratio
L_c/r_c	column slenderness ratio
M,M_i	moments at a section
M_{12}, M_{AB}, M_{AC}, M_{AB}, M_{BA}	end moments·
$M_{F_{AB}}$, $M_{F_{BA}}$	fixed end moments
M_j,M_{j_1}, M_{j_2}	joint moments
M_{max}	maximum moment that occurs at the top column's end
M_p	plastic moment of a section
M_{pc}	plastic moment of a column cross section
M_{rigid}	maximum moment that occurs at the top column's end when rigid joints are used
N_1 to N_6	shape functions for a beam-column element with semi-rigid joints
$\bar{N}_1$ to $\bar{N}_4$	shape functions for a beam-column element with rigid joints
P	axially applied load
P_{cr}	critical load
P_E	Euler load

$P_{i,ref}$	reference load for the the i^{th} loading condition
P_o	maximum load for a subassemblage with axially applied load only
P_{tot}	total applied load (for a specific type of loading)
P_u	ultimate load
P_y	squash load
Q, Q_1, Q_2	beam loads
Q_3	lateral column load
Q_{bal}	unbalanced lateral load
r	radius of gyration
R	ratio of connection stiffness to beam stiffness (eqn.7.2)
u, v	deformations at a general point
u_i, v_i, θ_i	deformations at node i
u', v', θ'	deformations of a point in the $x'-y'$ system of axes
V, V_i, V'_{AB}	shear forces
W_{ext}, W_{int}	external and internal work done
W^e_{int}	internal work done by an element
W^j_{int}	internal work done by a semi-rigid joint
x, y, x', y'	coordinates of a point w.r.t. x-y and $x'-y'$ systems of axes
$\bar{y}$	distance of centroid of a section from a reference axis
Z_y	elastic section modulus
ΔP_i	increment of the i^{th} applied load

Greek letters

α	angle between any two systems of axes
α_j, β_j	B-Spline coefficients

β	coefficient used by Chen and Lui ($= \frac{M_{pc}}{C_j}$)
δ_o	initial lateral deflection at a general point
ε	strain at a general point in the cross section
ε_L	non-linear component of the axial strain
ε_{sh}	strain at which strain-hardeneing starts
ε_y	yield strain
θ_j, $\theta_j 1$, θ_{j_2}	joint rotations
$\bar{\theta}^i_{j_1}$, $\bar{\theta}^i_{j_2}$	rotations of joints at nodes 1 and 2 in the deflection mode i
λ_p, λ_r	slenderness ratios for pin-ended and restrained columns
σ	stress at a general point in cross section
σ_a	allowable compressive stress (AISC specifications)
σ_C	compressive residual stress
σ_f	residual stress at flange tips
σ'_e	Euler critical stress (AISC specifications)
σ_T	tensile residual stress
σ_y	yield stress
σ_{fw}	residual stress at flange to web junction
σ_w	residual stress at web centre
Φ	connection rotation

Matrices

A	matrix relating deformations at a general point to nodal deformations
B	strain-displacement matrix
B_o	linear strain-displacement matrix
B_L	non-linear strain-displacement matrix
B^a_o	linear strain-displacement matrix: axial action

B_o^b	linear strain-displacement matrix: bending action
B_L^b	non-linear strain-displacement matrix: axial
D	elasticity matrix
G	row vector containing derivatives of shape functions: beam-column element
$\overline{G}$	row vector containing derivatives of shape functions: beam element
k_T	tangential element stiffness matrix
k_E	element linear stiffness matrix
k_G	element geometrical stiffness matrix
k_L	element displacement matrix
K_T	overall tangential stiffness matrix
N_{j_1}, N_{j_2}	row vector relating joint rotations to nodal deformations
p^e	element load vector: local coordinate system
p^g	element load vector: global coordinate system
P	overall load vector
P_o	vector of equivalent forces for initial deflections
T	transformation matrix
U	overall vector of nodal displacements
ΔP	incremental load vector
ΔU	incremental displacement vector
δ	displacement vector: a general point
δ^e	nodal displacement vector
ε	average strain vector
ε_i^e	average strain at load iteration no. i
ε_{i-1}^e	average strain at load iteration no. i-1
σ	resultant stress vector

CHAPTER–1

INTRODUCTION

1.1- Considerations in Design of Frames with Semi-Rigid Joints:-

When designing steel frames, BS5950 (1) recognizes three methods of design depending on the type of connections used. These design methods are:

(1) Simple design: in which the connections used are assumed to transmit no moment between the connected elements; the connections may be expected to undergo large rotations. In analysing frames with such connections, the beams are assumed to be simply supported. The connections are assumed to transmit shear forces only and hence they are sometimes termed as shear connections. The connections of this type are very light.

(2) Rigid design: in which the connections are assumed to develop full continuity between the connected elements. It follows that these connections are assumed, in theory, to permit no relative rotation of the elements connected. Elastic, inelastic or plastic analyses may be used to determine the internal forces in the structure. Such connections are relatively heavy since they are designed for both moment and shear.

(3) Semi-rigid design: in which the connections are assumed to transmit some of the moments between the connected elements and permit some relative rotation depending on their stiffness. These connections are intermediate between the other two types mentioned above.

Similar design methods are recognized by the AISC specifications (2). Simple and rigid design methods are also recognized in other specifications (3,4). Shear connections have always been commonly used in steel construction and this is especially true nowadays, due to the rising cost of labour, since they require the

least amount of site work. It has been shown experimentally (5) that even the most flexible shear connections do possess some degree of stiffness. Hence, they may rightly be classified as "semi-rigid connections". More interest has been directed recently towards the behaviour of steel frames with semi-rigid joints.

The most important aspect of connection behaviour is the moment-rotation ($M-\Phi$) relationship. Fig-1.1 shows typical $M-\Phi$ characteristics for a range of hypothetical connections. The stiffer the connection the higher is the $M-\Phi$ curve representing the behaviour of the connection. Perfectly rigid connections are represented by the vertical axis while pin connections are represented by the horizontal axis.

Semi-rigid joints, as compared with pin connections, have the effect of reducing the maximum moment that occurs within the beam length or at its ends. For example, if semi-rigid supports are used instead of simple ones at the ends of the beam of Fig-1.2, the maximum moment at the centre of the beam becomes less although moments are induced at the beam ends. If, on the other hand, the semi-rigid supports are used in place of fixed ends, the maximum moments at the beam ends are reduced. The mid-span moment, however increases due to the presence of semi-rigid joints. In both cases the use of semi-rigid end supports may result in lighter beam sections. Furthermore, the connections do transmit some of the restraint offered by the beams against column buckling. This results in shorter effective lengths of the columns and consequently leads to lighter column sections.

1.2- Objectives of the Present Investigation:-

Following the recommendations made by Jones (5), who studied

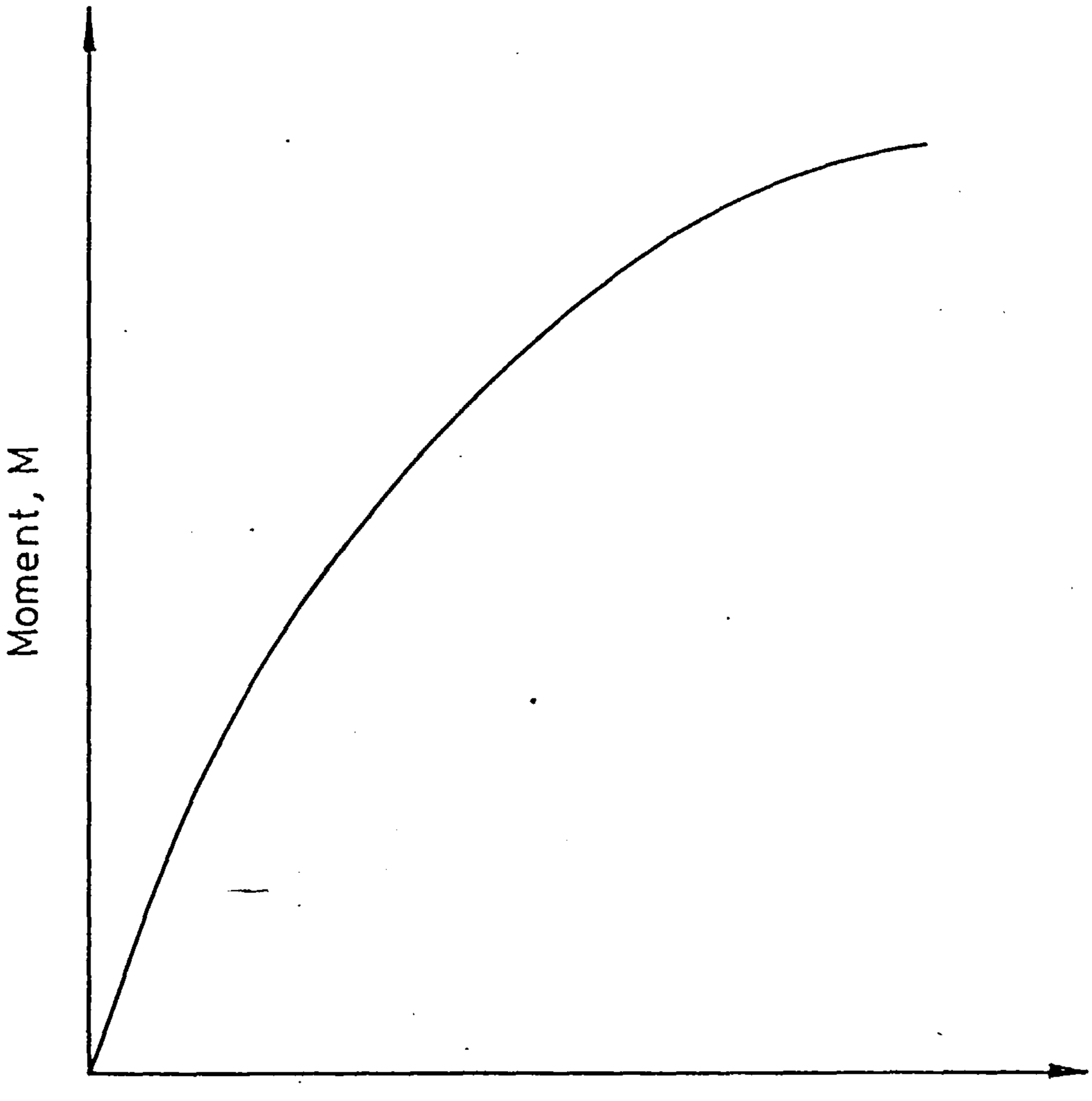

FIG.1·1 TYPICAL MOMENT-ROTATION CURVE FOR A SEMI-RIGID CONNECTION

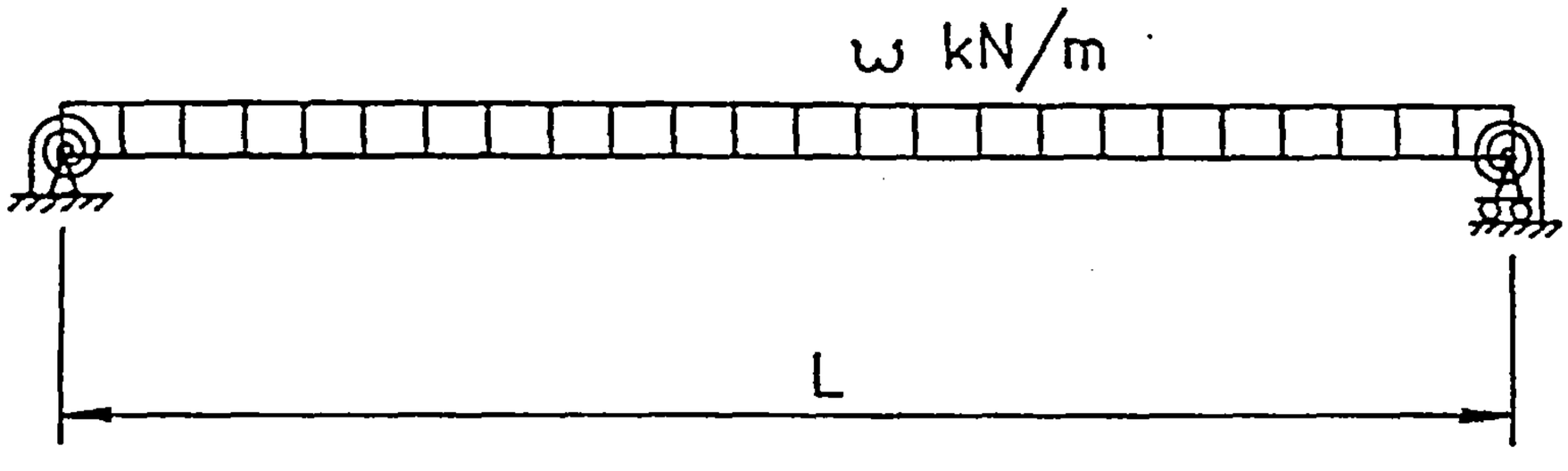

(a) A Beam with semi-rigid end supports

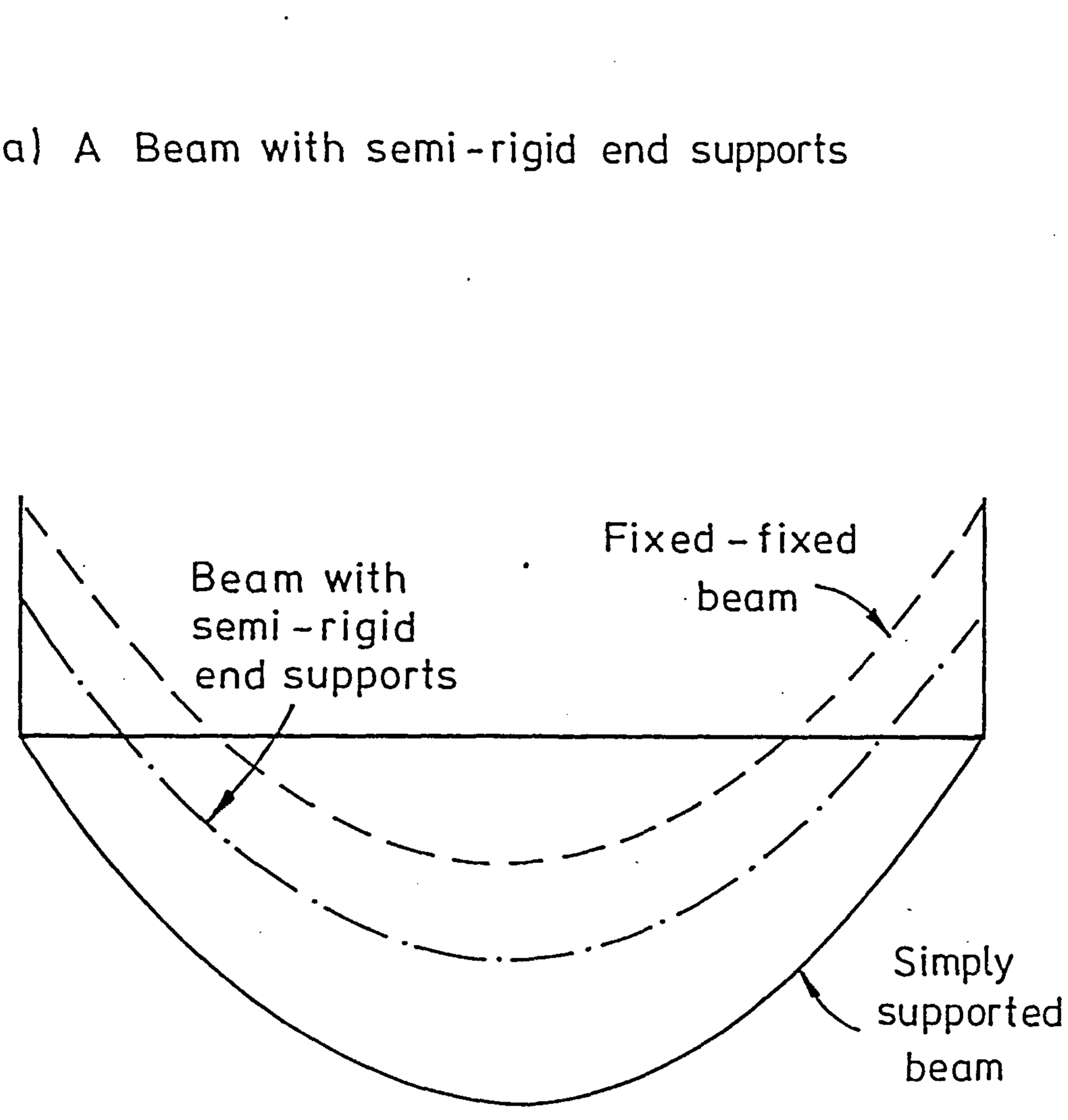

(b) Bending moment diagrams

FIG. 1·2 EFFECT OF SEMI-RIGID JOINTS ON THE BENDING MOMENTS IN THE BEAM

the behaviour of isolated columns with semi-rigid joints attached to rigid supports, the present investigation is aimed at removing this limitation by considering subassemblages. The family of substructures considered in this study are, in general, I-shaped subassemblages each consisting of a column and two beams connected at each column end by means of beam to column connections. Rigid, semi-rigid or pin connections may be assumed. The computer program developed by Jones for the study of isolated columns was rewritten and extended to analyse I-shaped subassemblages.

The beneficial effects of the semi-rigid connections which were mentioned in the previous section may be overestimated if infinitely rigid beams are used. For this reason, it was essential ,in extending Jone's work, to include flexible beams rather than rigid ones. Moreover, the presence of realistic beams with finite spans allows for the inclusion of more realistic loading conditions. In the present work, beam loads as well as axial and lateral column loads are considered, together with the loading sequence in which these loads are applied.

The complexity of the loading conditions considered in the present study results in some of the semi-rigid joints behaving in a loading, unloading and possibly reloading manner. Although provisions are made for constructing hysteresis M-Φ characteristics from any loading-unloading curves, only the loading-unloading-reloading path is considered in detail. This necessitates the consideration of only limited loading conditions which would restrict connection behaviour ,to loading unloading or reloading. Complete cyclic loading is not considered in this study.

The theoretical background of the modified program is

presented in chapter 3 while the program layout may be found in chapter 4. In its modified version, the program is capable of performing non-linear inelastic analysis of I-shaped subassemblages with semi-rigid connections. Unloading and reloading of connections is accounted for in the program. Beam loads as well as column loads are accepted by the program in addition to residual stresses, initial column deflections and small axial load eccentricities.

The program is used to simulate some experimental results obtained from tests made on both rigidly and flexibly connected frames. These comparisons are presented and discussed in chapters 5 and 6. In chapter 7, the results of a limited parametric study are presented. The main parameters varied are the type of connection, the beam flexibility and the loading condition. Finally, some conclusions and recommendations are made in chapter 8.

1.3- Limitations of the Present Investigation:-

The present work is bounded by the following limitations:

1- The frames considered here are limited to I-shaped subassemblages. Although, in theory, larger frames may be handled by the finite element procedure upon which the program is based, extra checks would be needed to ensure that assembly of the stiffness matrix and load vector are performed properly. In addition, the convergence criterion is based on fulfilling equilibrium of various segments of the frame, hence extra modifications may be needed if larger frames are to be considered.

2- Only the pre-buckling load-deflection behaviour is traced.

3- Although the applied loads may be either increasing or

decreasing in magnitude, full cyclic loading is not considered. This is due to the fact that such analyses would require complete hysteresis records of the connection M-φ characteristics. As mentioned earlier, the program does not yet fully consider such hysteresis.

4- The material considered is typical of mild steels which behave in an elastic-perfectly plastic fashion with or without strain hardening. Materials with non-linear stress-strain relationships have not yet been considered. Similar behaviour is assumed for compression and tension.

5- The present study is limited to in-plane behaviour only. Hence, no torsional effects are considered.

6- The present study covers no-sway frames only although, basically, sway frames may be handled by the program at least after very minor modifications.

7- Joint offset has been considered by modelling the panel zone by a rigid segment with length equal to half the depth of the column cross section. It has been shown that panel zone deformation is significant in the case of stiff connections (6,7) an effect not included in the present program.

CHAPTER-2

REVIEW OF LITERATURE OF STRUCTURES WITH SEMI-RIGID CONNECTIONS

2.1- The Column Problem:-

2.1.1- Pin-Ended Columns:

Probably the most important factor governing column design is the maximum load which may be resisted by the column before failure occurs. Assuming in-plane behaviour only, column failure may be categorized as follows:

(i) Elastic buckling

(ii) Squashing; or

(iii) Inelastic buckling

The earliest attempt to mathematically calculate the critical load for a column was made by Euler (8). He suggested the well known Euler formula in which the critical load, P_{cr} for a pin-ended column such as that shown in Fig-2.1a, may be expressed as

$$P_{cr} = \frac{\pi^2 EI}{L_c^2} \qquad (2.1)$$

in which EI is the flexural rigidity of the column and L_c is its length. Eqn-2.1 is based on a true bifurcation type of buckling (Fig-2.1b) for an initially straight elastic pin-ended column with the load perfectly concentric with respect to the member axis.

Provided that the column remains elastic and subject to the limitations of small deflection theory, eqn-2.1 still correctly predicts the critical load for an imperfect column with initial crookedness or load eccentricity (8,9). The load-deflection behaviour, however, is quite different. In the case of an imperfect column, the application of the axial load gives rise to lateral deflection even at low load levels. Eqn-2.1 predicts the load corresponding to the asymptote of the load-deflection curve.

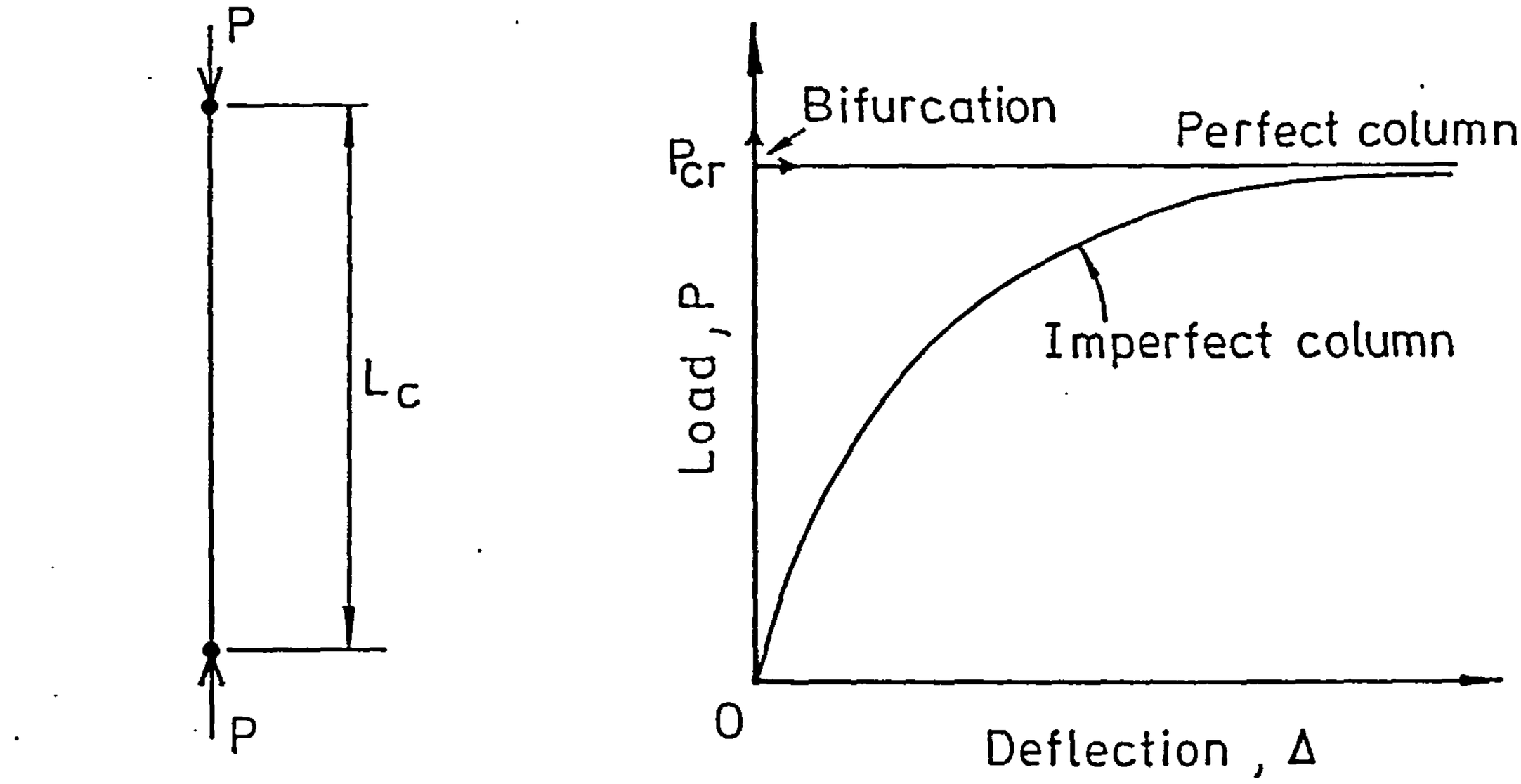

(a) A straight pin ended column

(b) Load-deflection curves

FIG.2·1 BEHAVIOUR OF PERFECT AND IMPERFECT COLUMNS

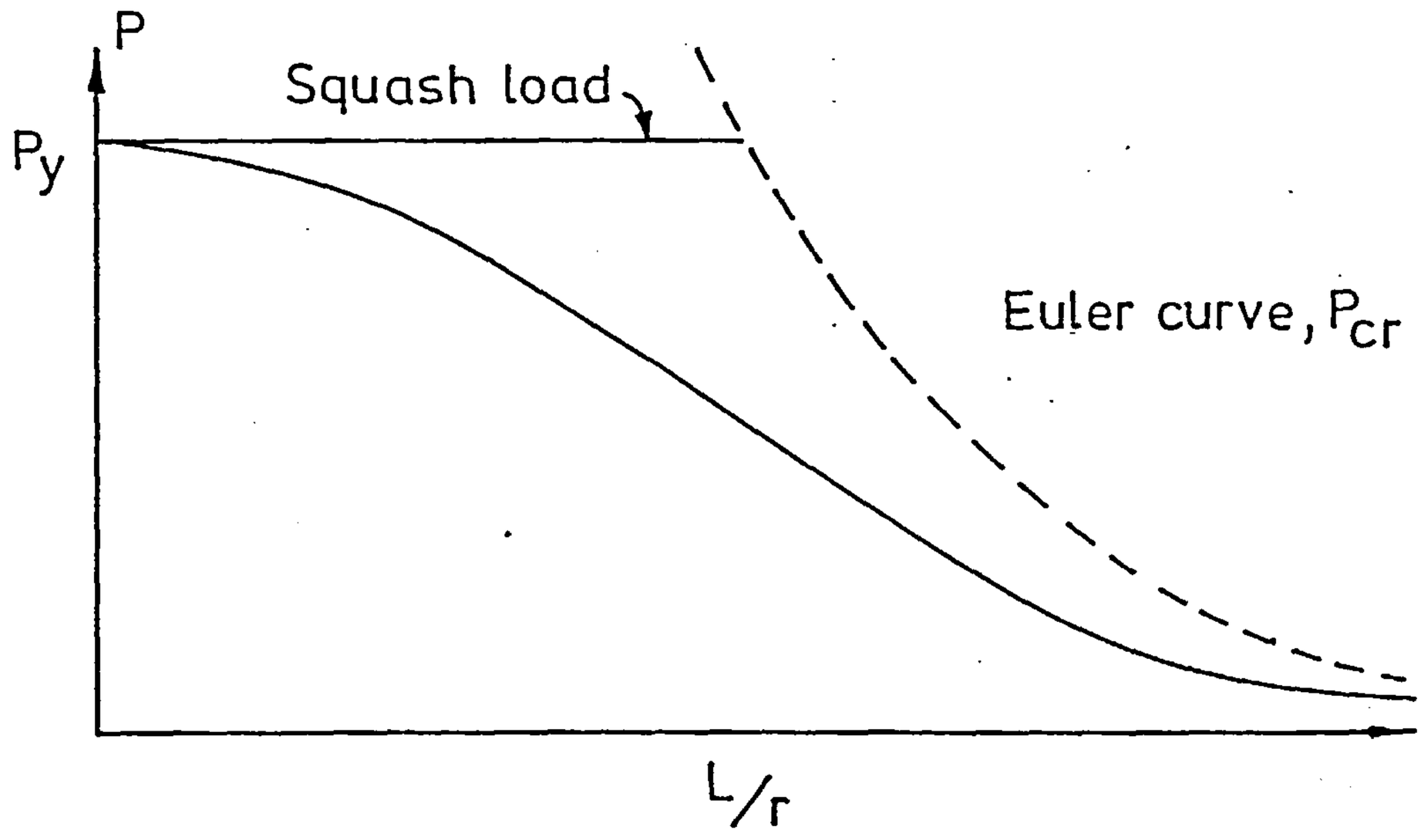

FIG.2·2 TYPICAL COLUMN STRENGTH CURVE

Tests on isolated columns (9,10) showed that eqn-2.1 gives reasonable predictions for the critical loads for the case of very slender columns. It starts to give erroneous predictions as it is applied to increasingly shorter columns. In no case can the column sustain a load greater than the "squash load" (10) given by

$$P_y = \sigma_y A \qquad (2.2)$$

in which

P_y = squash load

σ_y = yield stress; and

A = cross sectional area

If a column is of a medium slenderness, the failure is governed by inelastic buckling in which yielding takes place in the column as it buckles. The failure load in this case is less than that predicted by either of the above two equations.

In general, the failure load of a pin-ended column, is dependent on the slenderness ratio defined as the column length divided by the least radius of gyration of the column cross section. Slender columns sustain smaller loads than shorter ones. Fig-2.2 shows the relationship between the failure load and the slenderness ratio of a hypothetical column with a certain set of parameters. This curve would be constructed from data -obtained either theoretically or experimentally- consisting of the failure loads corresponding to a series of pin-ended columns with different slenderness ratios but with other factors constant. Also shown in Fig-2.2 are the Euler curve expressed by eqn-2.1 and the upper limit defined by the squash load given by eqn-2.2. From this figure, it may be seen that eqns-2.1 and 2.2 reasonably predict the failure loads for very slender and very

stocky columns respectively. Neither equation is correct when considering columns with medium slenderness ratios.

If any of the conditions, such as the column cross section or axis of buckling, is changed, the failure load of the column will be modified accordingly. Consequently, a different column strength curve is obtained. The column strength curves, therefore, serve as a useful tool in studying the effect of the various parameters governing column strength.

2.1.2- End-Restrained Columns:-

Pin-ended columns rarely exist in real structures. Most real columns have some form of end restraint provided by the other structural elements that are connected to the column ends. The most important type of end-restraint is that which is associated with the column end rotations. This restraint has the effect of changing the deflected shape of a column which would buckle in single curvature if pin-ended to one with internal points of inflection (Fig-2.3). The distance between these points, in the buckled position, is sometimes termed the effective length of the column(11) since the concept of effective length implies the use of an equivalent pin-ended column to represent the restrained one. As the effective length for no-sway columns is always less than or equal to the actual length, the failure load may be expected to be higher. Consequently the presence of rotational end-restraints has a beneficial effect.

The behaviour of isolated columns subject to real end-restraints has been extensively studied in the last few years. In what follows, some of the reported work on end-restrained isolated columns will be reviewed.

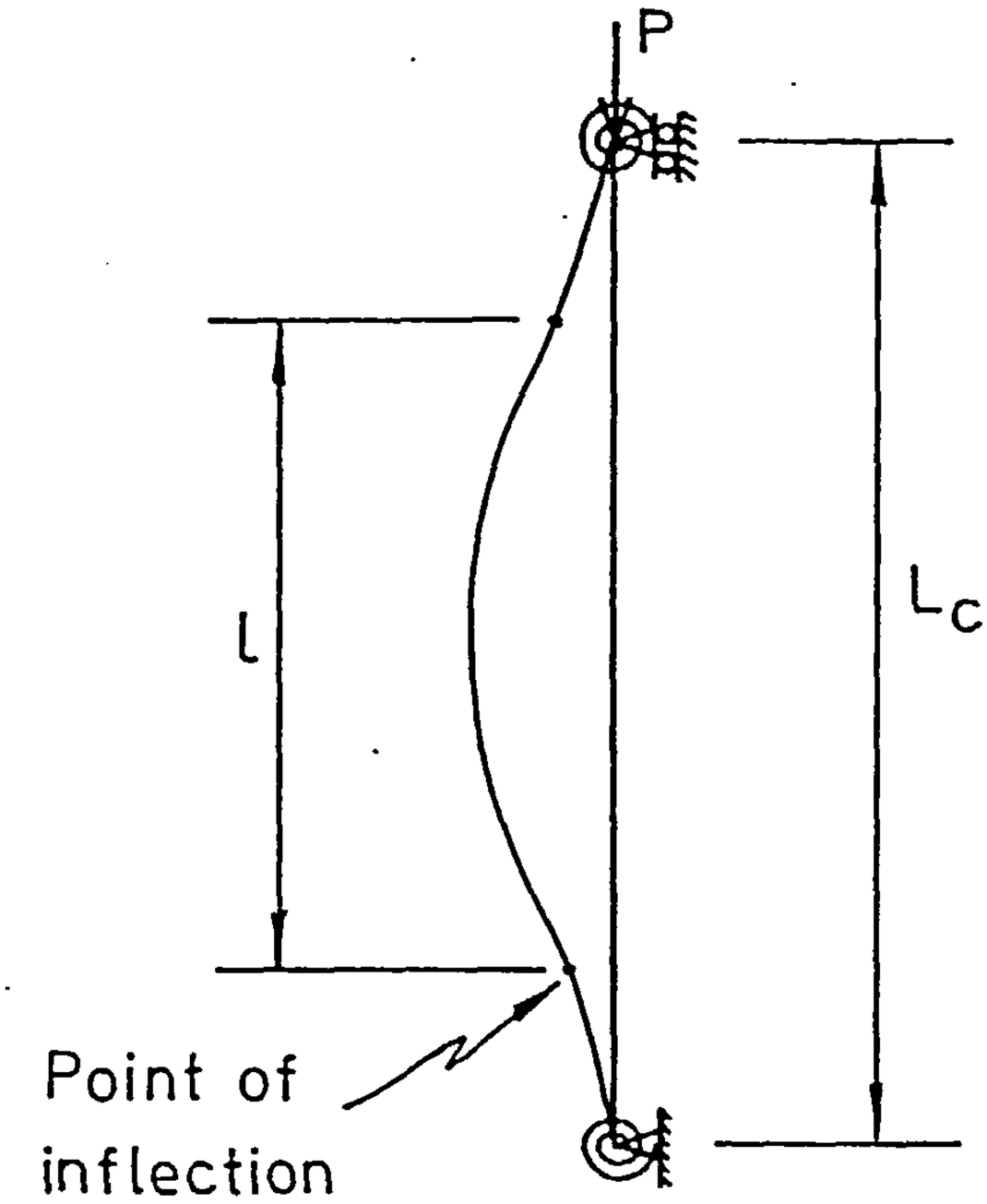

FIG.2·3 A COLUMN WITH SEMI-RIGID END SUPPORTS: EFFECTIVE LENGTH

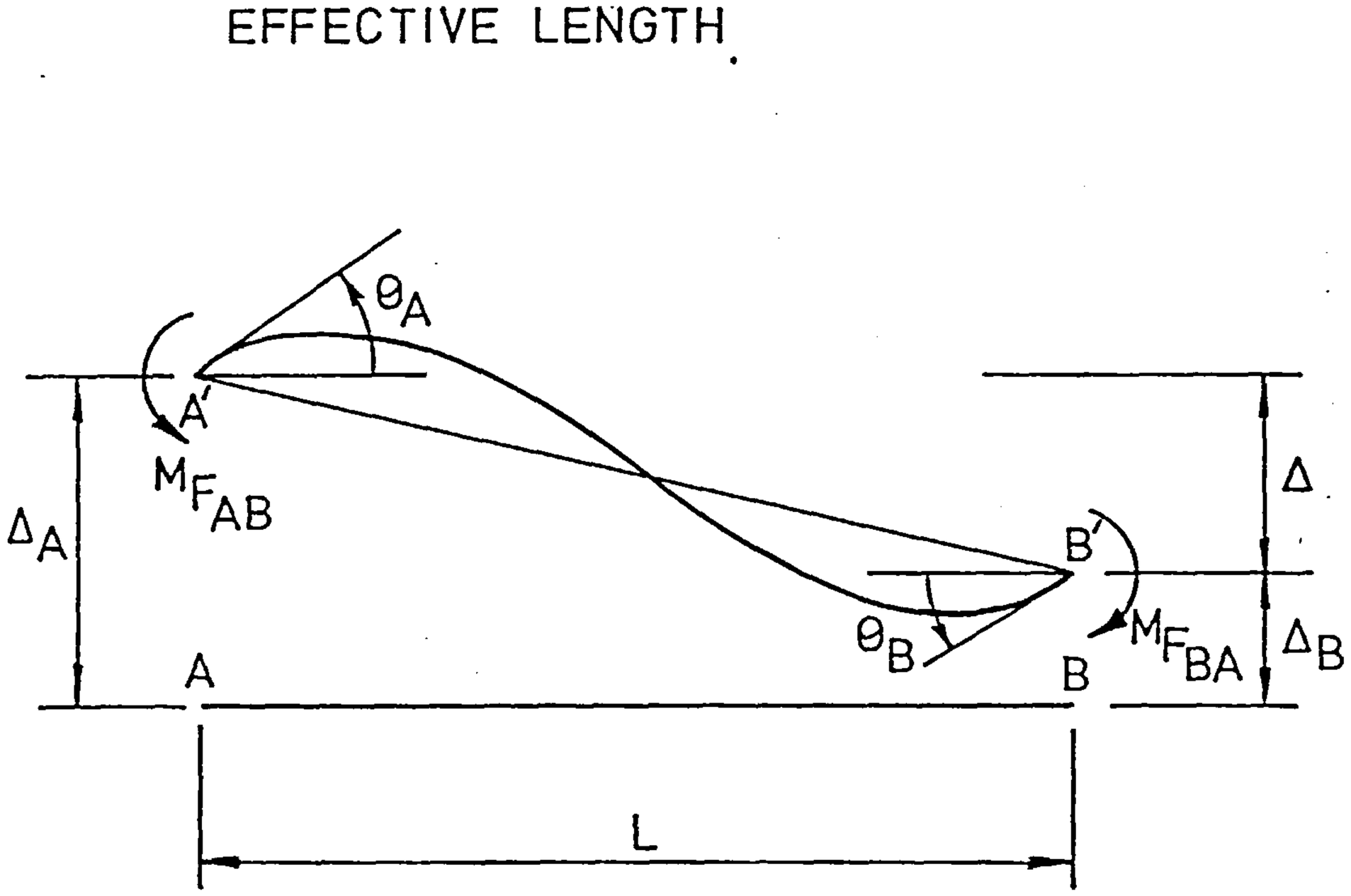

FIG. 2·4 A BEAM ELEMENT IN ITS ORIGINAL AND DEFLECTED POSITIONS

Jones (5) provided a comprehensive review of the research on the behaviour of columns with semi-rigid connections up to 1980. For this reason, apart from the work done by Jones, only work done after 1980 will be reported here. Jones developed a computer program to trace the load-deflection behaviour of an isolated column with semi-rigid joints up to its failure load. The program was based on a finite element analysis and accounted for the presence of geometrical and material non-linearities within the column and for the presence of semi-rigid connections. These connections were assumed to be attached to infinitely rigid beams. He used a non-linear connection characteristic to represent the M-Φ relationship. which was based on data from tests on semi-rigid joints (12) or was generated using formulae suggested by Frye and Morris (13). The program accounted for the effect of parameters such as residual stresses, axis of bending and cross section shape and size. He conducted a parametric study to investigate the influence of parameters such as the type of semi-rigid connection and the axis of bending on the behaviour of isolated columns.

Jones concluded that the presence of semi-rigid connections increased the maximum load above that of a pin-ended column especially for columns with slenderness ratios above 80. The change in the effective length factor of columns with semi-rigid end-restraints was reduced as stiffer connections were used. For a particular type of end restraint, the effective length factor does not change much over the range of slenderness ratios considered. Amongst the recommendations for future work he stated that realistic beams should be included in the analysis to eliminate the optimistic assumption of infinitely rigid beams. He further suggested that the work be extended to cover three

dimensional response. Although the post-buckling behaviour has little importance in the case of isolated columns, he recommended that such behaviour be traced especially when the behaviour of more realistic frames is sought.

Razzaq and Chang (14) addressed theoretically the problem of isolated columns with partial end restraint and initial imperfections. Their procedure was based on a finite difference approach in which the effect of semi-rigid end-restraint was idealized as a linear or bi-linear M-Φ relationship. A linear pattern of residual stresses was assumed. Material behaviour was assumed to be elastic-perfectly-plastic. Upon conducting a limited parametric study, the following conclusions were drawn. The effect of end-restraint has a dominant role on the behaviour of crooked columns without residual stresses but is even more pronounced when both initial crookedness and residual stresses are present. It was found that the connection moment at the attainment of the maximum load is an important factor in column response.

Sugimoto and Chen (15) developed a computer program based on the approximate deflection method (16). Bi-linear representation of the moment-rotation characteristics was used. The program was developed for three dimensional behaviour although only in-plane action was considered in a parametric study in which the effects of semi-rigid joints, axis of bending, size of column cross section and initial imperfections were considered. A set of column strength curves was constructed and used to investigate the separate effect of the parameters mentioned above. Also, by using the column strength curves for the restrained columns in conjunction with that of a pin-ended column, it was possible to determine the effective length factor (the

ratio of the effective length to the actual column length) corresponding to any particular column. The definition of the effective length adopted in their study was slightly different from that used in normal instability approaches. They defined the effective length of a restrained column as the length of an equivalent pin ended column which would sustain the same maximum load as the actual column over its actual length.

It was suggested that the effective length factor, k, for a restrained column may be calculated from the equation

$$k = 1.0 - 0.017 \frac{M_{pc}}{C_j} \qquad (2.3)$$

in which M_{pc} and C_j are the plastic moment of the column cross section and the initial stiffness of the connection respectively.

Sugimoto and Chen concluded that the deflections in the column decreased by 45%-89% in the range of L/r values of 40-160 due to the presence of modest end-restraints. Also, the maximum load of the restrained column increased in all cases. The effect of end restraint was found to decrease with increasing initial imperfections.

Vinnakota (17) studied the problem of isolated columns with end-restraints using a theoretical approach in which the finite difference method was employed. He considered a general mono-symmetrical section in the development. The material was assumed to be elastic-perfectly plastic. Initial crookedness was assumed to be present in the column. Linear, bi-linear or tri-linear representations were used for the M-Φ characteristics of the semi-rigid connections. Vinnakota conducted a parametric study in which column strength curves were constructed. He suggested that the effective length factor be

calculated from the formula

$$k = \frac{\pi^2 + 2\bar{\alpha}}{\pi^2 + 4\bar{\alpha}} \qquad (2.5)$$

in which $\bar{\alpha}$ is defined as $\frac{C_j}{EI/L}$.

2.2- Columns as Part of Frames:-

As mentioned in the previous section, real columns exist as parts of actual frames in which flexible beams are attached to one or both ends of the column by means of beam to column connections. In the theoretical approaches described above, the semi-rigid connections were assumed to be connected to infinitely rigid beams. Such an assumption overestimates the beneficial effect of the restraint. It follows that beam flexibility should be taken into account in any realistic assessment of the behaviour of restrained columns. A number of theoretical and experimental studies have been conducted to investigate the behaviour of frames with rigid or semi-rigid beam to column connections and some of these are reviewed in the following sections.

2.2.1- Types of Analyses of Rigidly Connected Frames:-

Many methods are available at present for the analysis of frames with rigid joints. The most basic methods are the slope deflection and moment distribution methods. Stability functions may be used to take into account the presence of axial forces in the members. A matrix analysis may be used to analyse large frames and this approach is well suited for use with digital computers.

2.2.1.1- Slope Deflection Methods:-

The slope deflection method (18), is based on expressing the

end moments of a beam in terms of the deformations at its ends. For a beam AB, which is deformed into the position $A'B'$ (Fig-2.4), the end moments M_{AB} and M_{BA} are expressed as

$$M_{AB} = \frac{EI}{L}(4\theta_A + 2\theta_B + \frac{6}{L}\Delta) + M_{F_{AB}} \qquad (2.6a)$$

$$M_{BA} = \frac{EI}{L}(2\theta_A + 4\theta_B + \frac{6}{L}\Delta) - M_{F_{BA}} \qquad (2.6b)$$

in which θ_A and θ_B are the rotations at ends A and B respectively, Δ is the difference between the lateral end deflections and $M_{F_{AB}}$ and $M_{F_{BA}}$ are the fixed end moments respectively. Considering the equilibrium at every joint in the structure results in a set of simultaneous equations which, upon solution, yield the unknown deformations. Using eqns-2.6, the end moments may be calculated. Once these moments are calculated, the moment at any point may easily be determined from equilibrium of the relevant part of the structure.

When an axial force is present in a member, to account for the reduced stiffness of the element equations 2.6 may be applied if the factors 4, 2 and 6 are replaced by the stability functions s, sc and s(1+c) respectively, the values of which depend solely on the ratio of the axial force present in the member to the Euler load of this member. The expressions for s, c and m may be found in many text books (18,19). The procedure is continued in the same way as the slope deflection method.

Vinnakota (20) studied the stability of rigidly connected braced L and Z shaped frames using the slope deflection method in which stability functions were used to account for the presence of axial forces in the members. Different types of applied loads and different beam span to column height ratios were considered. He concluded that

the beams framing into the column offer some restraint to the column against buckling provided that the beams are stronger than the column. If the beams were weaker than the column, no restraint was provided. Here, the strength of a member is characterized by the deformation at which the maximum strength of this member is attained (20). The same point was raised by Vinnakota in an earlier contribution (21).

2.2.1.2- **Moment Distribution Method:-**

The moment distribution (18) method was developed from the slope deflection equations. However it does not involve the solution of simultaneous equations and hence it gained wide acceptance shortly after it was first proposed by Hardy Cross (22). The procedure is started by calculating the fixed end moments. Secondly, the joints in the structure are released in succession. When any joint is released, the moments at the member ends meeting at the joint are not, in general, in equilibrium. Hence a balancing moment is distributed between the members according to their distribution factors which depend on the relative member stiffnesses. Also due to the release of the joint under consideration, a moment is induced at the far end of every member meeting at the joint depending on a carry over factor which for linear elastic analysis is equal to one half. The process is repeated until the moment at every joint converges to a value. Hence, the end moments are directly determined using the moment distribution method without the need to solve simultaneous equations.

2.2.1.3- **Matrix Methods:-**

When large structures are analysed, especially if digital computers are available, matrix analysis methods may be used. One of

these methods is the stiffness method which is based on slope deflection equation (2.18). The method involves systematically calculating the stiffness matrix and the load vector. The unknown deformations may then be found by solving the set of equations

$$\mathbf{K\,U = P} \qquad (2.7)$$

in which **K** is the stiffness matrix and **U** and **P** are the displacement and load vectors.

2.2.1.4- Finite Element Method:-

A more advanced method, which has become widely used in recent years, is the finite element method. Many specialized text books that explain the method in detail are now available (23,24,25). The mechanics of the method are very similar to those of the matrix stiffness method. According to this method, the structure is divided into a reasonable number of elements. The deformations at any point along any element are uniquely determined from the deformations at the element nodes using a set of shape functions. Using the approaches based on the principles of virtual work or energy conservation in conjunction with assumed strain-displacement relationships, the element stiffness matrices may be calculated. These matrices are then assembled to form the structural stiffness matrix. Likewise, the overall load vector is assembled from the vectors of fixed end forces of the elements. The equilibrium equations 2.7 are then solved for the displacement vector **U**. Next the strains, stresses and resultant forces at any point along any element may be calculated using the determined displacements. At present, there are a large number of computer programs which utilize the finite element method and which are

specifically prepared for research (26)

Corradi and Poggi (27) have developed a computer program for frame analysis which utilizes the finite element method of analysis. Non-linear behaviour was considered. Local plasticity was taken into account in the analysis by dividing the cross section into a number of layers. The program was used to analyse a number of multi-storey frames and was found to be satisfactory.

El-Zanaty et al (28) developed a computer program based on the finite element method. The program is capable of performing elastic and inelastic analyses. In addition to elastic-plastic analysis, elastic Eigen-value problems may be handled by the program. Only rigid joints were considered in all of these analyses. The effects of the presence of axial forces, residual stresses and strain hardening were all taken into account in the inelastic non-linear analysis. The program was used to solve a variety of problems. It was concluded that the non-linear terms in the strain-displacement relationships should be included if large change of geometry effects were to be considered. The elastic-plastic method of analysis was found to over-estimate the ultimate strength of frames under the action of lateral loads together with large axial loads and column slenderness ratios. For such frames the effect of gradual penetration of yielding influences the load-deflection behaviour. Residual stresses were found to have negligible effect on the ultimate strength. The effect of strain-hardening is more pronounced in large frames.

2.2.2- Inclusion of Semi-Rigid Joints in the Analysis of Frames:-

All of the methods of analysis described above were modified by different researchers to account for the presence of semi-rigid

connections at the ends of elements. Generally in these modifications, the moment-rotation characteristics of the joints were assumed to be linear with a slope equal to the initial stiffness of the connection although certain investigators used multi-linear relationships.

The slope deflection equations when semi-rigid connections are present take the general form (29)

$$M_{AB} = \frac{2EI}{L}A'(B'_{AA}\theta_A + B'_{AB}\theta_B + B'_{AC}\frac{\Delta}{L}) + C'_{AA}M_{F_{AB}} + C'_{AB}M_{F_{BA}} \qquad (2.8a)$$

$$M_{BA} = \frac{2EI}{L}A'(B'_{BA}\theta_A + B'_{AB}\theta_B + B'_{BC}\frac{\Delta}{L}) - C'_{BA}M_{F_{AB}} - C'_{BB}M_{F_{BA}} \qquad (2.8b)$$

where A', B'_{AA}, B'_{AB}, B'_{AC}, B'_{BA}, B'_{BB}, B'_{BC}, C'_{AA}, C'_{AB}, C'_{BA}, and C'_{BB} depend on the stiffness and size of the connection and are given in Table-2.1 (29). Δ is the lateral displacement of end B relative to end A taken as positive if downwards. The rotations and moments are assumed to be positive when they are counter-clockwise. The procedure then continues in exactly the same way as in the conventional slope deflection method.

The modified moment distribution process again follows the same procedure as the conventional method; the only difference is that the distribution and carry over factors change to those appearing in Table-2.2 (29).

In addition to the above methods, there are a number of basic analysis methods such as three moments and deformeter methods. These methods have also been modified for the presence of semi-rigid joints. A brief description of these methods was given by Jones (5). The methods are fully described elsewhere (30).

Table-2.1: Coefficients for Slope Deflection Method: Effect of Semi-Rigid Connections Included

Constant	Semi-rigid Joints with Finite Width	Rigid Joints (Zero Width)
A'	$\frac{1}{(1+2\alpha+3\alpha\beta)}$	1
B'_{AA}	$2 + 3\beta+6(1+\beta)\frac{b_{AB}}{L} + 3(2+\alpha+\beta)\frac{b_{AB}^2}{L^2}$	2
$B'_{AB} = B'_{BA}$	$1 + 3(1+\alpha)\frac{b_{AB}}{L} + 3(1+\beta)\frac{b_{BA}}{L} + 3(2+\alpha+\beta)\frac{b_{AB}.b_{BA}}{L^2}$	1
B'_{AC}	$3(1+\beta) + 3(2+\alpha+\beta)\frac{b_{AB}}{L}$	3
C'_{AA}	$1 + 2\beta+(1-\alpha+2\beta)\frac{b_{AB}}{L}$	1
C'_{AB}	$\beta + (\beta-2\alpha-1)\frac{b_{AB}}{L}$	0
B'_{BB}	$2 + 3\alpha + 6(1+\alpha)\frac{b_{AB}}{L} + 3(2+\alpha+\beta)\frac{b_{BA}^2}{L^2}$	2
B'_{BC}	$3(1+\alpha) + 3(2+\alpha+\beta)\frac{b_{BA}}{L}$	3
C'_{BA}	$\alpha + (\alpha-2\beta-1)\frac{b_{BA}}{L}$	0
C'_{BB}	$1 + 2\alpha + (1-\beta+2\alpha)\frac{b_{BA}}{L}$	1

N.B. $\alpha = \frac{2EI}{C_{j_l} L}$, $\beta = \frac{2EI}{C_{j_r} L}$ where C_{j_l} and C_{j_r} are the stiffness of the left and right connections respectively and L is the clear distance between connections

Table-2.2: Semi-Fixed Moments, Carry Over Factors and Rotational Stiffness: Effect of Semi-Rigid Joints Included

Constant	Semi-rigid Joints with Finite Width	Rigid Joints (Zero Width)
Simi-Fixed moment, M_{SAB}	$C'_{AA}M_{F_{AB}} + C'_{AB}M_{F_{BA}} - V'_{AB}b_{AB}$	$M_{F_{AB}}$
Carry Over Factor, $\bar{r}_{AB}$	$\frac{B'_{BA}}{B'_{AA}}$	0.5
End Rotation Stiffness, $\bar{S}_{MAB}$	$\frac{2EI}{L}\cdot\frac{B'_{AA}}{A'}$	$\frac{4EI}{L}$

Simitses and Vlahinos (31) employed the kinematics of the beam to column joint to analyse the flexibly connected two bar L shaped frame shown in Fig-2.5 which is subjected to a load with eccentricity e assumed positive if the load was within the length of the beam. Both linear and non-linear representation for the M-Φ data of the connection were considered. In the non-linear representation, a cubic polynomial was assumed. Only elastic behaviour was considered. Due to the non-linearity arising from the presence of non-linear M-φ representation, an incremental type of analysis was employed. They concluded that the critical load increases as connection stiffness increases. As the load eccentricity e increases in a negative sense (i.e. to the left of the column), the critical load decreases. In this case, the load-deflection curves possess points of maximum load. Positive values of e resulted in load-deflection curves which do not have such peak points. It was also concluded that neither the column slenderness nor the non-linearity of the M-φ relationship of the connection had any significant effect on the critical load.

Anderson and Lok (32) developed a procedure based on the matrix displacement method of analysis in which second order effects were taken into account. Elastic behaviour was assumed. The effect of the presence of the semi-rigid joints was accounted for by modifying the overall load vector using the overall stiffness matrix. It was claimed that this technique leads to savings in computer time and memory since the stiffness matrix is not changed whether or not semi-rigid joints are included. The effect of the presence of axial forces in the members was taken into account by employing the stability functions proposed by Livesley (33). Based on a limited study of the effect of semi-rigid joints on the effective length of the columns in

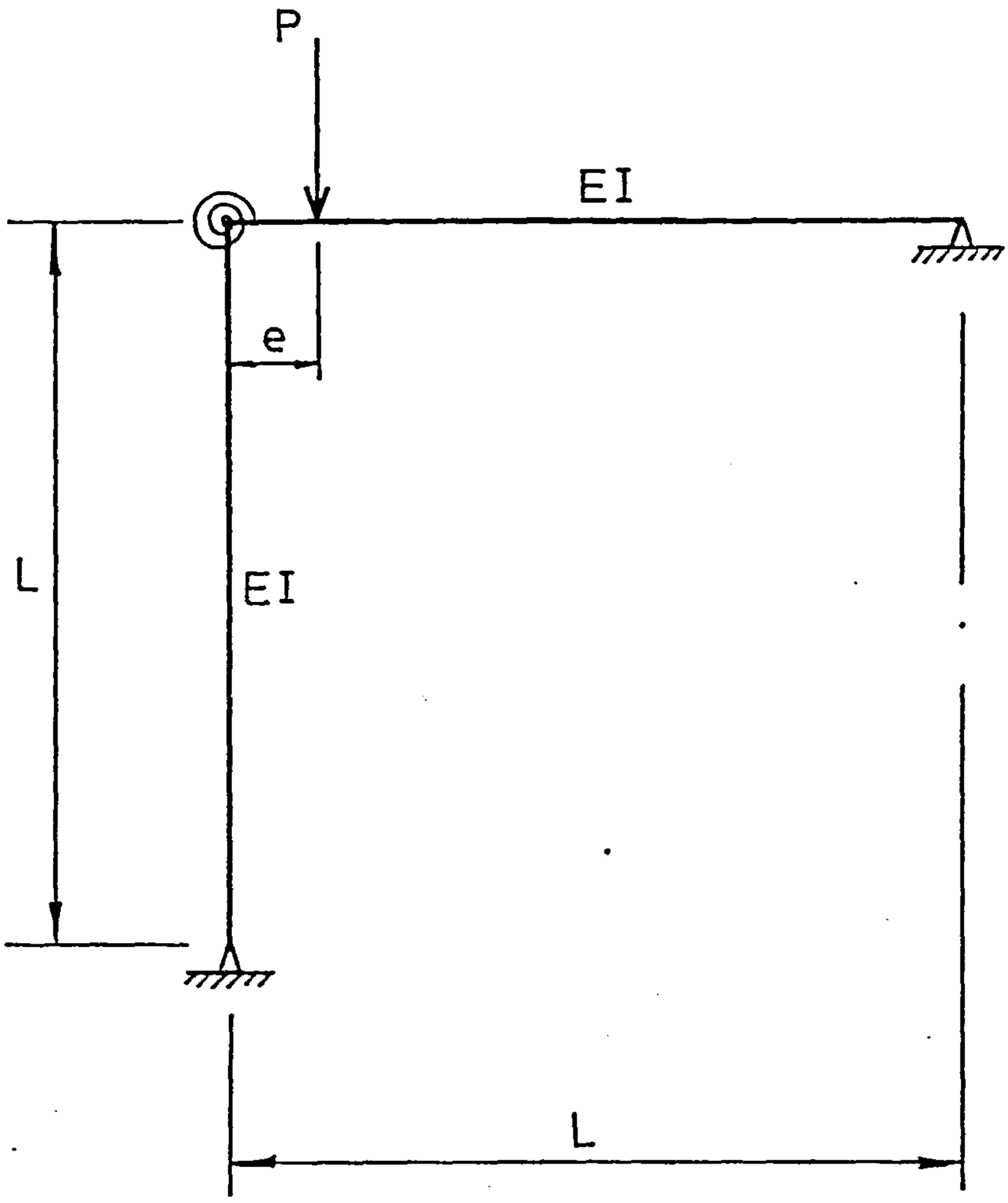

FIG. 2-5 FLEXIBLY CONNECTED FRAME ANALYSED BY SIMITSES AND VLAHINOS

braced frames, it was concluded that the traditional specifications of determining the effective length of columns were reasonable. It was also pointed out that the effective length factor decreases as the column length increases, since the connection becomes relatively more effective in restraining the columns. The method is now thought to be of limited use due to poor convergence when used with M-Φ curves for flexible low moment connections.

Chen and Lui (34) employed the stiffness method in which the overall tangent stiffness matrix was assembled from the element matrices. The element matrices were calculated on the basis that an element with two semi-rigid joints at its ends is treated as a substructure consisting of three sub-elements: two joint elements and one beam-column element (Fig-2.6). The total degrees of freedom for this substructure is ten: six corresponding to the beam-column element and two corresponding to each joint element. The element stiffness matrix was then reduced to a 6x6 matrix by condensing the extra two degrees of freedom relating to the two semi-rigid joints. The procedure was then carried out in the usual manner of matrix methods. Stability functions derived by Chen (35) were used to account for the presence of axial forces in the beam-column elements and an incremental-iterative type of analysis was used. The M-Φ data for the connections were represented by an exponential function. It was pointed out that the presence of semi-rigid joints must be taken into account when studying the behaviour of flexibly connected frames. In particular, the unloading of some of the connections must be considered. Load sequence is an important factor due to the non-linear nature of the problem. It was also concluded that the connection flexibility affects the moment distribution and drift of the frame.

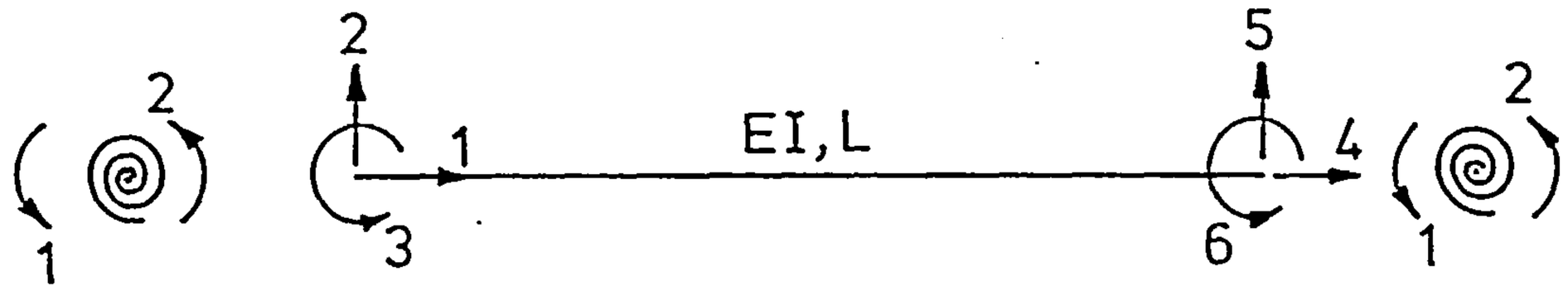

FIG. 2·6 MODEL ASSUMED BY CHEN AND LUI FOR BEAM-COLUMN ELEMENTS WITH SEMI-RIGID JOINTS

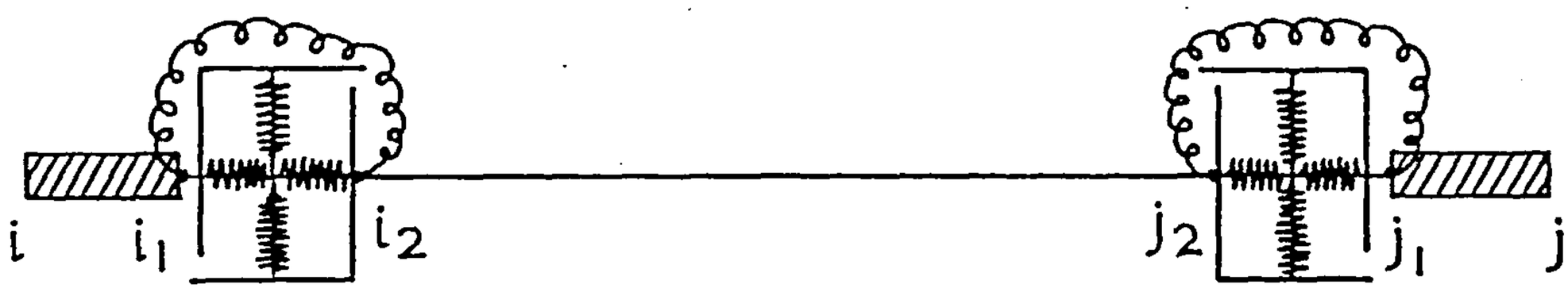

FIG. 2·7 MODEL ASSUMED BY COSENZA ET AL FOR BEAM – COLUMN ELEMENTS WITH SEMI-RIGID JOINTS

Cosenza, de Luca and Faella (36) also developed a computer program which utilized the stiffness matrix method of analysis. Large displacement effects were taken into account by the use of a second order analysis. Semi-rigid joints were modelled as extra sub-elements consisting of a short rigid segment and springs with axial, shear and rotational stiffnesses. The stiffness matrix of a sub-structure consisting of a beam-column element and one sub-element at each end (Fig-2.7) was developed. Then the matrix was reduced to a 6x6 matrix using static condensation of the internal degrees of freedom. Many alternatives for representing the M-Φ data of the connections were considered. A parametric study on the behaviour of multi-storey flexibly connected frames was conducted. It was concluded that the critical loads of frames increased when stiffer connections were used.

Poggi and Zandonini (37) extended the program developed by Corradi and Poggi (27) to include the effect of semi-rigid joints. The M-ϕ data were represented by a series of straight lines which closely follow the actual relationship. Unloading of some of the connections was also included.

2.3- Review of Tests on Frames with Rigid and Semi-Rigid Connections:-

Unlike the large variety of available analytical procedures, tests on actual steel frames are limited in number and scope. This is probably due to the fact that the testing of full scale steel frames is expensive since it requires large well equipped testing facilities. Moreover, only a very small fraction of such tests have been carried out on flexibly connected frames or subassemblages.

English and Adams (38) tested frames comprising of a column and one beam at each end connected by rigid beam to column connections.

They considered a variety of column height to beam span ratios. Both axial and lateral column loads were considered. The load-deflection behaviour and the sequence of formation of plastic hinges were studied in this series of tests. Aoki and Fukumoto (39) experimentally studied the behaviour of frames similar to those tested by English and Adams. Again, rigid joints were used. Eccentric axial column load was considered in this study. Bergquist (40) tested a single I-shaped subassemblage with flexible beam to column connections. Beam loads and an axial column load were considered. It was concluded in this test that the beams on the loading side did not offer any assistance to the column against buckling. All of these three studies are discussed in more detail in Secs.5.3, 5.2 and 5.4 respectively.

Lay and Galambos (41) conducted a series of tests on subassemblages similar to those tested by Aoki and Fukumoto. Rigid beam to column connections were used. An axial column load was applied to the column in the first load stage and, in the second stage, the column load was held constant while applying moments at the column ends by means of forces eccentric to the column. This stage was terminated at failure. The axial load and the moments and rotations at the joints and the strains in the members were recorded. From these measurements, it was possible to study the joint moment-rotation, deflections at various points on the frame and the strain distribution at certain cross sections corresponding to any desired load level. Theoretical procedures were also developed to predict the behaviour of the subassemblage.

From the above study, Lay and Galambos concluded that theoretical methods using equilibrium and compatibility and based on inelastic response of the beams and the beam-column reasonably

predicted the behaviour of the subassemblage. Conventional quasi-elastic analysis was less accurate. No instability of the subassemblage nor of the individual components was observed. Using non-linear member theory, the response of the individual members was predicted correctly. Plastic hinges formed at the advent of local buckling. After the formation of plastic hinges, simple mechanism theory correctly predicted the behaviour of the subassemblage.

Gent and Milner (42) conducted a series of tests on limited subassemblages each consisting of a column and two beams at each column end forming a three dimensional frame. Rigid beam to column connections were used. The loading sequence adopted was such that beam loads at the far ends of the beams were applied using turnbuckle arrangements. When the prespecified levels of beam loads were reached, an axially applied column load was increased from the zero condition until failure of the subassemblage occured. In this latter stage, the turnbuckles were clamped in position hence preventing the beam ends from undergoing any displacements relative to each other. Curves describing the load-deflection behaviour and showing the variation of the column end moment with the axial force in the column were constructed from test results. It was concluded that, if the column became plastic, moment shedding may occur although it did not have any significant effect on the ultimate load of the column. Bending action, however, indirectly influenced the ultimate capacity of the column by reducing the stability and inducing deformations analogous to initial deflections.

A 3 storey 2 bay x 1 bay full size, rigidly connected steel frame was tested by Wood et al (43) to investigate its behaviour under the action of service and ultimate loading conditions. Grade 43 steel was used for all frame members. Beam and axial column loads were

applied to the structure in four loading stages. The last stage was intended to bring the individual members and, if possible, the major axis beams to collapse. The test was conducted to verify a design method proposed in the Joint Committee Report published in December 1964 (44). According to this design method, major axis beams (which restrain the column about the major axis) are designed on the basis that their ends are fixed and that three plastic hinges form at collapse: two hinges at the ends and one within the beam length. Minor axis beams are designed elastically using a limited sub-frame consisting of the beam and the adjoining members in the plane of bending of the beam. The column is designed for limiting stresses calculated on the basis of a limited frame which includes the column under consideration and the members framing at either end. Using this sub-frame, the stresses due to the axially applied load and those resulting from beam bending, together with additional stresses resulting from the axial load acting through initial and additional lateral deflections, are calculated.

It was concluded, from the study conducted by Wood et al described above, that the method of column design proposed in the Joint Committee Report was accurate in designing the beams. Column design, however, was conservative. It was suggested that more research be done to accurately define criteria for collapse with increased plasticity.

Smith and Roberts (45) tested a 3 storey 2 bay x 2 bay rigidly connected steel frame for service and ultimate loading conditions. The study is similar in scope to that described above. Its main objective was to verify the Joint Committee design method which had been extended to high strength steels in a report published in May 1971 (46). Also this frame permitted the investigation of a wholly

internal column. The loading sequence was the same as in the study described above. It was concluded that the Joint Committee method was applicable to high grade steels as well as to mild steel. The method was found to result in safe design of internal columns.

Davison et al (47,48) conducted a series of tests on I-shaped subassemblages with semi-rigid beam to column connections. Two types of loads were applied in a two stage sequence. In the first stage one or two beam loads were applied to prescribed load levels. In the second stage, an axial column load was applied up to failure of the subassemblage. The proposed AISC LRFD beam-column design procedure (49) was used to predict the ultimate loads found in this series of tests. The predicted loads were found to be considerably lower than the experimental ones. The ability of the connections to transmit substantial amounts of beam restraint was advanced as the reason for the discrepancies between the design and test procedures. This series of tests is discussed in more detail in chapter 6.

Two multi-story flexibly connected frames were also tested by Davison et al (48,50) to investigate the behaviour of more realistic flexibly connected frames for realistic loading conditions.

2.4- Review of Semi-Rigid Beam to Column Connections:-

2.4.1- Experimental Studies:-

Numerous experimental investigations have been conducted on the behaviour of semi-rigid beam to column connections. It was concluded that the most important aspect in connection behaviour is the moment-rotation relationship. In-depth reviews of tests performed on semi-rigid connections were provided by Jones (5), Nethercot (51) and Goverdhan (52). In these reports, information is available on

individual details of the connections as well as the M-φ data obtained from tests made on the connection.

Davison et al (48,53) conducted a set of tests on a series of beam to column connections which ranged from flexible web cleat connections to an almost rigid extended end plate connection with all other variables e.g. column and beam sizes and material kept constant. The M-φ data from these tests were recorded. More details of the test procedure and the M-Φ data are presented in chapter 6.

2.4.2- Modelling of the Moment-Rotation Data:-

In order to include the effect of a semi-rigid connection in an analysis, it is important to model the M-Φ data by a reasonable and mathematically defined curve. First attempts considered linear and bi-linear representations while later attempts considered tri-linear, multi-linear and non-linear representations. Non-linear representation included polynomials of any desired degree and exponential functions with arbitrary constants to suit the data under consideration. The latest attempt to non-linearly represent the M-Φ data was based on using cubic B-splines which closely follow the actual data points. All of these representations have already been described in Sec-2.2 in the appropriate places. In chapter 3, a comparison between the polynomial and cubic B-spline representations for one set of data points is presented. Jones (5) pointed out that although polynomial representation results in good fitting of the moments and rotations, the slope of the M-Φ curve may be erroneously represented, in particular at higher values of rotation.

CHAPTER-3

ANALYSIS OF FRAMES WITH SEMI-RIGID JOINTS: FORMULATION

3.1- Introduction

The behaviour of real semi-rigid frames is highly non-linear. Any attempt to analytically closely simulate their behaviour must take into account the following sources of non-linearities:

(1) the presence of semi-rigid joints with non-linear M-Φ characteristics

(2) inelastic behaviour of some or all parts of the frame

(3) residual stresses which affect the point at which inelastic behaviour starts and also has a definitive role on the spread of yield over the cross sections and along the lengths of the frame members

(4) the presence of axial forces in the columns acting in conjunction with lateral displacements to increase the bending moments in these columns

(5) non-linear strain-displacement relations which arise from the consideration of large deflections

It is well known (23,53) that such analyses usually take the form of incremental-iterative procedures in which the structure is assumed to behave linearly within each load increment or iteration. One of the most common methods of analysis is the finite element method. The analysis proceeds with the assembly of a 'tangential' stiffness matrix $\mathbf{K}_T$ and an incremental load vector ΔP. The incremental equilibrium equation

$$\mathbf{K}_T \Delta U = \Delta P \qquad (3.1)$$

is then solved for the incremental displacement vector, ΔU . A Newton-Raphson iteration procedure may then be employed within each load increment until the required convergence is attained. Details of the

procedure will be given in chapter-4.

In this chapter, a formulation of the tangential stiffness matrix of a beam-column element is presented. In this formulation the element is assumed to be prismatic with two semi-rigid joints at its ends. Elastic behaviour is assumed. A method of dealing with the loss of stiffness due to spread of yield in all members, including the influence of residual stress, is used and will be explained later in this chapter. Also presented is a full account for the unloading-reloading behaviour of the connections which might occur at any load level depending on the loading sequence. The formulation is limited to two-dimensional, in-plane behaviour and the program will be applied herein only to non-sway subassemblages although the formulation can cover sway.

3.2- Shape Functions

Consider a beam-column which is in equilibrium under the action of a set of loads p^e . The deformed shape of the column which corresponds to these loads is shown in Fig-3.1. Also shown in this figure is the column's undeflected position which is taken to be the reference for the deflections. If an incremental load vector, Δp^e is applied, the deformations will be modified by an incremental displacement vector, $\Delta \delta^e$. The new deflected shape of the column is also shown in Fig-3.1. In both deformed positions, it is clear that, because of the presence of the semi-rigid joints at nodes 1 and 2, each of these nodes will have two rotations : one just to the left and the other just to the right. The difference between these rotations is the rotation of the joint itself. In the final deformed shape the deformation at any point A along the element length is given by

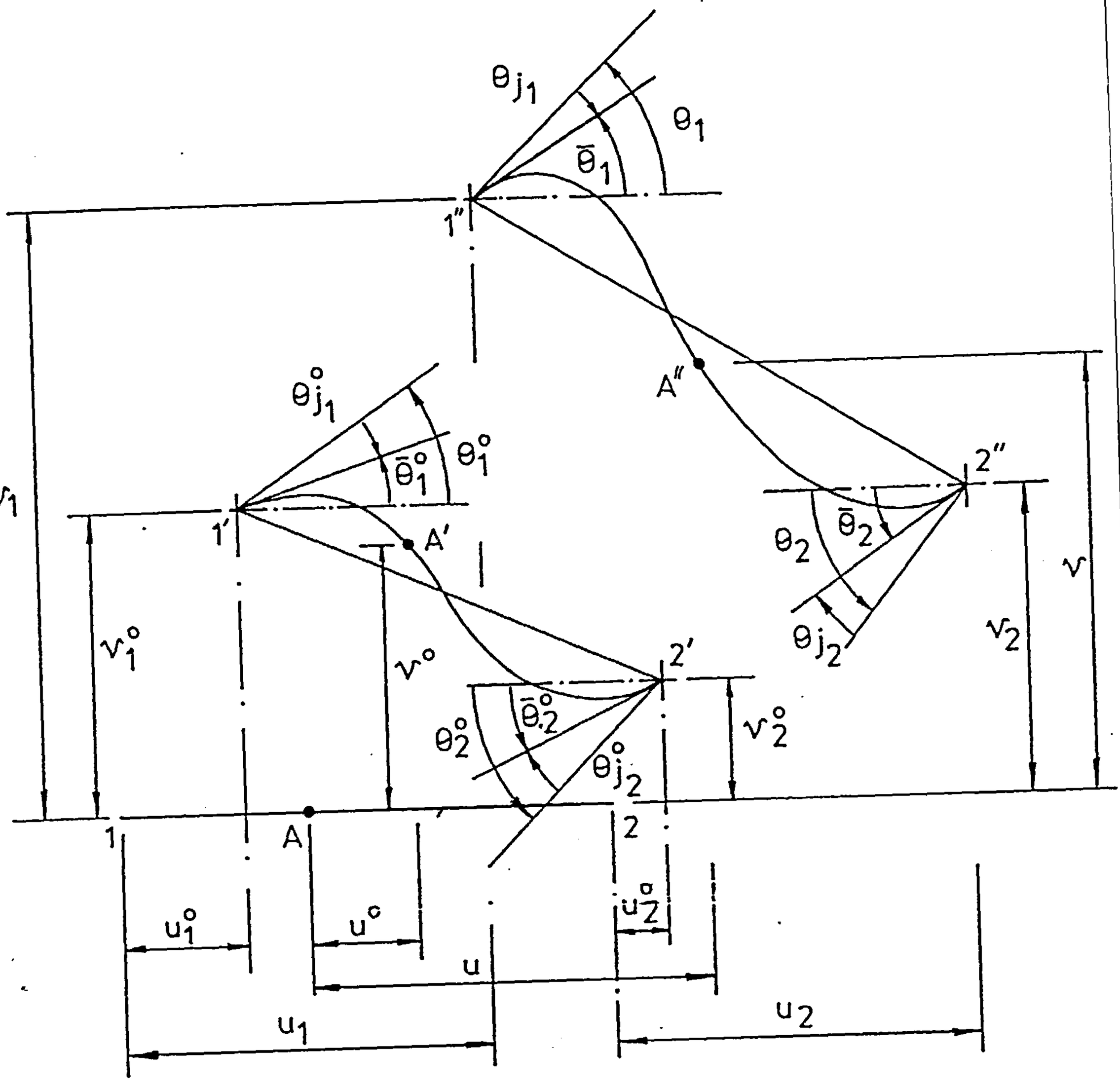

FIG. 3·1 A BEAM-COLUMN WITH SEMI RIGID JOINTS

$$\delta = \mathbf{A}\ \delta^{e} \tag{3.2-a}$$

in which

$$\delta = [u\ ,\ v]^{T} \tag{3.2-b}$$

$$\delta^{e} = [\ u_1\ v_1\ \theta_1\ u_2\ v_2\ \theta_2\ ]^{T} \tag{3.2-c}$$

and

$$A = \begin{bmatrix} N_1 & 0 & 0 & N_2 & 0 & 0 \\ 0 & N_3 & N_4 & 0 & N_5 & N_6 \end{bmatrix} \tag{3.2-d}$$

in which N_1 to N_6 are the shape functions that define the deflected shape of the element. The deflection modes defined by these functions are shown in Fig-3.2. Eqn-3.2 also applies to the deformed shape at the start of the load increment if the correct nodal deflections are used.

N_1 and N_2 are assumed to be linear in x, while N_3 to N_6 are assumed to be cubic polynomials of x. It is easy to confirm that N_1 and N_2 are given by

$$N_1 = 1 - r \tag{3.3-a}$$

and

$$N_2 = r \tag{3.3-b}$$

in which $r = \frac{x}{L}$ and L = element length.

To determine the expressions of N_3, N_4, N_5 and N_6 consider the shape functions of an element with rigid joints . Here the shape functions $\bar{N}_1$ to $\bar{N}_4$ represent the deflection modes of Fig-3.3 and are given by

$$\bar{N}_1 = 1 - 3r^2 + 2r^3 \tag{3.4-a}$$

$$\bar{N}_2 = L(\ r - 2r^2 + r^3) \tag{3.4-b}$$

$$\bar{N}_3 = 3r^2 - 2r^3 \tag{3.4-c}$$

and

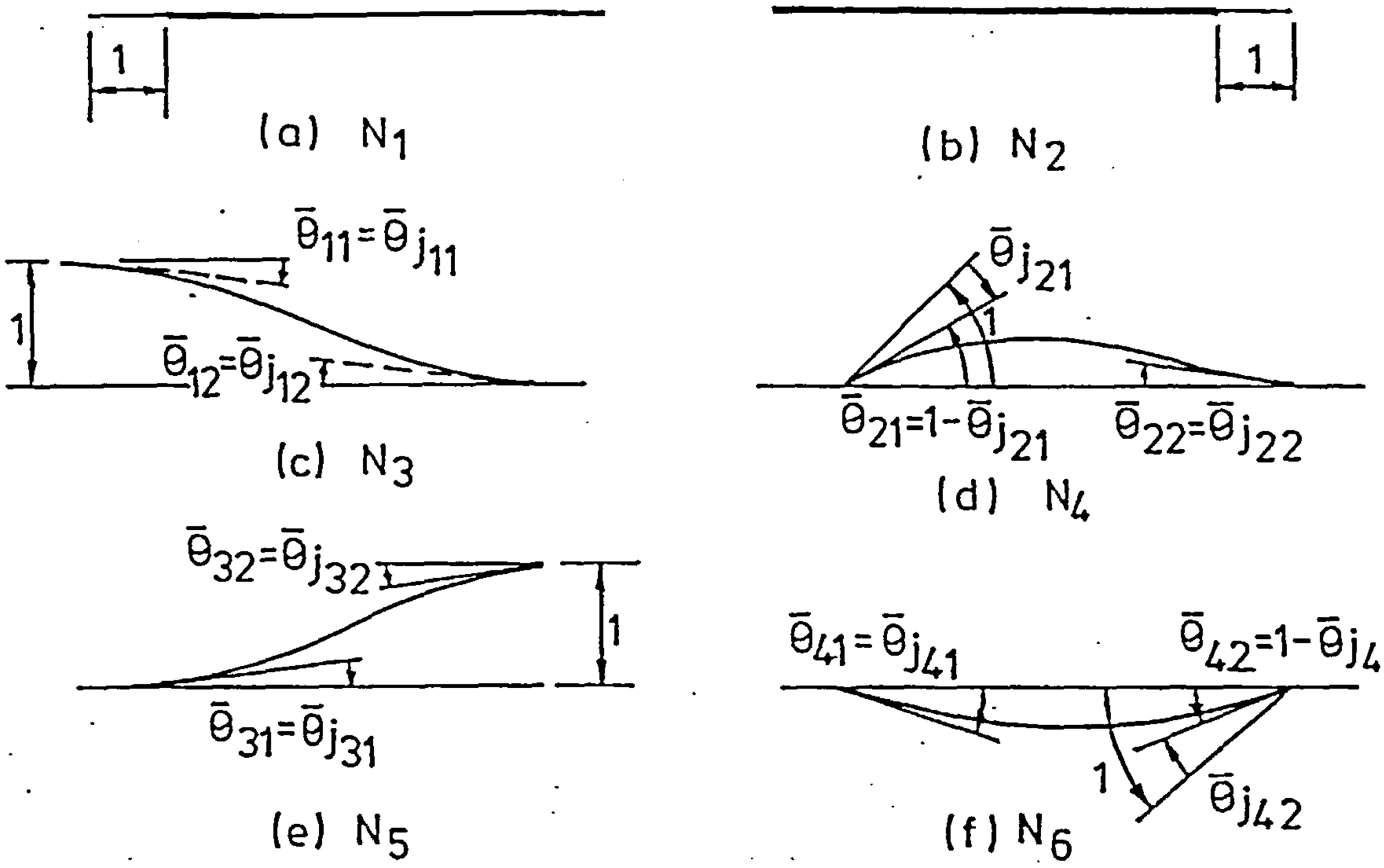

FIG.3·2 MODE SHAPES FOR AN ELEMENT WITH SEMI-RIGID JOINTS (UNIT DISPLACEMENTS)

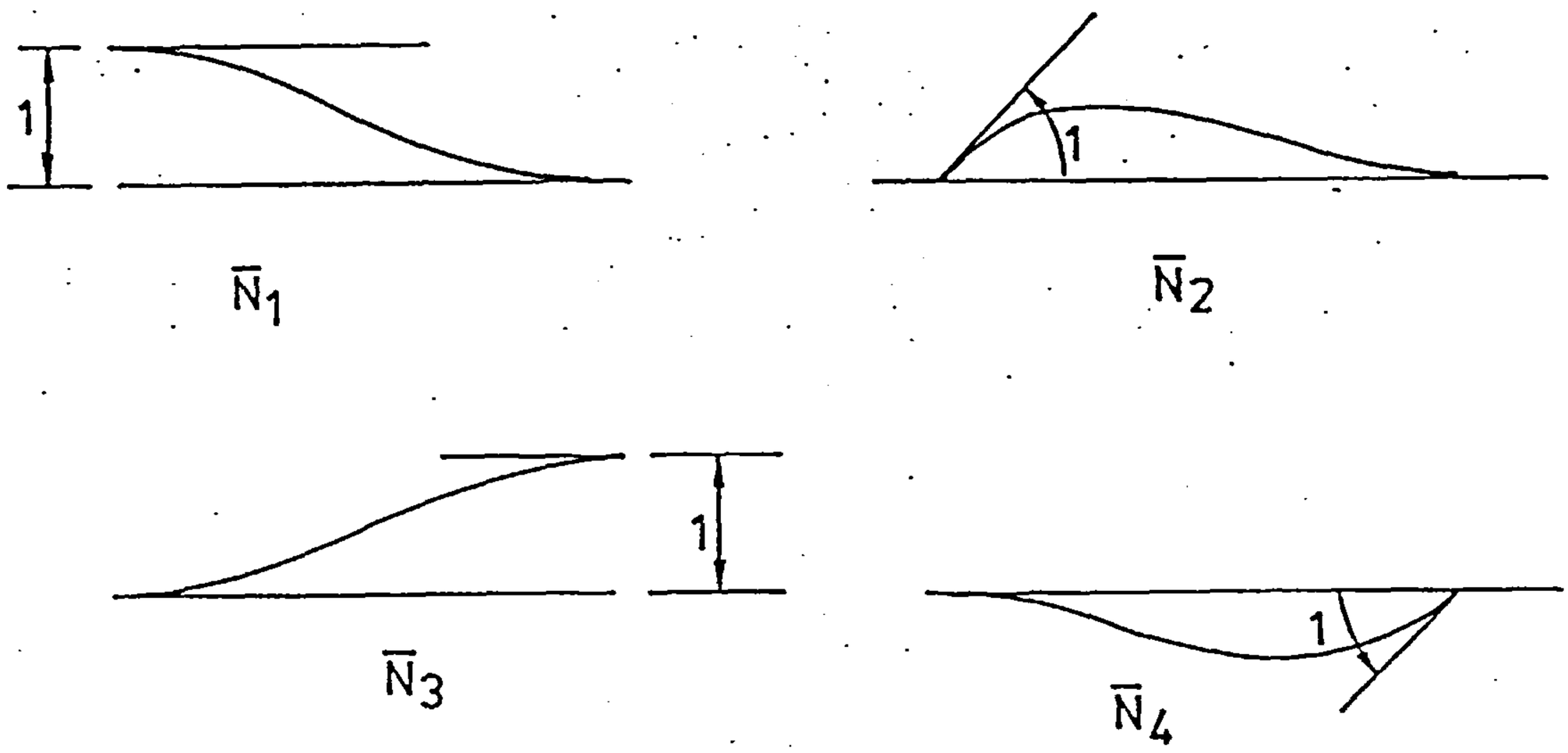

FIG. 3·3 MODE SHAPES FOR AN ELEMENT WITH RIGID JOINTS (UNIT DISPLACEMENTS)

$$\overline{N}_4 = L(-r^2 + r^3) \qquad (3.4\text{-d})$$

Careful consideration of the deflection modes of Fig-3.2c and Fig-3.3, reveals that the mode of Fig-3.2c may be represented by the function

$$N_3 = \overline{N}_1 - \overline{\theta}^1_{j_1} \overline{N}_2 - \overline{\theta}^1_{j_2} \overline{N}_4 \qquad (3.5)$$

Substituting for $\overline{N}_1$, $\overline{N}_2$ and $\overline{N}_4$ from eqns-3.4 into eqn-3.5

$$N_3 = 1 - \overline{\theta}^1_{j_1} Lr - (3- 2\overline{\theta}^1_{j_1} L - \overline{\theta}^1_{j_2} L)\, r^2 + (2- \overline{\theta}^1_{j_1} L - \overline{\theta}^1_{j_2} L)\, r^3 \qquad (3.6\text{-a})$$

Similarly it can be shown that

$$N_4 = L[(1- \overline{\theta}^2_{j_1})\, r - (2- 2\overline{\theta}^2_{j_1} - \overline{\theta}^2_{j_2})\, r^2 + (1- \overline{\theta}^2_{j_1} - \overline{\theta}^2_{j_2})\, r^3] \qquad (3.6\text{-b})$$

$$N_5 = \overline{\theta}^3_{j_1} L\, r + (3- 2\overline{\theta}^3_{j_1} L - \overline{\theta}^3_{j_2} L)\, r^2 - (2- \overline{\theta}^3_{j_1} L - \overline{\theta}^3_{j_2} L)\, r^3 \qquad (3.6\text{-c})$$

and

$$N_6 = L[-\overline{\theta}^4_{j_1}\, r - (1- 2\overline{\theta}^4_{j_1} - \overline{\theta}^4_{j_2})\, r^2 + (1- \overline{\theta}^4_{j_1} - \overline{\theta}^4_{j_2})\, r^3] \qquad (3.6\text{-d})$$

3.3- Strains and Stresses

It is well known that subject to the limitations of beam theory (but including large deflection effects) , the average strains at a cross section are related to the displacements at that section by the relation

$$\varepsilon = \left[-\left(\frac{du}{dx} + \frac{1}{2}\left(\frac{dv}{dx}\right)^2\right) \;,\; -\frac{d^2v}{dx^2} \right]^T \qquad (3.7)$$

This equation includes a non-linear term in the axial strain component.

Differentiating eqn-3.7 with respect to δ^e results in a relation between the incremental strain $d\varepsilon$ and incremental nodal displacements $d\delta^e$.

Since only the shape functions vary along the element length and referring to eqns.(3.2) and (3.7), $d\varepsilon$ is given by

$$d\varepsilon = -\left[\begin{bmatrix} \frac{dN_1}{dx} & 0 & 0 & \frac{dN_2}{dx} & 0 & 0 \\ & \frac{d^2N_3}{dx^2} & \frac{d^2N_4}{dx^2} & & \frac{d^2N_5}{dx^2} & \frac{d^2N_6}{dx^2} \\ 0 & & & 0 & & \end{bmatrix}\right.$$

$$\left. - \left(\frac{dv}{dx}\right) \begin{bmatrix} 0 & \frac{dN_3}{dx} & \frac{dN_4}{dx} & 0 & \frac{dN_5}{dx} & \frac{dN_6}{dx} \\ 0 & 0 & 0 & 0 & 0 & 0 \end{bmatrix}\right] d\delta^e \qquad (3.8)$$

or in short

$$d\varepsilon = \mathbf{B}\, d\delta^e \qquad (3.9)$$

where B is a strain-displacement matrix linear in δ . This matrix consists of a constant part and a linear one (with respect to δ) .

Hence we may write

$$\mathbf{B} = \mathbf{B}_o + \mathbf{B}_L \qquad (3.10)$$

where B_o is the constant strain-displacement matrix while B_L is the linear one.

Knowing the strains , the resultant stresses may be computed as

$$\sigma = D\ \varepsilon \qquad (3.11)$$

where

$$\sigma = [F \quad M]^T$$

in which F and M are the axial force and the bending moment at the section. In eqn-3.11, **D** is the elasticity matrix given by

$$D = \begin{bmatrix} EA & 0 \\ 0 & EI \end{bmatrix}$$

which, although at present assumed constant, would depend non-linearly on the current configuration of the structure as will be seen later in this chapter.

3.4- Stiffness Matrix

Following the procedure given by Zienkiewicz (23), the derivation of the tangential stiffness matrix follows from the application of the virtual work principles. Consider an element with two semi-rigid joints in equilibrium. Let p^e be the vector of applied loads at the element nodes and δ^e be the nodal displacement vector. If virtual displacements $d\delta^e$ are applied then W_{ext}, the work done by the external forces p^e is

$$W_{ext} = d\delta^{eT} \cdot p^e \qquad (3.12)$$

where

$$p^e = [F_1 \quad V_1 \quad M_1 \quad F_2 \quad V_2 \quad M_2]^T$$

The internal work, W_{int} on the other hand, is composed of two parts.

The first part is W^e_{int} the work done by the internal stresses through the virtual strains which result from the virtual displacements. This work may be expressed as

$$W^e_{int} = \int_0^L d\varepsilon^T \, \sigma \, dx = \int_0^L d\delta^T . B^T . \sigma \, dx \qquad (3.13)$$

The other part W^j_{int} the work done by the moments M_{j_1} and M_{j_2} in the semi-rigid joints through the rotations $d\theta_{j_1}$ and $d\theta_{j_2}$. This is given by

$$W^j_{int} = d\theta_{j_1} \, M_{j_1} + d\theta_{j_2} \, M_{j_2} \qquad (3.14)$$

Now if it is assumed that the moment in a joint is linearly related to its rotation, then

$$M_j = C_j \theta_j \qquad (3.15)$$

Referring to Fig.3-1, it can be observed that

$$\theta_{j_1} = -(\theta_1 - \bar{\theta}_1)$$

Noting that positive rotations are anticlockwise as indicated in Fig-3.2, it can be seen that the minus sign indicates that the joint rotation is clockwise (i.e. -ve). From eqns-3.2 (recognizing that $\bar{\theta}_1 = \frac{dv}{dx}$ for x=0)

$$\theta_{j_1} = -\begin{bmatrix} 0 & 0 & 1 & 0 & 0 & 0 \end{bmatrix} \delta^e + \begin{bmatrix} 0 & \frac{dN_3}{dx} & \frac{dN_4}{dx} & 0 & \frac{dN_5}{dx} & \frac{dN_6}{dx} \end{bmatrix} \delta^e$$

evaluated at x=0. Hence

$$\theta_{j_1} = N_{j_1} \, \delta^e \qquad (3.16)$$

in which

$$N_{j_1} = \begin{bmatrix} 0 & \frac{dN_3}{dx} & -1 + \frac{dN_4}{dx} & 0 & \frac{dN_5}{dx} & \frac{dN_6}{dx} \end{bmatrix}$$

similarly,

$$\theta_{j_2} = N_{j_2}\, \delta^e \qquad (3.17)$$

in which

$$N_{j_2} = \begin{bmatrix} 0 & \frac{dN_3}{dx} & \frac{dN_4}{dx} & 0 & \frac{dN_5}{dx} & -1 + \frac{dN_6}{dx} \end{bmatrix}$$

The derivatives $\frac{dN_3}{dx}$, $\frac{dN_4}{dx}$, $\frac{dN_5}{dx}$ and $\frac{dN_6}{dx}$ in the expressions for N_{j_1} and N_{j_2} in eqns-3.16 and 3.17 are evaluated at x=0 and x=L respectively. Substituting for θ_{j_1} and θ_{j_2} from eqns-3.16 and 3.17 and using eqn-3.15, eqn-3.14 may be written as

$$W^j_{int} = d\delta^{e^T} (N_{j_1}{}^T C_{j_1} N_{j_1} + N_{j_2}{}^T C_{j_2} N_{j_2}) \delta^e \qquad (3.18)$$

The total internal work done is the sum of the contributions from eqns-3.13 and 3.18 . This work must equal the external work done which is given by eqn-3.12. Hence,

$$d\delta^{e^T} p^e = d\delta^{e^T} [\int_0^L B^T \sigma \, dx + \left[N_{j_1}{}^T C_{j_1} N_{j_1} + N_{j_2}{}^T C_{j_2} N_{j_2} \right] \delta^e] \qquad (3.19)$$

Eqn-3.19 holds for any virtual displacement. Consequently, the term $d\delta^{e^T}$ may be cancelled out. Furthermore, eqn-3.19 may be rewritten as

$$\Psi(\delta) = [\int_0^L B^T \sigma \, dx + [N_{j_1}{}^T C_{j_1} N_{j_1} + N_{j_2}{}^T C_{j_2} N_{j_2}] \delta^e] - p^e \qquad (3.20)$$

in which $\Psi(\delta)$ represents the sum of external and internal forces. This quantity as seen from eqn-3.20 is a function of the nodal displacements. The first variation of Ψ with respect to δ^e then represents the tangential stiffness matrix (23). Hence

$$\frac{d\Psi}{d\delta^e} = \mathbf{K}_T = \int_0^L \mathbf{B}^T \frac{d\sigma}{d\delta^e}\, dx + \int_0^L \frac{d\mathbf{B}^T}{d\delta^e}\, \sigma\, dx$$

$$+ \left[\mathbb{N}_{j_1}{}^T C_{j_1} N_{j_1} + \mathbb{N}_{j_2}{}^T C_{j_2} N_{j_2} \right] \qquad (3.21)$$

From eqns-3.9 and 3.11, we have

$$\frac{d\sigma}{d\delta^e} = \mathbf{D}\, \frac{d\varepsilon}{d\delta^e} = \mathbb{D}\, \mathbf{B}$$

Hence, eqn-3.21, may be written as

$$K_T = \int_0^L B^T\, D\, B\, dx + \int_0^L \frac{dB^T}{d\delta^e} \sigma\, dx + \left[\mathbb{N}_{j_1}{}^T C_{j_1} N_{j_1} + \mathbb{N}_{j_2}{}^T C_{j_2} N_{j_2} \right]$$

or,

$$k_T = k_E + k_G + k_L \qquad (3.22)$$

where (using eqn-3.10 for the expression of B)

$$k_E = \int_0^L B_o{}^T\, D\, B_o\, dx + [\mathbb{N}_{j_1}{}^T C_{j_1} N_{j_1}$$

$$+ \mathbb{N}_{j_2}{}^T C_{j_2} N_{j_2}] \qquad (3.23a)$$

$$k_L = \int_0^L [\, B_o{}^T D B_L + B_L{}^T D B_o + B_L{}^T D B_L \,]\, dx \qquad (3.23b)$$

and

$$k_G = \int_0^L \frac{dB_L}{d\delta^e} \sigma \, dx \qquad (3.23c)$$

Returning to eqn-3.8, it is possible to separate axial strains from curvature and rewrite eqn-3.10 as

$$B = B_o + B_L = \begin{bmatrix} B_o^a & 0 \\ 0 & B_o^b \end{bmatrix} + \begin{bmatrix} 0 & B_L^b \\ 0 & 0 \end{bmatrix} \qquad (3.24)$$

where the superscripts a and b refer to axial and bending action respectively.

Using eqns-3.23 and 3.24, the various stiffness matrices of eqn-3.23 may be rewritten as

$$k_E = \int_0^L \begin{bmatrix} B_o^{a^T} EA B_o^a & 0 \\ 0 & B_o^{b^T} EI B_o^b \end{bmatrix} dx +$$

$$[M_{j_1}{}^T C_{j_1} N_{j_1} + M_{j_2}{}^T C_{j_2} N_{j_2}] \qquad (3.25a)$$

$$k_L = \int_0^L \begin{bmatrix} 0 & B_o^{a^T} EA B_L^b \\ B_L^{b^T} EA B_o^a & B_L^{b^T} EA B_L^b \end{bmatrix} dx \qquad (3.25b)$$

and

$$k_G = \int_0^L \begin{bmatrix} 0 \\ P \dfrac{dB_L^b}{d\delta^e} \end{bmatrix} dx \qquad (3.25c)$$

Now, the non-linear component of the axial strain (eqn-3.7) is given by

$$\varepsilon_L = -\frac{1}{2}\left(\frac{dv}{dx}\right)^2$$

Then, taking derivatives with respect to δ^b

$$d\varepsilon_L = -\left(\frac{dv}{dx}\right) d\left(\frac{dv}{dx}\right)$$

$$= -\left(\frac{dv}{dx}\right) G \; d\delta^b \qquad (3.26)$$

where G is given by

$$G = \left[\frac{dN_3}{dx} \quad \frac{dN_4}{dx} \quad \frac{dN_5}{dx} \quad \frac{dN_6}{dx}\right]$$

Hence since eqn-3.26 is similar in form to eqn-3.8

$$B_L^b = -\left(\frac{dv}{dx}\right) G \qquad (3.27)$$

which may be used in the calculations of K_L in eqn-3.25b. Next, the variation of B_L^b with respect to δ^e is required as it appears in the expression for k_G (eqn-3.25c). Taking variation of eqn-3.27 with respect to δ^e

$$dB_L^b = -\bar{G}\; d\delta^e\; G$$

where $\bar{G}$ is a 1x6 row vector given by

$$\bar{G} = [\, 0 \quad G \,]$$

Hence,

$$dB_L^{b^T} = - G^T d\delta^{e^T} \overline{G}^T$$

$$= - G^T \overline{G}\, d\delta^e$$

Equation 3-25c then gives

$$k_G = - \int_0^L \begin{bmatrix} 0 & \\ & \\ & G^T P G \end{bmatrix} dx = - \begin{bmatrix} 0 & 0 \\ & \int_0^L G^T P G \, dx \\ 0 & \end{bmatrix} \qquad (3.28)$$

where P is the axial force in the element assumed positive if compressive. The row vector $\overline{G}$ in the first bracket in eqn.3.28 is replaced by the row vector **G** since the latter is only 1x4.

The stiffness matrices as defined by eqns-3.25a, 3.25b and 3.28 may be computed using numerical integration .The only remaining obstacle is the determination of rotations $\overline{\theta}^m_{j_1}$ and $\theta^m_{j_2}$ for m=1,2,3,4 since they appear in the expressions for the shape functions of eqn-3.6. Employing the well known slope deflection equations in conjunction with the deflection mode of Fig-3.2c , for instance, the moments at nodes 1 and 2 may be expressed as

$$M_1 = \frac{2EI}{L}(-2\overline{\theta}^1_{j_1} - \overline{\theta}^1_{j_2} + \frac{3}{L}) = C_{j_1}\overline{\theta}^1_{j_1}$$

and

$$M_2 = \frac{2EI}{L}(-\overline{\theta}^1_{j_1} - 2\overline{\theta}^1_{j_2} + \frac{3}{L}) = C_{j_2}\overline{\theta}^1_{j_2}$$

Rearranging these two equations and solving for $\overline{\theta}^1_{j_1}$ and $\overline{\theta}^1_{j_2}$ the following may be obtained

$$\overline{\theta}^1_{j_1} = \frac{A_1 B_1}{H} \quad , \quad \overline{\theta}^1_{j_2} = \frac{A_1 B_2}{H} \qquad (3.29)$$

Similarly

$$\bar{\theta}^2_{j_1} = \frac{A_2 B_3}{H} \quad , \quad \bar{\theta}^2_{j_2} = \frac{\frac{2EI_c}{L} j_1}{H} \tag{3.30}$$

$$\bar{\theta}^3_{j_1} = \bar{\theta}^1_{j_1} \quad , \quad \bar{\theta}^3_{j_2} = \bar{\theta}^1_{j_2} \tag{3.31}$$

$$\bar{\theta}^4_{j_1} = \frac{\frac{2EI_c}{L} j_2}{H} \quad , \quad \bar{\theta}^4_{j_2} = \frac{A_2 B_4}{H} \tag{3.32}$$

in which

$$A_1 = \frac{6EI}{L^2} \quad , \quad A_2 = \frac{4EI}{L}$$

$$B_1 = \frac{2EI}{L} + C_{j_2} \quad , \quad B_2 = \frac{2EI}{L} + C_{j_1}$$

$$B_3 = \frac{3EI}{L} + C_{j_2} \quad , \quad B_4 = \frac{3EI}{L} + C_{j_1}$$

$$H = \frac{1}{2} A_1 A_2 + A_2 (C_{j_1} + C_{j_2}) + C_{j_1} C_{j_2}$$

If any of the joints at the element ends is rigid, the corresponding stiffness, C_j, is equal to ∞ reducing the rotation to zero as may be seen from eqns.3.29-3.32.

3.5- Connection Modelling

3.5.1- Numerical Representation of Moment-Rotation Curves:-

Various approximations for the M-Φ curves for joints have been proposed. A linear representation (Fig-3.4a) corresponding to the initial slope is the simplest although it ignores the loss of stiffness observed at higher rotation levels. A better approximation is a bi-linear relationship (Fig-3.4b) in which the initial slope is replaced with a shallower line at a certain level of rotation. Tri-linear (Fig-3.4c) and multi-linear (Fig-3.4d) representation may also be used.

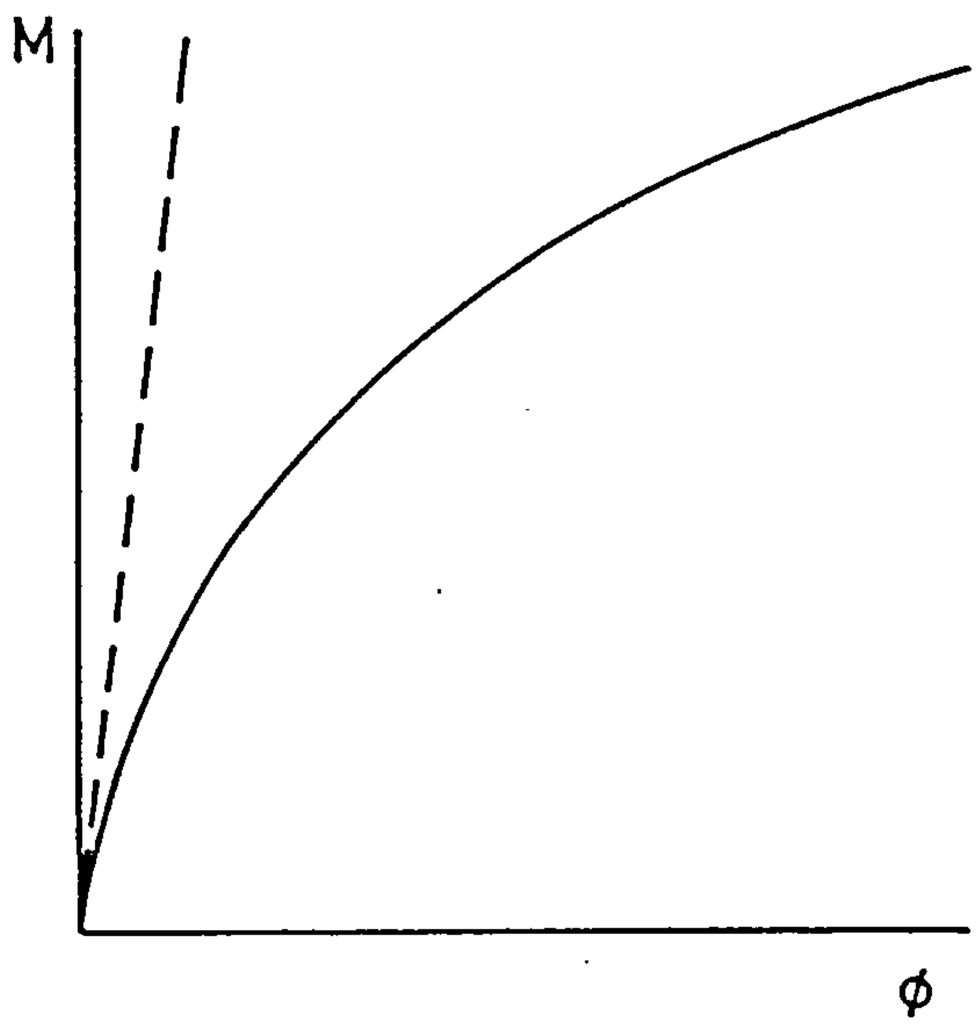

(a) Linear

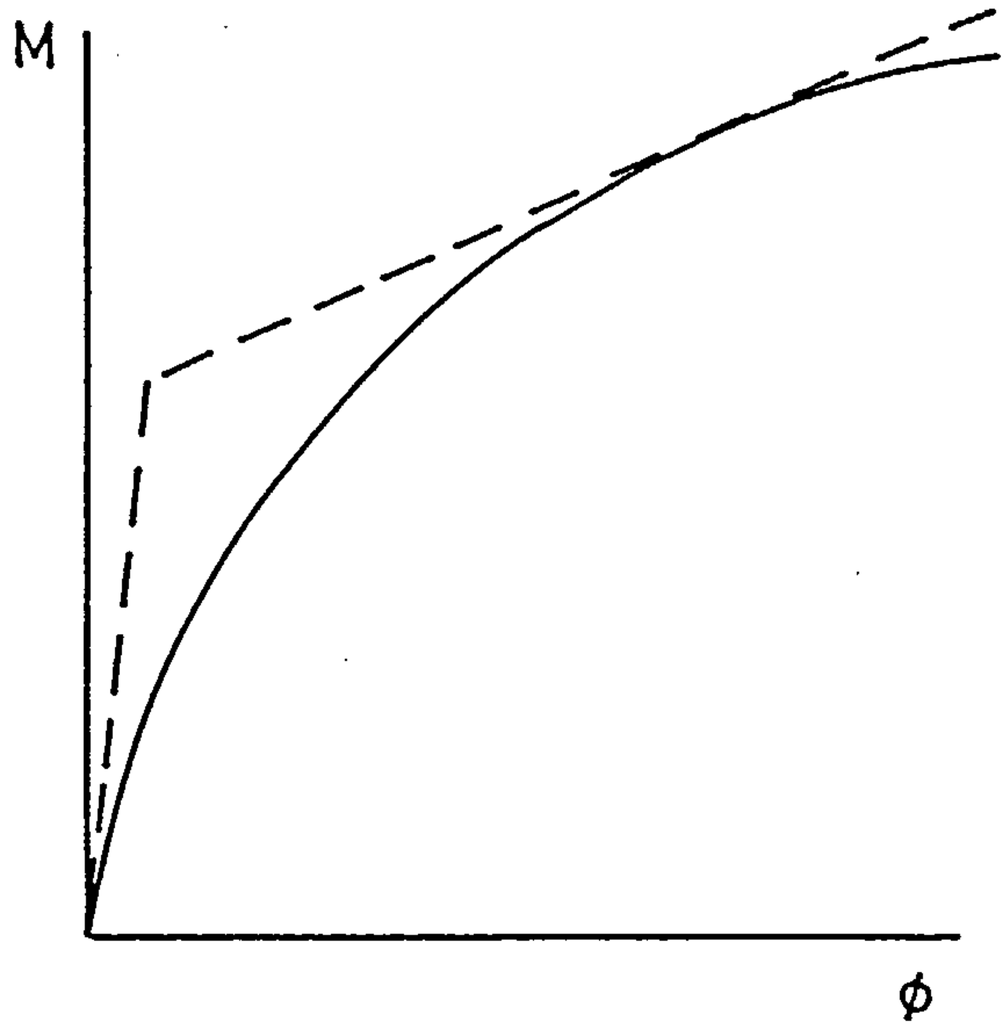

(b) Bi – linear

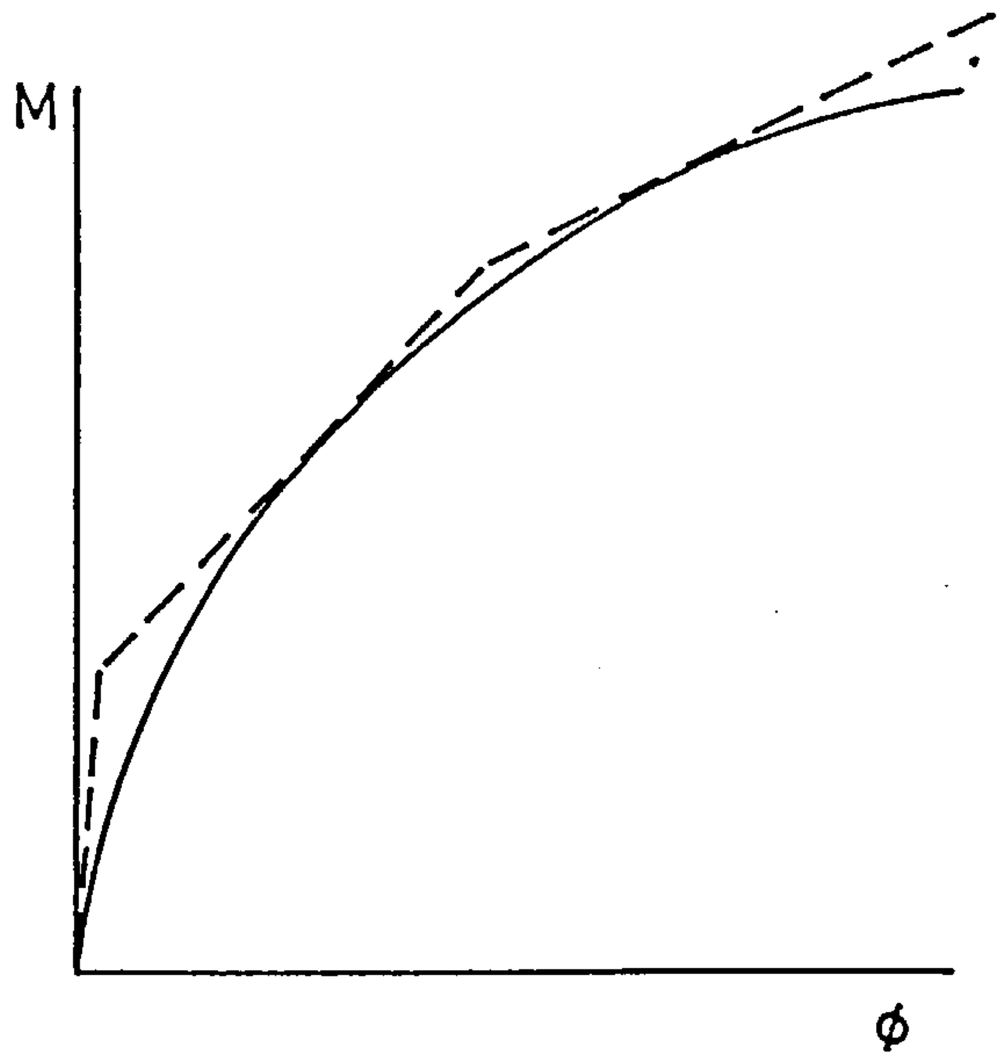

(c) Tri – linear

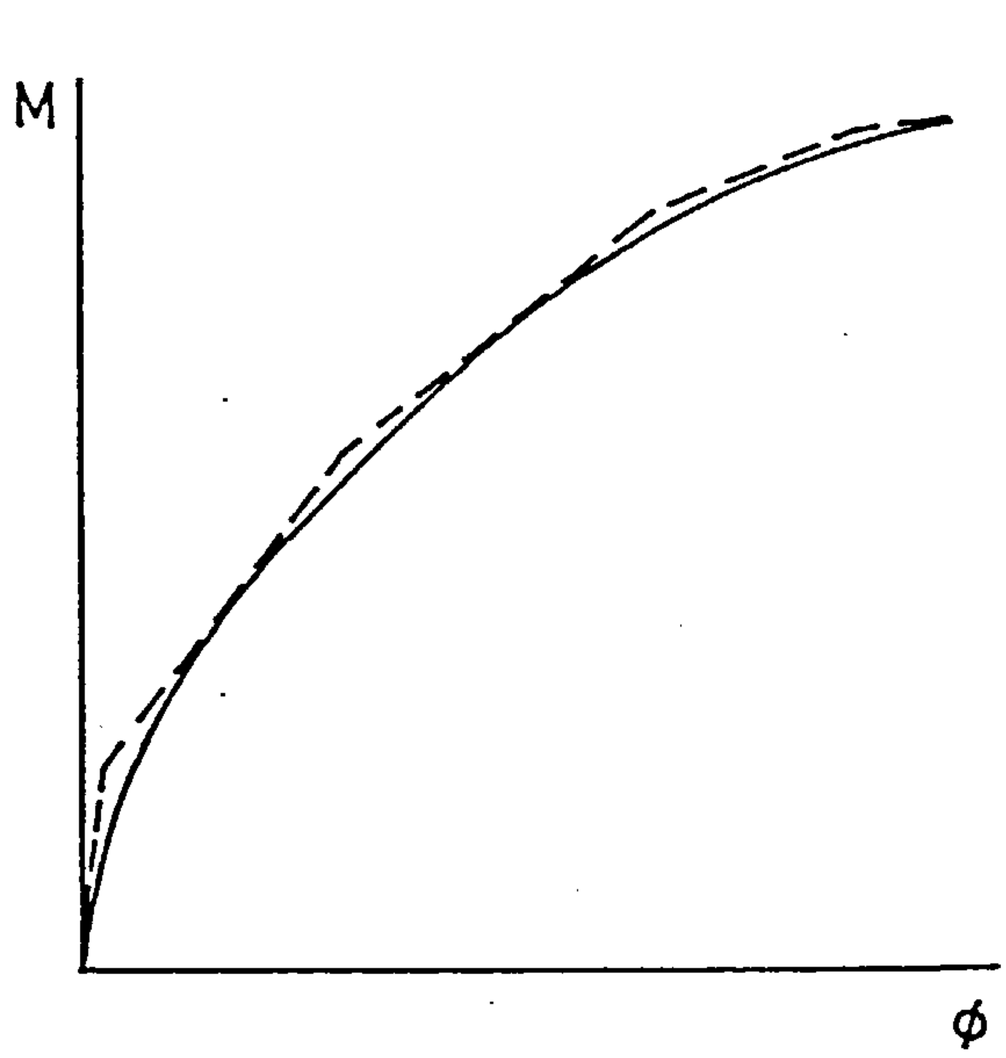

(d) Multi – linear

FIG. 3·4 DIFFERENT TYPES OF M – ϕ REPRESENTATION

Razzaq (14), Sugimoto and Chen (15) and Vinnakota (17) have employed some of these approaches to analyse single restrained columns, whilst Zandonini and Poggi (37) have used multi-linear curves for the analysis of complete frames.

In order to closely represent the M-Φ curves, good quality approximations are needed. Possible curve fitting techniques include the use of either polynomial or B-spline curves. In the former the M-Φ data is represented by the single polynomial

$$\Phi = a_0 + a_1.M + a_2.M^2 + \cdots + a_n.M^n$$

The coefficients a_n are found by minimizing the error in M using least square methods. Jones et al (5) pointed out that although polynomials may give a close approximation to the moments (or rotations), they may be very poor in approximating the slope of the curve especially at higher values of rotation.

A cubic B-spline (54) is uniquely represented in the form

$$\phi(M) = \sum_{j=0}^{3} \alpha_j M^j + \sum_{j=1}^{h} \beta_j (\langle M-k \rangle)^3$$

in which

h = number of knots that divide the entire range of the function domain. Knots k are suitably chosen by the user.

$\langle M-k \rangle$ = M-k for (M-k) > 0

= 0 for (M-k) < 0

and α_j and β_j are coefficients determined by least square methods.

Fig-3.5 shows a comparison between B-spline and polynomial fitting techniques. Clearly, the B-spline approximation is superior. It has therefore been adopted in the present study.

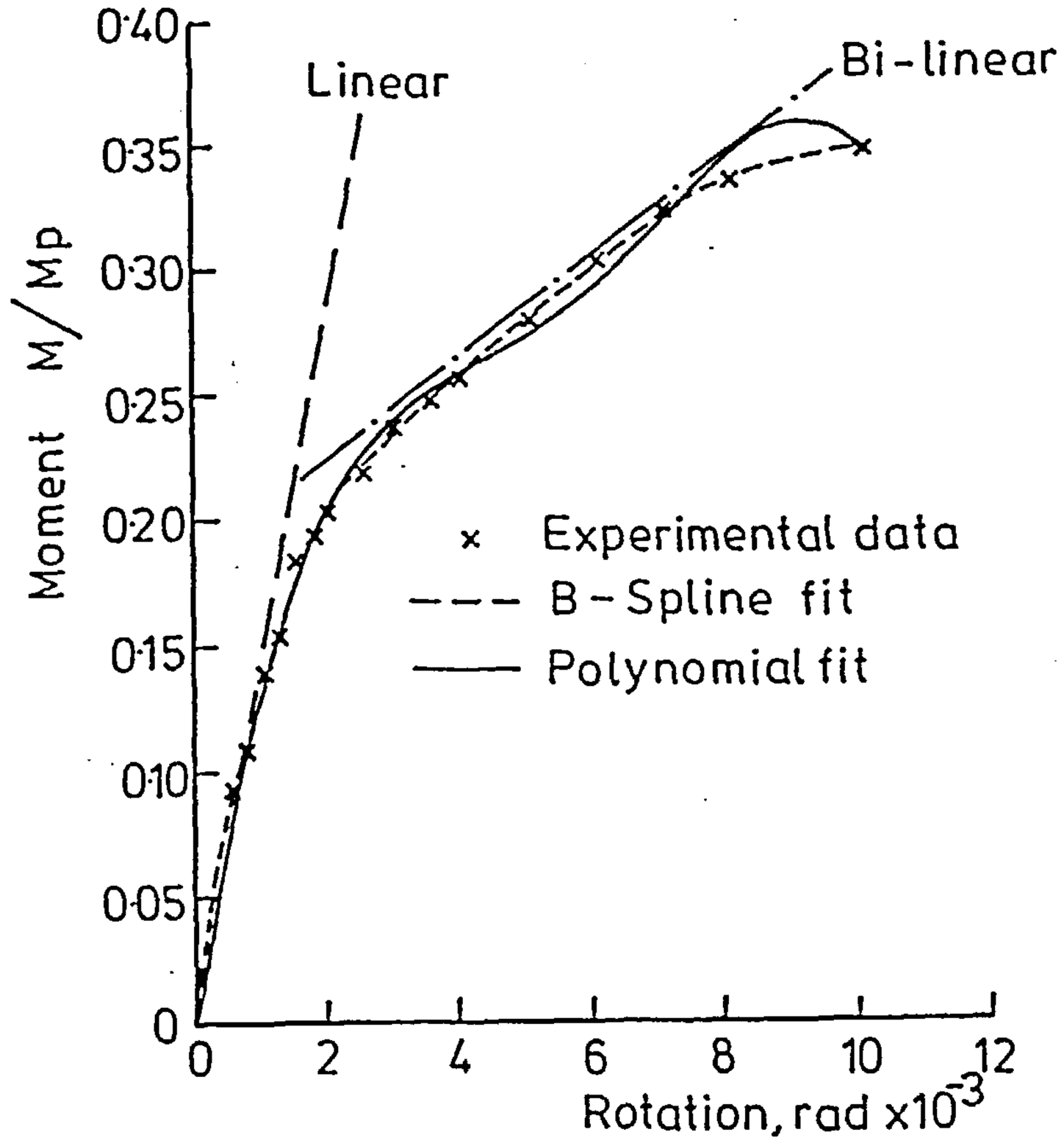

FIG. 3·5 COMPARISON OF MOMENT-ROTATION IDEALISATION

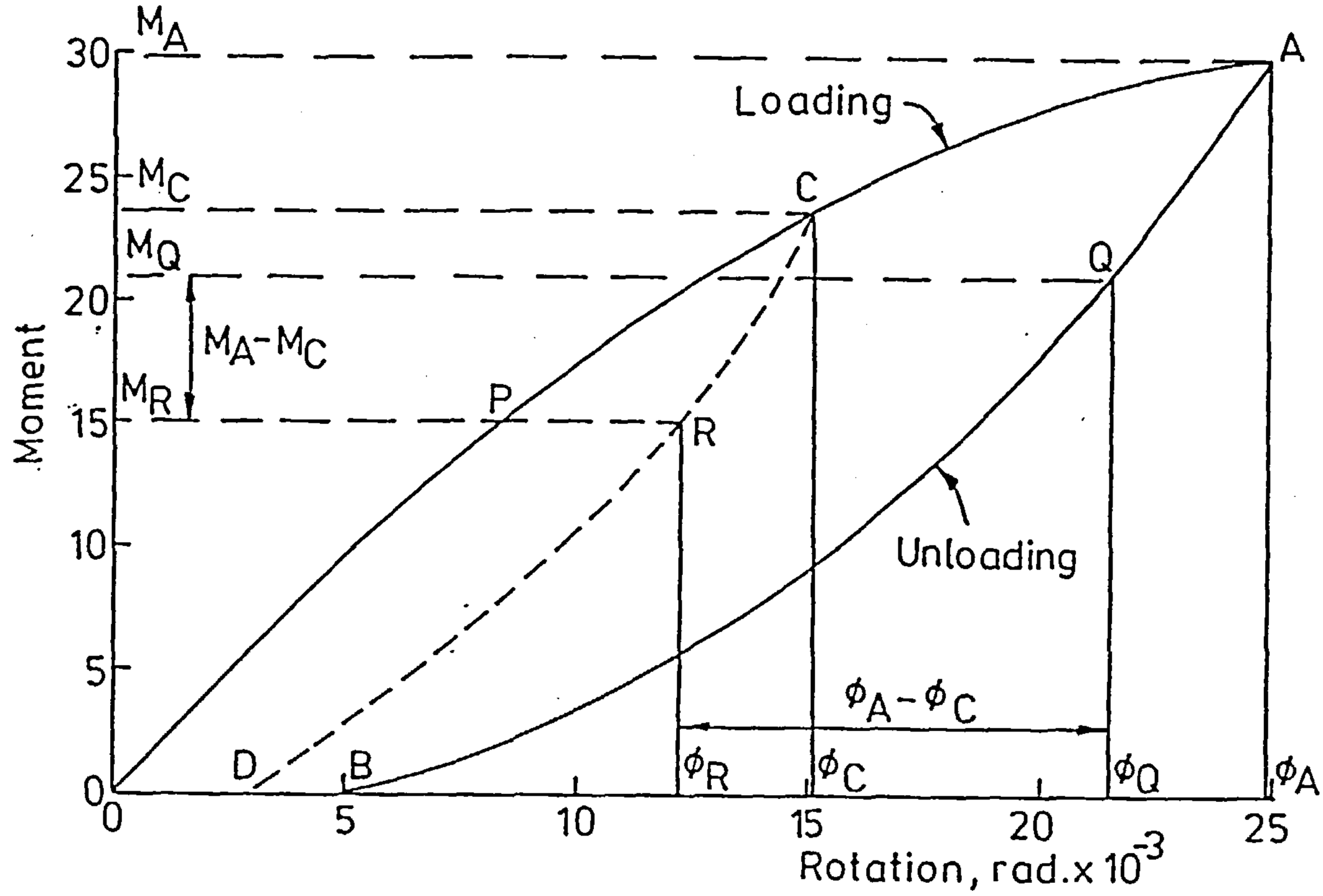

FIG. 3·6 TYPICAL M−φ RELATIONSHIP INCLUDING UNLOADING

3.5.2- Joint behaviour in unloading and reloading conditions:-

It is well known that connections exhibit different behaviour when loading and unloading (52). Fig-3.6 shows typical loading and unloading M-Φ curves based on results taken from reference 52 and elsewhere (50,51). The connection is loaded up to a moment M_a along the path OPA. The connection is then unloaded and follows path AQB. When operating in a structure, the connection may or may not reach point A. In fact, generally, it may be assumed that the connection follows the path OPCRD. The path CRD may be constructed from the path AQB by simply moving curve AQB so that points A and Q coincide with points C and R. In other words, there is a one to one relation between the general points R and Q. It is easy to demonstrate from Fig-3.6 that the difference between moments at points Q and R is equal to M_a-M_c while the difference in rotation is $\theta_a-\theta_c$. Point C at which unloading starts may be detected by a decrease in the moment (or the rotation).

In the absence of sufficient M-Φ data for the unloading and reloading conditions on which the above behaviour may be based, the portion AQB and consequently CRD has been assumed to be a straight line. The joint has therefore been assumed to behave linearly when unloading. If the joint is reloaded, it is assumed that it would follow the linear path DRC after which it follows the loading path CA until any further unloading condition occurs.

3.5.3- Offset of connection

In frame analysis, the various members of the frame are normally represented by their centre lines. This means that the member properties are assumed to be concentrated along these lines. Consequently, any joint that connects two or more members is assumed to

occupy no volume as indicated in Fig-3.7b, which may therefore be regarded as the analytical model for the beam and column of Fig-3.7a. Such a representation is acceptable only if the column is bent about its minor axis i.e. the connection is made to the column web, since connection to the column flanges will involve a significant offset of the connection from the column centre line. A suitable model for this case is shown in Fig-3.7c. This comprises a normal beam column element with a semi-rigid joint, together with a stiff portion with a length of D/2 where D is the depth of the column section. The panel between the column's centre line and the column flange is assumed to have infinite flexural and axial rigidities since the depth is very large. Node B is internal to this model and hence it could be condensed out (25). Consequently the analysis will not yield the deformations at node B which are important in calculating the internal forces in beam AB. Since the portion BC is of a large stiffness, it will only undergo rigid body motion and hence the deformations at node B can be easily obtained by simple transformation. Having condensed out node B, the analysis procedure continues in the usual manner since the model is reduced to a beam-column with six degrees of freedom.

The effect of the actual position of the connection was investigated by analysing the subassemblage of Fig-3.8 in which the column was bent about its major axis. A beam load of 100 KN was applied initially and then held constant while applying an axial load P up to failure. Both fully rigid and very flexible web cleat connections were used for the comparison.

Fig.3.9 shows the total force in the column plotted against the central deflection. It is clear that for the rigid connection the inclusion of the effect of the actual position of the connection is of

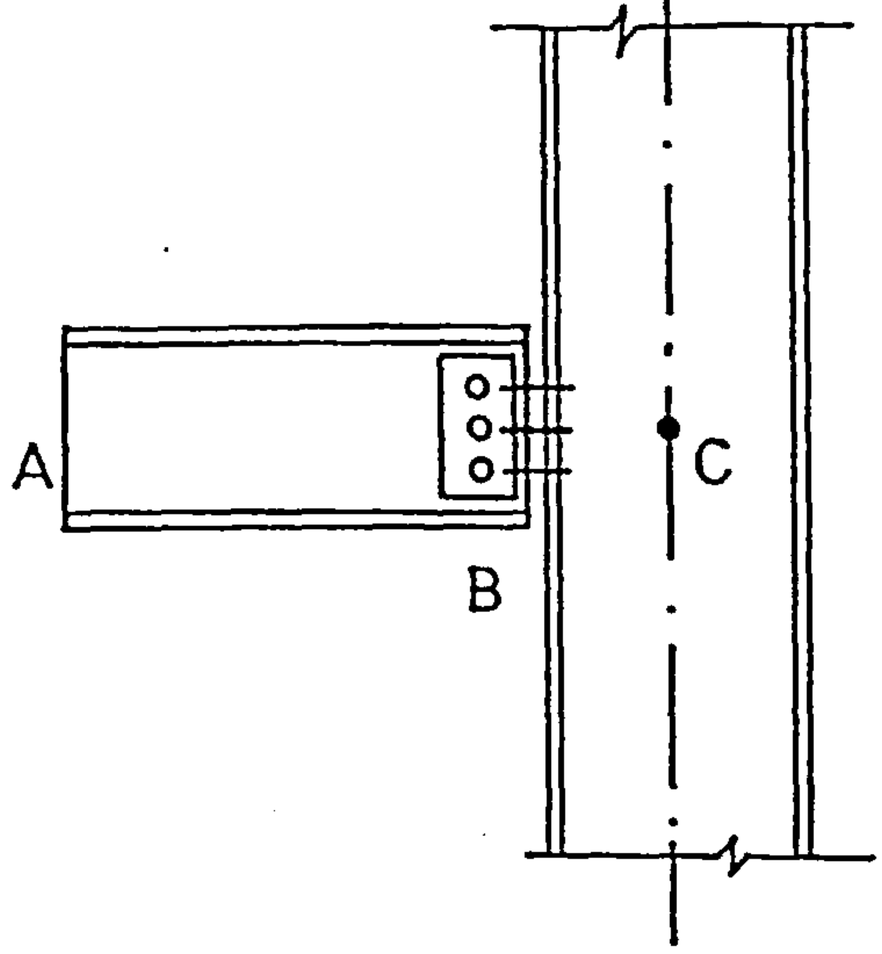

(a) Actual joint

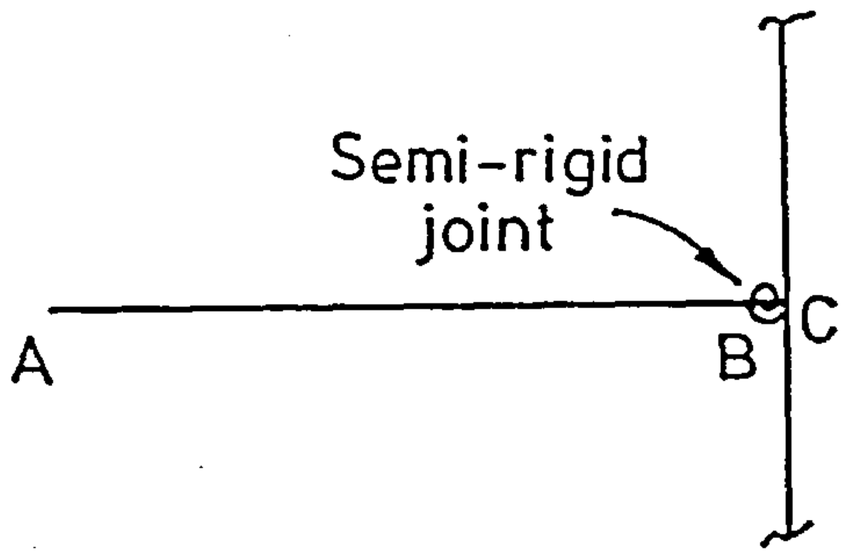

(b) Model neglecting joint offset

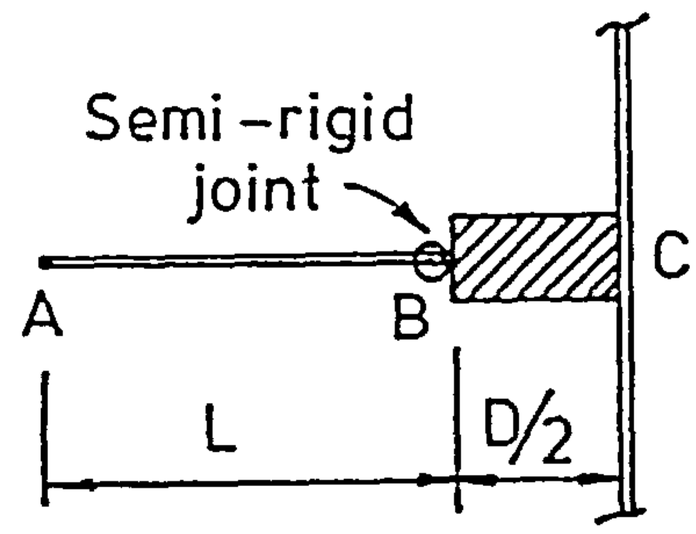

(c) Model including joint offset

FIG. 3·7 IDEALISATION OF PRACTICAL CONNECTIONS

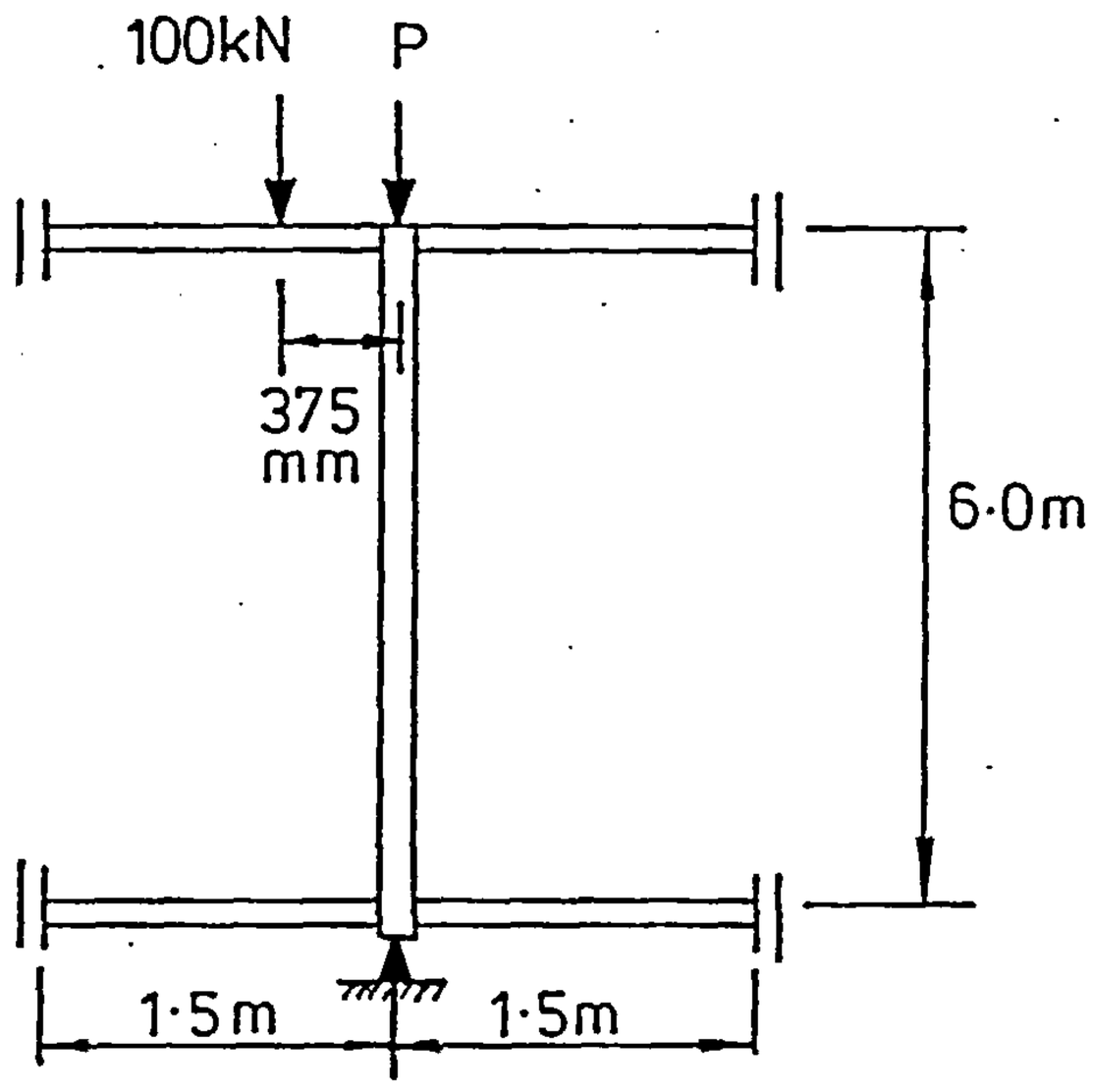

FIG. 3·8 SUBASSEMBLAGE ANALYSED FOR INFLUENCE OF JOINT OFFSET

little significance. In the case of web cleat connections, however, the force-deflection paths are quite different, although the failure loads are practically the same. Fig-3.10 shows the variation of the moments in the left beam, right beam and the column at the top joint of Fig-3.8 for the case of web cleat connections. It can be seen that the rigid segments have a considerable effect on the distribution of moments at the top joint.

3.6- Section Properties:-

3.6.1- Evaluation of Section Properties for a General Elastic Section:-

One of the most important steps in a nonlinear analysis is the determination of section properties characterized in a two dimensional frame analysis by the axial and flexural rigidities EA and EI. As mentioned in sec-3.3, the elements in the structure are assumed to be prismatic. If any element ,however, behaves inelastically, this assumption is not correct since E is not constant which causes EA and EI to vary along the element. Average axial and bending rigidities may be used ,hence restoring the validity of this assumption. In the present procedure, the quantities EA and EI are calculated at each node of every element and average values are then used in the analysis.

The axial and flexural rigidities with respect to an axis x-x in the general section shown in Fig-3.11 are given by the following relations

$$EA = \int_A E_{eff}\, dA \qquad (3.36a)$$

and

$$EI = \int_A E_{eff}\, y^2\, dA \qquad (3.36b)$$

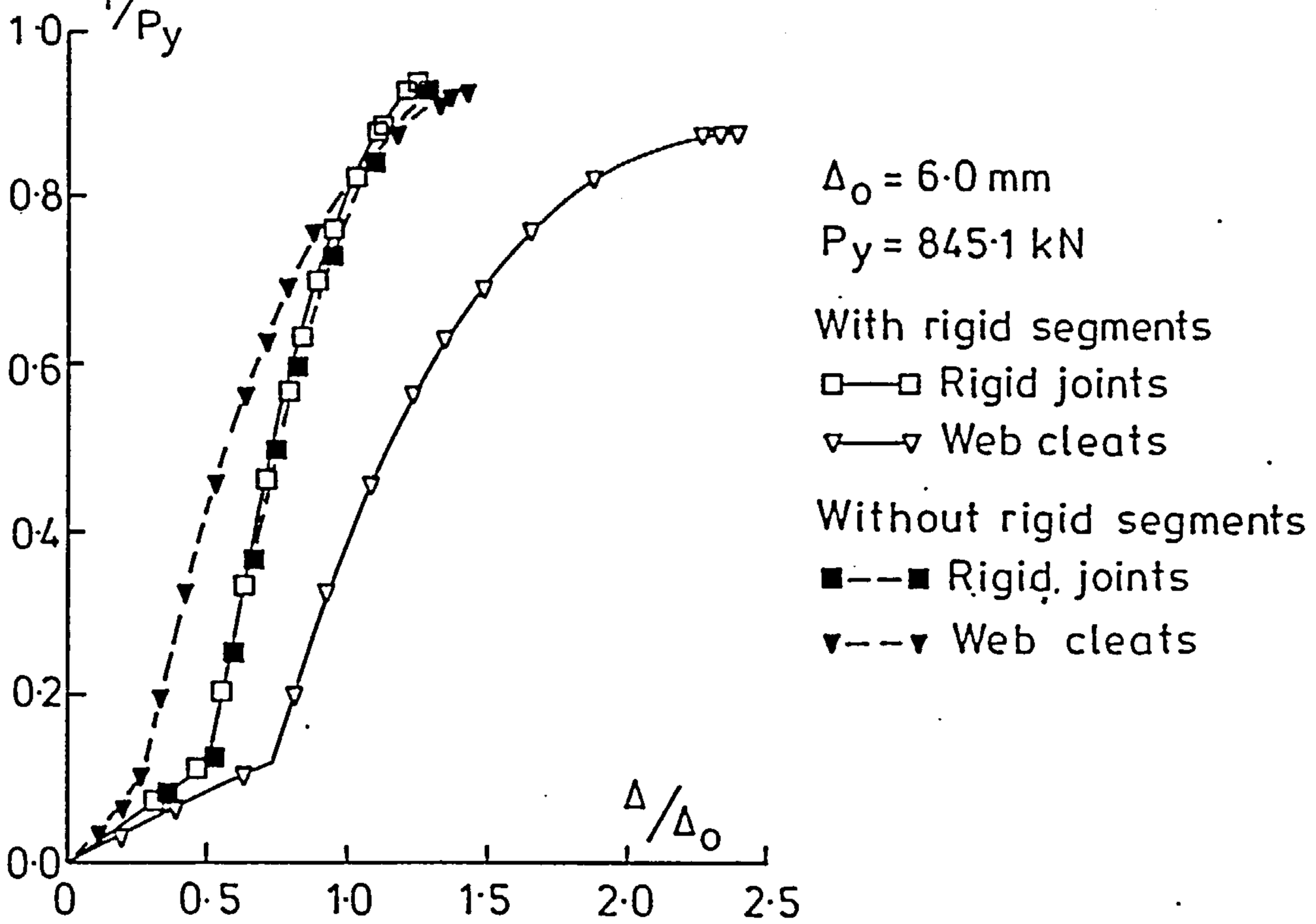

FIG. 3·9 LOAD-DEFLECTION CURVES FOR THE SUBASSEMBLAGE OF FIG. 3·8

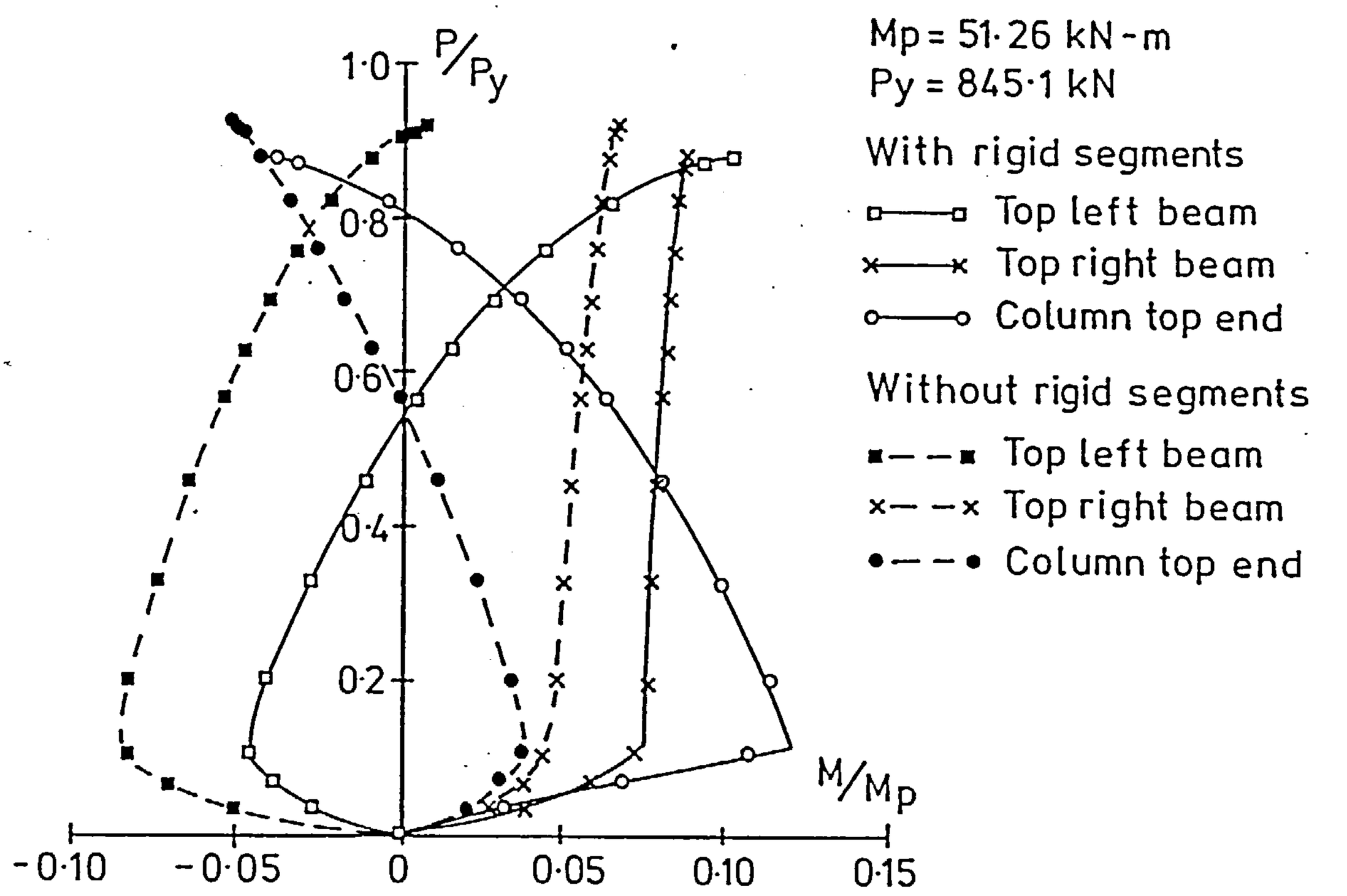

FIG. 3·10 LOAD-MOMENT CURVES FOR THE SUBASSEMBLAGE OF FIG. 3·8: WEB CLEATS

where E_{eff} is the effective modulus of elasticity which depends on the stress-strain curve for the material and y is the distance from the infinitesimal area dA to the x-x axis.

In analysis, the quantity EI should refer to an axis passing through the centroid of the section. If the x-x axis is at a distance $\bar{y}$ from the centroid, the flexural rigidity $\overline{EI}$ about an axis passing through the centroid is

$$\overline{EI} = EI - \bar{y}^2.A \qquad (3.37)$$

where EI is given by eqn-3.36b and A is the area of the section calculated from

$$A = \int_A dA \qquad (3.38)$$

and $\bar{y}$ is given by the expression

$$\bar{y} = \frac{\int_A y\, E_{eff}\, dA}{\int_A E_{eff}\, dA} \qquad (3.39)$$

3.6.2- Spread of Yield:-

In an actual analysis, the section is usually elastic at the lower levels of loading. Although not obligatory, the section properties are calculated with respect to a centroidal axis. Therefore, the distance $\bar{y}$ is equal to zero. Hence, equation 3-37 reduces to eqn-3.36b and either one of these equations may be used in calculating EI. However, as yielding progresses, $\bar{y}$ becomes nonzero and the flexural rigidity must be calculated using eqn-3.37.

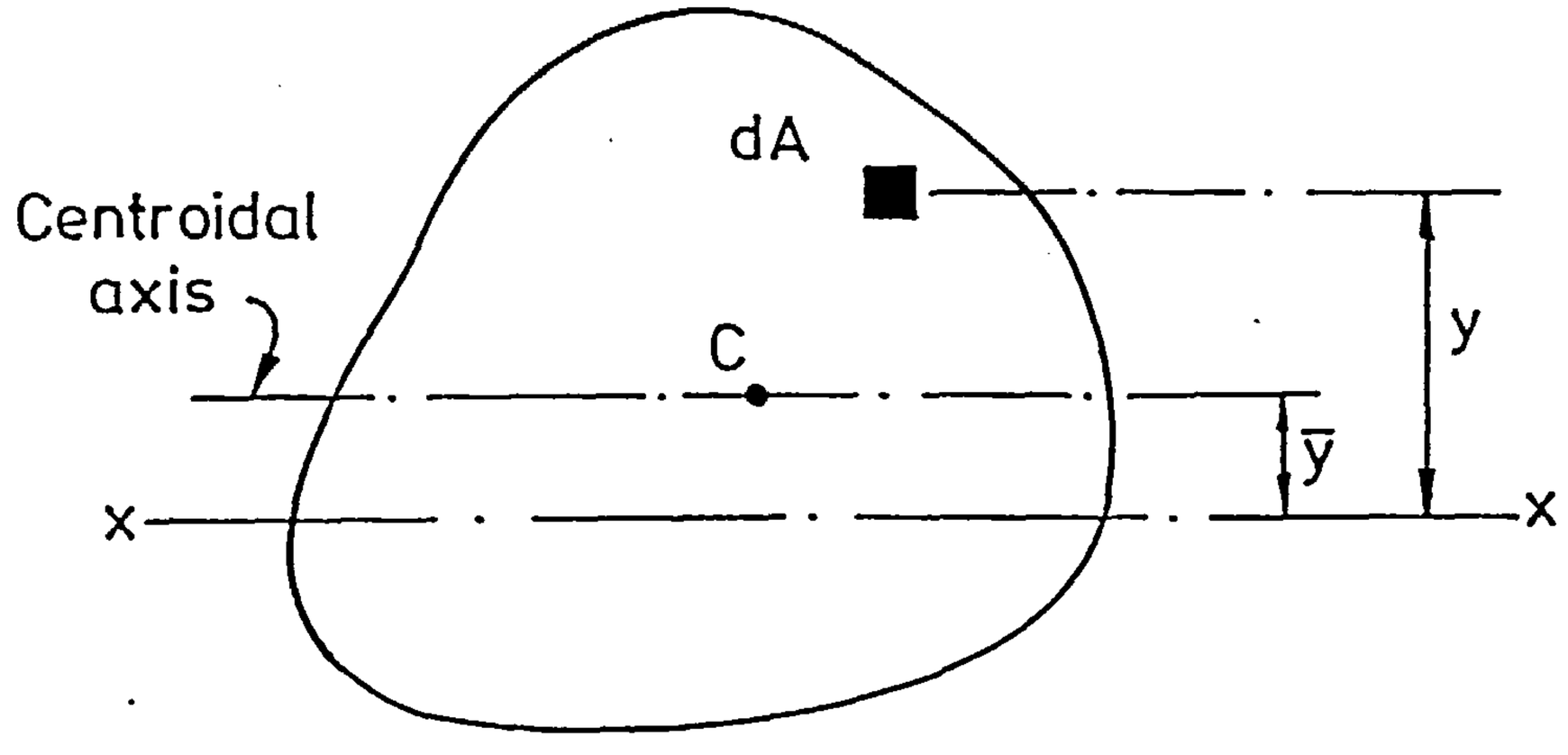

FIG. 3·11 A GENERAL CROSS-SECTION

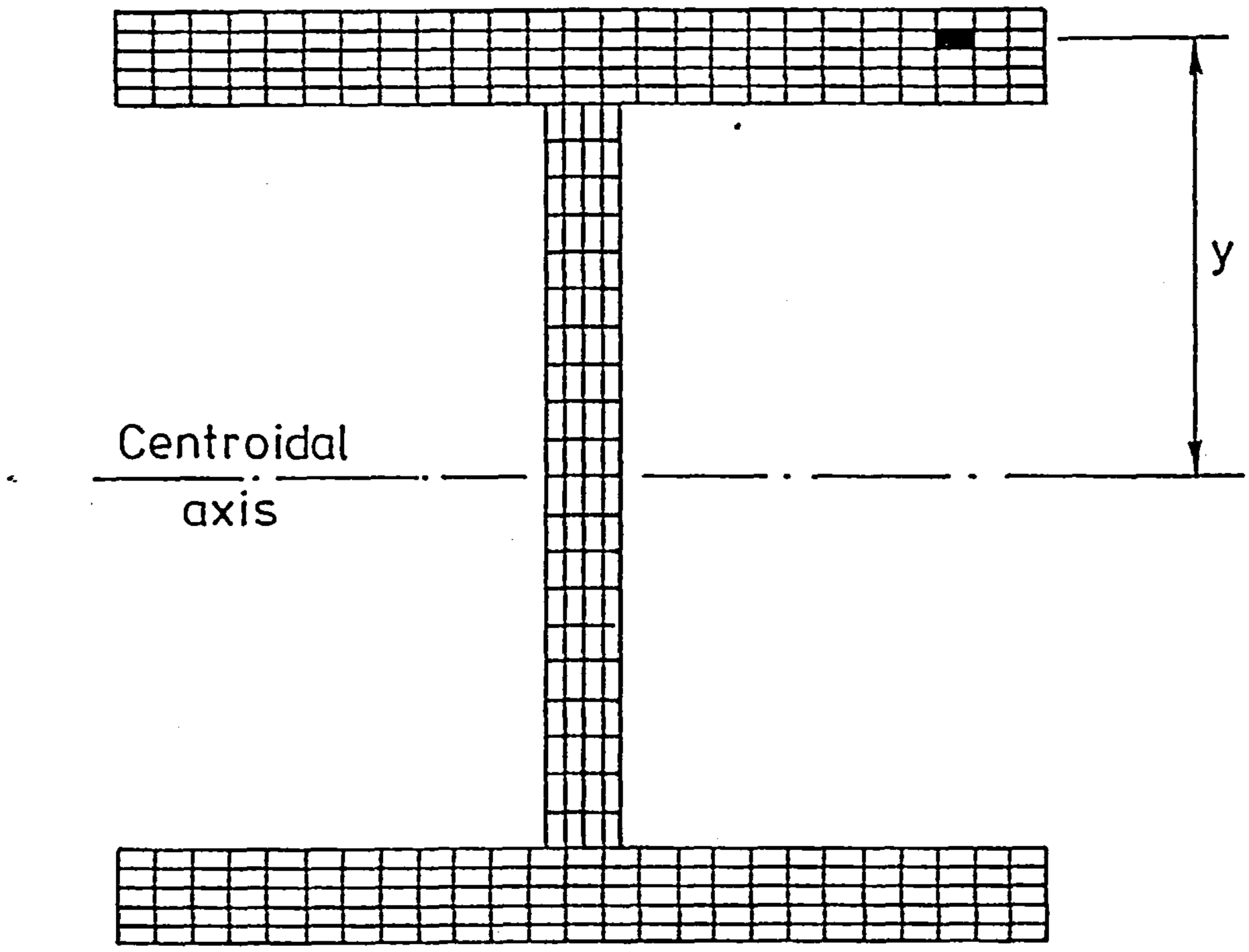

FIG. 3·12 A GENERAL I–SHAPED CROSS-SECTION:
SUBDIVISION FOR APPROXIMATE CALCULATION
OF SECTION PROPERTIES AND INTERNAL FORCES

An approximate method of determining the section properties to monitor the spread of yield in thin sections was suggested by Nethercot(55). This method involves the division of the section into a large number of sub-elements as shown in Fig-3.12. The axial and bending rigidities with respect to the centroid of the original (unyielded) section can be calculated from the following relations

$$EA = \sum_{i=1}^{N} E_{eff}^{i} \cdot \Delta A_i \qquad (3.40a)$$

and

$$EI = \sum_{i=1}^{N} E_{eff}^{i} \cdot y_i^2 \cdot \Delta A_i \qquad (3.40b)$$

where N is the number of sub-divisions in the section. These equations are the same as eqns-3.36 but replacing integrals by summations. Again the flexural rigidity as obtained from eqn-3.40b should be corrected by the quantity $(-\bar{y}^2 A_{eff})$ where

$$\bar{y} = \frac{\sum E_{eff}^{i} \, y \, \Delta A}{\sum E_{eff}^{i} \, \Delta A} \qquad (3.41)$$

which is, once more the same as eqn-3.39 but with summations instead of integration. The area A_{eff} which appear in the correction of EI is the area of the part of the section that remains elastic.

In two dimensional analysis, if a doubly symmetric section has partly yielded, and provided that the residual stress pattern is doubly symmetric, the section retains symmetry about at least one of its axes of symmetry. It is possible , therefore, to carry out the above calculations on only half the section. The resulting properties

may then be multiplied by 2 to give the correct values. This is very useful in maintaining a low computer cost while ensuring that the section properties are calculated to a high degree of accuracy.

3.6.3- Stress-strain Relationship:-

Since in eqns-3.40 and 3.41, E_{eff} is dependent on the stress-strain curve, it is essential to adopt a stress-strain curve which simulates the behaviour of the material. In the present study, a general elastic-perfectly plastic with strain hardening characteristics is adopted. Fig-3.13 shows a typical curve which is reasonable for most steels. Any reasonable values may be assumed for the yield stress, σ_y, modulus of elasticity, E, strain hardening modulus, E_{st} and the strain at which strain-hardening commences, ϵ_{st}. The yield strain, ϵ_y may readily be calculated from the assumed values of σ_y and E.

Once the normal strain at a point is calculated, it is a simple matter to enter Fig-3.13 with this value of strain and to determine the effective modulus of elasticity E_{eff} which is to be used in eqns-3.40 and 3.41. If the normal strain is ϵ, the effective modulus of elasticity may be determined from the following relations

$$E_{eff} = E \qquad -\epsilon_y < \epsilon < \epsilon_y \tag{3.42a}$$

$$= 0 \qquad \epsilon_y < \epsilon < \epsilon_{st} \quad \text{or} \quad -\epsilon_{st} < \epsilon < -\epsilon_y \tag{3.42b}$$

$$= E_{st} \qquad \epsilon > \epsilon_{st} \quad \text{or} \quad -\epsilon_{st} > \epsilon \tag{3.42c}$$

The total normal strain at any point consists of a direct axial strain and a bending strain. Both of these strains result from the applied loads. In addition, a residual strain may be present in the section. The distribution of this strain is frequently highly irregular. Approximate patterns are usually assumed (5). Such assumed

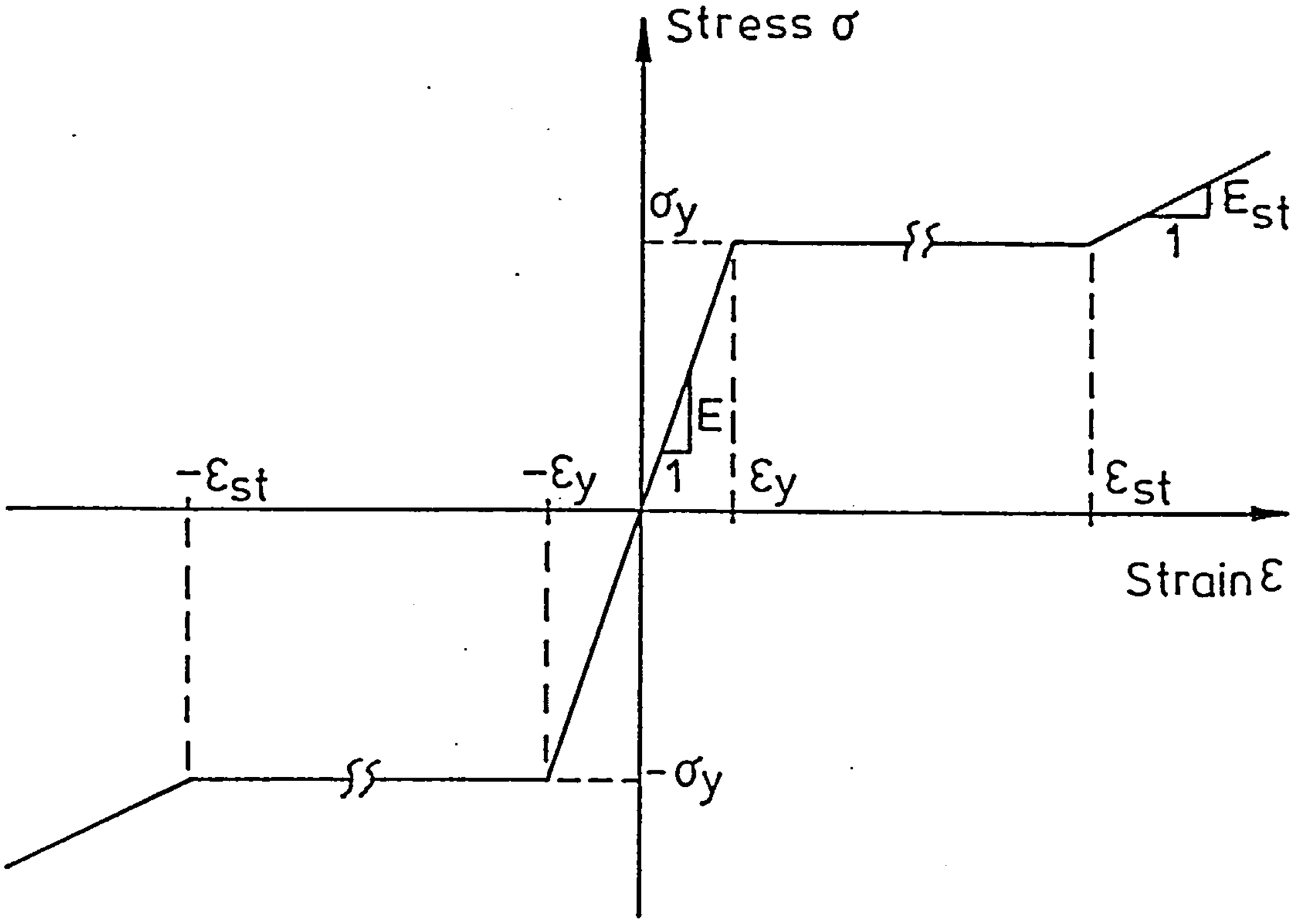

FIG. 3·13· IDEALIZED STRESS-STRAIN RELATIONSHIP

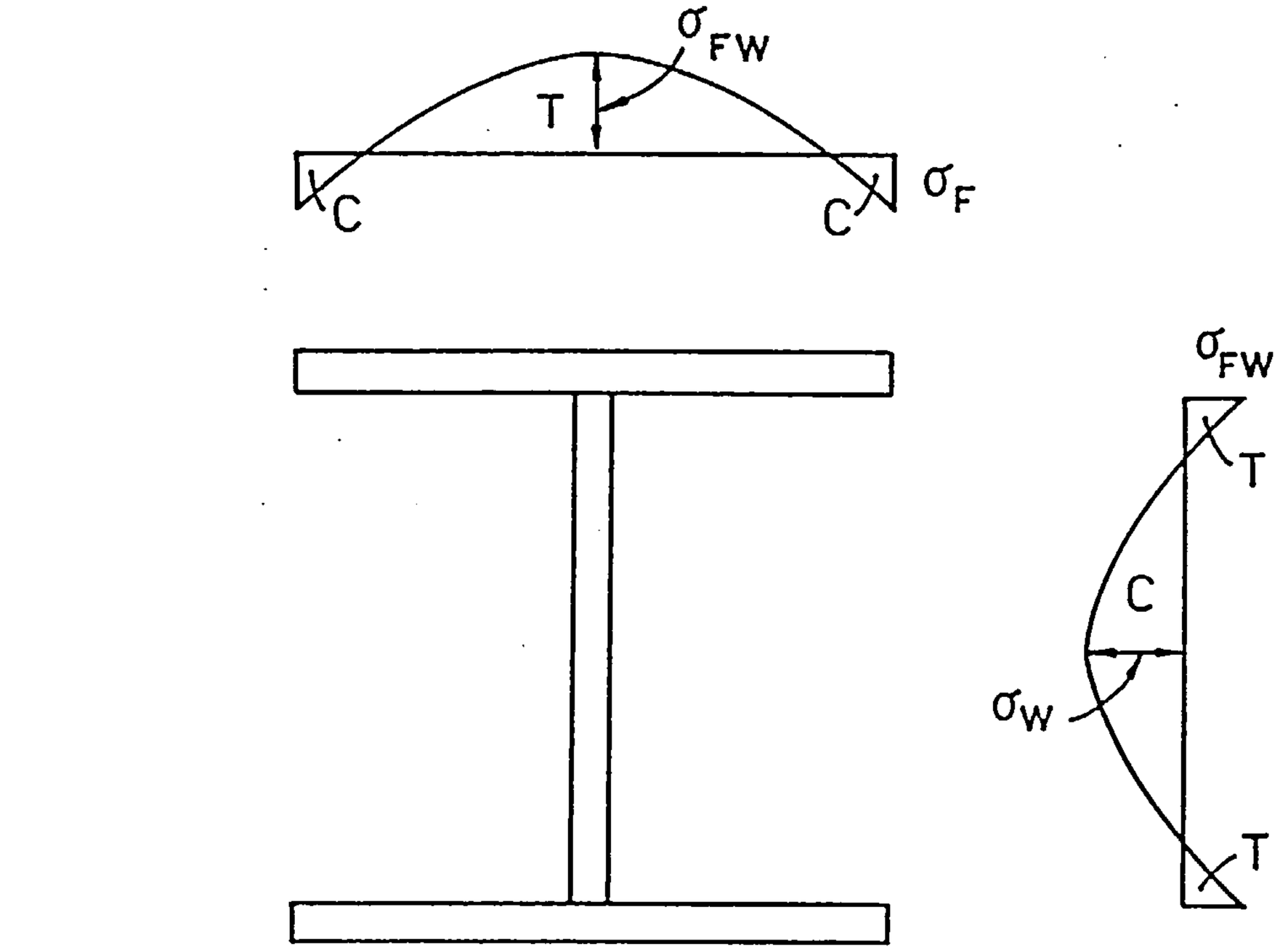

FIG. 3·14 AN APPROXIMATE PATTERN FOR RESIDUAL STRESSES: PARABOLIC DISTRIBUTION (YOUNG)

patterns would be given as input data to the analysis program. A more detailed explanation of the various patterns accepted by the program will be given in Sec-3.8. If the average axial strain and the curvature at the section are known, the normal strain at any point in the section may be calculated from

$$\varepsilon = \varepsilon^a - y\ \phi^b + \varepsilon^r \qquad (3.43)$$

where ε^a , ϕ^b and ε^r are the average axial strain and the curvature at the section and the residual strain at the point under consideration. In the present study, the distance y refers to an axis passing through the centroid of the original (unyielded) section. The strains due to the applied loads may be calculated from eqn-3.8 at the points x=0 and x=L. Hence, for rigid joints

$$\begin{bmatrix} \varepsilon_1 \\ \phi_1 \\ \varepsilon_2 \\ \phi_2 \end{bmatrix}_n = \begin{bmatrix} \varepsilon_1 \\ \phi_1 \\ \varepsilon_2 \\ \phi_2 \end{bmatrix}_{n-1} + \begin{bmatrix} \frac{1}{L} & 0 & \theta_1 & \frac{-1}{L} & 0 & 0 \\ 0 & \frac{6}{L^2} & \frac{4}{L} & 0 & \frac{-6}{L^2} & \frac{2}{L} \\ \frac{1}{L} & 0 & 0 & \frac{-1}{L} & 0 & \theta_2 \\ 0 & \frac{-6}{L^2} & \frac{-2}{L} & 0 & \frac{6}{L^2} & \frac{-4}{L} \end{bmatrix} \Delta\delta^e \qquad (3.44)$$

in which L is the length of the element and the rotations θ_1 and θ_2 are shown in Fig-3.1 and the subscripts 1 and 2 refer to nodes 1 and 2 of the element respectively.

3.7- Internal Stresses and Forces

The stress at any point in a section may easily be found if the strain at that point is known. The strain at this point may be calculated from eqn-3.43. With the help of Fig-3.13, the stress may be found using the following equation:

$$\sigma = E\,\varepsilon \qquad \text{for} \quad 0 < \varepsilon < |\varepsilon_y|$$

$$= \sigma_y \qquad \text{for} \quad |\varepsilon_y| < |\varepsilon| < |\varepsilon_{st}| \qquad (3.45)$$

$$= \sigma_y + E_{st}\,(\varepsilon - \varepsilon_{st}) \qquad \text{for} \quad \varepsilon > \varepsilon_{st}$$

$$= -\sigma_y + E_{st}\,(\varepsilon - \varepsilon_{st}) \qquad \text{for} \quad \varepsilon < -\varepsilon_{st}$$

Next, the internal axial force F and the moment M about an axis passing through the midpoint of the section may be found from the relations

$$F = \sum_{i=1}^{N} \sigma\, dA \qquad (3.46)$$

$$M = \sum_{i=1}^{N} \sigma\, y\, dA \qquad (3.47)$$

where y is measured from an axis passing through the midpoint of the unstressed section.

3.8- Inclusion of Initial Imperfections:-

3.8.1- Residual Stresses:-

As mentioned in Sec-3.6.3, the total strain at any point in the cross section is the sum of the applied strains which result from the applied loading and the residual strain. Residual strains in rolled shapes arise from differential cooling after rolling. In the case of welded sections, residual strains are due to welding. The distributions of the residual strains over the cross section is usually highly

complicated. Simple patterns were adopted to approximately represent the distribution of residual strains. Such patterns were based on experimental measurements. In what follows, reference will be made to residual stresses rather than residual strains since it is the stresses that are usually reported in the literature. Obviously, the stresses are related to the strains by the modulus of elasticity (since it is assumed that the entire section remains elastic in the absence of the applied strains). Only I-shaped sections will be considered herein since the whole study is limited to such sections.

A pattern with parabolic distributions of residual stresses across the flanges and the web is usually assumed for the rolled sections produced in the U.K. (5). This pattern was suggested by Young (56) based on a series of experimental observations. Fig-3.14 shows this type of distribution. Young suggested that values for the residual stresses at the flange tips σ_f , the flange-to-column junction, σ_{fw} and the centre of the web, σ_w be given by

$$\sigma_f = 165\left(1 - \frac{A_w}{1.2\,A_f}\right) \quad N/mm^2 \qquad (3.48a)$$

$$\sigma_{fw} = -100\left(0.7 + \frac{A_w}{A_f}\right) \quad N/mm^2 \qquad (3.48b)$$

$$\sigma_w = 100\left(1.5 + \frac{A_w}{1.2A_f}\right) \quad N/mm^2 \qquad (3.48c)$$

in which A_w is the area of the web and A_f is the area of both flanges. The residual stresses at any point in the flanges may be calculated by assuming a parabolic equation which must, if applied at the flange tips and the flange-to-web junction, give the values given by eqns-3.48a and 3.48b. Similarly, the stresses in the web are found from parabolic

equations which must satisfy the conditions at the flange-to-web junction and the centre of the web as given by eqns-3.48b and 3.48c.

The residual stresses found in rolled shapes produced in the U.S.A. are usually represented by the pattern shown in Fig-3.15 (5,57). In this pattern, the stresses are assumed to vary linearly along the flanges. The maximum values occur at the flange tips and the flange-to-web junction. These values are given by

$$\sigma_f = 0.3\ \sigma_y \tag{3.49a}$$

$$\sigma_{fw} = -0.3\ \sigma_y \frac{A_f}{A_w + A_f} \tag{3.49b}$$

in which σ_y is the yield stress of the material and A_f and A_w are the areas of one flange and the web respectively. The residual stresses are assumed to be constant throughout the web with a value equal to σ_{fw}.

For welded sections a simple rectangular pattern is assumed (5). This pattern is shown in Fig-3.16. The areas around the weld are assumed to have high residual tension given by

$$\sigma_T = -0.9\ \sigma_y \tag{3.50a}$$

while a low residual compression given by

$$\sigma_C = 0.1\ \sigma_y \tag{3.50b}$$

is assumed elsewhere in the section.

The present program accepts all of the above patterns. A multiplying factor which may be different from unity is used in order to use the patterns in cases where the severity of the residual stresses varies from the values given above. In addition to the above

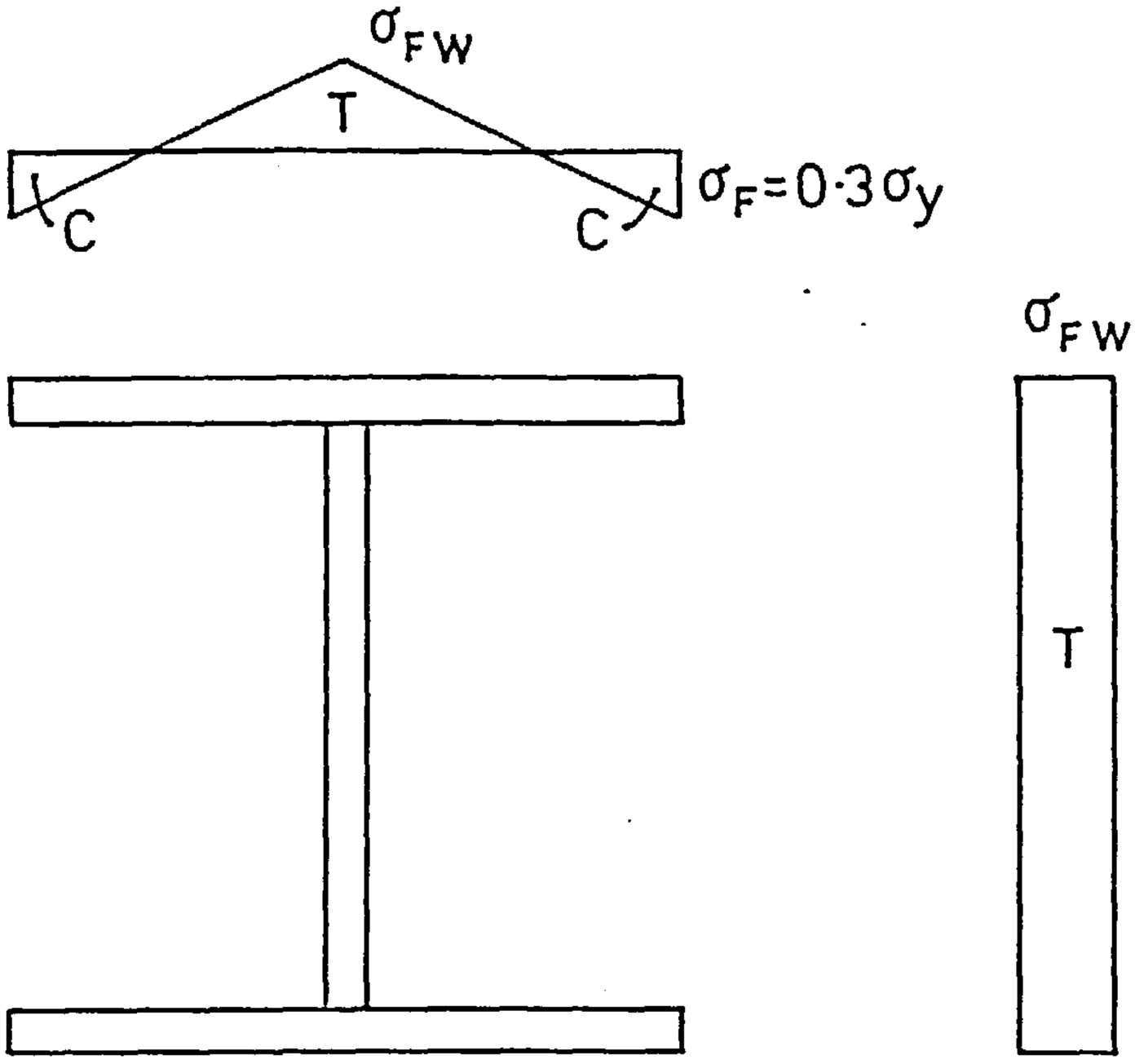

FIG.3·15 AN APPROXIMATE PATTERN FOR RESIDUAL STRESSES: LINEAR DISTRIBUTION (LEHIGH)

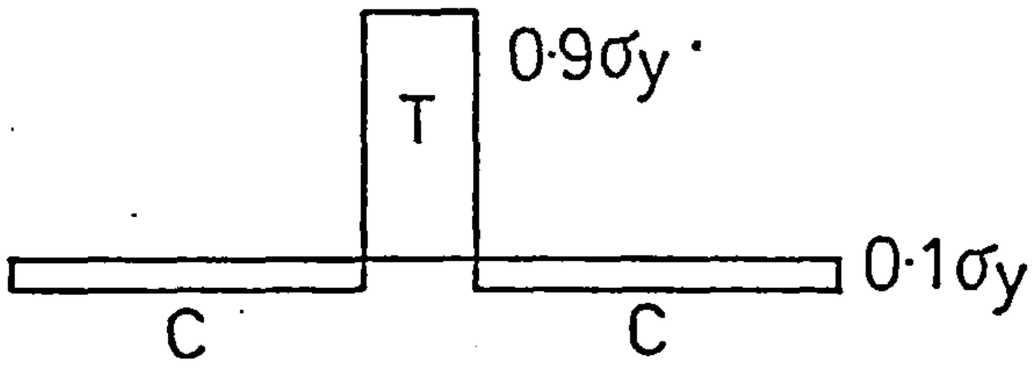

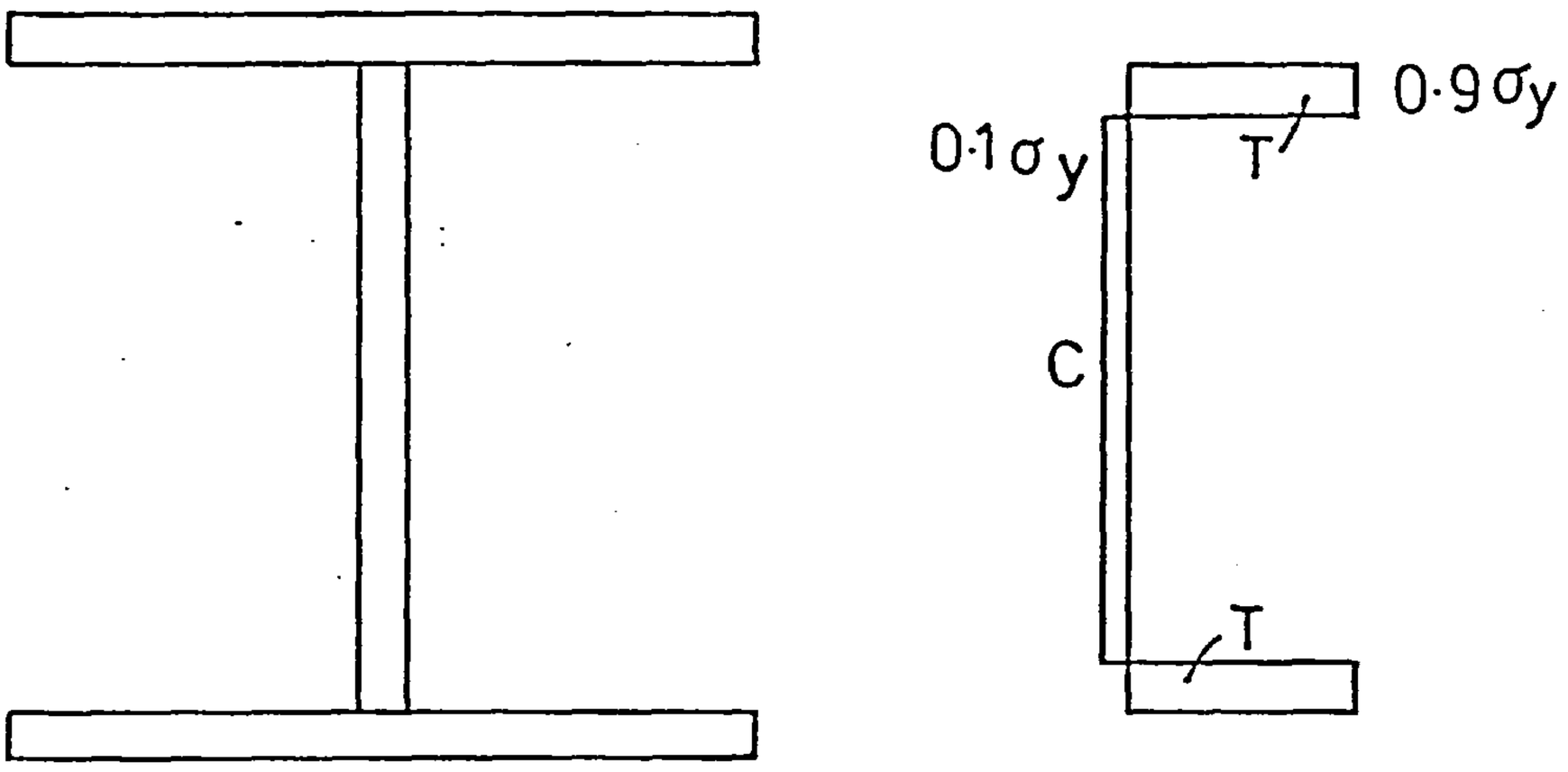

FIG. 3·16 AN APPROXIMATE PATTERN FOR RESIDUAL STRESSES: RECTANGULAR DISTRIBUTION (WELDED)

patterns, two more patterns are accepted by the program. One of these patterns is a parabolic distribution similar to that of Fig-3.14 (the one mentioned above) but with values for σ_f, σ_{fw} and σ_w treated as input data that has to be chosen by the user. In the second of these additional patterns, the residual stresses at a number of specified points along the flanges and the web are given to the program as input data. Straight lines are then assumed by the program in order to calculate the stresses at any other point in the section.

It must be noted that in any of the above patterns, static equilibrium must be satisfied. Such equilibrium requires that the residual force F_r and the residual moment M_r about any axis must equal to zero. The equilibrium check is automatically made by the program in the first two patterns. Here, only the residual force need be checked since the symmetrical patterns must yield zero moment. In the welding stress pattern, the area around the weld may be pre-chosen in such a way that the residual force is zero. In the last two patterns, since values at the key points in the pattern are chosen by the user, a complete check of the static equilibrium must be ensured by the user. The program can only calculate the residual force and the residual moment about the horizontal and vertical axes and print appropriate warning messages if necessary.

3.8.2- Initial Out-of-straightness:-

In practice, it is seldom possible to find a perfectly straight column. All columns do possess some degree of out-of-straightness due to cooling after rolling. Specifications allow for a small amount of crookedness to be present in the column. A common value for the maximum initial lateral deflection that is allowed to be

present in a column is one thousandth of the column's length (1,2).

The variation of the initial deflection along the length of the column is not always simple. The initial out-of-straightness has been experimentally measured in a range of column sizes in Sweden (58) and Japan (59). A half sine wave is usually assumed for the initial deflections. Hence, the initial deflection δ_o at any point along the column is given by (Fig-3.17)

$$\delta_o = a_o \sin \pi \frac{x}{L} \qquad (3.51)$$

in which a_o is the initial central deflection and L is the length of the column.

The presence of the initial out-of-straightness in a column in conjunction with the applied axial load has the effect of inducing additional bending moments in the column. Consequently, additional lateral deflections will result.

In a finite element model, a set of imaginary lateral forces and moments, P_o, which would have the same effect as that of the initial deflections may be used (5,60). This set of loads is obtained by multiplying the geometrical stiffness matrix, K_G, and the vector of the initial deflections δ_o which contain lateral deflections and rotations calculated using eqn-3.51 and its derivative. Hence

$$P_o = K_G \delta_o \qquad (3.52)$$

In eqn-3.50, the geometric stiffness matrix depends on the axial load, P, in the column. In an incremental analysis, a load increment ΔP is used in the calculation of K_G instead of the total load P. At the start of the load application, the only lateral deflections present in the column are the initial deflections. Hence, eqn-3.51 may

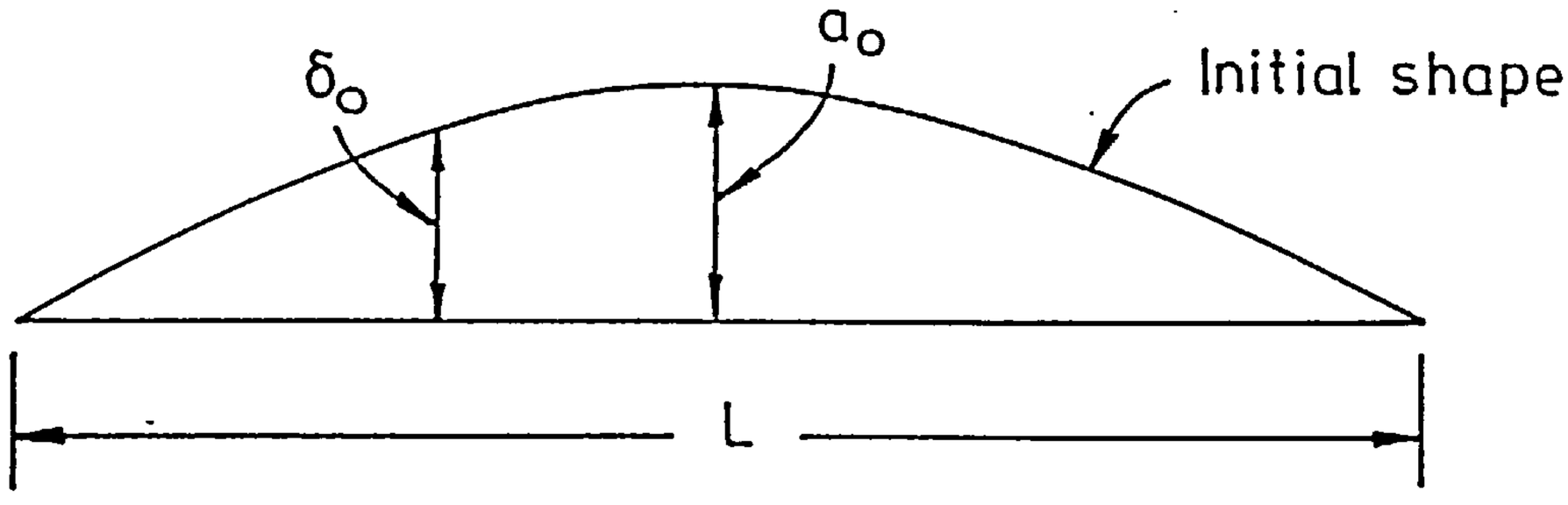

FIG. 3·17 AN APPROXIMATE SHAPE FOR INITIAL DEFLECTIONS IN A COLUMN

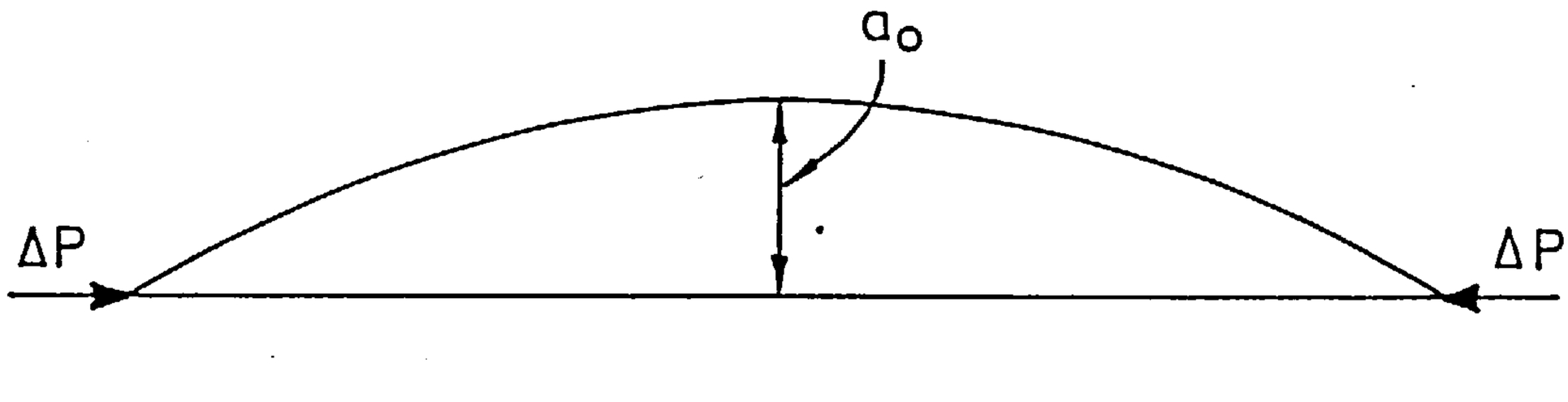

(a) First load increment

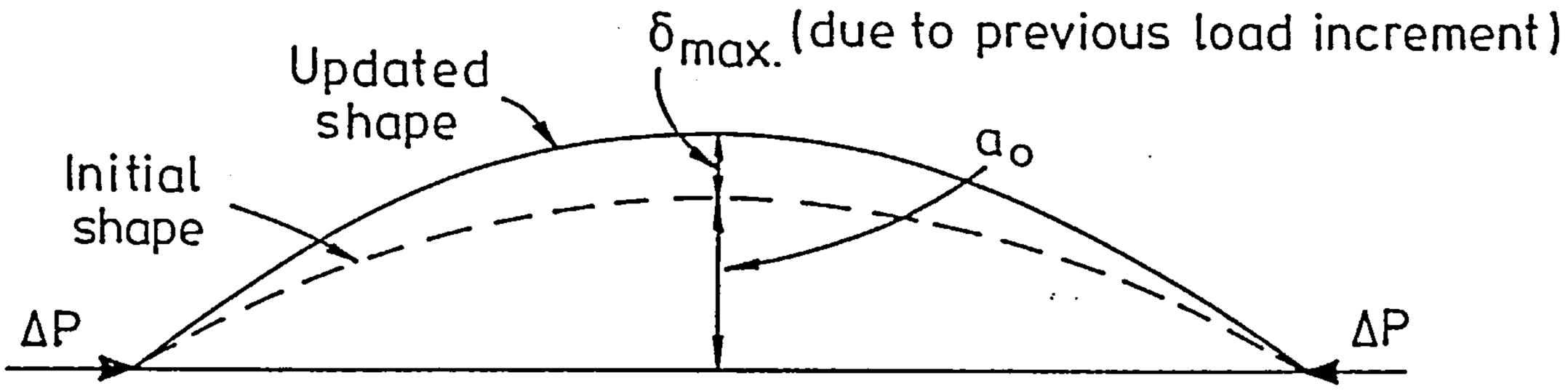

(b) Second load increment

FIG. 3·18 INITIAL AND UPDATED SHAPES

be used to calculate the set of lateral loads keeping in mind that K_G corresponds to a load increment ΔP (see Fig-3.18a). At the end of this load increment, an additional set of lateral deflections is induced. Hence, at the start of the next load increment, the lateral deflections that have to be used in eqn-3.51 consists of the initial deflection δ_o and the additional deflections $\Delta\delta$ (Fig-3.18b). In other words, the updated deflected shape of the column must be used in the determining P_o.

3.8.3- Axial Load Eccentricity:-

A small amount of eccentricity is usually inevitable in the application of axial loads in real structures. Therefore, it is necessary that the analysis program allows for such an eccentricity. In the present program, only equal eccentricities at the top and the bottom of the column, as shown in Fig-3.19, are considered. The effect of a load eccentricity, e , is to add a moment M_e given by

$$M_e = P \cdot e$$

to the top of the column and another moment with the same magnitude but with opposite sign to the lower end of the column. Once more, in incremental analysis, ΔP should be used instead of P .

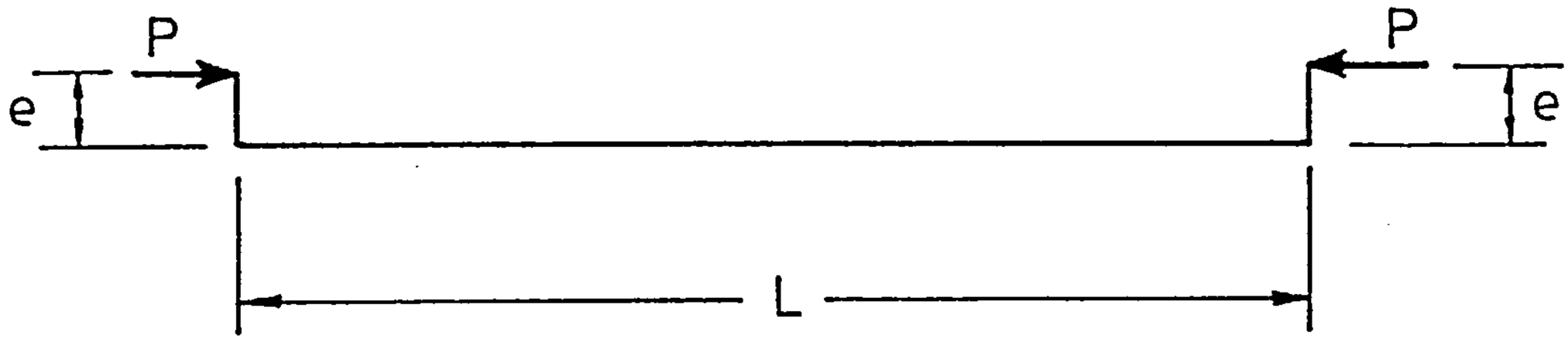

FIG.3·19 INCLUSION OF LOAD ECCENTRICITY

CHAPTER–4

COMPUTER PROGRAM

4.1- Program Layout:-

The theoretical background described in the previous chapter has been implemented in a computer program using FORTRAN 77 language. The program was developed on a PRIME computer available at the University of Sheffield and later was slightly modified to run on an IBM computer which is also available at the university. An incremental-iterative type of analysis which utilizes the finite element method was adopted. In the finite element model beam-column elements with six degrees of freedom were used. The program was intended to analyse subassemblages of the general type shown in Fig-4.1 which comprises four beams connected to a column by means of four semi-rigid connections. The program also deals with frames with less than four beams and is restricted to two-dimensional response.

The program consists of a large number of routines each performing a specific task. The main steps of the procedure followed in the program for analysing a structure are shown in the flow chart of Fig-4.2. These steps include:

(i) read and interpret input data

(ii) calculate the element stiffness matrices and the the element fixed end forces.

(iii) assembly of the overall stiffness matrix, K_T and the incremental load vector, ΔP

(iv) solution of the global equilibrium equation

$$K_T \Delta U = \Delta P \qquad (4.1)$$

for the incremental displacement vector ΔU

(v) update the generalized strains at every node

(vi) calculate section properties and the internal forces at both

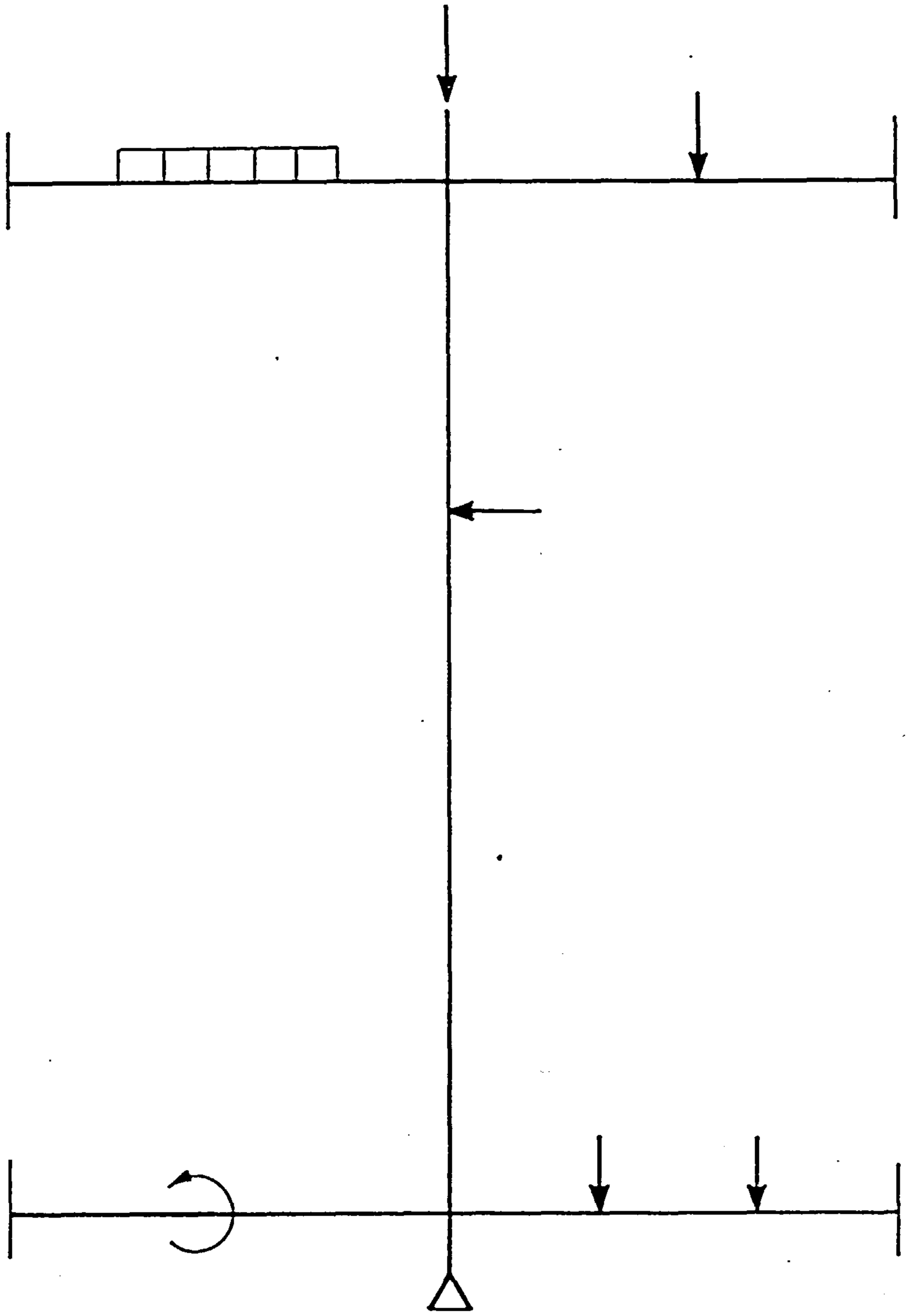

FIG. 4·1 A GENERAL TYPE OF SUBASSEMBLAGE

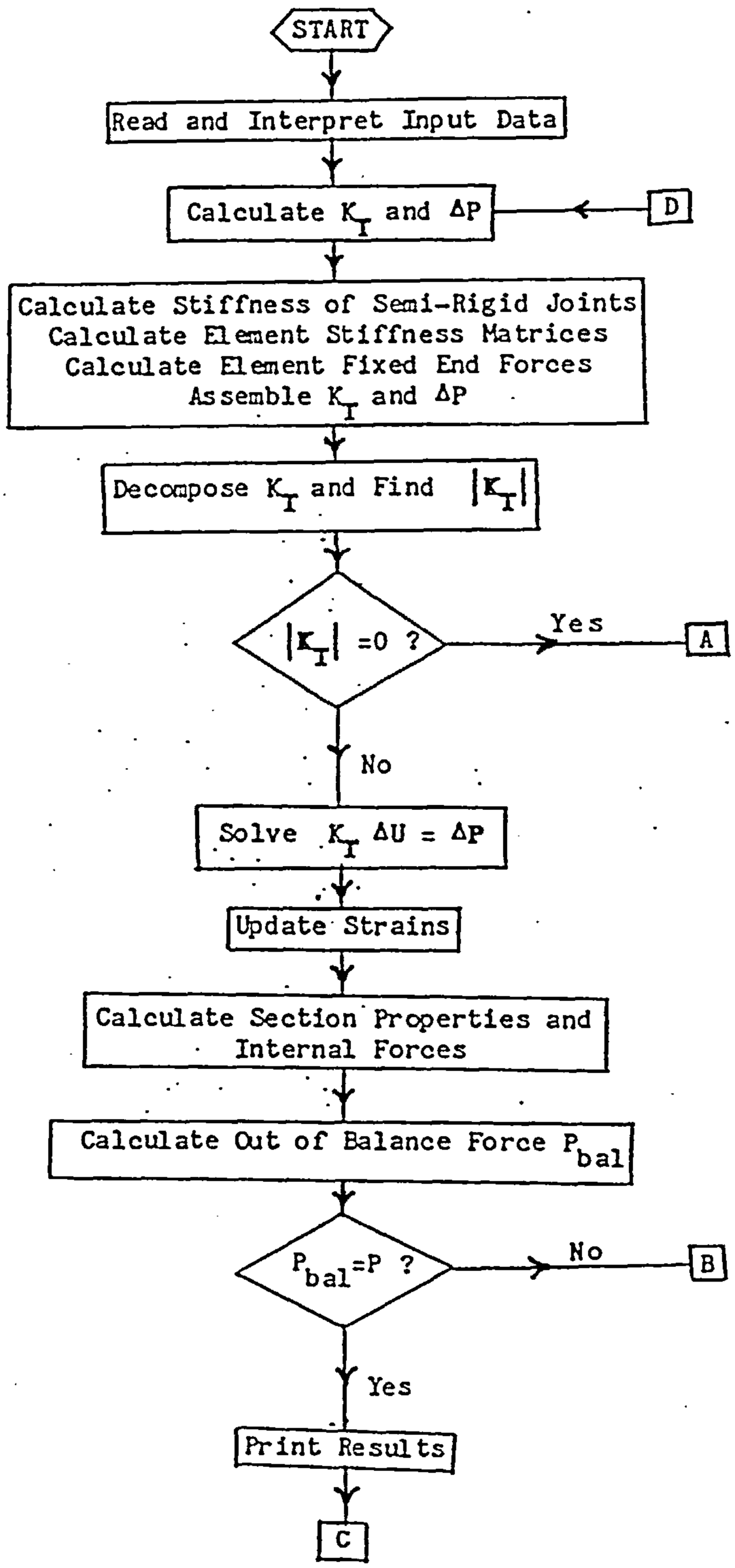

Fig-4.2: COMPUTER PROGRAM FLOW CHART

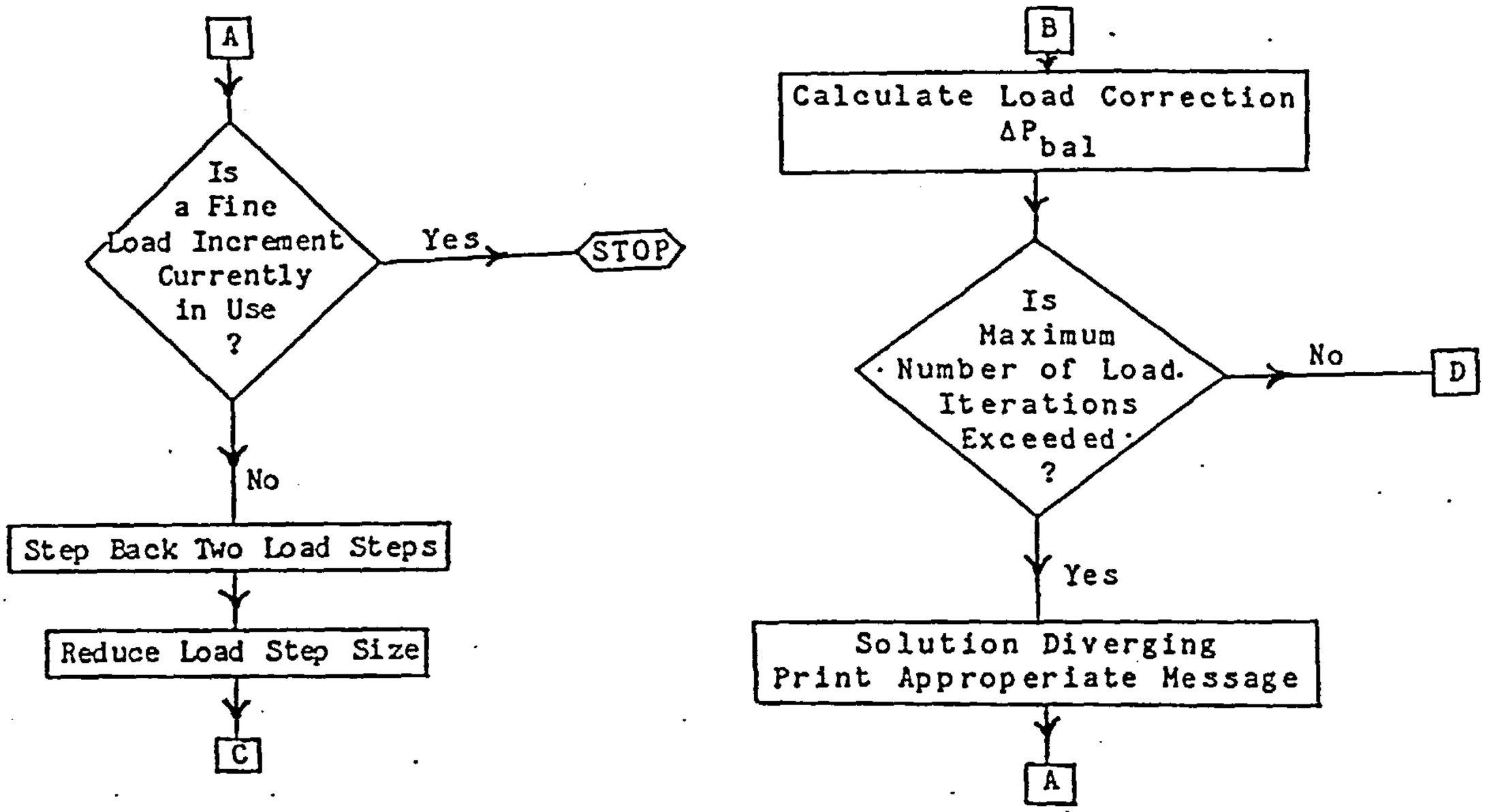

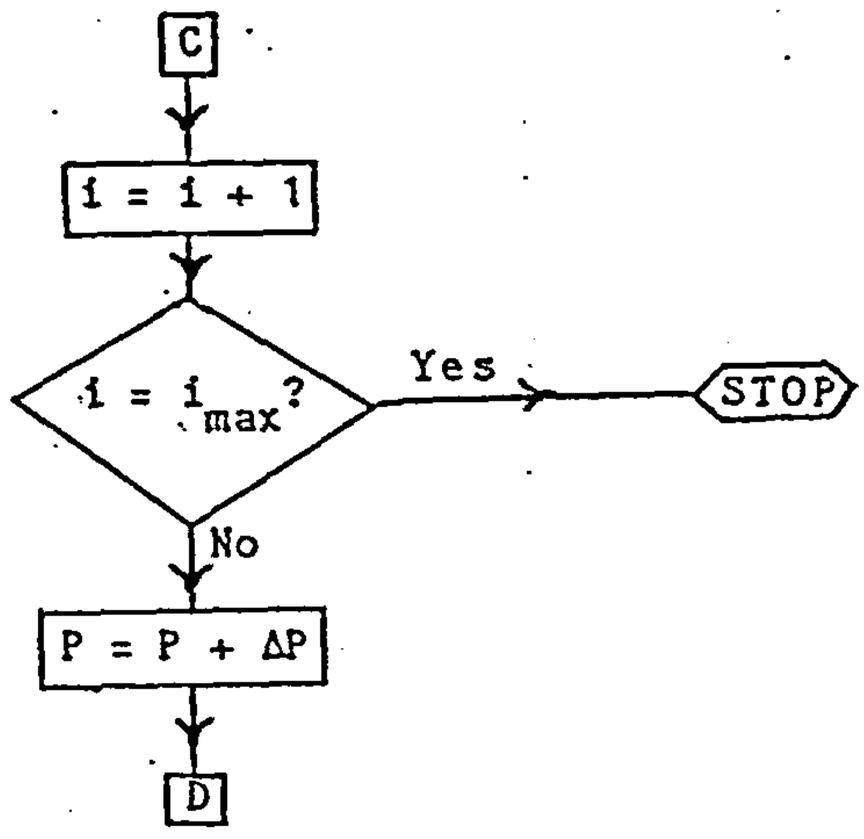

K_T = Overall Stiffness Matrix

ΔP = Incremental Load Vector

ΔU = Incremental Displacement Vector

i = Load Incement Number

i_{max} = Prespecified Number of Load Increments

Fig-4.2: (Continued)

nodes of each element

(vii) perform Newton-Raphson iterative procedure

(viii) print results; and

(ix) increment the applied loads to start another load increment.

In the following sections, each of these steps will be described in more detail. In addition, some other special facilities which are available in the program will be presented.

4.2- Reading Input data:-

As in any other analysis, the first step in the procedure is to read input data which define the problem in hand. The input data was divided into three separate main categories:

(1) General data: which define general aspects of the problem such as:

(a) structural geometry

(b) discretization of the structure, i.e. defining mesh size, nodal coordinates and element connectivity.

(c) type of analysis, i.e. whether elastic or inelastic type of analysis is required.

(d) accuracy level which controls the convergence criterion of the solution.

(e) type, location and history of the applied loads.

(f) type of residual stress pattern

(2) Section data: which consists of the cross-sectional dimensions for the sections used for the column and those for the beams. The section is assumed to be composed of three plates: a web and two flanges. Rectangular sections may also be considered. Sectional dimensions are given, for each plate, in the form of the maximum and

minimum values along the x and y axes with respect to an arbitrary point of origin which is usually taken as the centroid of the section. Internally, the program calculates the required properties.

The section data also include the axes of bending for the column and the beams. Material properties characterized by defining the key points in the stress-strain curve of Fig-3.13 are included in this type of data. The section data also include the residual stresses in the section in the cases where these stresses are to be given by the user. The program internally calculates the residual stresses at every sub-element of the cross section (as described in Sec-3.8.1).

(3) Joint data: the main part of this data is a previously prepared numerical representation of the M-Φ relationship of every connection used. Different relationships may be used for the connections in the structure. A separate computer program was developed for the purpose of determining the numerical representation for any M-Φ relationship; this latter program uses a B-Spline curve fitting technique. The joint stiffness and the rotation corresponding to a given moment may be calculated from the numerical representation using routines in the NAG computer library which is implemented on the main computers used at the University of Sheffield.

In addition, the joint data include an integer variable which specifies one of the following options pertaining to the loading-unloading behaviour of each of the connection:

(i) one M-Φ curve used for both loading and unloading

(ii) one M-Φ used for loading and an other for unloading and

(iii) one M-Φ curves used for loading and a straight line used for unloading and reloading.

Both PRIME and IBM computers permit the use of more than one

data file. Hence, each of the above sets of data is included in a separate file. This allows independently change any of these sets of data; for example, when analysing the same structure using different connections, only the joint data need be changed.

4.3- Calculation of the Element Stiffness Matrix and the Vector of Element End Forces:

4.3.1- The Element Stiffness Matrix:-

The total stiffness matrix is computed for every element in the structure with reference to the local axes shown in Fig-4.3. As was seen in chapter 3, this matrix is given by

$$k_T = k_E + k_G + k_L \qquad (4.2)$$

where

k_E = elastic stiffness matrix based on small deflection theory.

k_G = geometric stiffness matrix which depends on the axial force in the element

k_L = displacement matrix which depends on the deflected shape at the start of the load increment.

An explicit expression for each of these matrices is given in chapter 3. A numerical integration scheme was used to calculate these matrices. Four Gauss points along the element length were assumed in the scheme. The use of cubic shape functions enables that the integrations involved in the calculations of all of the above matrices be evaluated exactly using four Gauss points (23).

All of the above matrices are evaluated by one routine although only one matrix can be evaluated at any one time. Hence, any

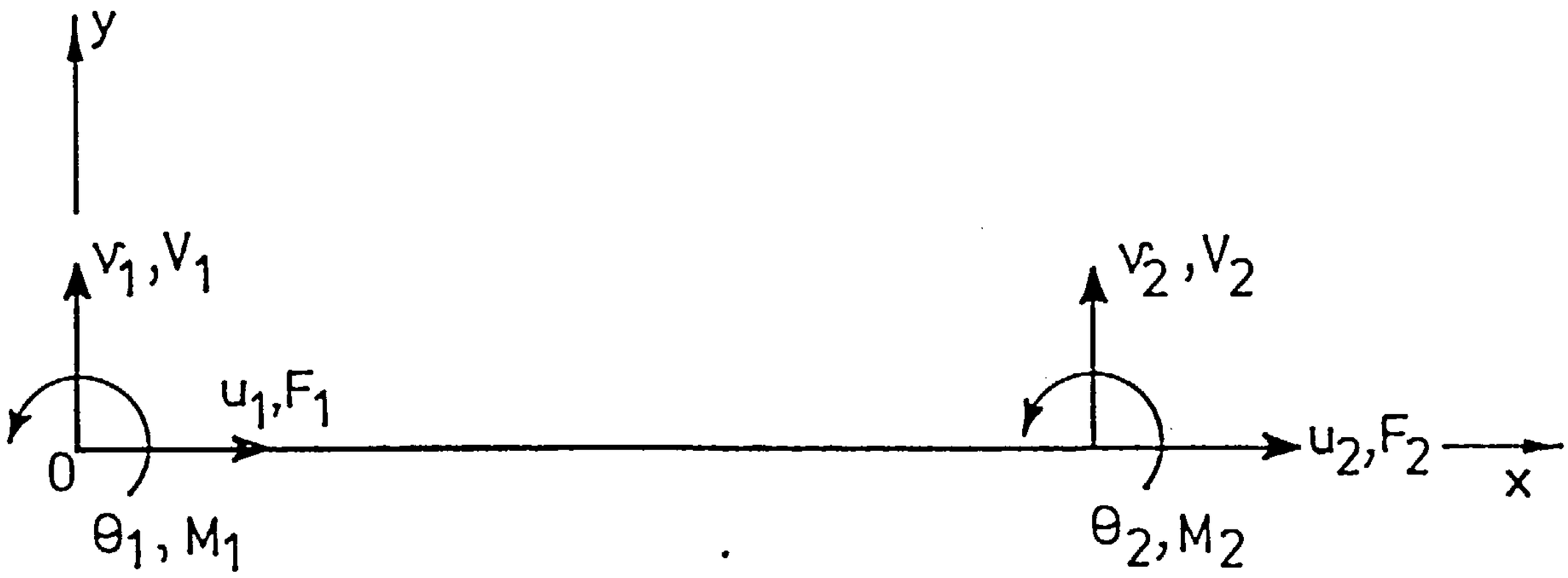

FIG. 4·3 A BEAM – COLUMN ELEMENT : LOCAL CO-ORDINATE AXES, DEGREES OF FREEDOM AND END FORCES

combination of the matrices that appear in eqn.4.1 may be used. Among the arguments passed to the routine are the joint stiffnesses of the two semi-rigid connections which are assumed at the nodes. Obviously, if any of these connections are rigid, a very large value should be used for the joint stiffness.

A special routine calculates the stiffnesses for the semi-rigid joints from the information given in the joint data. A routine in the NAG computer library is used for this purpose. It is to be noted that the independent variable in the M-Φ relationship is taken to be the moment not the rotation. The joint moment is taken to be equal in magnitude but opposite in sign to the moment at the end of the beam attached to this joint. The routine also calculates the rotation of the joint corresponding to any given moment. This helps in keeping track of the M-Φ curves of the connections.

4.3.2- Element Fixed End Forces:-

Four different types of applied loads are acceptable by the program as indicated in Fig-4.4. These types are:

(1) an axial load: assumed to act along the x-axis of the element at which the load is applied (Fig-4.4a). However, at present, this load is treated by the program as being applied to the top of the column not to a general point.

(2) a concentrated lateral load: this load may be applied to any element at a general point as shown Fig-4.4b. A downward load is assumed to be positive.

(3) a uniformly distributed load: which may also be applied to any element and have the same positive direction as the concentrated load. Fig-4.4c shows this type of loading.

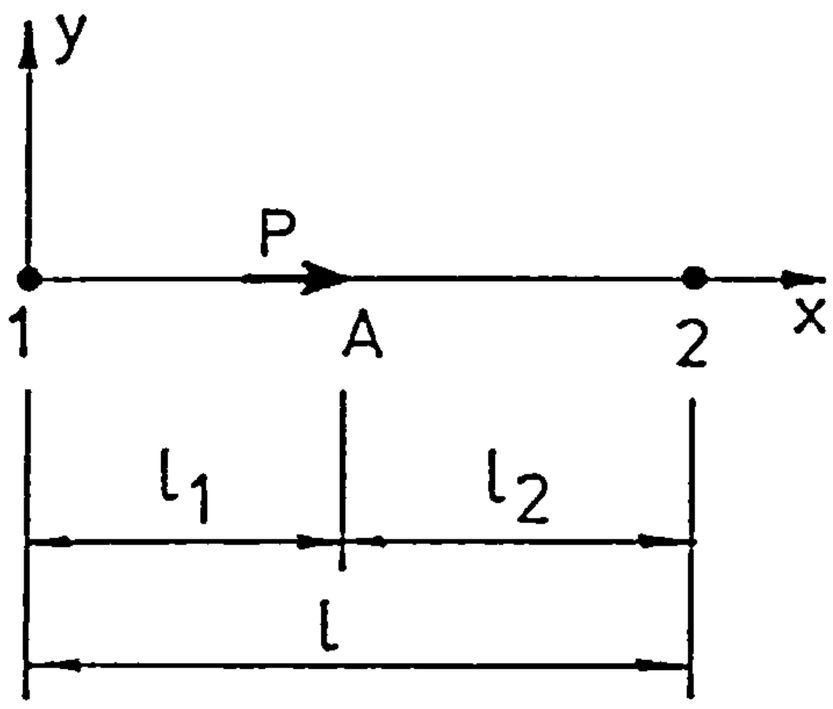

(a) A concentrated axial load

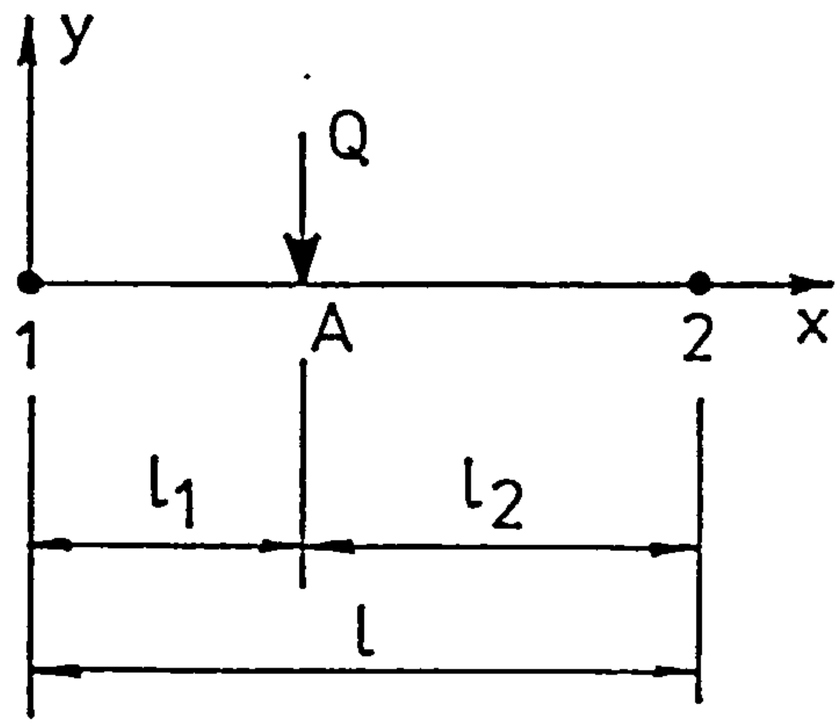

(b) A concentrated lateral load

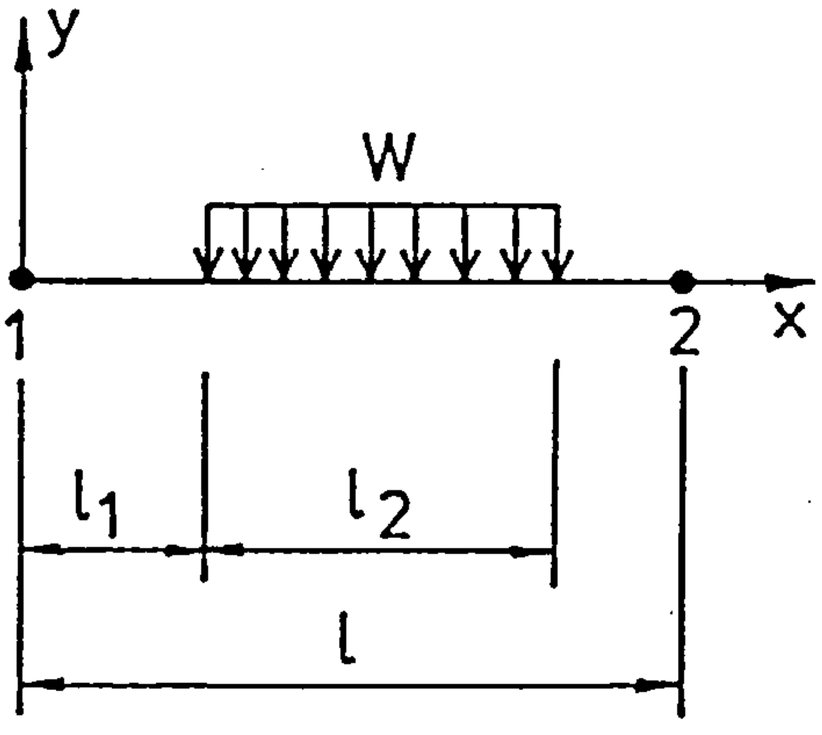

(c) A uniformly distributed load

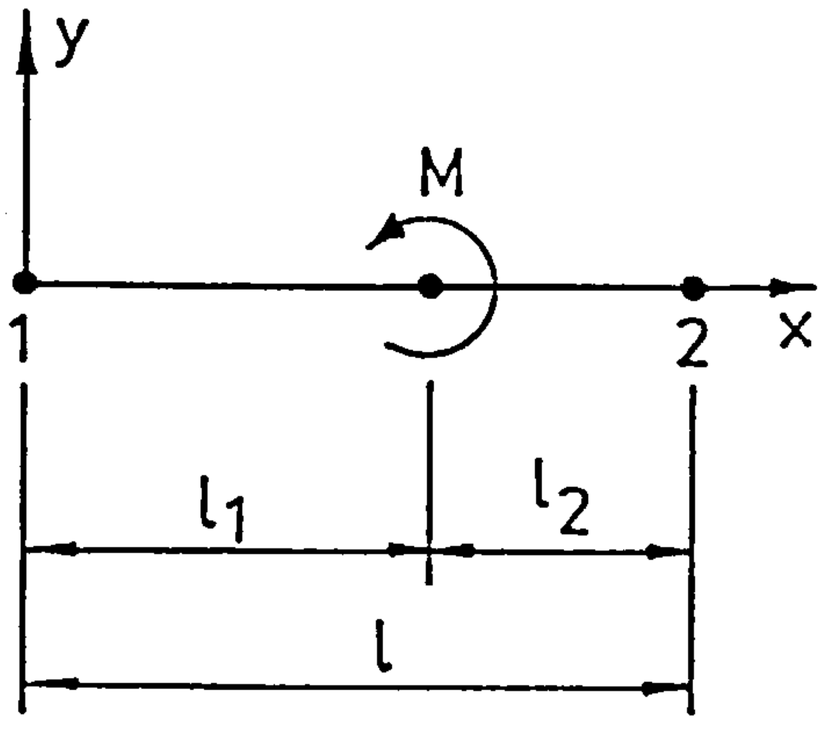

(d) A concentrated moment

FIG.4·4 TYPES OF ACCEPTABLE APPLIED LOADS

Generally, the load covers only a part of the element.

(4) a concentrated moment (Fig-4.4d) which may be applied to any element.

A reference value for each of these types of load is given in the general input data. The program then calculates the vector of fixed end forces corresponding to this reference load and directly assembles it into an overall reference load matrix in which every column corresponds to one type of loading. This assembly procedure is carried out after axes transformation whenever necessary. It must be noted that the fixed end forces ,at present, do not include the effect of the presence of the semi-rigid joints. It is not usually a difficult task to include such an effect. However, since the present study is only concerned with concentrated loads, this shortcoming is not of importance. Semi-rigid joints have no effect of the fixed end forces corresponding to a nodal load. Hence, by introducing an extra node at the applied load, the correct load vector is obtained. This extra node will probably be needed if the load was not nodal to increase the accuracy of the analysis.

4.3.3- Transformation:

Fig-4.5 shows the local coordinates for column and beam elements as well as the global axes which are common to all elements. It follows that stiffness matrices and vectors of fixed end forces for all beam elements must be modified since axes transformation is required.

Shown in Fig-4.6 are two sets of axes both having the same origin. The coordinates of any point A in the $x'-y'$ system is related to the coordinates of the same point in the x-y system by the relations

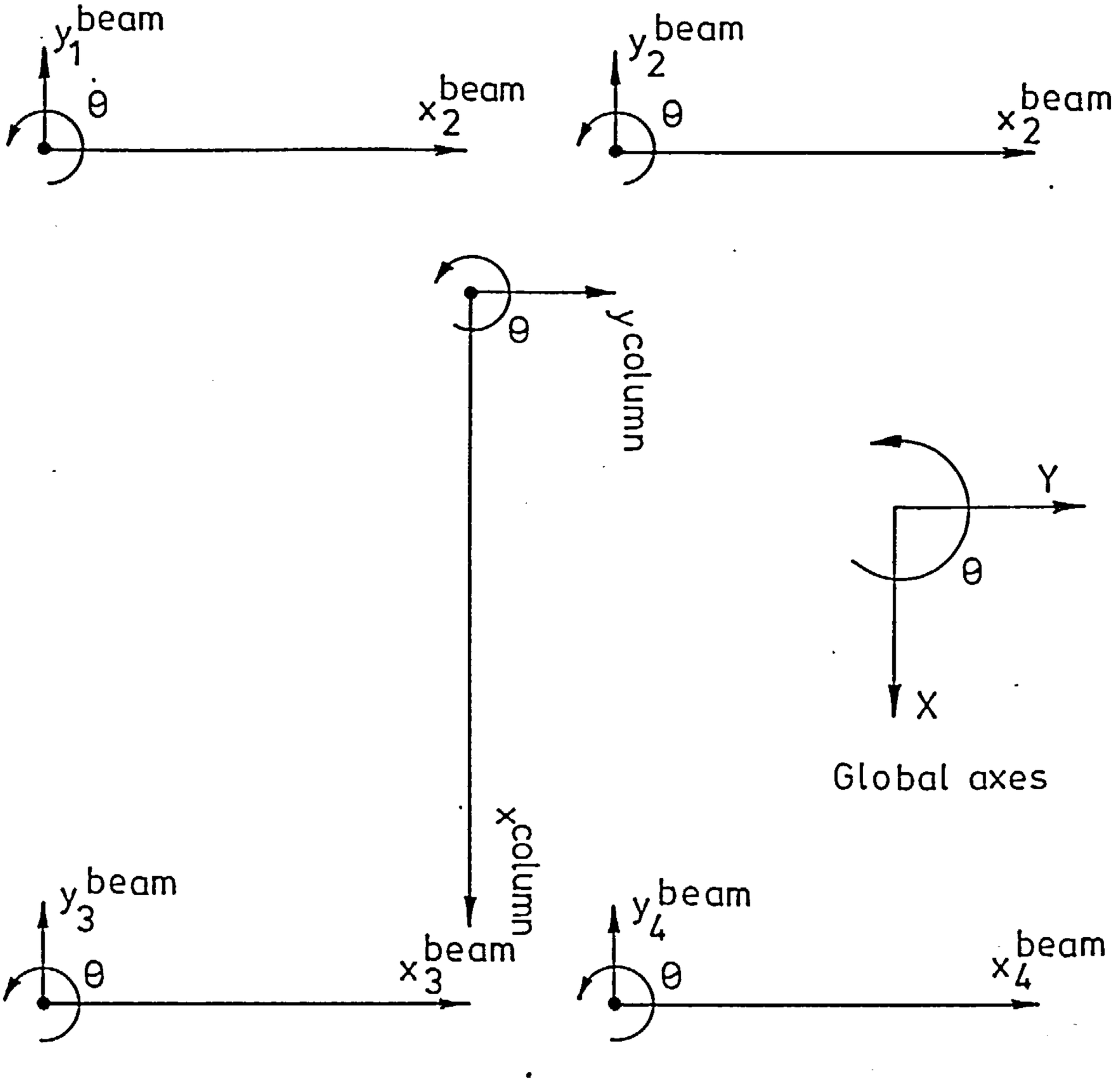

FIG.4·5 LOCAL AND GLOBAL AXES

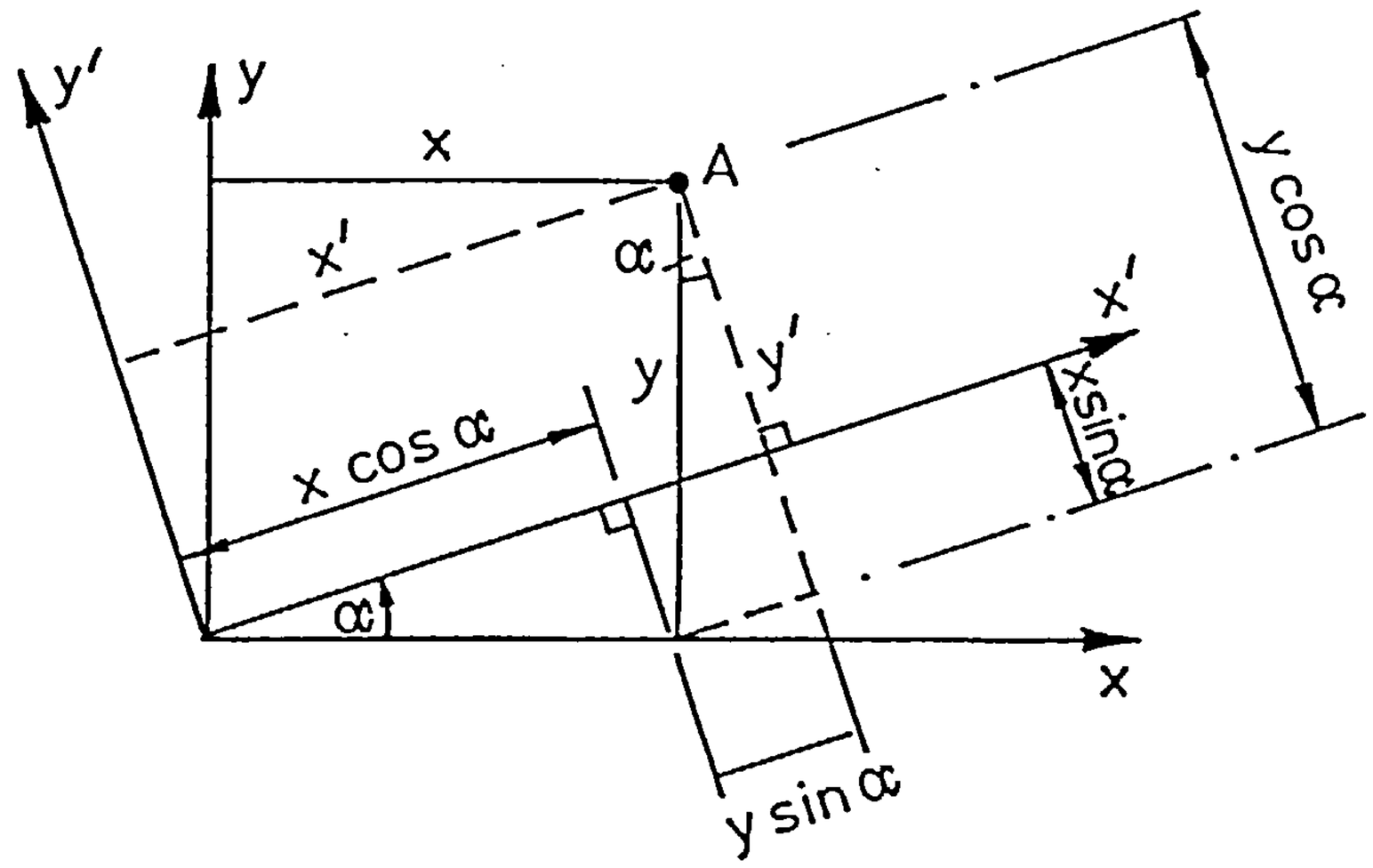

FIG.4·6 AXES TRANSFORMATION

$$x' = x\cos\alpha + y\sin\alpha \qquad (4.3a)$$

$$y' = -x\sin\alpha + y\cos\alpha \qquad (4.3b)$$

Eqns-4.2 is applicable to the transformation of translational deformation components at any point. It is also applicable to the transformation of forces from one coordinate system to an other. Let the displaced position of point A of Fig-3.1 with respect to the global coordinate system, x-y, be defined by the deformation components u, v, and θ. Also, let this point be defined in the local coordinate system, $x'-y'$ by the deformation components u', v' and θ'. The relation between the two sets of deformations is given by

$$\begin{bmatrix} u' \\ v' \\ \theta' \end{bmatrix} = \begin{bmatrix} \cos\alpha & \sin\alpha & 0 \\ -\sin\alpha & \cos\alpha & 0 \\ 0 & 0 & 1 \end{bmatrix} \begin{bmatrix} u \\ v \\ \theta \end{bmatrix} \qquad (4.4)$$

which is obtained by applying eqn-4.2. The rectangular matrix is the transformation matrix that defines the relation between the two sets of deformations. For the two node element shown in Fig-3.1, the transformation matrix, T is

$$T = \begin{bmatrix} \cos\alpha & \sin\alpha & 0 & 0 & 0 & 0 \\ -\sin\alpha & \cos\alpha & 0 & 0 & 0 & 0 \\ 0 & 0 & 1 & 0 & 0 & 0 \\ 0 & 0 & 0 & \cos\alpha & \sin\alpha & 0 \\ 0 & 0 & 0 & -\sin\alpha & \cos\alpha & 0 \\ 0 & 0 & 0 & 0 & 0 & 1 \end{bmatrix} \qquad (4.5)$$

For this element and in line with eqn-4.4, we have

$$\delta^e = T\,\delta^g \qquad (4.6)$$

where δ^e and δ^g are the local and global sets of nodal deflections

respectively. It follows that the set of end forces in the global system are related to that in the local system by the relation

$$p^g = T^T p^e \qquad (4.7)$$

in which T^T is the transpose of T.

Now, assume that the equilibrium equation for the element under consideration is

$$k_T^e \delta^e = p^e \qquad (4.8)$$

where k_T^e is the total stiffness matrix of the element. Then by substituting for δ^e from eqn-4.6, we have after premultiplying both sides of eqn-4.8 by T^T and applying eqn.4.7

$$T^T k_T^e T \delta^g = p^g$$

or

$$k_T^g \delta^g = p^g$$

in which p^g is given by eqn-4.7 and k_T^g is given by

$$k_T^g = T^T k_T^e T$$

The inclination angle, α, is calculated from the nodal coordinates as

$$\alpha = \tan^{-1}\left(\frac{y_2 - y_1}{x_2 - x_1}\right)$$

4.4- Assembly of Global Stiffness Matrix and Load Vector:-

The structural stiffness matrix is assembled from the element stiffness matrices in the usual manner as described in text books

(23,24,25). It is based on the relation between the local degrees of freedom in an element and their corresponding global degrees of freedom. In the present program, the property that the structural stiffness matrix is a banded one has been employed. This is useful in saving computer time and space. The stiffness matrix is stored in a compacted form to save computer memory. The procedure for assembling a compacted banded matrix is well documented in the literature.

The total load vector, P_{tot} is computed from the reference load matrix in which, as mentioned earlier, every column corresponds to a different load. Based on the load pattern for any specific applied load, P_i, a load increment ,ΔP_i, is calculated and the contribution of this load to the total load vector is calculated as the result of multiplying this load increment and the column in the reference load matrix corresponding to this load. Hence, if we denote by $P_{i,ref}$ the i^{th} column in the reference load matrix, the total load vector P_{tot} in the j^{th} load stage is

$$P_{tot} = \sum_{i=1}^{N} \frac{\Delta P_{i,j}}{P_{i,ref}} P_{i,ref} \qquad (4.9)$$

where N is the number of applied loads. Load incrementation is explained in more detail in Sec-4.10.

4.5- Solution of Simultaneous Equations:-

The next step in the analysis is to solve the incremental equation 4.1 for the incremental displacement vector.

4.5.1- Boundary Conditions:-

The assembled tangential stiffness is singular before

applying the boundary conditions(23,24). This means that it cannot be decomposed. However, it becomes non-singular when the boundary conditions are applied. These boundary conditions define the deformation components in a certain number of degrees of freedom. The most common boundary conditions are those in which deformation components are restrained .i.e

$$u_i = 0 \qquad (4.10)$$

where u is any deformation component and i is its identification number. The condition of eqn-4.10 may be achieved by assuming zero values for all but the diagonal elements in the row and column corresponding to the i^{th} degree of freedom. Hence

$$K_{i,j} = K_{j,i} = 0.0 \qquad \text{for } j = 1,N$$

and

$$K_{i,i} = 1.0$$

Where N is number of degrees in the structure.

It must be noted that, because of the way the semi-rigid joints are being included in the analysis, the rotation at an end which is connected to an infinitely rigid base with a semi-rigid joint must be assumed to be restrained. Of course, since the stiffness of the semi-rigid joint is less than that of a fixed end, the rotation at the end of the element is actually equal to the rotation of the semi-rigid joint itself.

4.5.2- Cholesky's Method of Solving Simultaneous Equations:-

This method is adopted since it is convenient in decomposing symmetric banded matrices. The method is well explained in many text books (25,61). It starts with decomposing the structure stiffness matrix into an upper triangular form. The load vector is also modified

in the same way as if it were an extra column in the stiffness matrix. Finally, the unknown displacements are found by back substitution.

The method fails if any of the diagonal elements of the matrix became negative during the process of decomposition. However, it was pointed out in reference 61 that this condition occurs only if the matrix was not positive-definite. It is well known that the stiffness matrix is positive-definite as long as the structure remains stable(23,24,25). Hence, the condition stated for failure of the method is taken to be an indication of structural instability.

4.6- Updating the Strains:-

Incremental average strains, $\Delta\varepsilon$, at element nodes due to the incremental displacements are calculated from eqn-3.44. The total strains are then updated. If the total strain vector ε^{e}_{i-1} for an element at the end of the previous load increment, is known, the strain vector corresponding to the end of the current load increment is given by

$$\varepsilon^{e}_{i} = \varepsilon^{e}_{i-1} + \Delta\varepsilon^{e}$$

where $\Delta\varepsilon^{e}$ is the element strain vector resulting from the current load increment.

These updated strains , along with any residual strains are used in calculating the section properties and the internal forces at both nodes of every element.

4.7- Calculating Section Properties and Internal Forces:-

As explained in Secs-3.6 and 3.7, section properties and internal end forces are calculated using an approximate method in which

the section is divided into a large number of sub-elements and summing up the contributions of these sub-elements. The importance of this step is that it enables monitoring the spread of yield along the element length and across the cross section. The analysis process includes an iterative procedure which is performed in every load increment. This procedure involves the calculation of a set of out-of-balance forces corresponding to the set of applied loads. These out of balance forces can be calculated only if the internal forces are known.

4.8- Load Iteration Procedure:-

In non-linear analysis, the external load is usually applied in a number of increments. The structure is assumed to behave linearly in each load increment. The deformations are updated after each load increment. The predicted response of the structure using this approach departs away from the true one. Fig-4.7 qualitatively shows the actual and predicted load-deformation curves of a structure. The gap between the two curves increases as the load increases. This means that, in every load increment, there is an amount of error in the prediction of the response. This error accumulates as more load increments are applied.

4.8.1- Newton-Raphson Iterative Procedure:-

To overcome this problem, an iterative procedure is required within every load increment. One of the most common iterative methods used in the structural analysis is the Newton-Raphson method. It serves as a corrector to the predicted response of the structure. The procedure which involves incremental and iterative processes is usually termed an incremental-iterative analysis. Assume that the structure's response corresponding to a load P is known. The first step in the next

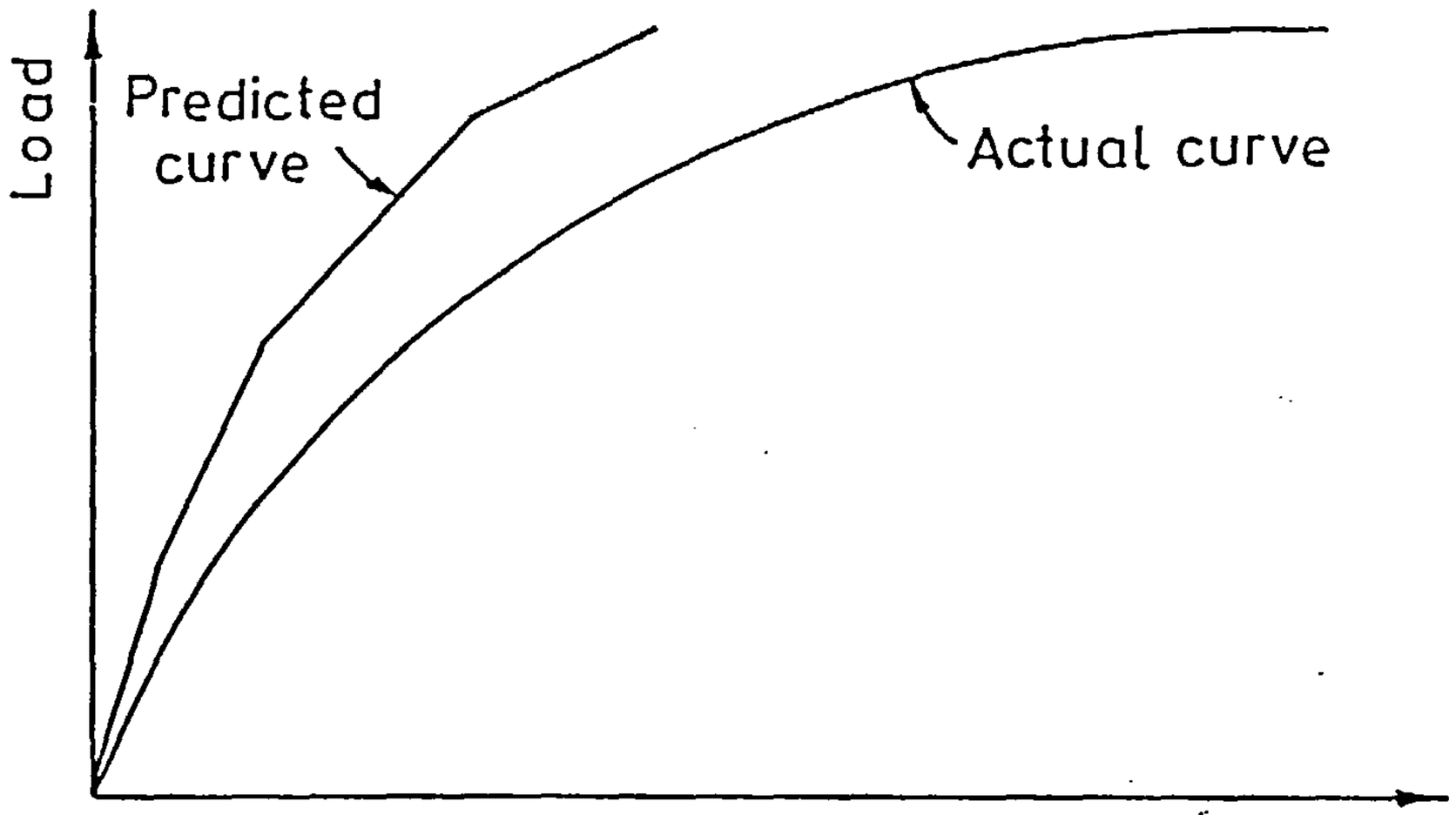

FIG.4·7 PREDICTION OF LOAD – DEFLECTION CURVE USING INCREMENTAL ANALYSIS

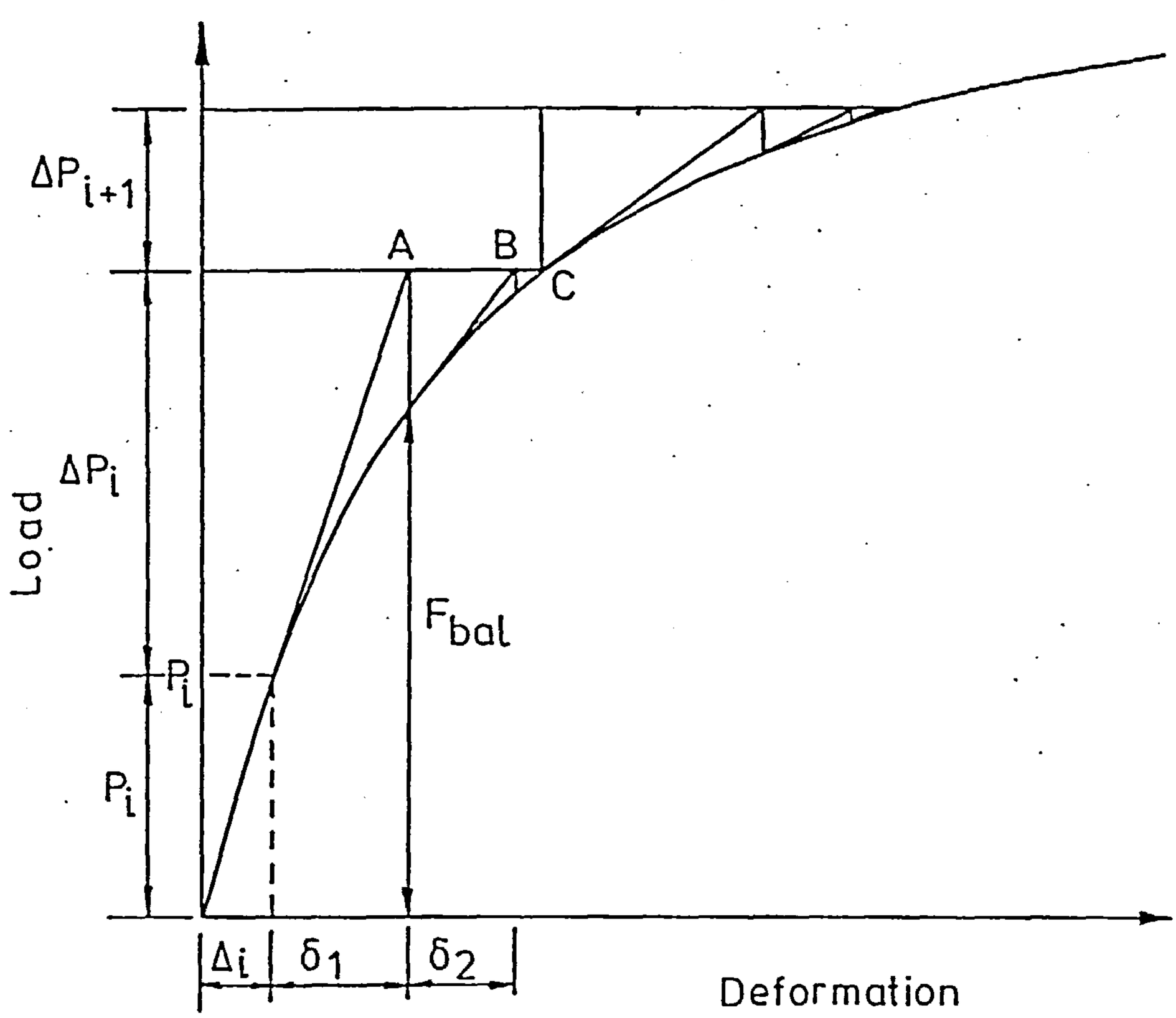

FIG.4·8 PREDICTION OF LOAD – DEFLECTION CURVE USING INCREMENTAL ITERATIVE PROCEDURE

load increment is to calculate the tangential stiffness matrix which depend on the current status of the structure. A load increment is then applied and the deformations are updated. Hence point A in Fig-4.8 is determined. The Newton-Raphson procedure is then carried out. An out-of-balance force which depends on the updated deformations is calculated. If point A is not on the actual curve, the out-of-balance force will be different from the applied load. A corrective load equal to the difference between the applied load and the out-of-balance force is then applied to the structure. This step is done after recalculating the tangential stiffness matrix using the updated deformations. This process determines point B on Fig-4.8. This procedure is repeated until the corrective load becomes sufficiently small to assume that point C on the actual curve of Fig-4.8 is reached. The next load increment is then applied and the whole process is repeated. In this way, a close approximation to the actual response is obtained.

4.8.2- Modified Newton-Raphson Procedure:-

A modified version of the Newton-Raphson method may also be used. The method is the same as the one described above except in that, to reduce computer time, the tangential stiffness matrix is not computed at every iteration. This method, however, results in that more iterations are required to achieve the same accuracy. Bearing in mind that the adopted procedure for calculating section properties and internal forces requires a large number of arithmetic operations (multiplications, divisions, ... etc) and logical tests, it is desirable to keep the number of iterations per load increment to a minimum. In other words, the savings obtained by not recomputing and decomposing the stiffness matrix in the modified Newton-Raphson method,

is, at least to some extent, offset by the need to perform a large number of computations to calculate section properties and internal forces. For this reason, the original Newton-Raphson method was adopted in this study.

4.8.3- Calculation of Out-of-Balance Forces:

The calculation of the out-of-balance forces depends on the type of the applied load. In the present program, a separate routine calculates the out-of-balance force for each type of loading. Since distributed loads were not considered in the present study, there is no routine available for calculating the out-of-balance force for this type of load; it may be easily added if required. In what follows, the calculations of the out-of-balance forces corresponding to an axial load, a concentrated lateral load and a concentrated moment are described.

(1) Axial load:-

As mentioned earlier, although the input data permits the consideration of axial loads which are applied at any general point in the structure, the program considers only one axial load which is assumed to be applied at the top of the column. The out-of-balance force corresponding to this type of loading may be determined by considering the equilibrium of half the subassemblage shown in Fig-4.9. The force, F_{bal} is simply taken to be the force at the centre of the column. This force must counteract any beam reactions and directly applied column load. Hence,

$$F_{bal} = P + R_{B_l} + R_{B_r} \qquad (4.11)$$

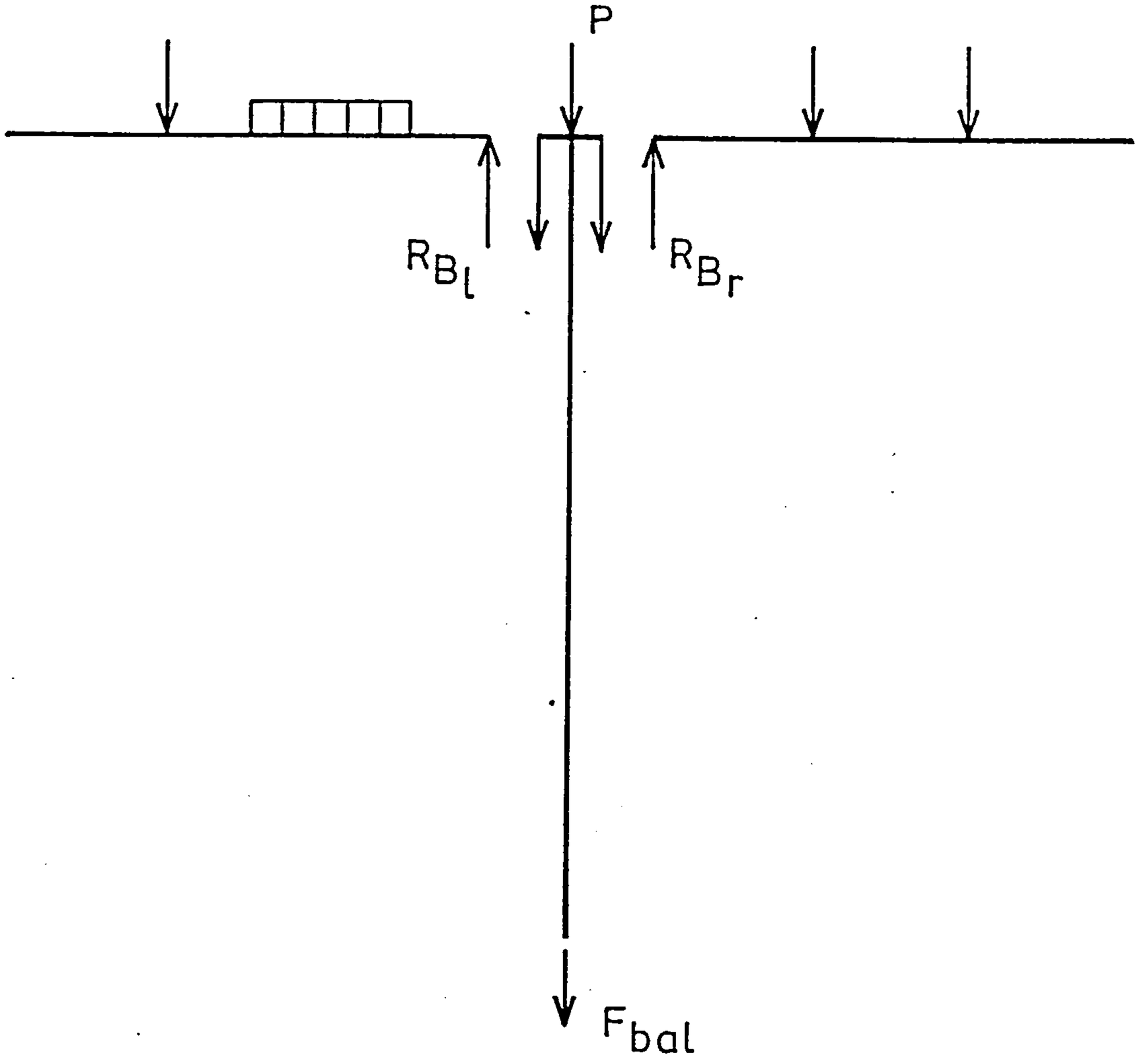

FIG.4·9 FREE BODY DIAGRAM FOR THE CALCULATION OF OUT OF BALANCE FORCE DUE TO THE COLUMN LOAD

where R_{B_l} and R_{B_r} are the left and right beam reactions respectively.

If the boundary conditions at the far ends of the beams are such that the vertical deflections are not restrained, the force, F_{bal} is equal to the sum of the applied column and beam loads.

(2) Concentrated Lateral Loads:-

The out-of-balance force due to a concentrated lateral load is taken to be the algebraic sum of the shear forces just to the left and just to the right of the applied load in consideration. These shear forces are calculated by considering the equilibrium of the segment to which the load is applied (i.e the column or any one of the beams).

Consider a subassemblage of the general type shown in Fig-4.1 and assume that the column is acted upon by a set of lateral loads. Let the out-of-balance force corresponding to a load Q be required. The column may then be divided into two segments separated at the load in consideration as shown in Fig-4.10 in which the free body diagrams for these two segments are shown. In Fig-4.10, the column is rotated by an angle 90° for convenience only. Summing up moments about point A for the left part gives

$$M_1 = M_1 + M_{2,1} - F_{2,1}(\Delta_1-\Delta_2) - \sum_{i=1}^{N_1} Q_i a_i$$

where

N_1 = the number of concentrated lateral loads, Q_i applied to the left of the considered load.

M_1 = the internal moment at point A

$M_{2,1}$ = the internal moment just to the left of point B

$F_{2,1}$ = the internal force in the column just to the left of point B

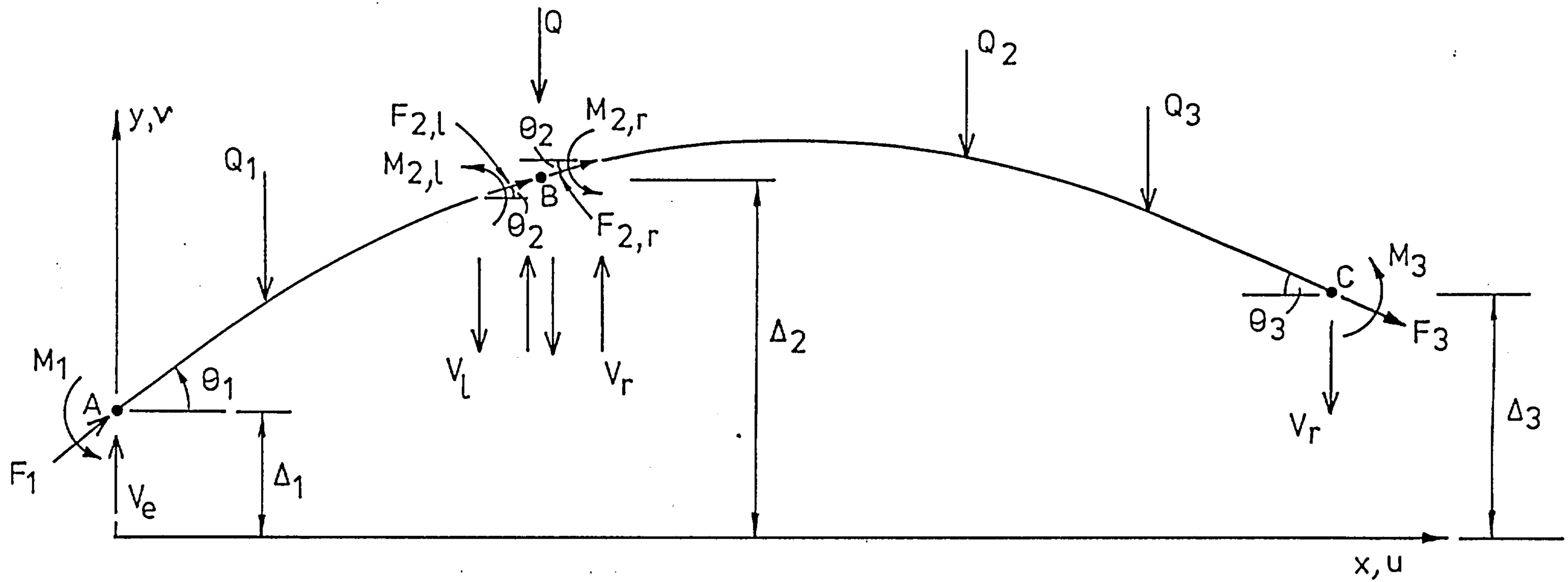

FIG. 4·10 FREE BODY DIAGRAM FOR A FRAME MEMBER FOR THE CALCULATION OF OUT-OF-BALANCE FORCE DUE TO A LATERAL LOAD Q

Δ_1 = total deflection (including initial) at point A

and

Δ_2 = total deflection (including initial) at point B

The shear force, V_1 just to the left of the load is

$$V_1 = \frac{M_1}{l_1} \tag{4.12}$$

Similarly, taking moments about point C of Fig-4.10, we get

$$M_r = M_{2,r} + M_3 - F_{2,r}(\Delta_2 - \Delta_3) + \sum_{i=1}^{N_2} Q_i a_i$$

where

N_2 = the number of concentrated lateral loads, Q_i applied to the right of the considered load.

M_3 = the internal moment at point A

$M_{2,r}$ = the internal moment just to the right of point B

$F_{2,r}$ = the internal force in the column just to the right of point B; and

Δ_3 = total deflection (including initial) at point C

The shear force just to the right of the load Q is then given by

$$V_r = \frac{M_r}{l_r} \tag{4.13}$$

The out of balance force may then be computed from the shear forces computed by eqns-4.11 and 4.12. Hence,

$$Q_{bal} = V_r - V_l$$

(3) Concentrated Moment:-

In this case, the out-of-balance moment is calculated as the algebraic sum of the moments just to the right and just to the left of the applied moment. These moments are taken directly from the calculated internal moments at the node at which the moment is applied.

4.8.4- Convergence Criterion:-

The Newton-Raphson iterative procedure as described in Sec-4.8.1 is carried out within each load increment until the analysis converges to the true equilibrium path. In other words, the corrective load ΔF_{bal} given by the relation

$$\Delta F_{bal} = P - F_{bal}$$

must satisfy the inequality

$$\frac{\Delta F_{bal}}{F_{bal}} = c \qquad (4.13)$$

where c is a pre-specified tolerance factor usually ranging between 0.001 and 0.01. Eqn.4.13 is applied to every applied load regardless of the status of the load (i.e. whether it is changing or constant at the present load increment). In this way, simultaneous convergence is obtained for all applied loads.

4.9- Printing Out Results:-

For every load increment, some important results are written in separate computer files. These results include:

(1) The total force in the column, the central deflection and the

moments and rotations at top and bottom ends of the column. This information is mainly used in plotting the P-Δ and interaction curves.

(2) M-Φ results for all the semi-rigid connections. These results are used in plotting the M-Φ curves as inferred from the analysis. They help in understanding the behaviour of the different connections.

(3) The moments and rotations at the left beam, the right beam and the column at the top and bottom ends of the column. Such information is useful in determining the variation of these moments and rotations during the loading process with the total force in the column.

(4) The flexural rigidity, EI, for all the elements along with the joint stiffnesses for all the semi-rigid joints. This information is useful in two ways:

(i) it helps in observing the spread of yield along the lengths of the columns and the beams.

(ii) the information may be used in calculating the G-values at the top and bottom of the column. These G-values are required for determining the effective length factor of the column following the AISC recommendations(2).

4.10- Incrementation of the Applied Loads:-

Once the actual response of the structure corresponding to a certain load level is accurately traced, the load is then incremented to continue the analytic procedure. A method of independently incrementing the applied loads was used. In this method, a load pattern

is given as input data for every applied load. Each of these patterns define the history of the corresponding load i.e. whether the load is increasing, decreasing or constant. It also defines the rate at which the load is to be incremented or decremented. A reference load value for each load is also included in input data.

The whole loading process is broken down into a number of load stages. In any one stage, any load may only increase, decrease or maintain its current value. In this way, very complicated load patterns may be considered.

Fig-4.11 shows an example of a loading process in which two loads P_1 and P_2 are applied. In this example, $(\alpha_{1,1}P_{1,ref})$ and $(\alpha_{2,1}P_{2,ref})$ were applied in the first load stage in which N_1 load increments were used. In the second load stage, $(\alpha_{1,2}P_{1,ref})$ and $(\alpha_{2,2}P_{2,ref})$ were applied in N_2 load increments. The load increments, $\Delta P_{1,1}$ and $\Delta P_{2,1}$ in the first load stage may be calculated from

$$\Delta P_{1,1} = \frac{\alpha_{1,1}P_{1,ref}}{N_1}$$

and

$$\Delta P_{2,1} = \frac{\alpha_{2,1}P_{2,ref}}{N_1}$$

while the load increments $\Delta P_{1,2}$, $\Delta P_{2,2}$, in the second load stage are given by

$$\Delta P_{1,2} = \frac{\alpha_{1,2}P_{1,ref}}{N_2}$$

and

$$\Delta P_{2,2} = \frac{\alpha_{2,2}P_{2,ref}}{N_2}$$

These load increments are then used to determine the contributions of

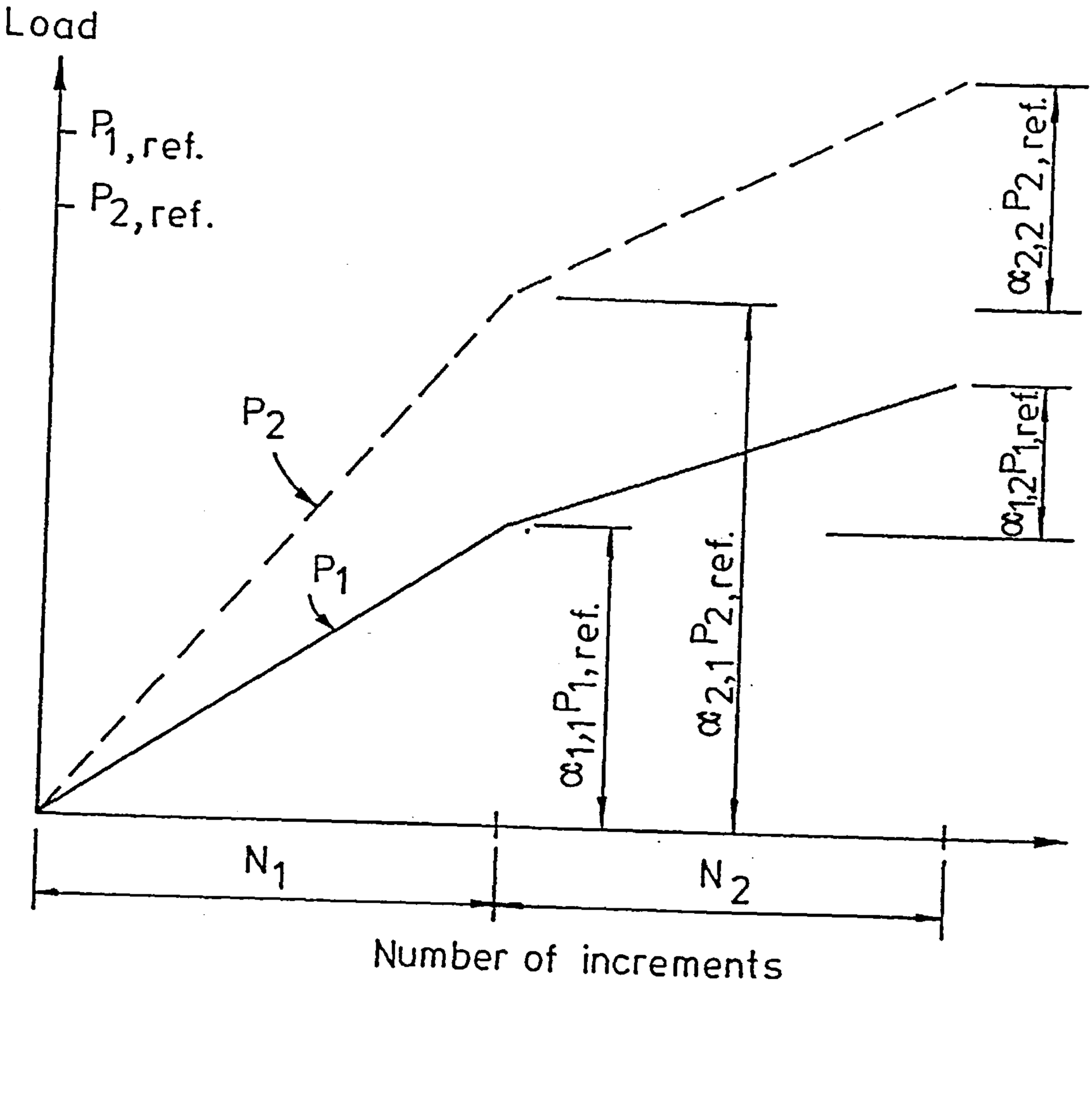

FIG. 4·11 AN EXAMPLE OF LOAD PATTERNS

the loads P_1 and P_2 to the total load vector as described in Sec-4.4.

In addition to the automatic load incrementation, the program includes an option in which the load may be manually changed. In this case, the program reads the new load level from the input data. It then works out the load increment as being the difference between the new load and the previous one.

4.11- Special Facilities:-

In addition to the steps described above, the program includes some special facilities which provide more flexibility to the application of the program. These facilities may be termed: restart and step back facilities.

4.11.1- Restart Facility:-

This facility is very useful when it is desirable to stop the analysis at some specified load to check on the predicted behaviour of the structure, such as, the spread of yield or the internal moments at a specified point. Once such checks were made, the analysis may then be restarted from the last load level.

The facility involves writing all the important variables to an unformatted file before coming to a stop. When the program is rerun, all these variables are read from this file. This procedure is achieved by declaring all the important variables in a number of common blocks and then using a special facility in the FORTRAN computer language to load all these variables into a number of one-dimensional arrays. These arrays may then be written to or read from the unformatted file whenever needed.

4.11.2- Step-back Facility:-

This facility is useful in automatically reducing the load

step when a failure condition is detected. Hence the maximum load may be determined with a reasonable accuracy. Once a failure condition has been detected while using a coarse load increment depending on the load pattern given in the input data, the programs then takes two actions:

(1) it steps back two load steps,

(2) it then continues the analysis using a fine load step. This load step is equal to a tenth of that calculated from the load pattern.

The facility is performed in a similar way as the restart facility. At the end of the i^{th} load increment, all the variables which may change value during the analysis and correspond to the $(i-1)^{th}$ load increment are read from an unformatted file and written to an other unformatted file. The current values for the variables are then written to the first file. Hence at the start of any load increment, the values for the variables corresponding to the last two load increments (i and i+1) are stored in two separate files. The method of storing this information is the same as described for the restart facility. Once the step-back facility is required, the information corresponding to the (i-1) increment may be readily read from the appropriate file.

5.1-Introduction:-

Any computer program that is intended to be used in analysing practical structures needs to be checked against experimental and possibly other theoretical results. This is to ensure that the program correctly represents the behaviour of the structure. Extensive checks have been made on the computer program described in chapter 4. These checks are presented in this chapter and in chapter 6. Both rigidly and flexibly connected structures have been considered. The structures that are presented in this chapter may be classified into three categories as follows:

(1) Rigidly connected frames with eccentrically applied axial column loads: in these frames, rigid beam to column connections are used. Only column loads were applied with or without small eccentricity.

(2) Rigidly connected frames with combined axial and lateral column loads: in which, as in the above category, rigid beam to column connections were used. A lateral column load was applied after the application of a pre-specified axial load.

(3) Flexibly connected frames with axial column load: in this category, flexible beam to column connections were used. A set of beam loads was applied in such a way that the full capacities of the connections were reached. Then an axial load was applied to the column head until failure occurred.

In the next sections, a detailed description and discussion of the comparisons corresponding to each of the above categories are presented. In addition, some design approaches will be utilized in these comparisons.

5.2- Rigidly Connected Frames with Eccentrically Applied Axial Column Loads:-

5.2.1- Description of Experimental Tests:-

The first stage of program verification is a comparison of the analyses produced by the computer program with the experimental results reported by Aoki and Fukumoto (39). These experimental results are obtained from tests made on the frame of Fig-5.1. The frame comprises a column and a beam at either end. Beam to column connections were found to behave as rigid joints. The column section was welded up from plates as shown in Fig-5.1 while the beams were made of rolled 194x150x9x6 shapes. Both the column and the beams were allowed to bend about their minor axes. Residual stresses in the column section were measured in a total of 30 specimens. The average shape of these residual stresses is represented by a solid line in Fig-5.2 which is based on data obtained from Fukumoto (65). A mean compressive stress of $0.31\sigma_y$ in the flanges was reported. Initial out of straightness was measured in 60 specimens (65) . It was found that the initial deflection at the column centre varied between 0.16 and 2.8 times $\frac{L_c}{10,000}$ where L_c is the column length (39). Although the reported nominal yield stress is 320N/mm^2, the average yield stress as computed from stub column tests was about 390N/mm^2 (39).

In the experimental program, Aoki and Fukumoto tested a series of frames of different column and beam lengths. A restraint parameter R defined by

$$R = 1.5 \frac{I_b}{L_b} \frac{L_c}{I_c} \qquad (5.1)$$

was varied between 0 and 1.0. In eqn-5.1, I_b and I_c represent the

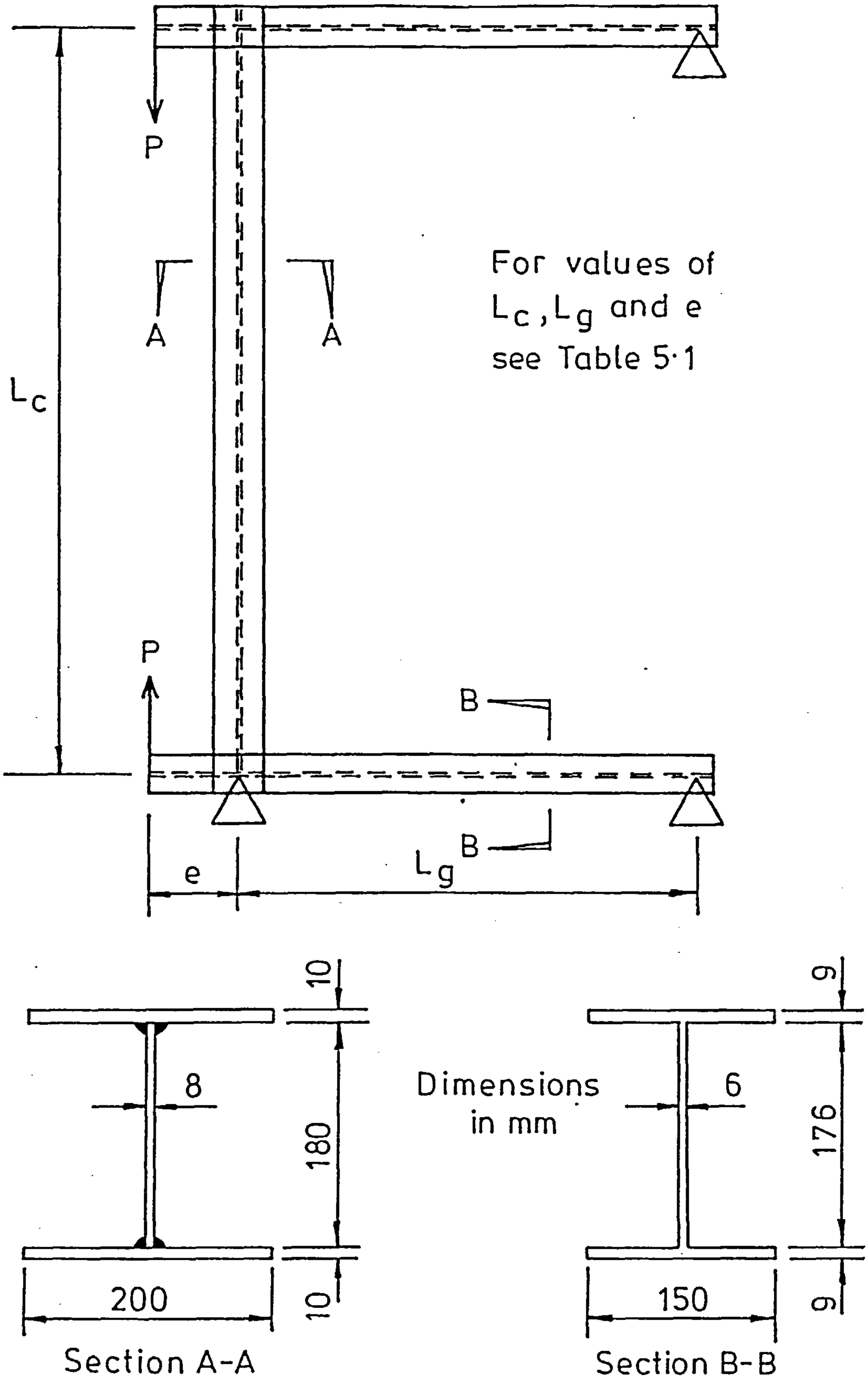

FIG. 5·1 SUBASSEMBLAGE TESTED BY AOKI & FUKUMOTO

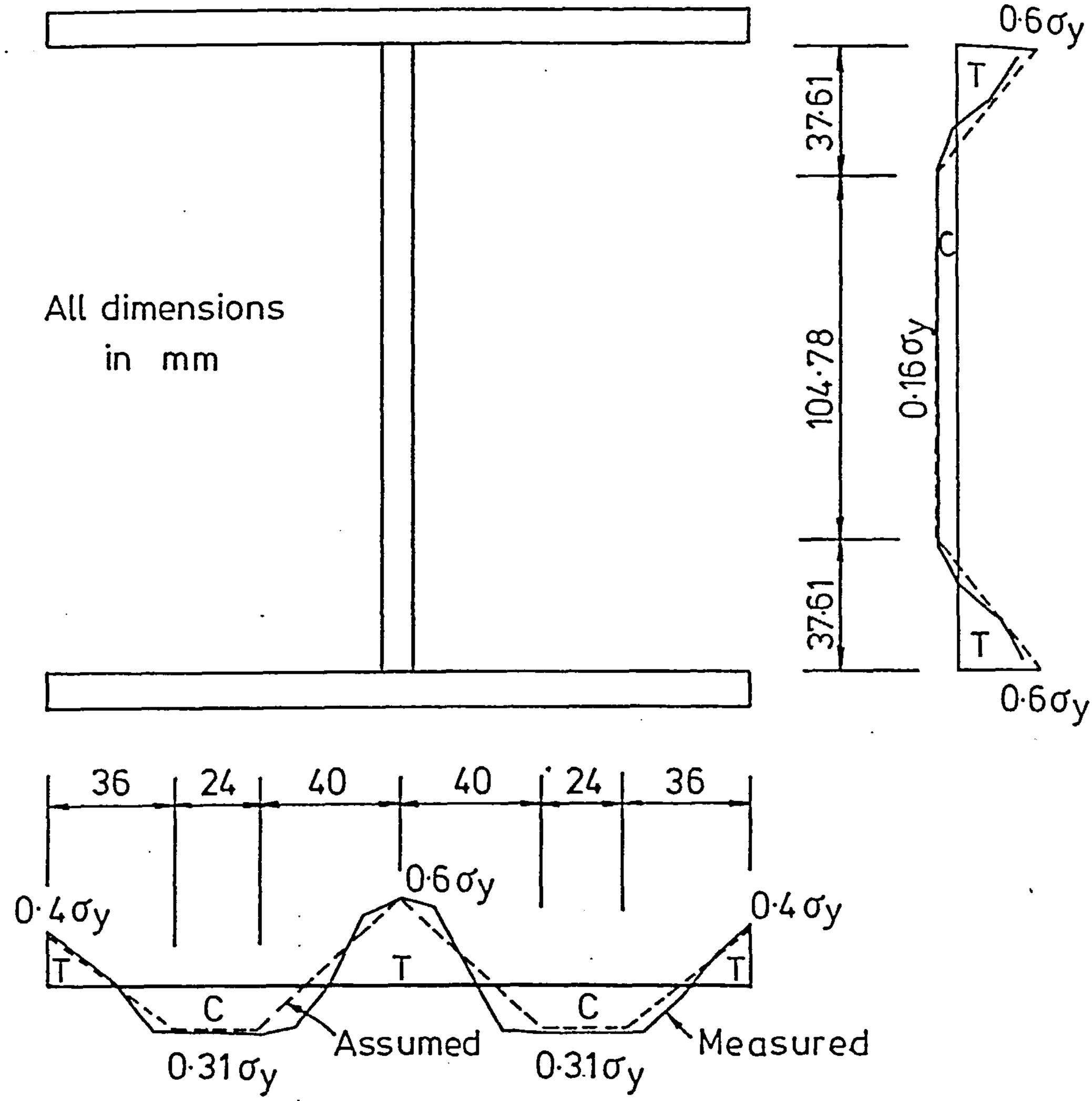

FIG.5·2 RESIDUAL STRESSES IN COLUMN SECTION OF FIG. 5·1 (WELDED)

second moment of area of the beam and column cross sections respectively and L_b is the beam span. The axial load was applied with a small load eccentricity which was was given the values of 0.0, r/20 and r/10 where r is the radius of gyration of the column cross section. The column slenderness ratio had values of 40, 70 and 100.

5.2.2- Comparisons Between Analytical and Experimental Results:-

The program was used to analyse the subassemblage of Fig-5.1 with the parameters mentioned above. One value of R corresponding to unity was used. A linear pattern for the residual stresses, shown in Fig-5.2 as the dotted line, was assumed. The initial out of straightness is assumed to be of a sinusoidal shape with a maximum value as indicated in Table-5.1 along with the assumed geometrical dimensions (column and beam lengths).

Table-5.2 shows a comparison between the maximum loads obtained by the program and those obtained from the experiments. In general, the two sets of loads were in close agreement with differences always within ± 5%.

Fig-5.3 shows a comparison between the analytical and experimental load deflection curves corresponding to a slenderness ratio of 40 and ZERO load eccentricity. The two curves are very close together indicating good agreement. Similarly, Figs-5.4 and 5.5 show the analytical and experimental load deflection curves corresponding to slenderness ratios of 70 and 100 with a load eccentricity of r/10 (i.e. 5mm). Again, the agreement between the two sets of curves is clear.

Shown in Fig-5.6 are the variations of the moment at the column end with the increasing column load for the cases considered in Figs-5.3 to 5.5. In each case, the moment in the column increases with

Table-5.1: Geometrical Dimensions and Maximum Initial Out of Straightness Assumed in the Analytical Simulations of the Subassemblage of Fig-5.1

L/r	L_c (mm)	L_b (mm)	$\frac{\Delta_o}{L_c}$ x10^4		
			e = 0.0 mm	e = 2.5 mm	e = 5.0 mm
40.0	1980.0	1210.0	-1.5	-0.5	-2.0
70.0	3465.0	2120.0	-2.8	-1.3	-2.8
100.0	4950.0	3025.0	-1.0	3.0	-0.5

N.B. initial column deflections to the left are assumed positive (Fig-5.1)

Table-5.2: Analytical Maximum Loads for the Subassemblage of Fig-5.1

Load Eccentricity (mm)	Slenderness Ratio					
	40.0		70.0		100.0	
	P_{max} (kN)	%age diff	P_{max} (kN)	%age diff	P_{max} (kN)	%age diff
0.0	2078.0	1.3	1881.0	4.2	1383.5	-2.0
2.5	2074.0	-0.1	1775.5	2.8	1337.0	-2.9
5.0	2049.0	4.5	1645.0	4.4	1156.0	0.6

N.B. %age diff = $(P_{max} - P_{exp})x100/P_{exp}$ where P_{max} and P_{exp} are the analytical and experimental maximum loads respectively.

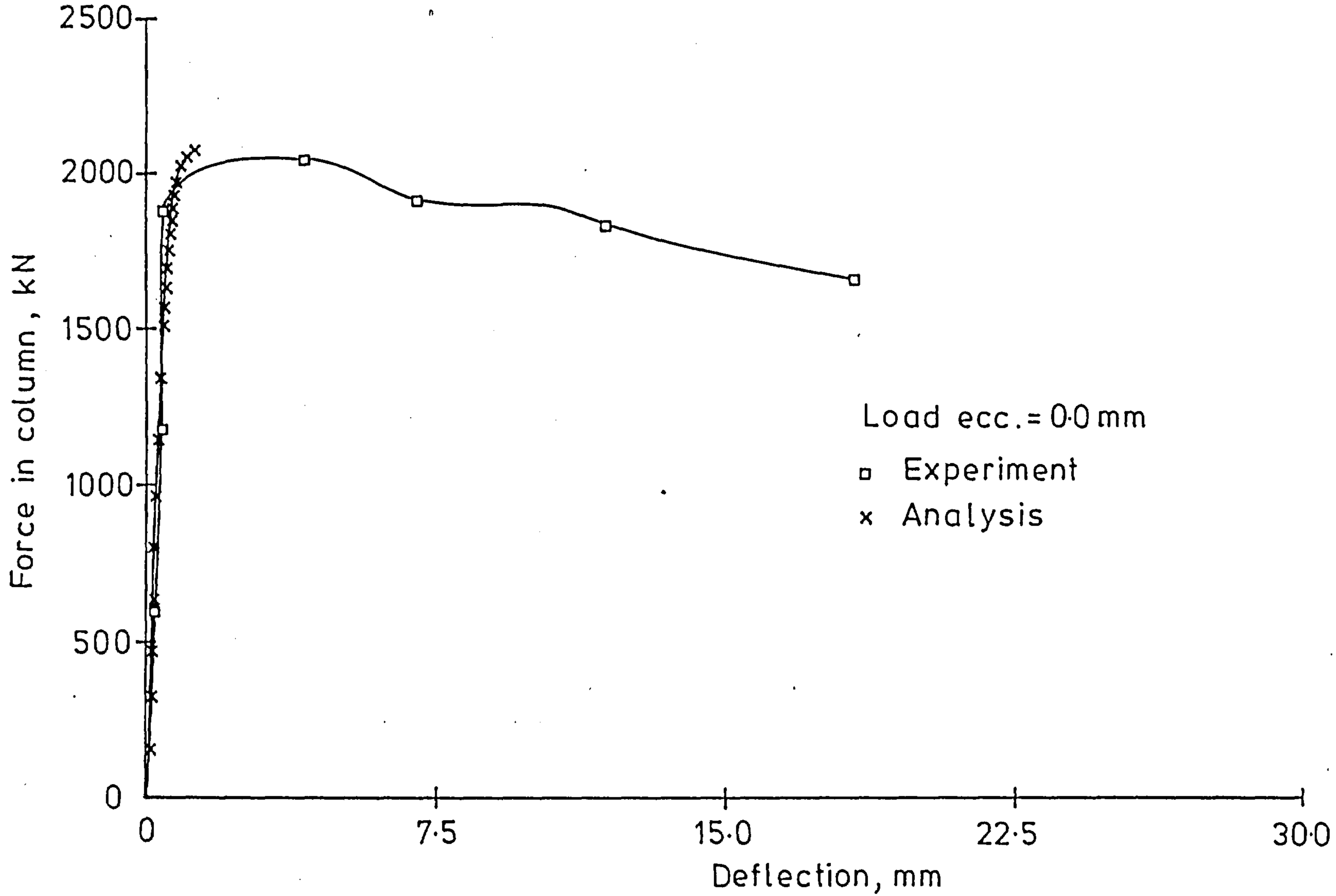

FIG. 5·3 LOAD – DEFLECTION CURVES FOR CASE A1 ($L/r = 40$)

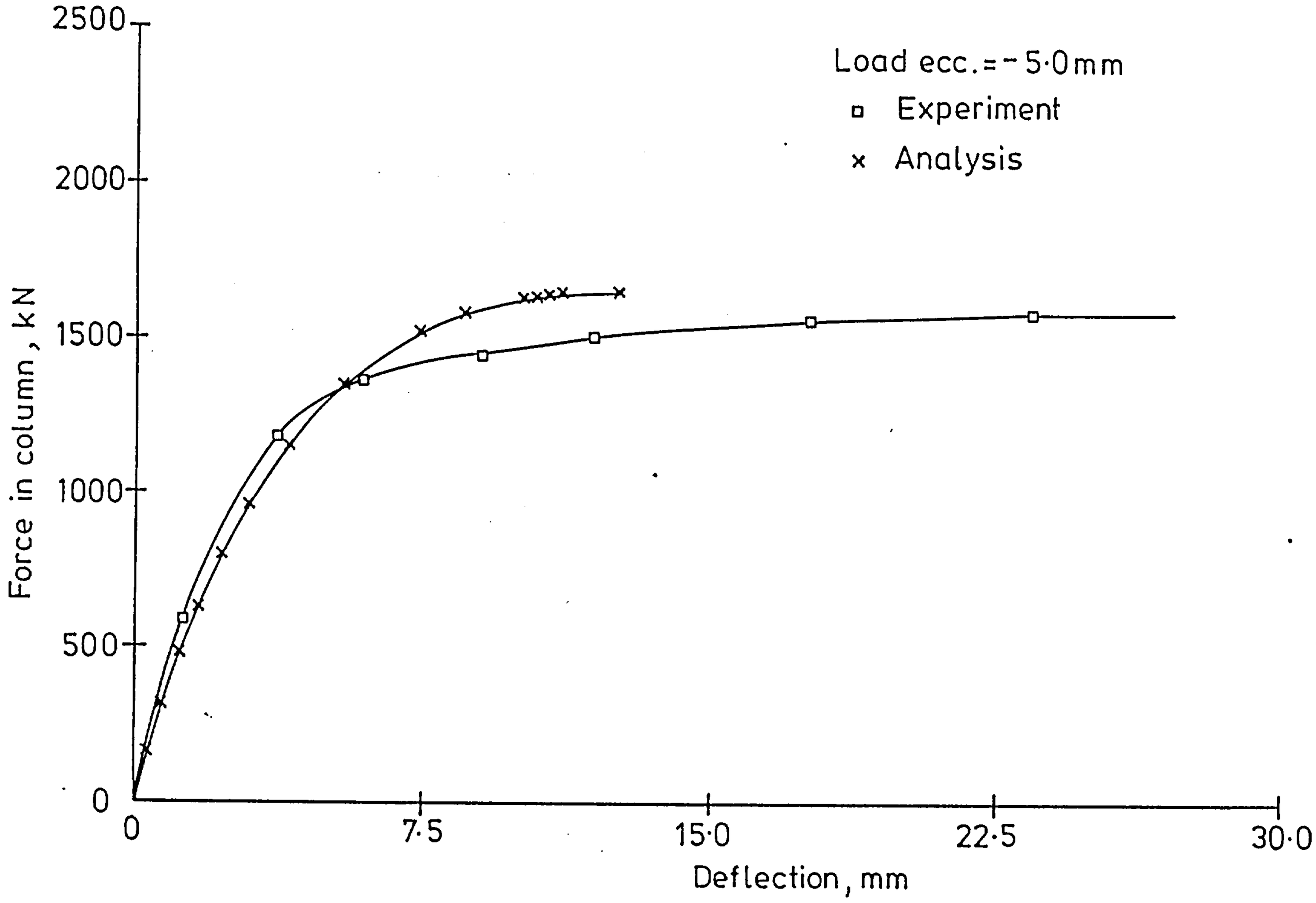

FIG. 5·4 LOAD - DEFLECTION CURVES FOR CASE B3 ($L/r = 70$)

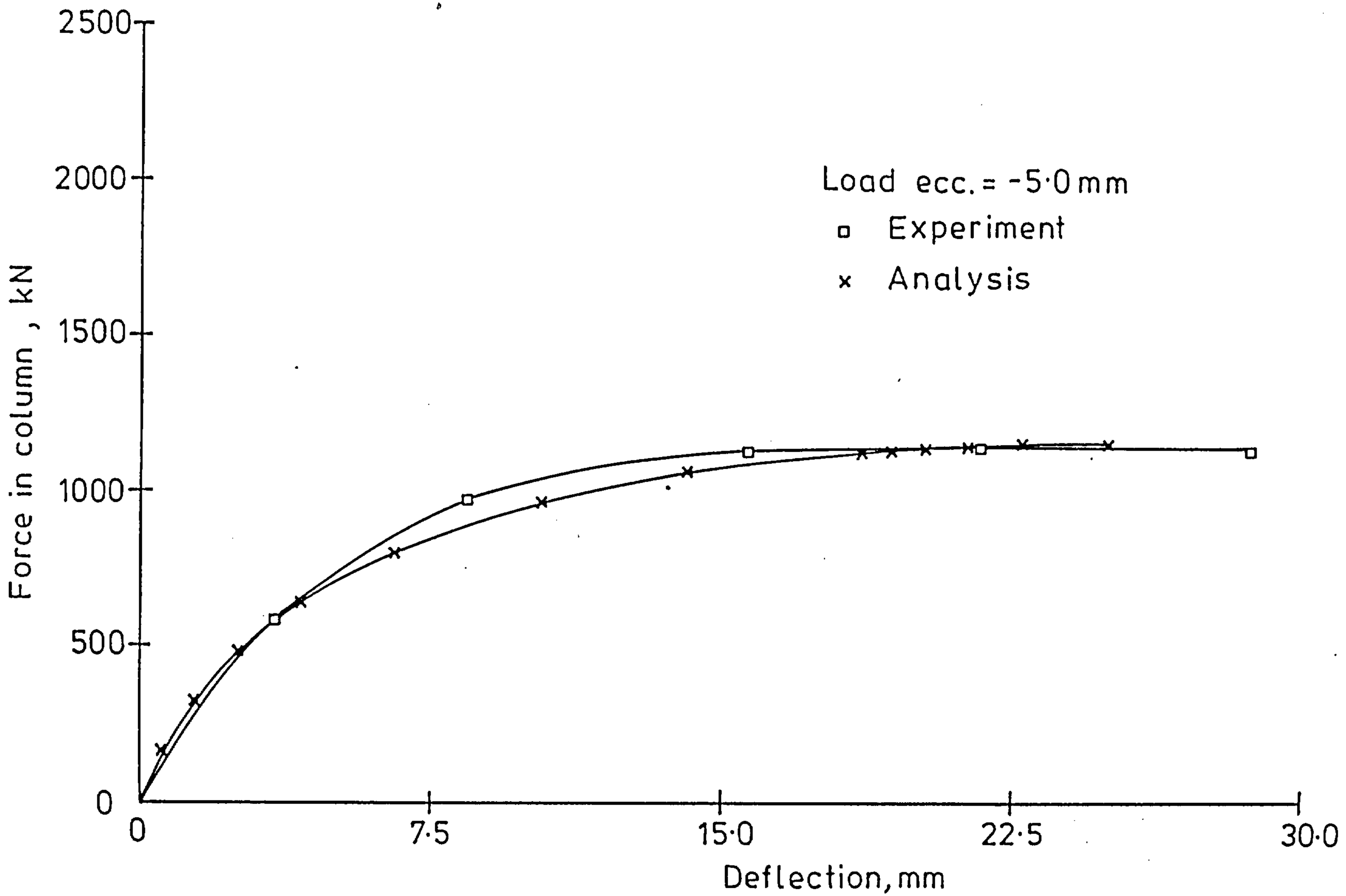

FIG.5·5 LOAD – DEFLECTION CURVES FOR CASE C3 ($L/r = 100$)

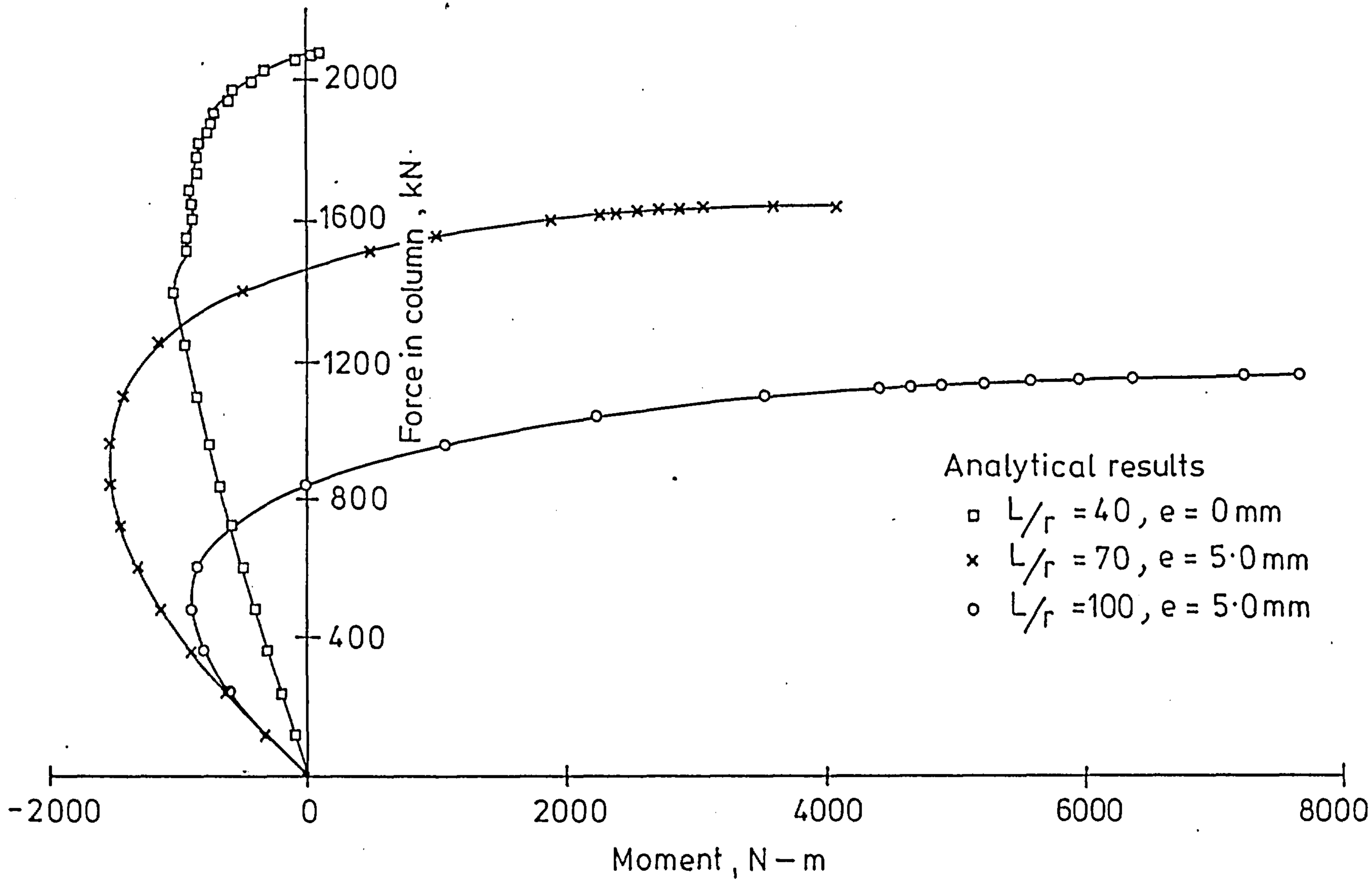

FIG. 5·6 VARIATION OF MOMENTS AT TOP END OF COLUMN

increasing column load until it reaches a maximum value. After attaining the maximum value, the moment decreases until it becomes zero and then changes sign. This reduction commences as the column starts to yield at its end (thus it becomes more flexible), hence redistributing stresses to the (now relatively stiffer) elastic members. This observation was also pointed out by Gent and Milner(42) in their tests on subassemblages similar to that shown in Fig-5.1. It may be seen that the relation between the column load and the moment in the case of L/r=40 and e=0.0mm is almost linear up to a point just before the maximum moment. In the cases of eccentric load (L/r=70 and 100), nonlinearity is more pronounced at lower load levels.

In Fig-5.7, the maximum loads for all the cases considered (Table-5.2) are plotted against the applied moments (load times eccentricity). Both experimental and analytical results are shown. It is clear that for all cases moments are small since the eccentricities used had small values. As mentioned above, the agreement between the experimental and the analytical results is close.

5.2.3- Calculation of Maximum Loads for the Cases of Concentric Axial Load Using Effective Lengths:-

The maximum loads for the subassemblage of Fig-5.1 under the action of concentric loads were computed for slenderness ratios of 40, 70 and 100 using the concept of effective length in conjunction with column strength curves. Three different methods were considered. These methods are:

(a) A method involving frame instability using stability functions,

(b) The method recommended by the BS5950 Part 1 The Use of Structural Steel in Buildings (1); and

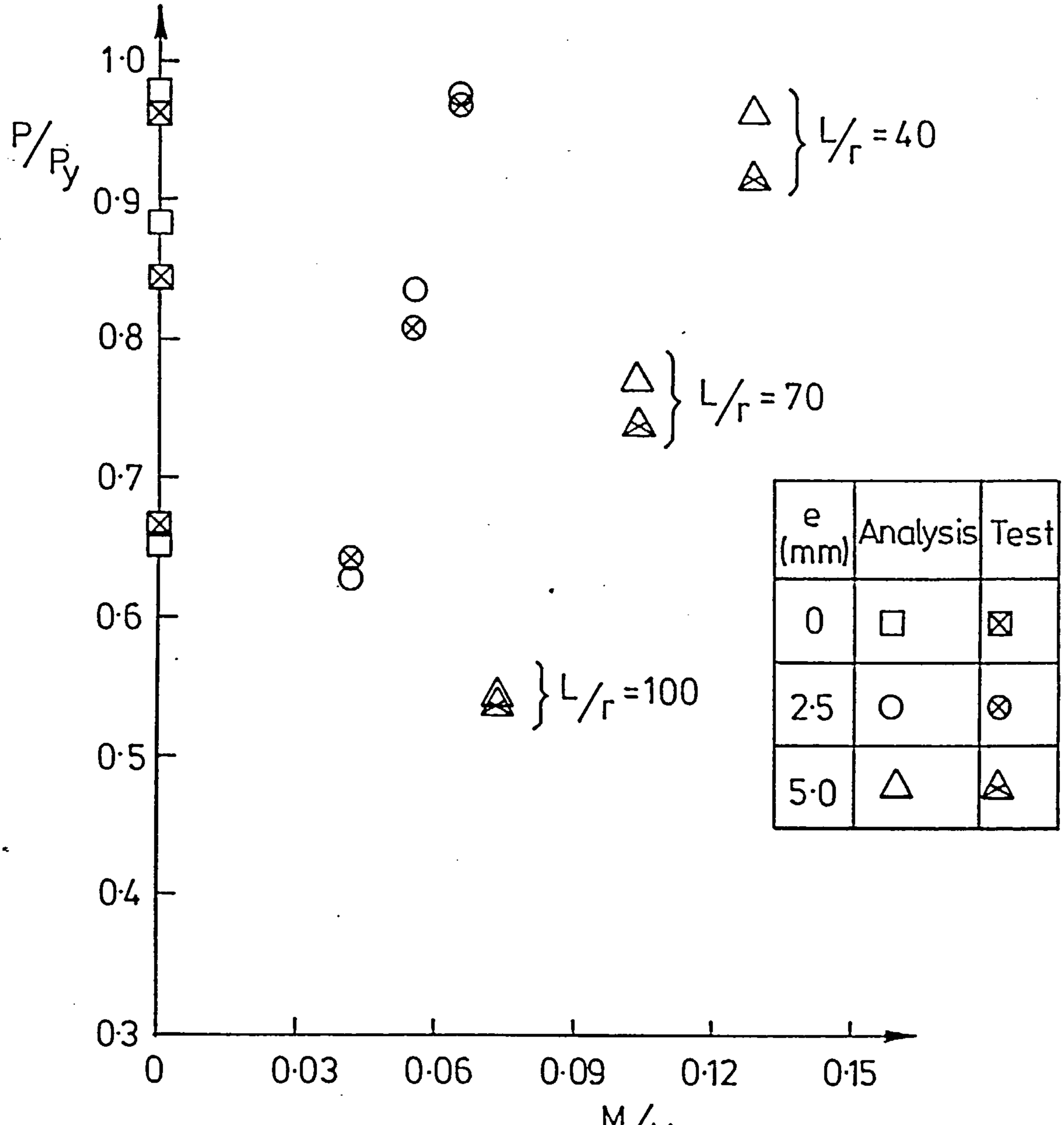

FIG. 5·7 INTERACTION PLOT FOR THE SUBASSEMBLAGE OF FIG. 5·1

(c) The method recommended by the AISC specification (2).

Two column strength curves were used. These curves are shown in Fig-5.8. The first curve was constructed using the author's program for a pin ended column. The other is the ECCS curve b which is appropriate for the group of sections including welded sections bent about their minor axes (63). Descriptions of each method as well as detailed calculations using these methods for L/r = 70 are presented below.

1- Stability Functions:-

This method may be found in many standard books that deal with frame instability (e.g. 18, 19). Consider the non-sway beam-column of Fig-5.9a. The moments at the ends of the member may be expressed by the slope deflection equation which includes the effect of the presence of the axial force. Hence,

$$M_{12} = k (s \theta_1 + sc \theta_2) \qquad (5.2)$$

in which s and c are stability functions depending on the level of the axial force, and k is the stiffness of the member defined as k = EI/L. In the case of no axial force, s and c take the values of 4 and 0.5 respectively hence reducing eqn-5.2 to the well known slope deflection equation for a beam element,

$$M_{AB} = 2 k (2 \theta_A + \theta_B) \qquad (5.3)$$

Applying eqn-5.3 for the moments at joint A and end B of the subassemblage of Fig-5.9b and eliminating θ_{BA} yields

$$M_{AB} = -3 k_b \theta_{AB} \qquad (5.4)$$

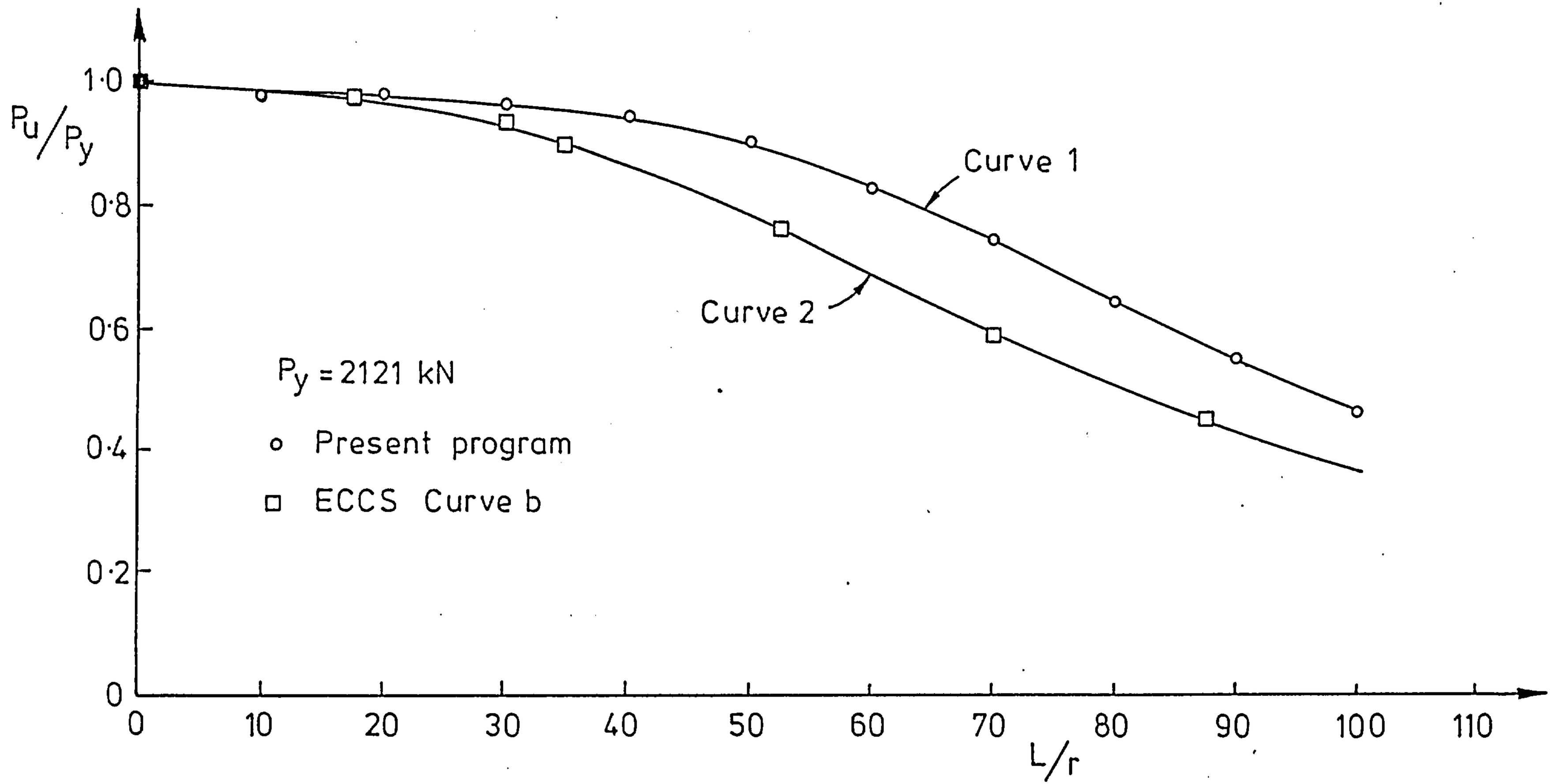

FIG. 5·8 COLUMN STRENGTH CURVES FOR A PIN-ENDED COLUMN

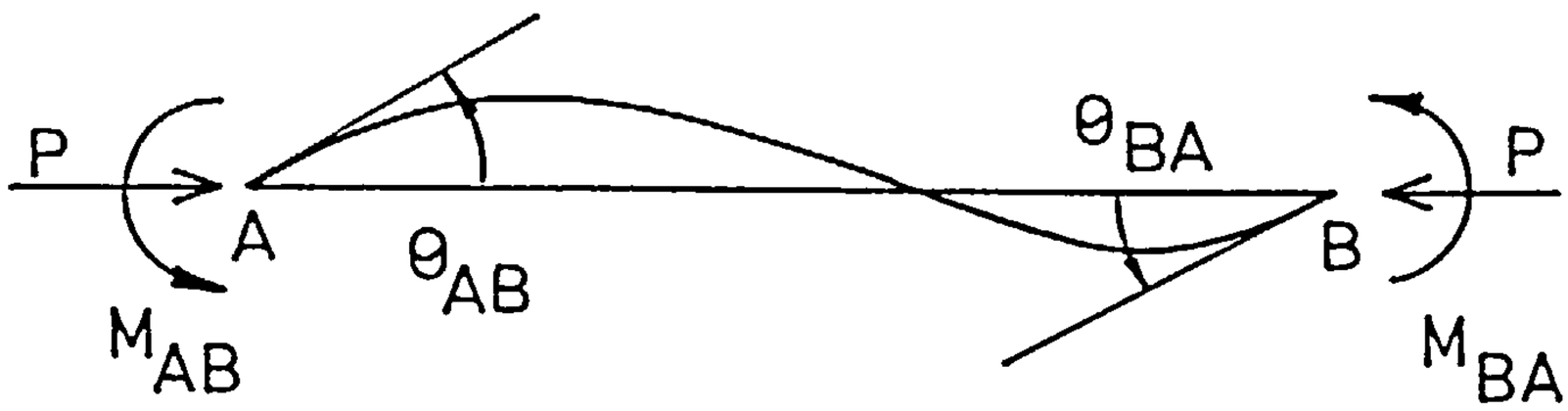

(a) Beam-column element

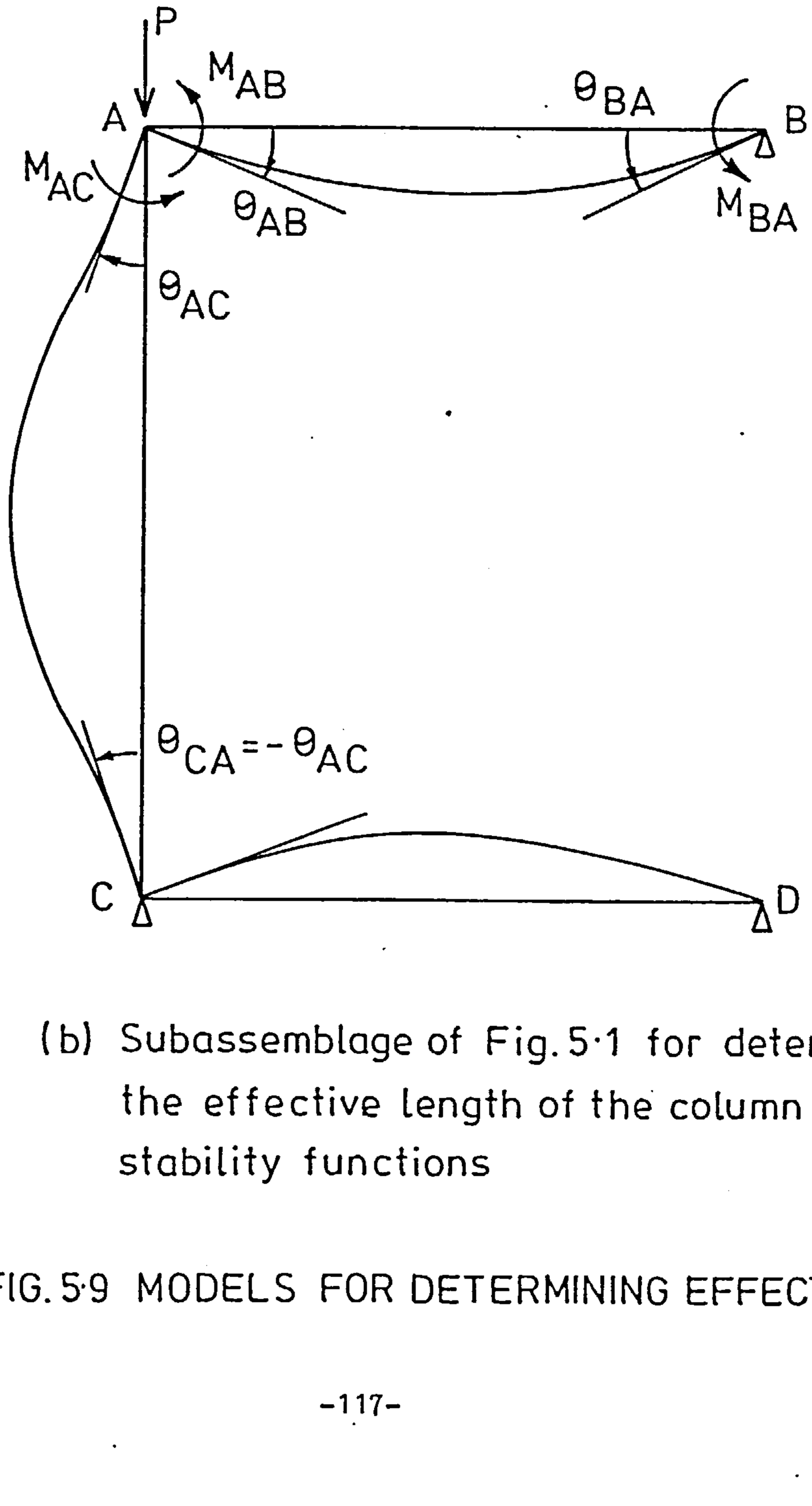

(b) Subassemblage of Fig. 5·1 for determining the effective length of the column using stability functions

FIG. 5·9 MODELS FOR DETERMINING EFFECTIVE LENGTH

in which k_b is the stiffness of the beam defined as EI_b/L_b. Now applying eq-5.2 for the moment M_{AC} at joint A of the subassemblage of Fig-5.9b bearing in mind that the end rotations, θ_{AC} and θ_{CA} are equal in magnitude and opposite in direction, then

$$M_{AC} = - k_c \, s \, (1-c) \, \theta_{AB} \qquad (5.5)$$

in which k_c is the stiffness of the column. Equilibirium of joint A requires that

$$M_{AB} + M_{AC} = 0 \qquad (5.6)$$

Hence, substituting for M_{AB} and M_{AC} from eqs-5.4 and 5.5 in eqn-5.6, the following relation is obtained

$$s(1-c) = - \frac{k_b}{k_c} \qquad (5.7)$$

In eqn-5.7, the right hand side is known and both s and c are dependent on the ratio of the axial force that is present in the column to the Euler load for this column. Tables for determining the stability functions s and c may be found in text books. Hence, eqn-5.7 may be solved for the ratio of the critical axial force to the Euler load. The effective length factor may then be calculated as the square root of the inverse of this ratio.

For the subassemblage under consideration (with $L/r = 70$), k_b and k_c are equal to 491216N.m and 792856N.m respectively. Hence eqn-5.7 gives

$$s(1-c) = -1.85865$$

hence,

$$\frac{P_{cr}}{P_E} = 1.635$$

The effective length factor may then be determined as 0.783. The effective slenderness ratio is then 0.783x70 = 54.8. Entering Curve-1 of Fig-5.8 with this slenderness ratio gives the ratio of the maximum load to the squash load for the column as 0.875. i.e. the maximum load is 1856kN. As the value of R was held constant for all the considered cases, eqn-5.7 is valid for all cases. Hence the same effective length factor is used to determine the effective slenderness ratios corresponding to L/r values of 40 and 100. Again using curve-1 of Fig-5.8, the maximum loads corresponding to L/r values of 40 and 100 may be found to be 2057kN and 1421kN respectively.

2- BS5950 approach:-

In the approach of Appendix E, the effective length factor is determined on the basis of using stiffness distribution factors for the top and the bottom of the column under consideration in conjunction with specially prepared charts for the effective length factor(5.4). The distribution factors for the subframe are given by

$$\bar{k}_i = \frac{\sum k_c}{\sum k_c + \sum k_b^i} \qquad (5.8)$$

in which

i =1 relates to top end of the column

=2 relates to bottom end of the column

k_c = I/L for the column

k_b^1 = I/L for top beam; and

k_b^2 = I/L for bottom beam

For the case considered above (L/r=70), the column and beam I/L values are $3849mm^3$ and $2385mm^3$ respectively. Hence the stiffness distribution factors for the top and the bottom of the column are

$$\bar{k}_1 = \bar{k}_2 = \frac{3849}{3849 + 0.5\ 2385} = 0.763$$

in which the factor 0.5 in the denominator is used to account for the fact that the far beam ends are hinged whereas the charts in BS5950 are based on fixed beam ends.

From the effective length factor charts the effective length factor may be found to 0.83. Upon entering curve-1 of Fig-5.8 with an effective slenderness ratio of 0.83x70=58.1, a maximum load of 1803kN is obtained. Once more, the stiffness distribution factors are the same for all the considered slenderness ratios. Hence the effective slenderness ratios corresponding to 40 and 100 are 33.2 and 83 respectively. The maximum loads corresponding to these cases are 2040kN and 1319kN respectively.

3- AISC Approach:-

The method recommended by the AISC specifications involves the use of beam to column stiffness ratios, G_{top} and G_{bottom} for the top and bottom ends of the column (2). The stiffness ratio for any joint is given by

$$G = \frac{\sum I_c/L_c}{\sum I_b/L_b} \qquad (5.9)$$

in which the summation, as in eqn-5.8, indicates summing the contributions of similar members. The beam stiffness, I_b/L_b,

corresponding to any beam with its far end hinged is multiplied by 1.5. Alignment charts (2) may then be used to evaluate the effective length factor. The maximum load may then be found in the same way as mentioned in the above two methods.

For the subassemblage of Fig-5.1, the value of G at the top and that at the bottom of the column is equal to 1.076 (which is the inverse of R calculated using eqn-5.1). From the alignment charts, the effective length factor may be found to be 0.78. Now following the same procedure of using the column curve of Fig-5.8, the maximum loads corresponding to slenderness ratios of 40, 70 and 100 may be found to be 2057kN, 1856kN and 1421kN respectively.

Table-5.3 shows a comparison between the maximum loads obtained by the above three methods as well as those obtained from the tests and the present analyses. It can be seen that all three methods described above gave close predictions of the maximum loads even though these methods are based on elastic effective length factors. However, it should be pointed out that the the use of the effective length factors was in conjunction with a column strength curve in which the parameters pertaining to the subassemblage under consideration were closely simulated. In addition, this column curve was constructed by a program in which full account was taken of yielding. In other words, the inelastic behaviour of the column was accounted for, at least partially, by the use the column strength curve of Fig-5.8.

The computations which led to Table-5.3 were repeated for all the cases but with the use of the column strength curve known as ECCS curve b (63) and reproduced in Fig-5.8 as curve-2. This curve is applicable to a family of shapes which include welded shapes bent about their minor axes. It can be seen by comparing Tables-5.3 and 5.4 that,

Table-5.3: Maximum Loads * in kN: Comparison of Different Approaches for Predicting the Load Carrying Capacity of the Column of Fig-5.1: Concentric Loads

Approach	Slenderness ratio		
	40.0	70.0	100.0
Stability functions	2057.0	1856.0	1421.0
BS5950	2040.0	1803.0	1319.0
AISC	2057.0	1856.0	1421.0
Experiments	2052.0	1834.0	1411.0
Present program	2078.0	1881.0	1383.5

* Based on the use of elastic effective length factors in conjunction with a column strength curve constructed using the present program

Table-5.4: Maximum Loads * in kN: Comparison of Different Approaches for Predicting the Load Carrying Capacity of the Column of Fig-5.1: Concentric Loads

Approach Approach	Slenderness ratio		
	40.0	70.0	100.0
Stability functions	1980.0	1620.0	1120.0
BS5950	1941.0	1510.0	1039.0
AISC	1973.0	1620.0	1120.0
Experiments	2052.0	1834.0	1411.0
Present program	2078.0	1881.0	1383.5

* Based on the use of elastic effective length factors in conjunction with ECCS column strength curve b

in all cases, the use of the ECCS curve resulted in lower estimates of the maximum loads. The reason for this is that the column curve constructed by the program is always above the ECCS curve except at very low slenderness ratios where both curves coincide as the ECCS curve is an approximate lower bound to the strength for the family of shapes.By comparing the maximum loads estimated by the ECCS curve with the experimental ones, it may be concluded that the use of the ECCS curve appears to be rather conservative for the cases under consideration.

5.2.4- Calculation of the Maximum Loads for the Subassemblage Under the Action of Eccentrically Applied Axial Load:-

When the axial load is applied with an eccentricity, a moment as well as the axial load act simultaneously on the column. The effect of the moment is to introduce additional deflections in the column through which the axial load produces additional moments in the column. This is known as the interaction between the applied moments (in this case the axial load times load eccentricity) and the applied axial load. Design specifications usually recommend the use of interaction formulae which account for the presence of both types of loads. In this section, the recommendations given by two design specifications are presented.

(1) AISC Specification:-

The AISC specification (2) recommends that the following two interaction formulae be satisfied

$$\frac{P}{P_{cr}} + \frac{M\ C_m}{M_m(1 - \frac{P}{P_E})} \leq 1.0 \qquad (5.10)$$

and

$$\frac{P}{P_y} + \frac{M}{1.18\ M_p} \leq 1.0 \qquad (5.11)$$

in which

P = the applied axial load

M = the applied moment

P_{cr} = critical load given by $1.7\ A_g \sigma_a$

P_E = Euler load

P_y = squash load

C_m = coefficient whose value can be taken as

$$0.6 - 0.4 \frac{M_1}{M_2} \geq 0.4$$

M_m = maximum moment that can be resisted by the member in the absence of axial load. For columns bent about their weak axes, M_m should be taken as M_p since no lateral torsional buckling takes place.

M_p = plastic moment

σ_a = allowable compressive stress corresponding to the effective slenderness ratio of the column.

For the subassemblage of Fig-5.1, the coefficient C_m is equal to 1.0. The Euler and the critical loads are given in Table-5.5 for all the slenderness ratios considered. In all these cases, M_m is equal to 79.1kN.m. The critical load is based on an effective length factor of 0.78 which corresponds to a value of G of 1.076. In eqn-5.10, the applied moment, M, is considered to be equal to P times the eccentricity, e. Solving eqn-5.10 for P, results in the required maximum loads that can be resisted by the subassemblage. These maximum

Table-5.5: Euler and Critical Loads Used in the AISC Interaction Formulae Relating to the Column of Fig-5.1

Slenderness Ratio	40.0	70.0	100.0
P_e (kN)	6913.0	2257.0	1106.0
P_{cr} (kN)	1933.0	1673.0	1345.0

N.B. The values in this table are based on an effective length factor of 0.78 which corresponds to G = 1.076

Table-5.6: Maximum Loads in kN Calculated by AISC and BS5950 Specifications for the Column of Fig-5.1: Eccentric Loads

L/r	Load eccentricity, e (mm)	AISC-Spec	BS5950
40	2.5	1786.0	1733.0
	5.0	1665.0	1558.0
70	2.5	1456.0	1460.0
	5.0	1330.0	1332.0
100	2.5	980.0	1041.0
	5.0	910.0	973.0

loads are shown in Table-5.6 for the considered slenderness ratios and eccentricities. Upon solving eqn-5.11 for P, the maximum load was found to be 2007kN and 1905kN for 2.5mm and 5mm eccentricities respectively. These loads are well above those obtained from the solution of eqn-5.10.

(2)- BS5950 recommendations:-

BS5950 recommends that two checks be made:-

i- Local capacity check : which is governed by the equation

$$\frac{P}{P_y} + \frac{M}{M_p} \leq 1.0 \qquad (5.12)$$

This equation is applicable for semi-compact sections. The cross section of the column of the subassemlage of Fig-5.1 is categorized as semi-compact.according to BS5950.

ii- Overall buckling check: which may be done in two ways

a- simplified approach which is governed by the formula

$$\frac{P}{P_{cr}} + \frac{m\ M}{\sigma_y\ Z_y} \leq 1.0 \qquad (5.13)$$

in which m is a factor depending of the relative values and signs of the end moments, σ_y is the yield stress and Z_y is the elastic section modulus about the y-axis of the section.

b- more exact approach in which the following equation should be satisfied

$$\frac{M}{M_c\ (\frac{1 - P/P_{cr}}{1 + 0.5\ P/P_{cr}})} \leq 1.0 \qquad (5.14)$$

in which M_c, for semi-compact sections, is defined as $\sigma_y \ Z_y$.

In eqns-5.13 and 5.14, P_{cr} is taken as the compressive design strength times the gross area of the section.

For the subassemblage of Fig-5.1, the effective length factor is 0.83. Hence the compressive strengths given in BS5950 for the kL/r values of 33.2, 58.1 and 83 are 362N/m^2, 299N/mm^2 and 210N/mm^2 respectively. Consequently the values of P_{cr} are 1969kN, 1626kN and 1142kN respectively.

The solution of eqn-5.12 leads to maximum loads of 1988kN and 1870kN for the 2.5mm and 5.0mm eccentricities respectively. Upon solving eqns-5.13 and 5.14, it was found that eqn-5.14 always governed the load carrying capacity of the column. The maximum loads corresponding to the considered slenderness ratios and load eccentricities are shown in Table-5.6,

5.3- Rigidly Connected Frames Under the Action of Combined Axial and Lateral Column Loads:-

5.3.1- Description of Test Program:-

In the second stage of program verification, the present computer program was used to simulate some of the tests conducted by English and Adams (38). In this series of tests, frames of the general type shown in Fig-5.10 were tested to examine their behaviour under the action of the applied loads shown in the figure. The frame comprises a column and one beam at either end which is connected to the column by means of a rigid beam to column connection. A variety of column and beam length combinations was used, although in this section, only two combinations are considered. Table-5.7 contains the geometrical

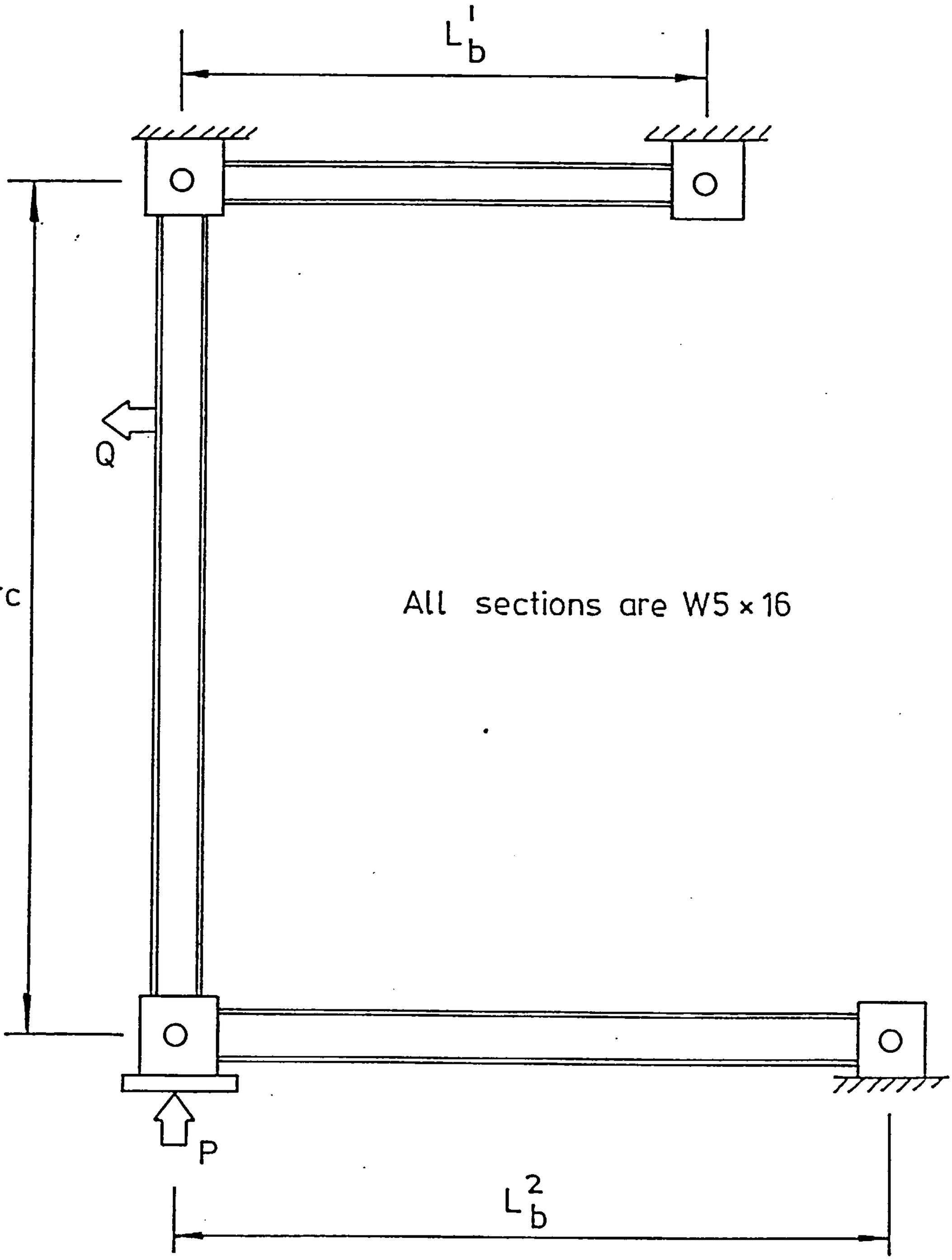

FIG. 5·10 SUBASSEMBLAGE TESTED BY ENGLISH & ADAMS

Table-5.7: Geometrical Dimensions and Location of Lateral Loads for the Subasemblage of Fig-5.10

Case	L_c (mm)	L_b^1 (mm)	L_b^2 (mm)	Location of Lateral Load
BC-5	4320.0	3050.0	4265.0	Midheight
BC-6	6096.0	3050.0	4265.0	Upper Third Point

Table-5.8: Comparison of Maximum Loads in kN for the Subassemblage of Fig-5.10

Case	Maximum Load (kN)		%age diff
	Experiment	Analysis	
BC-5	34.71	34.7	-0.03
BC-6	57.41	57.4	-0.02

N.B. %age diff = $(Q_{anal} - Q_{exp})x100/Q_{exp}$ where Q_{anal} and Q_{exp} are the analytical and experimental maximum lateral loads respectively.

dimensions of the frame corresponding to the two cases considered. Also shown in Table-5.7 is the location of the point of application of the lateral column load.

All sections were made of W5x16 shapes of CSA G40.12 steel of a specified minimum yield stress of 303N/mm^2 (38). The average value for the yield stress was found to be 361N/mm^2. A mean value for the strain hardening modulus was found to be 4.96kN/mm^2 which commences at a mean strain of 0.017. All lengths were cold straightened by rotarizing. Rather low residual stresses resulted from such treatment. Fig-5.11 shows the average measured residual stresses as reported in ref 64.

The set of applied loads consisted of an axially applied column load and a lateral column load. The axial load was applied first up to a pre-specified maximum value. Then the lateral load was applied up to failure. The loads, deflections and rotations at specified points were recorded.

5.3.2- Analytical Results:-

The frame of Fig-5.10 was analysed using the present computer program. The geometrical dimensions for the two considered cases are shown in Table-5.7. A yield stress of 353N/mm^2 was assumed. The modulus of elasticity, E, was taken to be 204kN/mm^2 while that of strain hardening was assumed to be 5kN/mm^2. A linear pattern of residual stresses with a maximum compressive stress of 0.1 σ_y was assumed. This pattern is shown as dotted lines in Fig-5.11. Although the column was cold straightened, a small amount of crookedness was assumed to be present. The maximum initial deflection was assumed to be $\frac{L_c}{10,000}$. As in the experimental procedure, the loads were applied in two load stages.

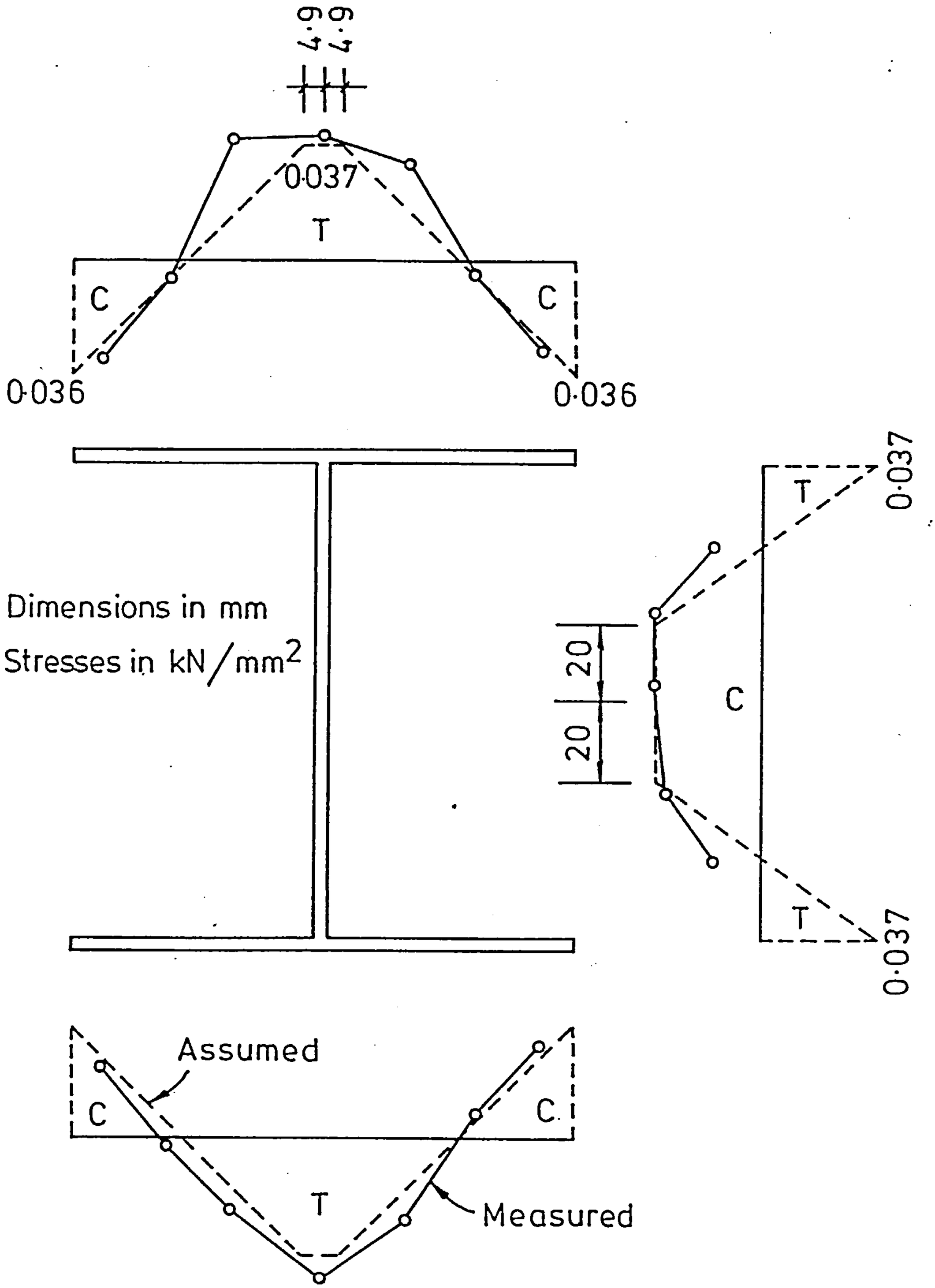

FIG. 5·11 RESIDUAL STRESSES IN W5 x 16 SECTION

The full pre-specified axial load was applied in the first load stage in ten equal load increments. In the second load stage, the lateral column load was applied until failure occured. Throughout this operation, the axial column load was maintained at a constant value.

5.3.3- Discussion of Results:-

Table-5.8 shows a comparison between the predicted and the experimental maximum lateral loads for the two cases considered in this study. It is evident from this table that there is good agreement between the two sets of maximum loads. Shown in Figs-5.12 and 5.13 are the analytical and experimental load deflection curves for the two considered cases. Generally, the analytical load deflection curve followed the same trend as the experimental curve. However, the difference in the deflections at any particular load is not small especially at higher load levels.

In Fig-5.12, two extra curves are shown. The first one was obtained by English and Adams (38) using an elastic-plastic analysis which take account of the formation of plastic hinges at various sections along the column and the beams. The other curve is obtained from a "plastic zone" computer program developed at the University of Alberta (28). In this latter program, both axial and lateral loads were applied simultaneously. It is clear that both the Alberta and the present programs produced very close load-deflection curves.

5.4- Flexibly Connected Frames Under the action of Axial Column Loads:-

5.4.1- Description of Experimental Program:-

The third type of frame that was analysed by the program in order to compare its results with experimental tests is the subassemblage of Fig-5.14. This subassemblage was tested by Bergquist

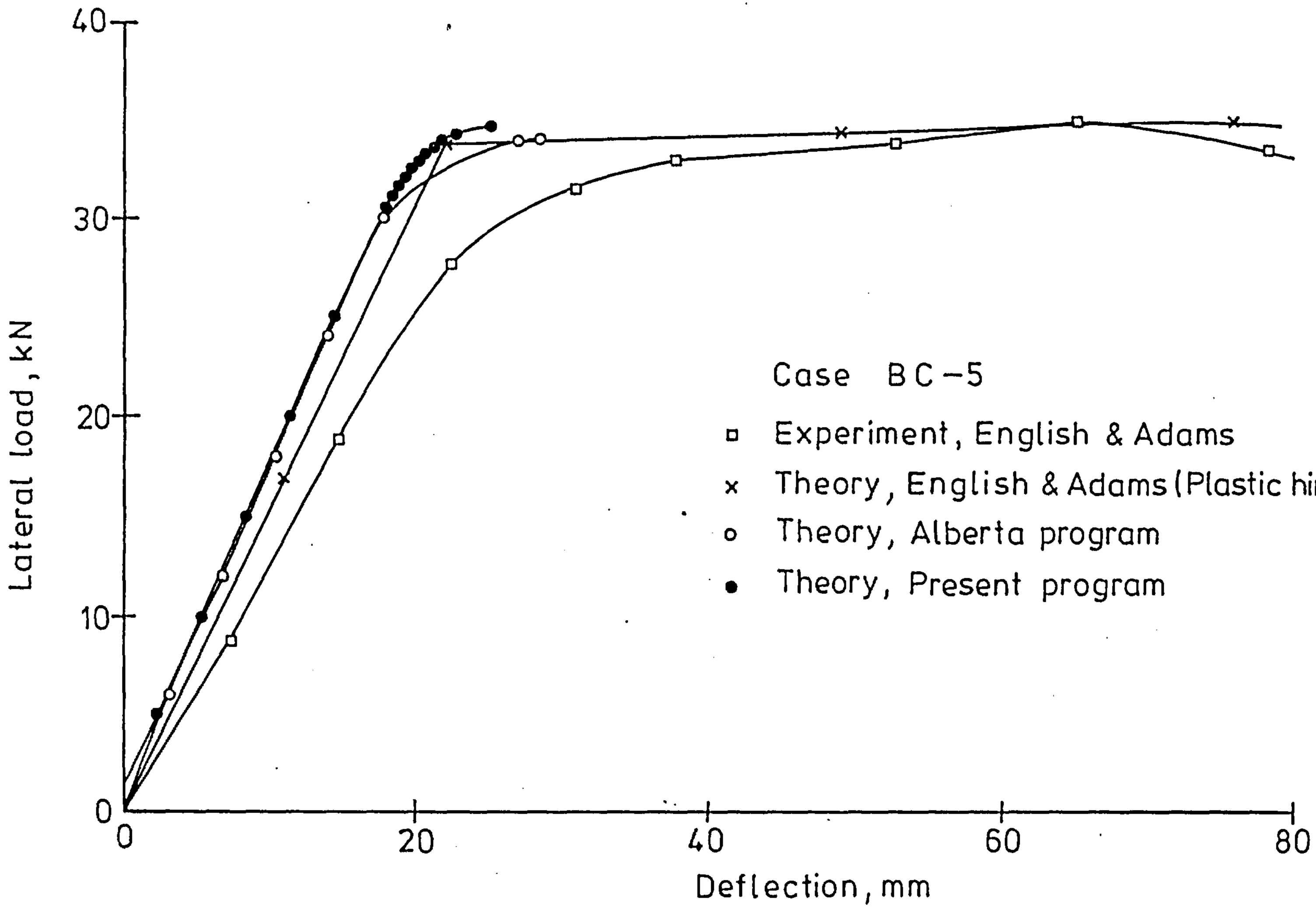

FIG. 5·12 LOAD-DEFLECTION CURVES FOR A RIGID FRAME (ENGLISH & ADAMS)

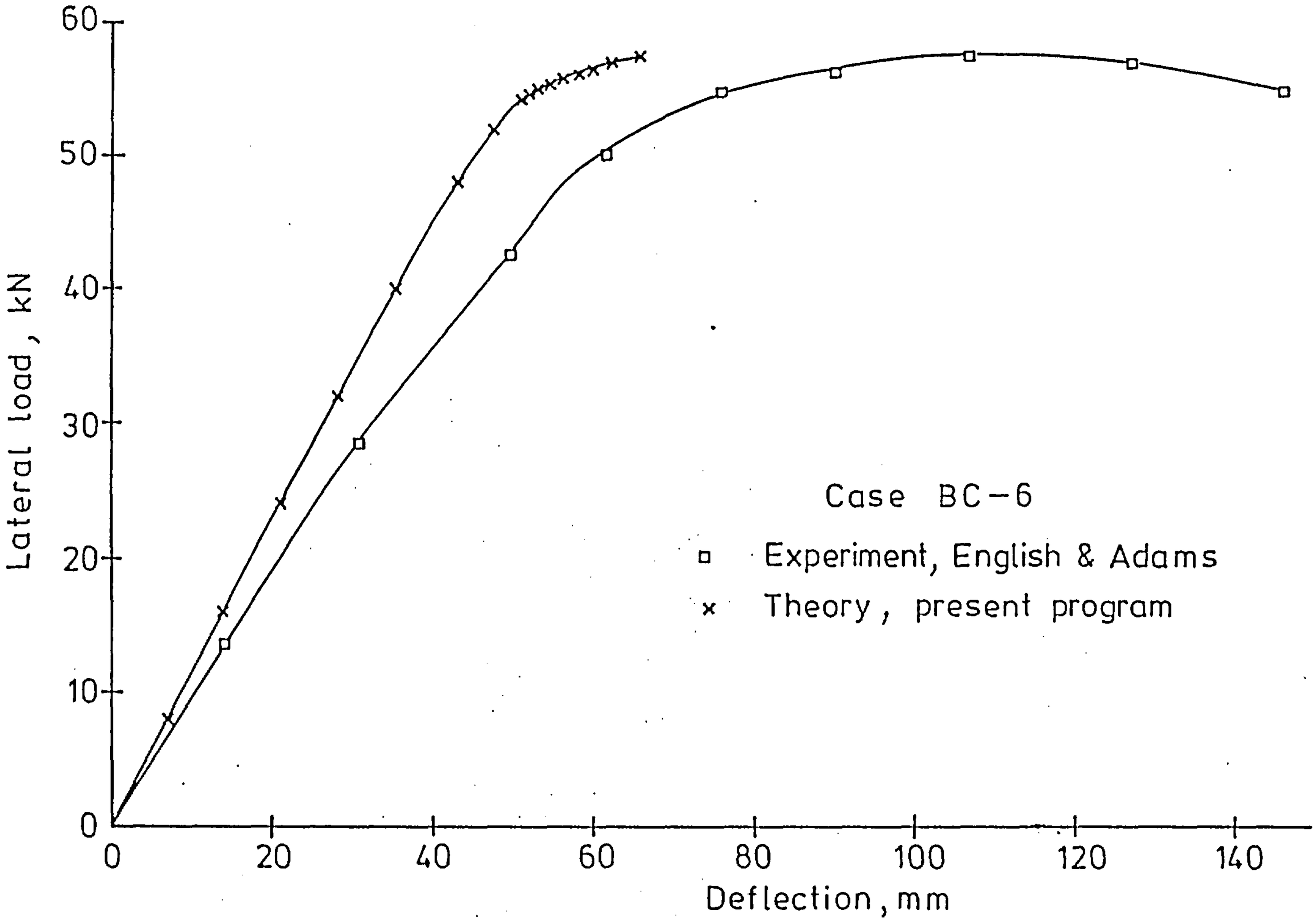

FIG.5·13 LOAD-DEFLECTION CURVES FOR A RIGID JOINTED FRAME (ENGLISH & ADAMS)

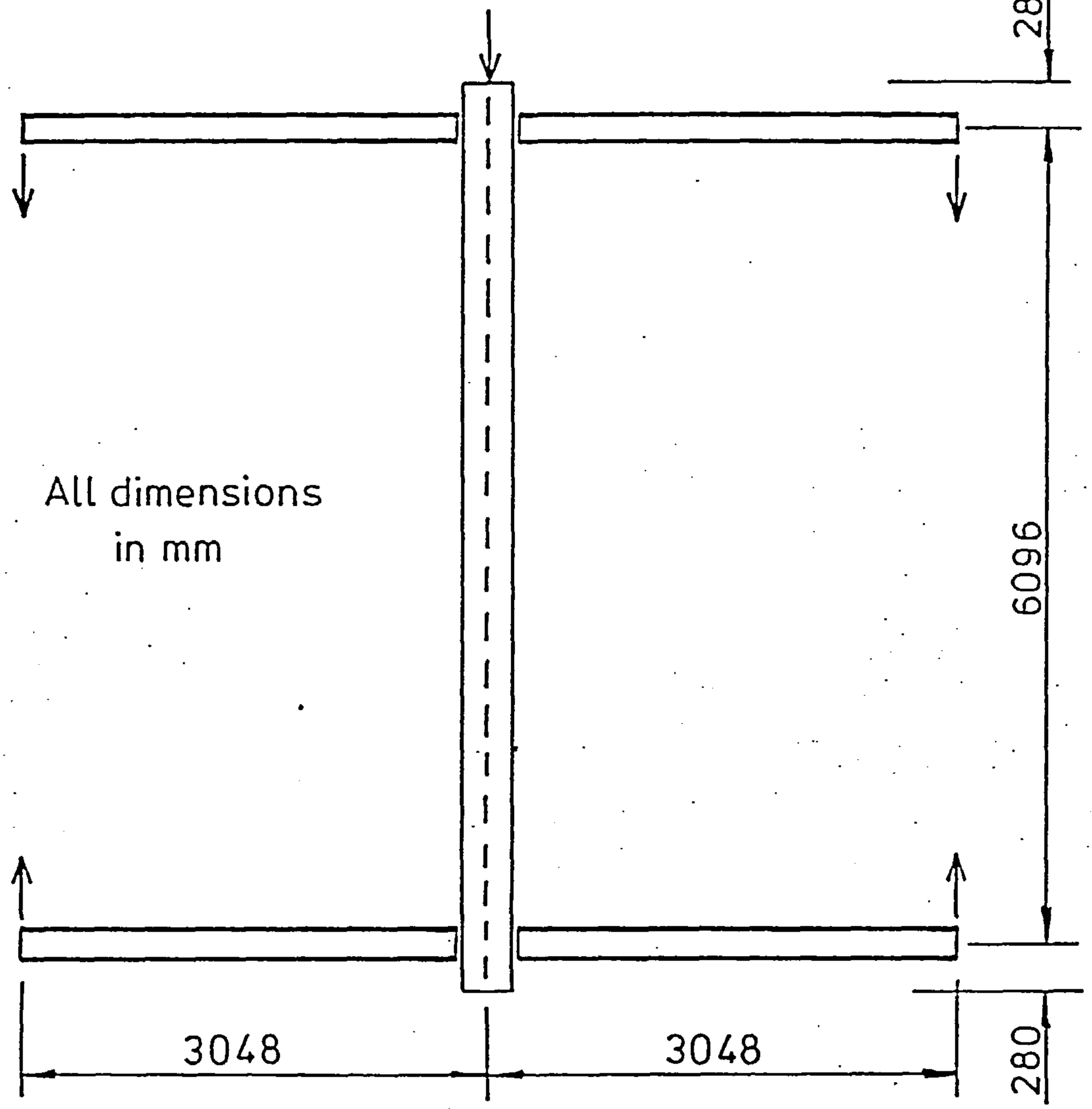

FIG. 5·14 SUBASSEMBLAGE TESTED BY BERGQUIST

(40). It comprised a column and two beams connected at each end by flexible beam to column connections. The column was a W10x29 shape and was allowed to bend about its minor axis. All beams were W10x21 shapes and were allowed to bend about their major axes. Flexible double web cleat beam to column connections were used.

The M-Φ characteristic for a typical connection is shown in Fig-5.15a. This moment-rotation curve was obtained by conducting a separate test on a connection similar to that used in the subassemblage but connected to the flanges of the column rather than the column web. It was found that this difference in connection detail appeared to have a significant effect of the stiffness of the connection(40). Shown in Fig-5.15b is the M-ϕ relationship for the top connections as inferred from limited measurements taken during the subassemblage test. Bergquist reported that the initial stiffness of the connection was reduced from 1.028×10^6 in the connection test to 0.4×10^6 N.m/rad in the subassemblage test.

In the subassemblage tests, a concentrated load was applied at the far end of each beam parallel to the column by α self contained system consisting of a hydraulic tension ram, 25mm threaded rod and a 44.5kN tension load all connected in series, so that all loads were equal. This resulted in all connections following their loading M-ϕ curves which were found to be very close to each other indicating similar connection behaviour (40). This stage of loading resulted in the whole connection capacity (Fig-5.15b) being consumed. Shut-off valves were attached to the rams to permit independent operation of the left and right rams (40). By shutting the valves, it was also possible to hold the rams in any desired position. In the second stage of loading, the valves were closed whilst a concentric axial load was

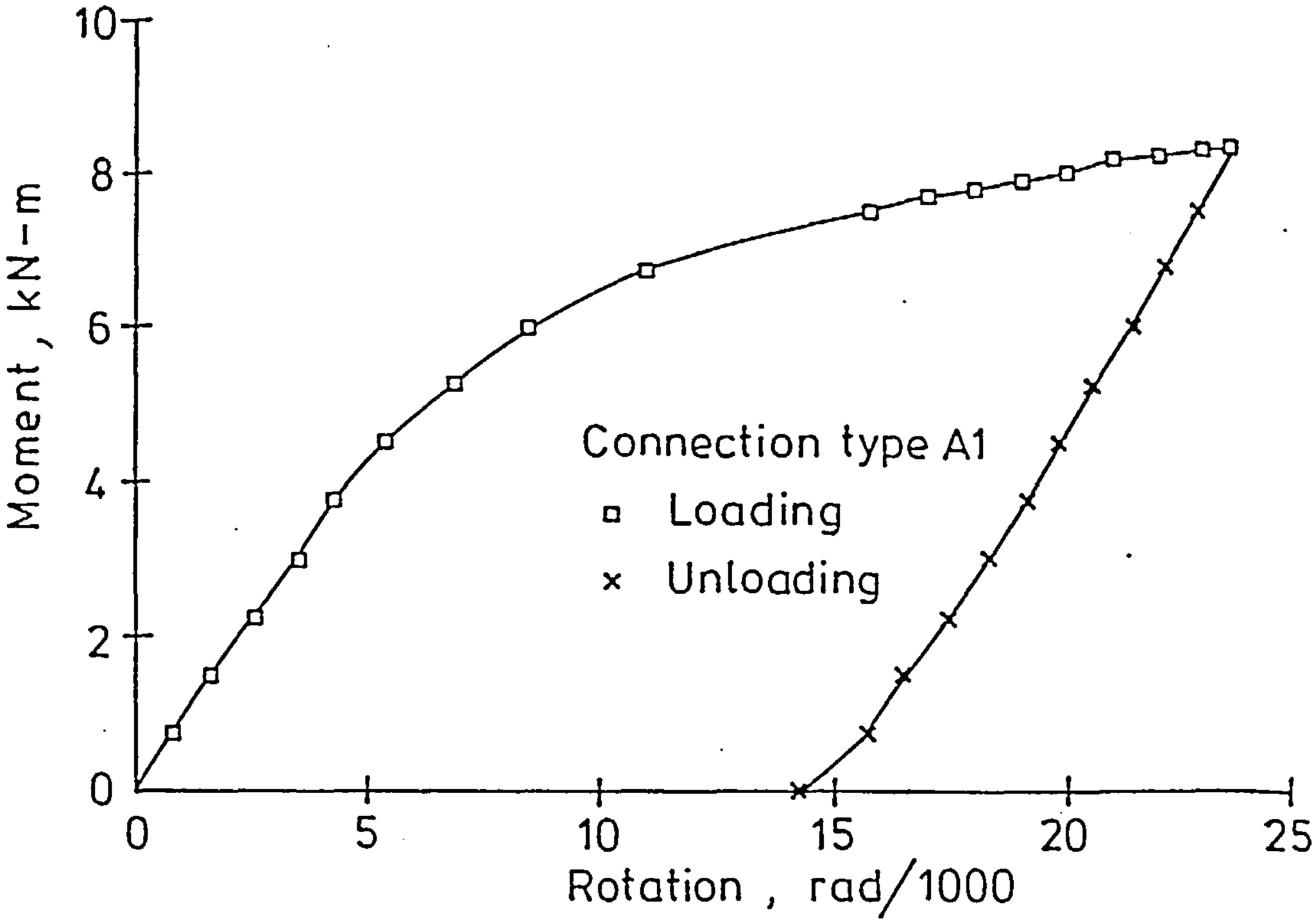

FIG. 5·15 a MOMENT-ROTATION CURVES FROM JOINT TESTS (BERGQUIST)

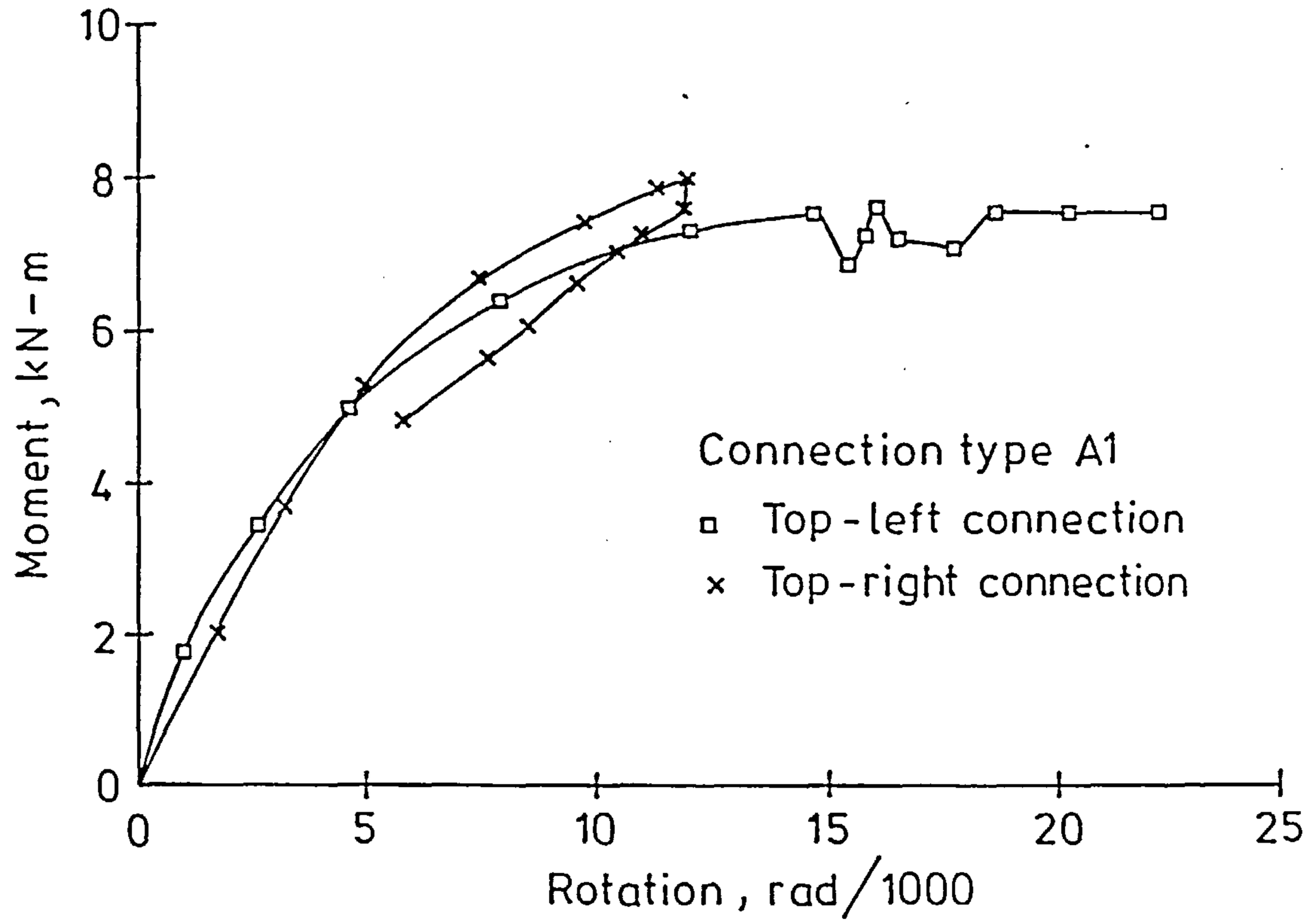

FIG.5·15b MOMENT-ROTATION CURVES AS INFERRED FROM BERGQUIST SUBASSEMBLAGE TESTS

increased until a sufficient number of data points (load and deflection) had been obtained while ensuring that the column did not yield. These data points were used in a Southwell plot in order to estimate the maximum load of the subassemblage. As the axial load was applied the left connections unloaded, while those on the right continued to load following a flat platau. The loading and unloading paths for the top connections are shown in Fig-5.15b. The load-deflection curve obtained from this test is shown in Fig-5.16. The test was terminated at a load level corresponding to about 87% of the maximum load which was found (using the Southwell plot) to be 547kN.

5.4.2- Comparisons of Analytical and Experimental Results:-

The subassemblage of Fig-5.14 was analysed using the present program. The M-ϕ curve shown in Fig-5.17 was used to represent the behaviour of all the connections. The loading part of this curve up to a rotation of about 0.014 radians is the same as the loading curve of Fig-5.15b. For rotations greater than 0.014 radians, an almost horizontal flat portion was assumed to represent the flat portion of Fig-15b. The unloading curve in both figures is the same. A half sine wave was assumed for the initial deflections with a maximum central deflection of 0.000425L (where L is the length of column from centre to centre of beams). This maximum value is the same as that obtained from the Southwell plot of the load-deflection results. As in the subassemblage test, the beams were assumed to be connected to the column web at about 280mm from each column end. A linear residual stress pattern in which the stresses vary between $\pm 0.3\sigma_y$ was assumed to be present in the column and beam sections. A yield stress of 365N/mm^2 was assumed while the modulus of elasticity was taken to be

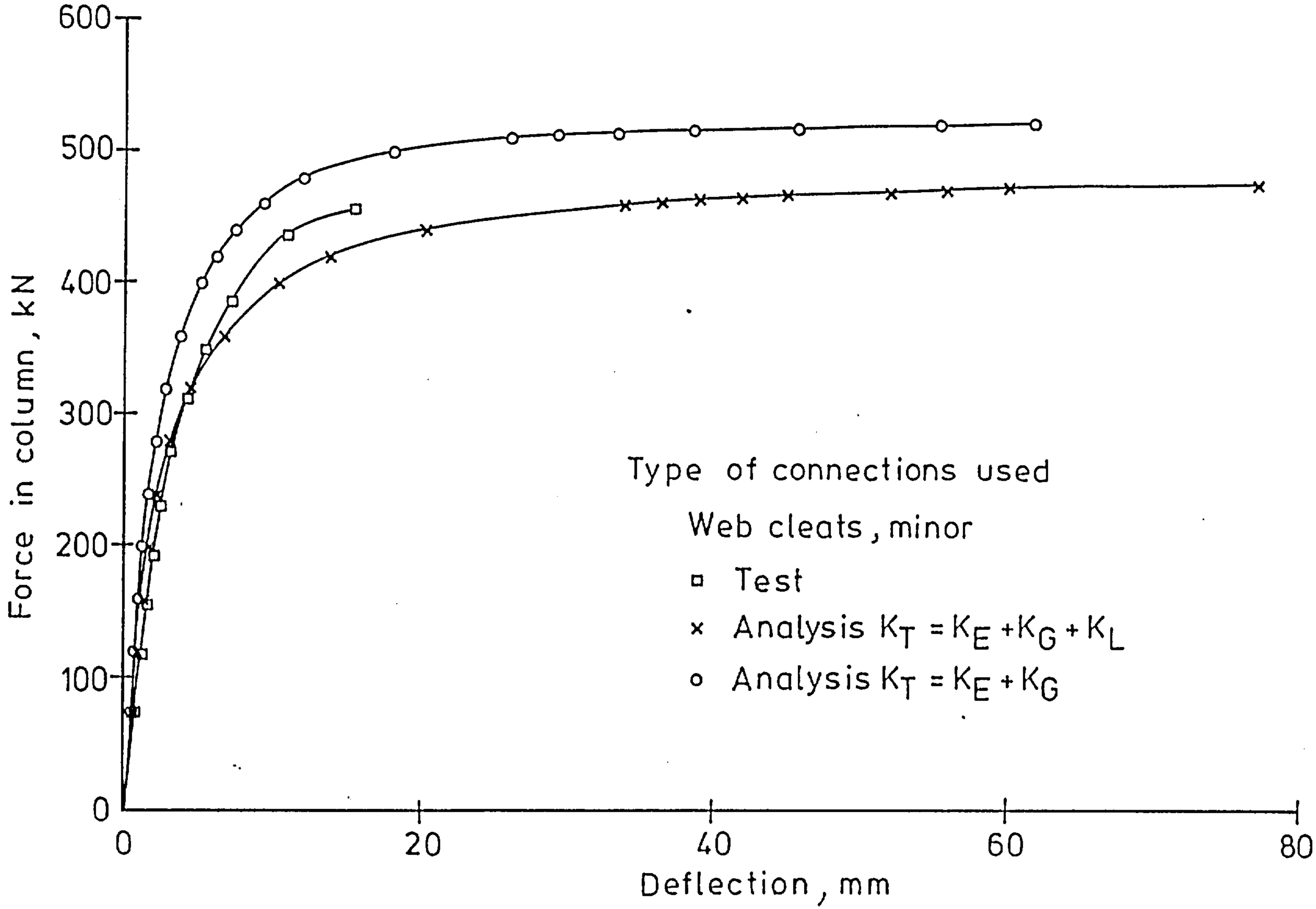

FIG.5·16 LOAD-DEFLECTION CURVES FOR BERGQUIST SUBASSEMBLAGE

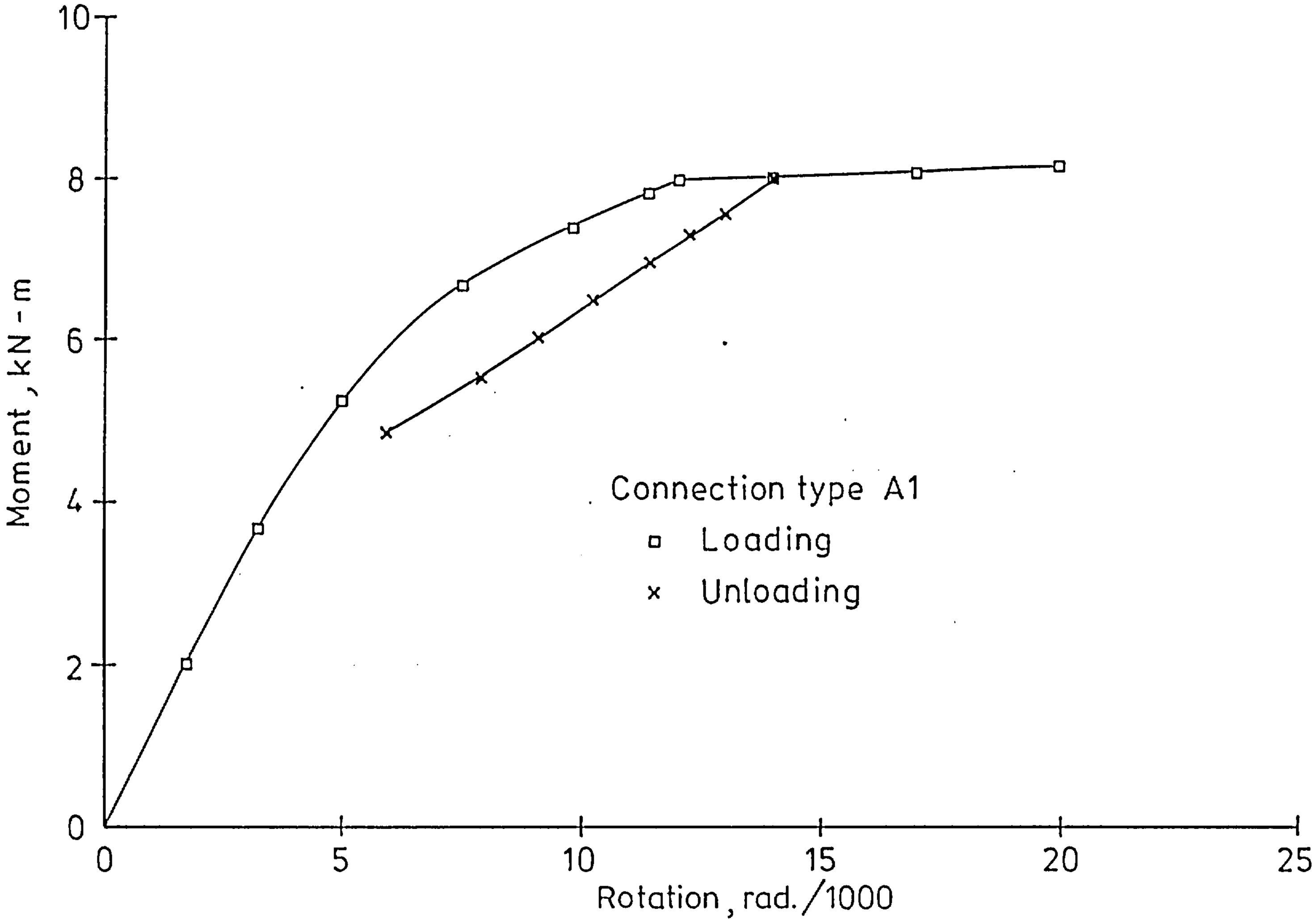

FIG. 5·17 MOMENT-ROTATION CURVES ASSUMED FOR THE BERGQUIST SUBASSEMBLAGE

215kN/mm^2. The yield stress was calculated from the reported plastic moment for the column section which is 52.67kN-m. The value of E was calculated using the reported EI value (determined from a test on a pin-ended column) in conjunction with the cross sectional dimensions of the column cross section. Since, as pointed out earlier, upon closing the shut-off valves, the beam ends could not undergo translational displacement in the direction of the beam loads, these ends were assumed to be hinged in the second loading stage in which the column load was applied. The beam ends were assumed to undergo no horizontal deflection at any stage. i.e zero side sway was assumed.

The analytical maximum load that could be resisted by the subassemblage was found to be 476kN which is 13.0% below the Southwell load. The load-deflection curve obtained from the analysis is shown in Fig-5.16. From this figure, it is clear that the analytical curve closely agrees with the experimental one. It should be pointed out that, as has already been mentioned, the experimental curve was terminated at a load level which is about 87% of the load predicted by the Southwell plot. The test was terminated at this stage because yielding was imminent. This was also confirmed by the analytical results in which it was found that the column started to yield at a load just below the maximum load. Consequently, it may be concluded that the load predicted by the Southwell plot is rather high since the Southwell plot can only predict the elastic maximum load of the structure. This point is further supported by the shape of the experimental P-Δ curve for which the tangent is almost horizontal indicating that the subassemblage was on the verge of failure when the test was terminated. It follows that the maximum load predicted by the Author's program as well as the analytical P-Δ curve may be accepted as

a very reasonable match to the experimental behaviour.

5.4.3- Discussion of Results:-

Careful consideration of the program output revealed that all sections remained elastic for almost all the loading stage. Not until the attainment of a load of 475kN did the column started to yield. However, there was an appreciable amount of yielding was present at the failure load (the reduced value of the flexural rigidity, EI, was about 75% of the elastic value). The fact that the column yielded prior to the attainment of the maximum load, makes it inappropriate to consider the problem as an elastic one.

It is interesting to investigate the effect of boundary conditions at the beam and column ends on the behaviour of the subassemblage. This is especially true since the boundary conditions at these ends were not well defined in the test. For instance, it was not reported in reference 40 whether the beam ends were prevented from horizontal movement or not. Moreover,closing the shut-off valves may only result in preventing the top beam ends from movements relative to the bottom beam ends. Both beam ends on one side of the subassemblage may still move parallel to the column length. It is not known whether the horizontal movements at the top and bottom column ends were restrained or not.

A possible variation of the boundary condition assumed in the original analysis (described above) of the subassemblage of Fig-5.14 is one in which the beam ends are free to move horizontally (but not vertically) while both column ends are prevented from horizontal movement. As before, the lower column end may not move vertically. The maximum load in this case was only slightly reduced (less than 1%

lower). If, on the other hand, the beam ends as well as the lower column end were assumed to be hinged while the top column end was assumed to be a free end, the maximum load increases above that of the original analysis by more than 55%.

It follows that, while the boundary conditions assumed in the original comparison resulted in a reasonable prediction of the behaviour of the subassemblage, it is very important, in a test, to adopt a well defined set of boundary conditions. This should enable any analytical procedure to closely simulate such boundary conditions. In the test of the subassemblage of Fig-5.14, it seems that the set of boundary conditions is somewhatof a mixture of the three sets mentioned above.

The subassemblage of Fig-5.14 was also analysed assuming the original boundary conditions (i.e. hinged beam ends and a roller support at the lower column end) but using the assumptions of small deflection theory. In other words, the displacement stiffness matrix that appears in eqn-3.22 is assumed to be identical to zero. Also, in calculating the strains at the element nodes, the non-linear term that appears in the expression for the axial strain (eqn-3.8) was neglected. The maximum load in this case was found to be 522kN which is about 4.5% below the Southwell load. The P-Δ curve for this case is shown in Fig-5.17 for comparison. Although the maximum load is closer to the Southwell load, the P-Δ curve deviates slightly from the experimental one.

It is of interest to inspect the variation of the beam and column moments at the column's top end as the force in the column increases. Fig-5.18 shows such relationships. It may be observed from this figure that the beam moments start from very large values. This is

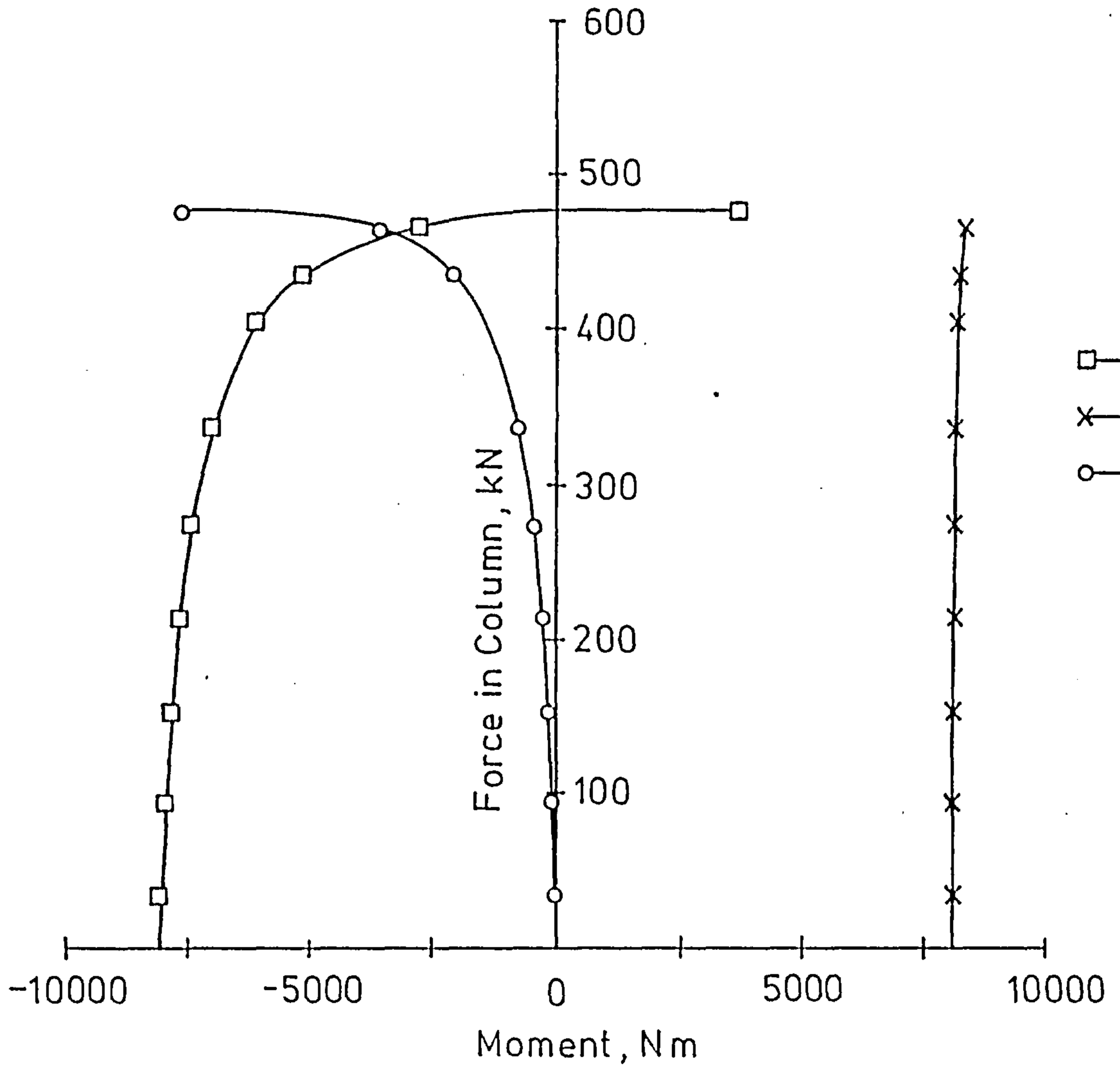

FIG. 5·18 VARIATION OF MOMENTS AT TOP END OF COLUMN (BERGQUIST SUBASSEMBLAGE)

due to the application of rather small beam loads through large lever arms in the first load stage. The maximum values of the beam loads were, in fact, slightly above 1% of the failure load that was applied to the column. Due to symmetry of the applied beam loads, the column moment in the first stage was practically zero. As the column load was increased in the second load stage, the column moment increased monotonically until failure of the column. The moment in the left beam decreased resulting in unloading of the left connection. The moment in the right beam stayed almost at a constant value keeping the right connection in a loading condition.

5.4.4- Effect of Beam Flexibility:-

The subassemblage of Fig-5.14, but with very large beam sections representing infinitely rigid beams, was analysed by the program to study the effect of beam flexibility on the maximum load and the load-deflection behaviour. The maximum load in this case was found to be 487kN. Comparing the maximum load obtained from the (original) analysis with this load suggests that the effect of beam flexibility is to reduce the maximum load by about 2.3%. It seems, therfore, that the beams are quite stiff as compared to the connection stiffness.

Lui and Chen (66) made an attempt to include the effect of beam flexibility on the behaviour of rectangular frames with semi-rigid joints. He proposed a combined beam and connection stiffness, C_j^*, expressed as

$$C_j^* = \frac{2EI_b}{L_b}\left[\frac{1}{1+\frac{2EI_b}{C_j L_b}}\right] \qquad (5.11)$$

in which

EI_b = flexural rigidity of the beam

L_b = beam span; and

C_j = initial connection stiffness

Eqn-5.11 applies only to rectangular frames in which the beams are bent in single curvature. The frame must be symmetrical and all the joints must be of similar characteristics. The use of eqn-5.11 permits the reduction of the frame problem to an equivalent column problem with end-restraints which may be dealt with rather more easily.

If the conditions at the far ends of the beams are different from those corresponding to the frame for which eqn-5.11 is applicable, a similar expression may still be derived. For the subassemblage of Fig-5.14 with the far beam ends hinged, the combined beam and connection stiffness is given by

$$C_j^* = \frac{3EI_b}{L_b}\left[\frac{1}{1 + \frac{3EI_b}{C_j L_b}}\right] \qquad (5.12)$$

which is similar to eqn-5.11 except in the replacement of 2 by 3 in the expression for the beam stiffness.

For the subassemblage of Fig-5.14, EI_b is 9400 kN.m^2 and C_j is equal to 450 kN.m/rad. Hence using eqn-5.12 the combined beam and connection stiffness is found to be 429 kN.m/rad which is 95% of C_j. Here, only one beam at each column end was taken into account since the connection which connects the beam on the other side of the column has almost zero stiffness in the column load stage. Comparing the initial connection stiffness with the combined beam and connection stiffness, it may be seen that the effect of beam flexibility is very minor. This

has already been pointed out from the comparisons of the maximum loads for the subassemblages with flexible and infinitely rigid beams. This low effect is due to the fact that the connection is very flexible when compared with the beam stiffness defined in this case as $\frac{3EI_b}{L_b}$.

5.5- Conclusions:-

The computer program presented in chapter 4 was used to simulate some of the experimental results in which rigidly and flexibly connected frames were tested. Both axial and lateral column loads were considered in the simulations of the rigidly connected frames. Beam loads and an axially applied column load were applied to the flexibly connected frame. The analytical results were found to compare reasonably well with the experimental results. The program may therefore be regarded as acceptable for performing any additional analyses of rigidly or flexibly connected frames of the general type shown in Fig.5.1 or 5.14.

It was pointed out in Sec-5.4.2 that the boundary conditions adopted in any test must be well defined in order that analytical procedures is able to closely simulate test results. In the next chapter a series of subassemblages with semi-rigid connections will be considered for further verification of the computer program.

CHAPTER-6

PROGRAM VERIFICATION: PART II

COMPARISONS WITH TESTS ON SUBASSEMBLAGES WITH SEMI-RIGID JOINTS

6.1- Introduction:-

In chapter-5, the computer program described in chapter-4 was verified for the analysis of a variety of cases including rigid frames and a semi-rigid frame. The agreement between the analytical and experimental results was seen to be acceptable. Although the rigid frames behaved inelastically, the semi-rigid one was elastic for almost the whole loading process. Furthermore, in this latter frame, the applied loads were limited to an axially applied loading. It is desirable to check the program performance in the cases where:

(1) the loading pattern is more complicated as this is the case that would be encountered in real frames.

(2) the frame (especially the column), behaves inelastically for an appreciable part of the loading process. This is also what might be expected in real frames.

In this chapter, the program was used to analyse a series of subassemblages consisting of a column and four beams. The data for these subassemblages is taken from the results of an experimental program that was carried out in the University of Sheffield. Different types of semi-rigid joints were used. The M-ϕ curves for these connections was based on an experimental joint test series that was also conducted as part of the same investigation. A brief description of the joint tests and the smoothing of the M-ϕ characteristics is given in Sec-6.2.1 and 6.1.2. In Sec-6.2.3, a description of the subassemblage test series is given. The results of the program analyses of the subassemblage series are presented and a discussion of the comparisons between the analytical and experimental results is given in Sec-6.3.

6.2- Experimental Data:

Two series of experimental tests were conducted by Davison (47,48,53) at the University of Sheffield. The first series consisted of tests on semi-rigid connections ranging from flexible web cleat connections to almost rigid extended end plate connections. The aim of this series was to experimentally determine the M-Φ characteristics of this range of connections. The second series included tests on full scale subassemblages to trace their behaviour up to failure. Each subassemblage consisted of four beams attached to a column by means of four semi-rigid connections. The connections used in this series were of the same types as those tested in the first series.

6.2.1- Joint Tests:

The joint test series included tests on connections of the following types (48,53):

(1) web cleats

(2) flange cleats

(3) seat and web cleats

(4) flush end plate

(5) extended end plate

Most of these connections were tested when attached to both column flanges and column webs i.e. for major and minor axis column bending as shown in Table-6.1, which has been extracted from the more comprehensive table of ref 53. A cruciform test arrangement of the type shown in Fig-6.1 was used in which two beams were connected to two identical connections which were, in turn, connected to both sides of a short column. 254x102x22UB sections were used for the beams while 152x152x23UC sections were used for the column. Load cells were mounted

Table-6.1 : Joint Tests

Test	Type of Connection	Column Axis of Bending	Connection Components
JT/01B	Web Cleats	Minor	80x60x8 RSA
JT/06	Web Cleats	Major	80x60x8 RSA
JT/07	Flange Cleats	Minor	top : 80x60x8 RSA bottom : 125x75x8 RSA
JT/08	Flange Cleats	Major	top : 80x60x8 RSA
JT/08			bottom : 125x75x8 RSA
JT/09	Web and Seat cleats	Minor	bottom : 80x60x8 RSA web : 125x75x8 RSA
JT/10	Web and seat cleats	Major	same as JT/09
JT/11	Flush End Plate	Minor	265x125x12 MS plate
JT/12	Flush End Plate	Major	265x125x12 MS plate
JT/13	Extended End Plate	Major	350x135x15 MS plate

Table-6.2 : Initial Joint Stiffnesses for the Considered Range of Connections

Connection	Initial Stiffness (From smooth curves) x 10^5 N.m/rad	
	Major	Minor
Web Cleats	84.4	101.6
Flange Cleats	207.0	326.7
Web and Seat Cleats	214.6	332.6
Flush End Plate	319.1	424.2
Extended End Plate	491.0	-

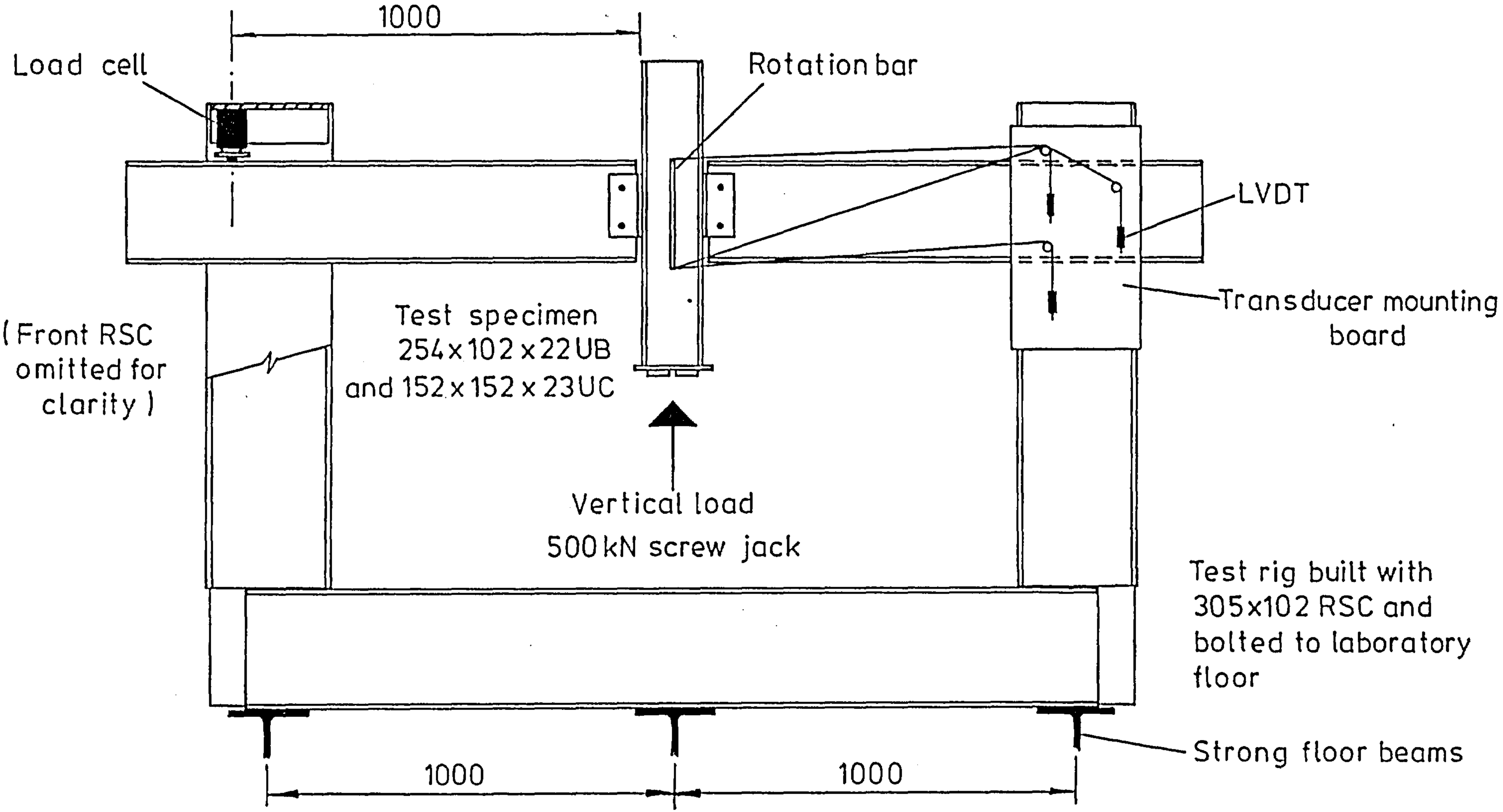

FIG. 6·1 JOINT TEST APPARATUS (REPRODUCED FROM REF. 53)

at the far ends of the beams to monitor the reactions at those points. Rotations at the faces of the column were measured using taught wires and linear variable displacement tranceducers (LVDT). A single load was applied to the column which was resisted by the reactions at the two beam ends. The bending moment at the connections was taken to be the result of multiplying the beam reactions by their lever arms (see Fig-6.1). A micro computer based data logging system was used to monitor the connection behaviour.

The M-ϕ relationships for the connections mentioned above are shown in Figs-6.2 to Fig-6.10, from which it is clear that the left connection behaves differently from the right one in almost all tests. It is also noticed that, although the M-Φ curves have general trends in which the joint stiffnesses are reducing over most of the range of rotations, they exhibit a high degree of local irregularities. Such irregularities may include portions in which the slope is negative which is ,obviously, not acceptable in physical terms. These irregularities are, in fact due to the experimental procedure and are explained in ref 53.

6.2.2 Smoothing of the Moment-Rotation data:

As was pointed out in the previous section, the M-Φ characteristics contained a high degree of local irregularities. In order to use these data in theoretical studies, it is necessary to obtain the smooth M-Φ curves which exhibit the general trend of the experimental behaviour of the connections. The procedure adopted for smoothing the M-Φ data was to obtain a plot of the original (experimental) data points for both left and right connections on a single graph. A smooth curve can then be drawn such that it passes in

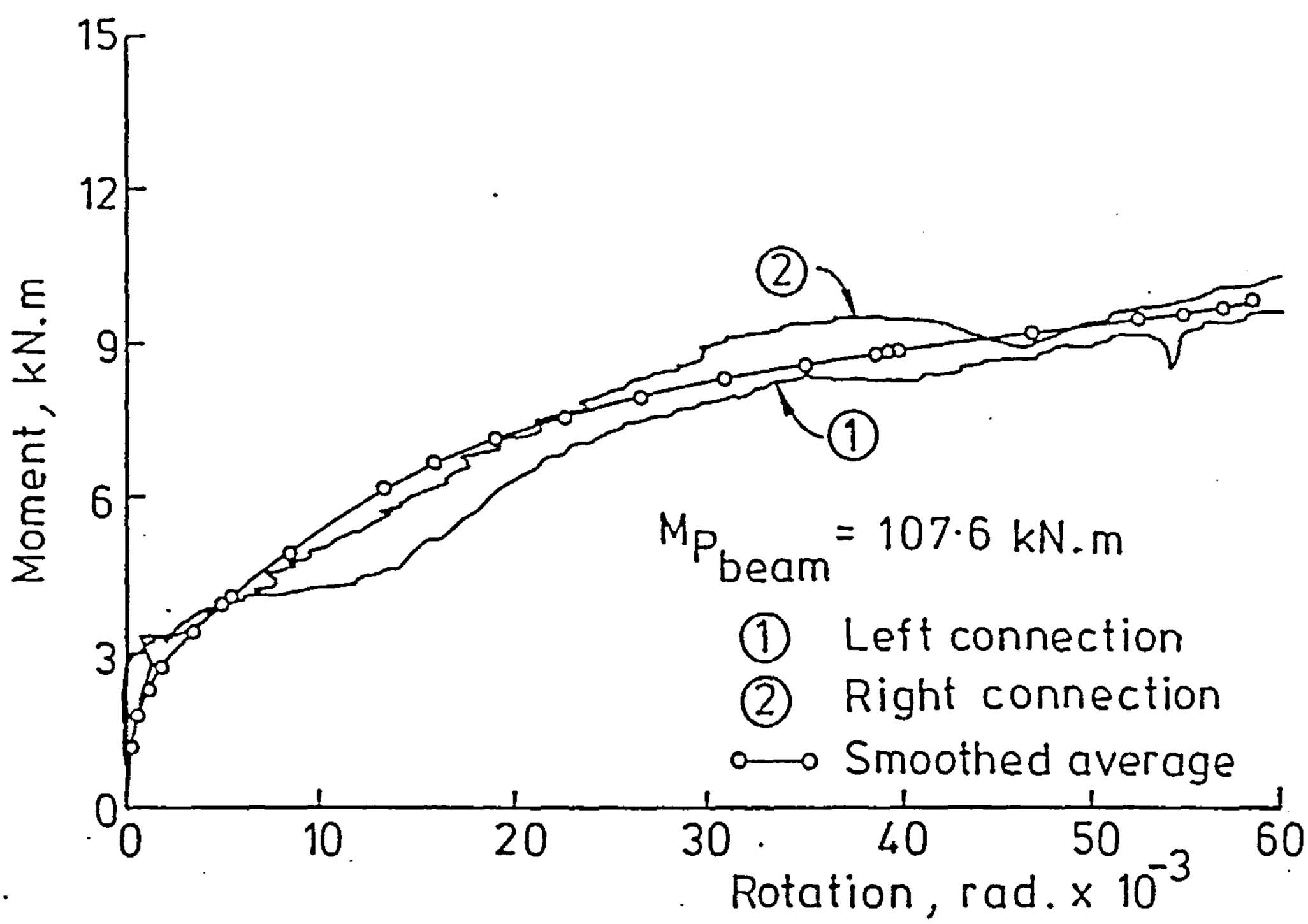

FIG.6·2 MOMENT-ROTATION CURVES FOR WEB CLEAT CONNECTION TO COLUMN WEB

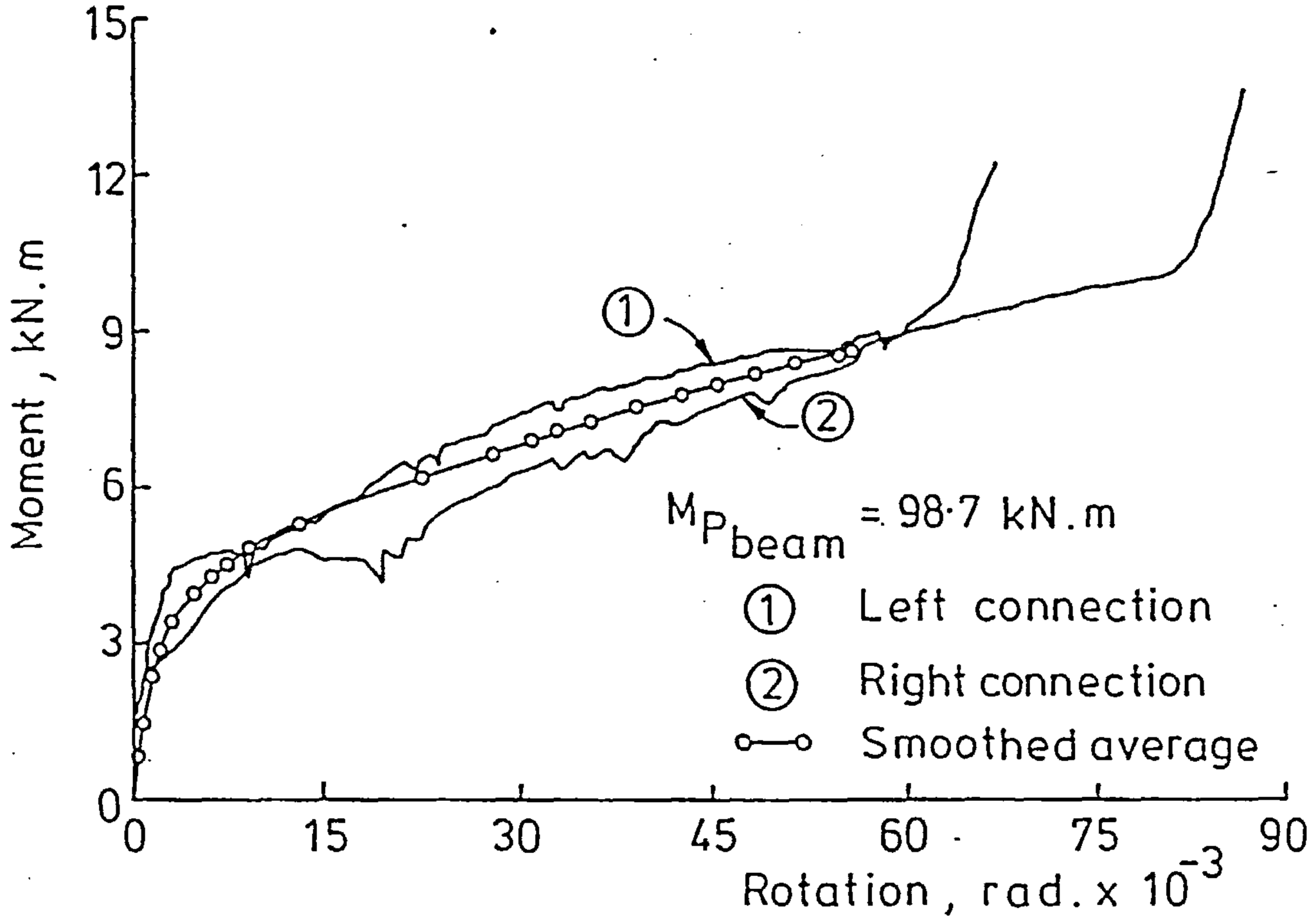

FIG. 6·3 MOMENT-ROTATION CURVES FOR WEB CLEAT CONNECTION TO COLUMN FLANGES

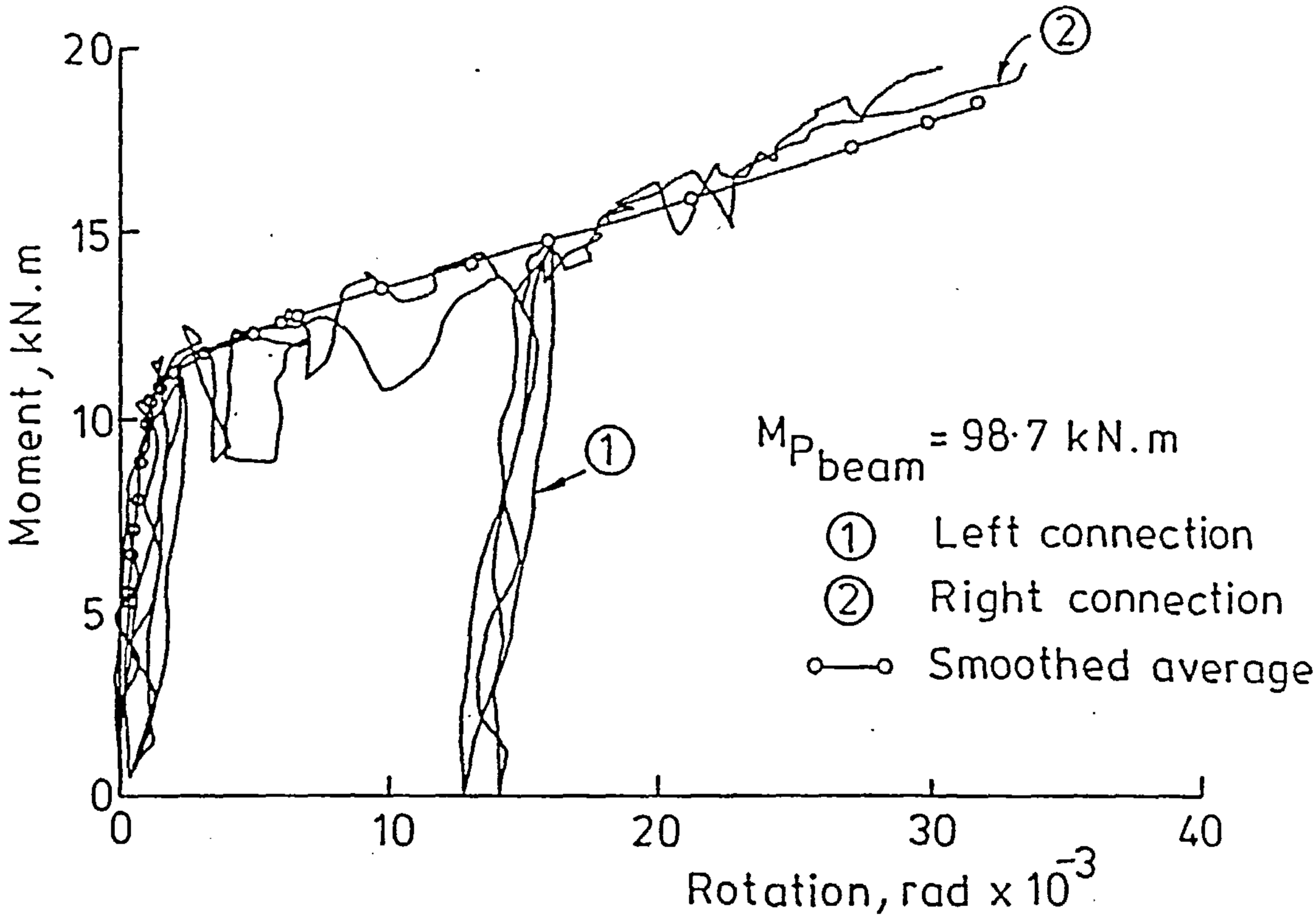

FIG. 6·4 MOMENT-ROTATION CURVES FOR FLANGE CLEAT CONNECTION TO COLUMN WEB

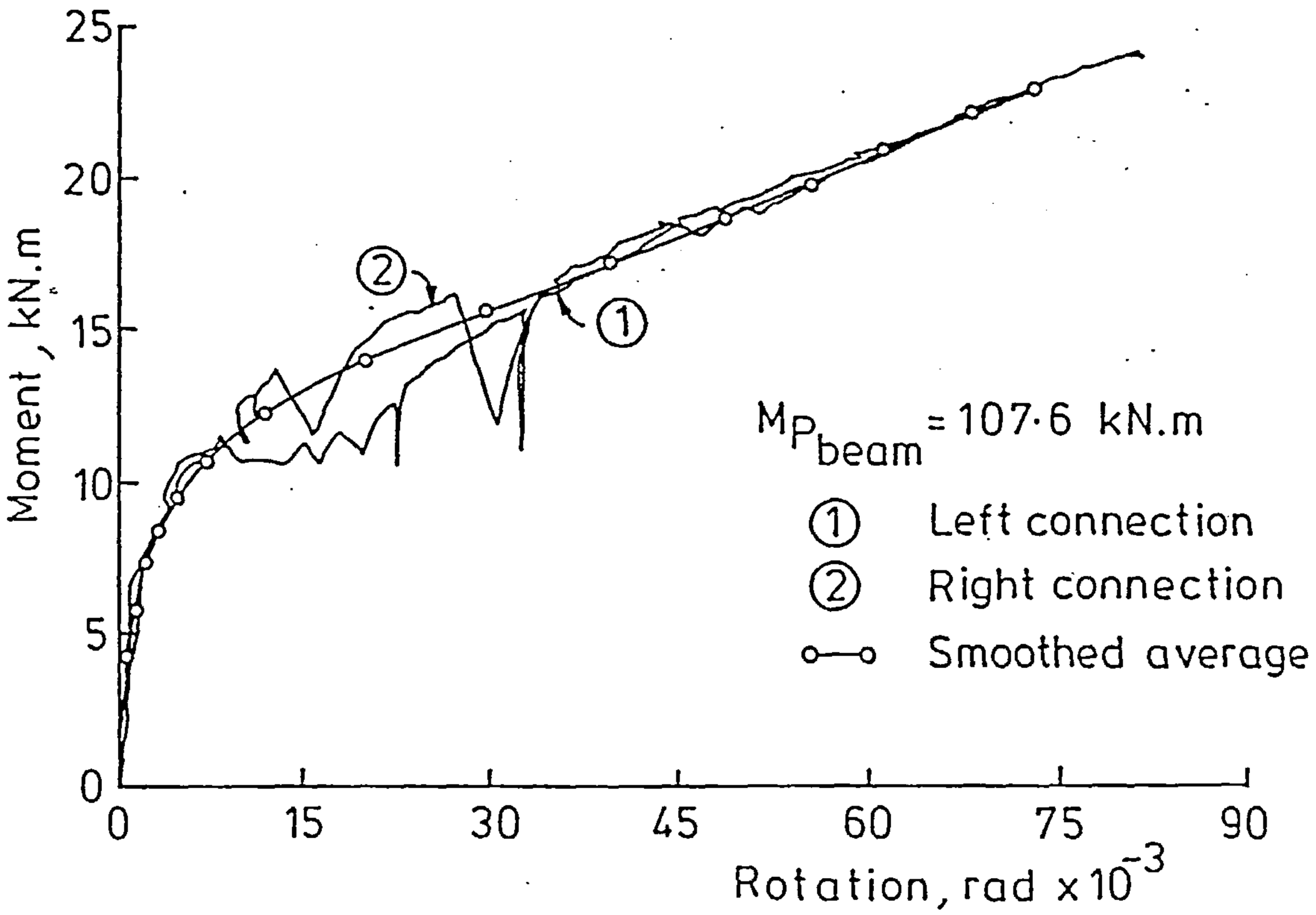

FIG. 6·5 MOMENT-ROTATION CURVES FOR FLANGE CLEAT CONNECTION TO COLUMN FLANGES

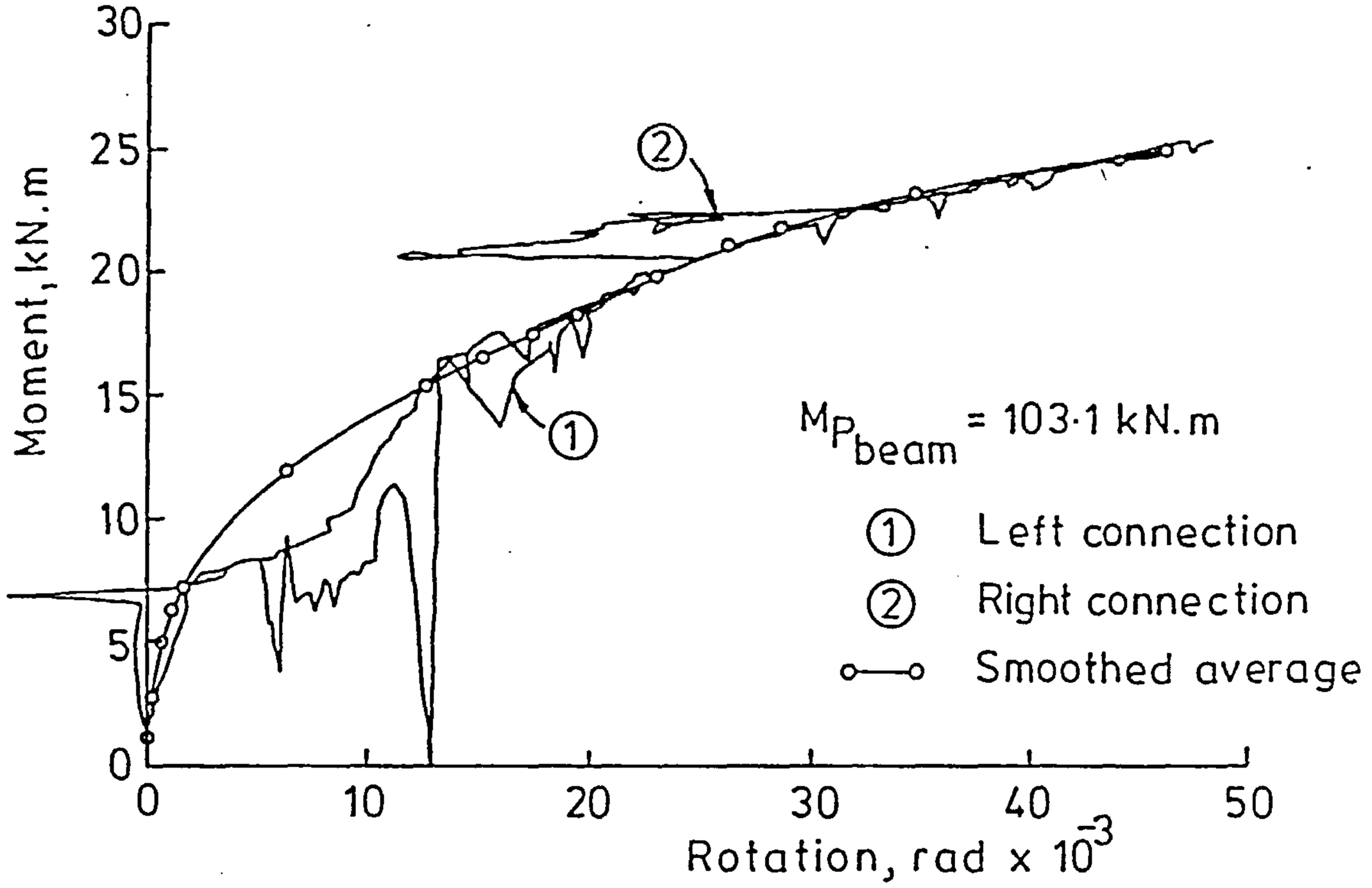

FIG. 6·6 MOMENT-ROTATION CURVES FOR WEB AND SEAT CLEAT CONNECTION TO COLUMN WEB

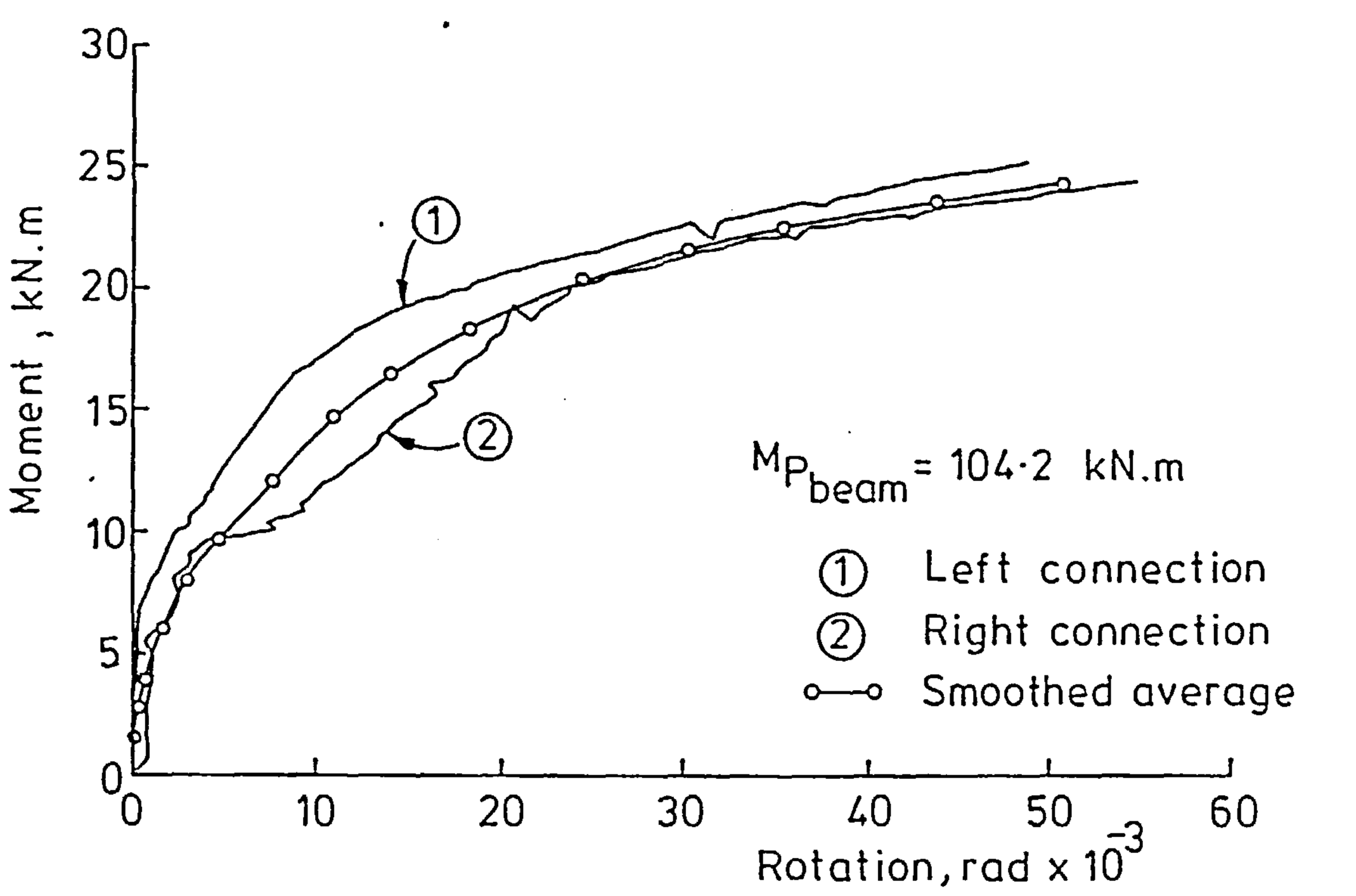

FIG. 6·7 MOMENT-ROTATION CURVES FOR WEB AND SEAT CLEAT CONNECTION TO COLUMN FLANGES

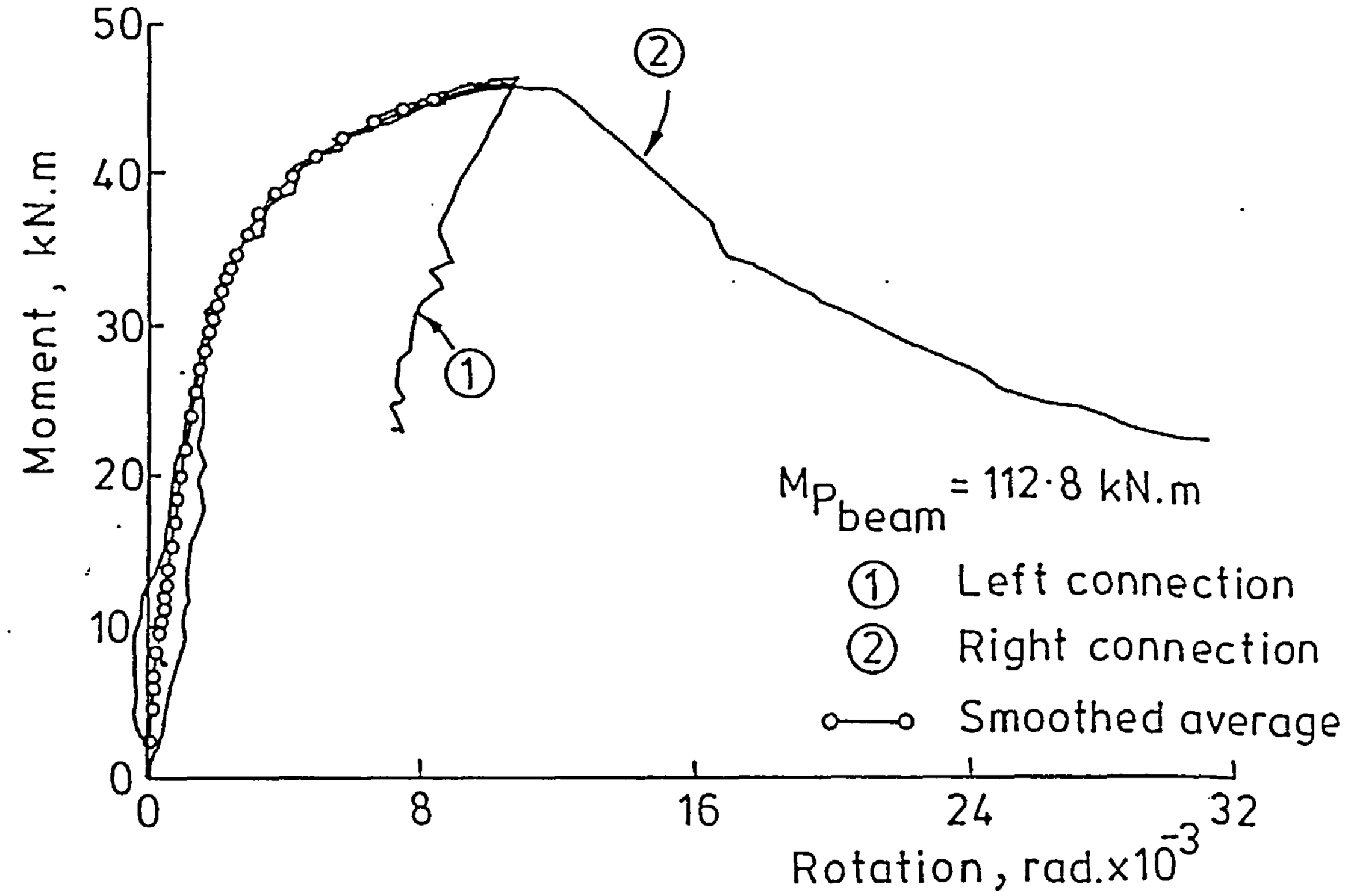

FIG. 6·8 MOMENT-ROTATION CURVES FOR FLUSH END PLATE CONNECTION TO COLUMN WEB

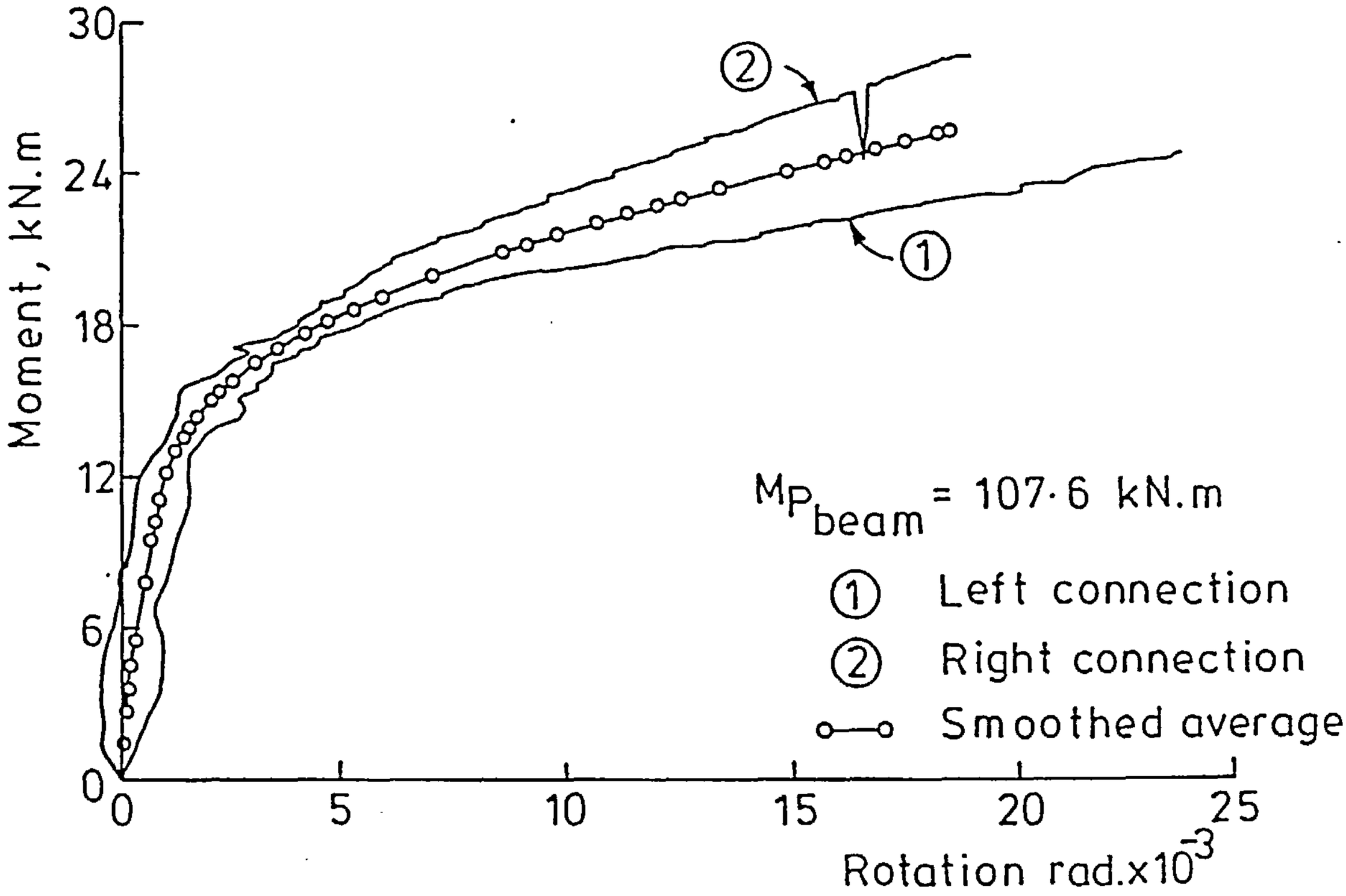

FIG. 6·9 MOMENT-ROTATION CURVES FOR FLUSH END PLATE CONNECTION TO COLUMN FLANGES

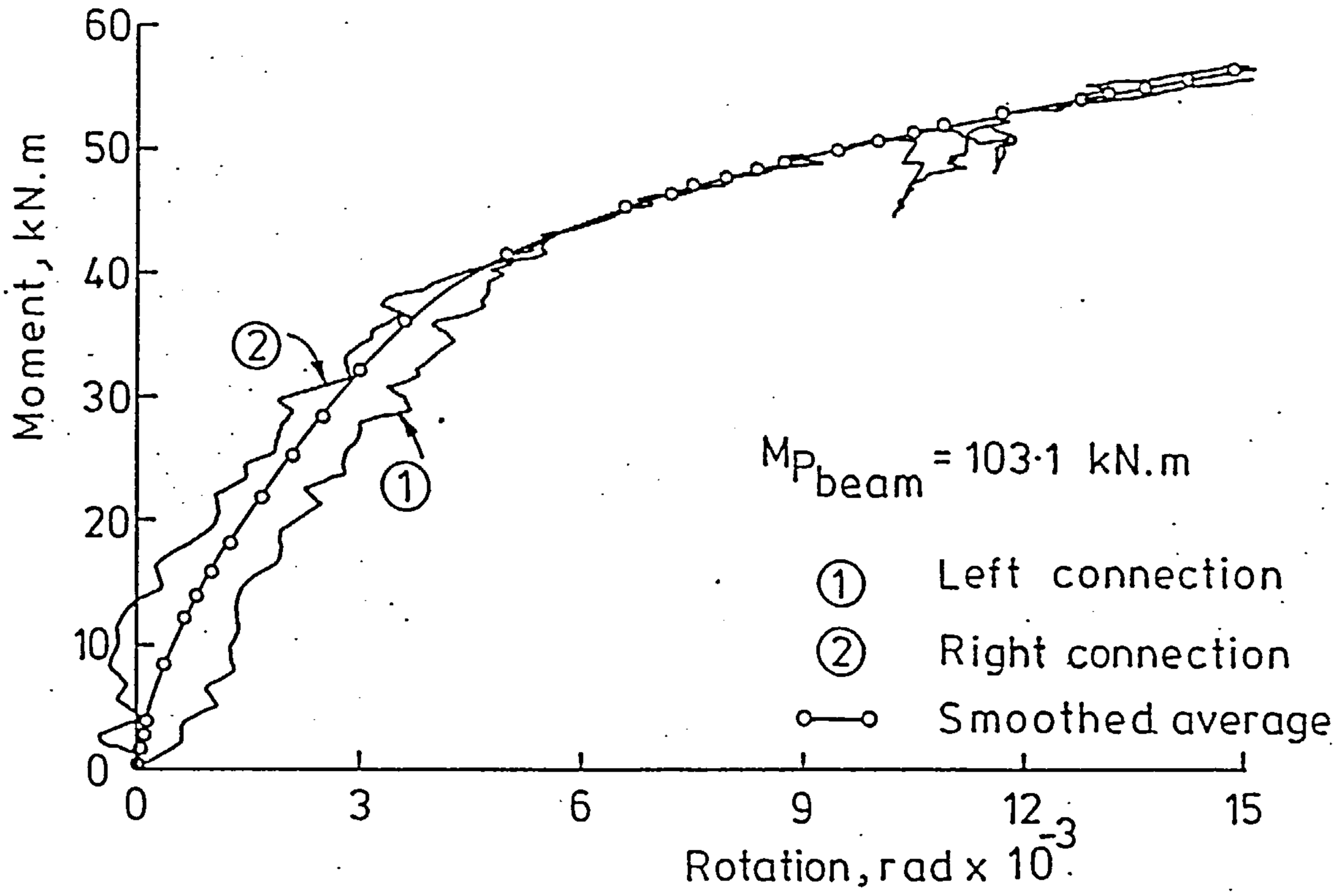

FIG. 6·10 MOMENT - ROTATION CURVES FOR EXTENDED END PLATE CONNECTION TO COLUMN FLANGES

between the two sets of points. In the cases where the connection was tested for loading and unloading behaviour e.g. the case of flange cleat connections to the column web, only the loading behaviour was considered. In some tests, slippage occurred in one of the connections. This resulted in large discontinuities in the M-ϕ characteristics. This sort of behaviour was disregarded by only considering the first and last points in the specific discrepancy in question. The moments and rotations at any number of points may then be extracted from the smooth curve. To ensure that the slope is continuously reducing, these points may then be numerically represented by a B-spline curve fit from which the slopes at these points may easily be found. Small adjustments to the smooth curve are carried out if necessary. Particular care is needed in smoothing the early part of the M-Φ data as this is the region of most significance for the analysis of actual frames. The smooth curve obtained from the final trial may then be numerically represented by a B-spline function and used in further frame analysis as required.

The M-Φ data for the series of connections mentioned in the previous section has been smoothed in the manner described above. The smoothed curves for all the connections of Table-6.1 are also shown in Figs-6.2 to 6.10. The curves for all connections attached to the column flanges are shown in Fig-6.11 while those for the connections attached to the column web are shown in Fig-6.12. These two sets of curves show the difference in the behaviour for these conditions. As the early part of any M-Φ curve is the most important, the curves shown in Figs-6.11 and 6.12 are reproduced in Fig-6.13 and Fig-6.14 to a larger scale for the range of rotations from 0 to 0.010 radians. It is noticed from these last two figures that, as expected, the connection performance

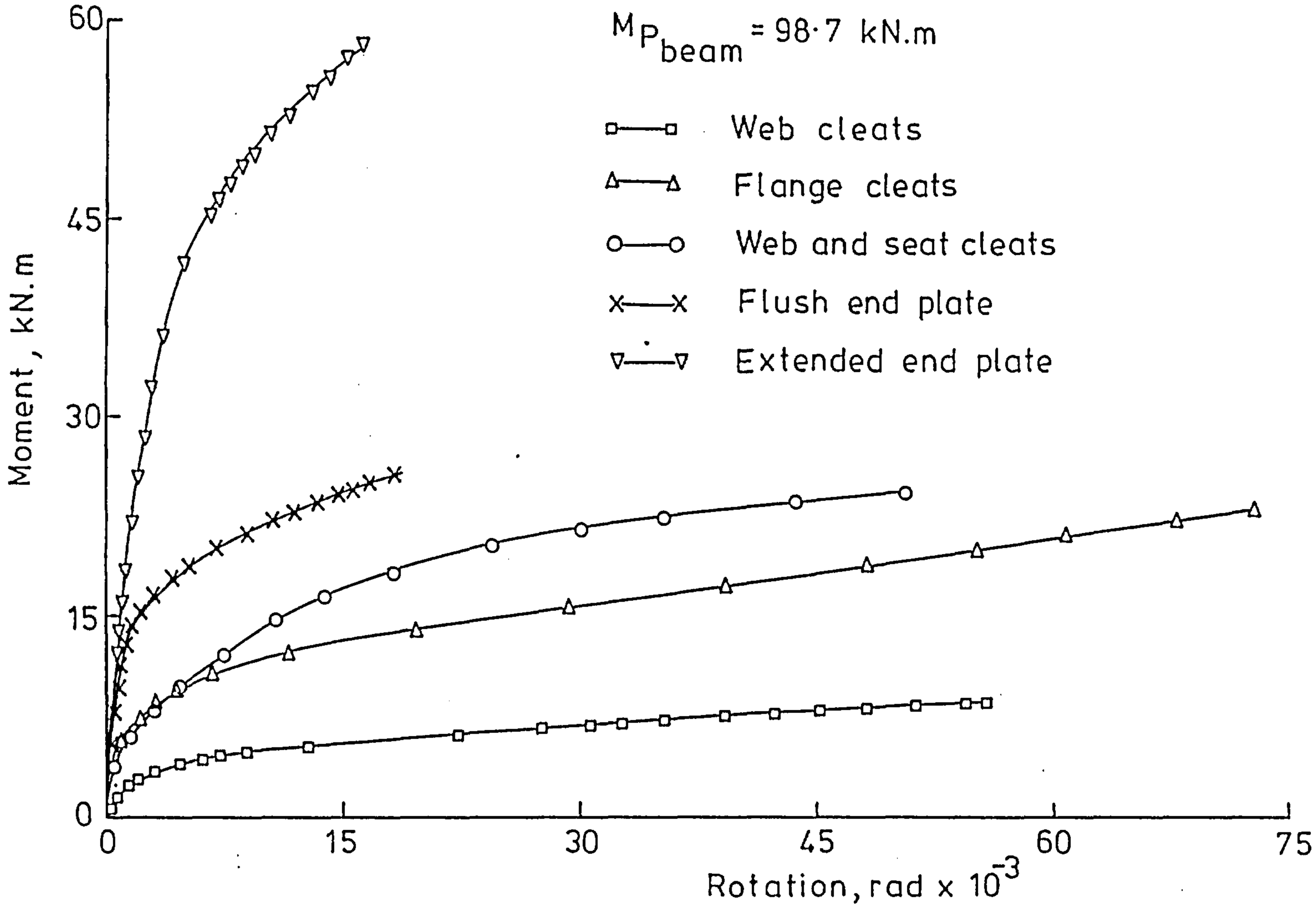

FIG. 6·11 SMOOTHED MOMENT-ROTATION CURVES FOR THE RANGE OF TESTED CONNECTIONS (MAJOR AXIS)

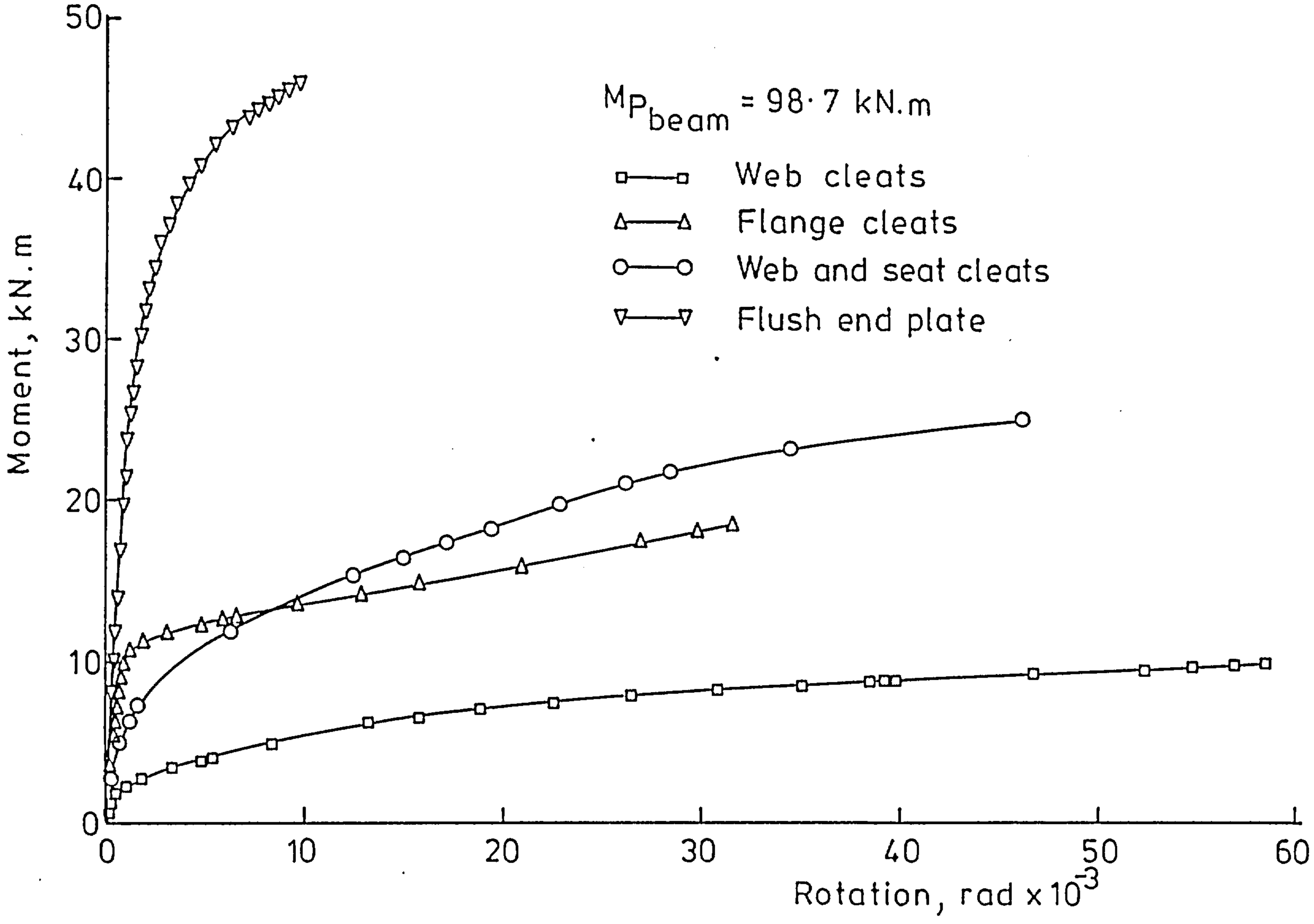

FIG. 6·12 SMOOTHED MOMENT-ROTATION CURVES FOR THE RANGE OF TESTED CONNECTIONS (MINOR AXIS)

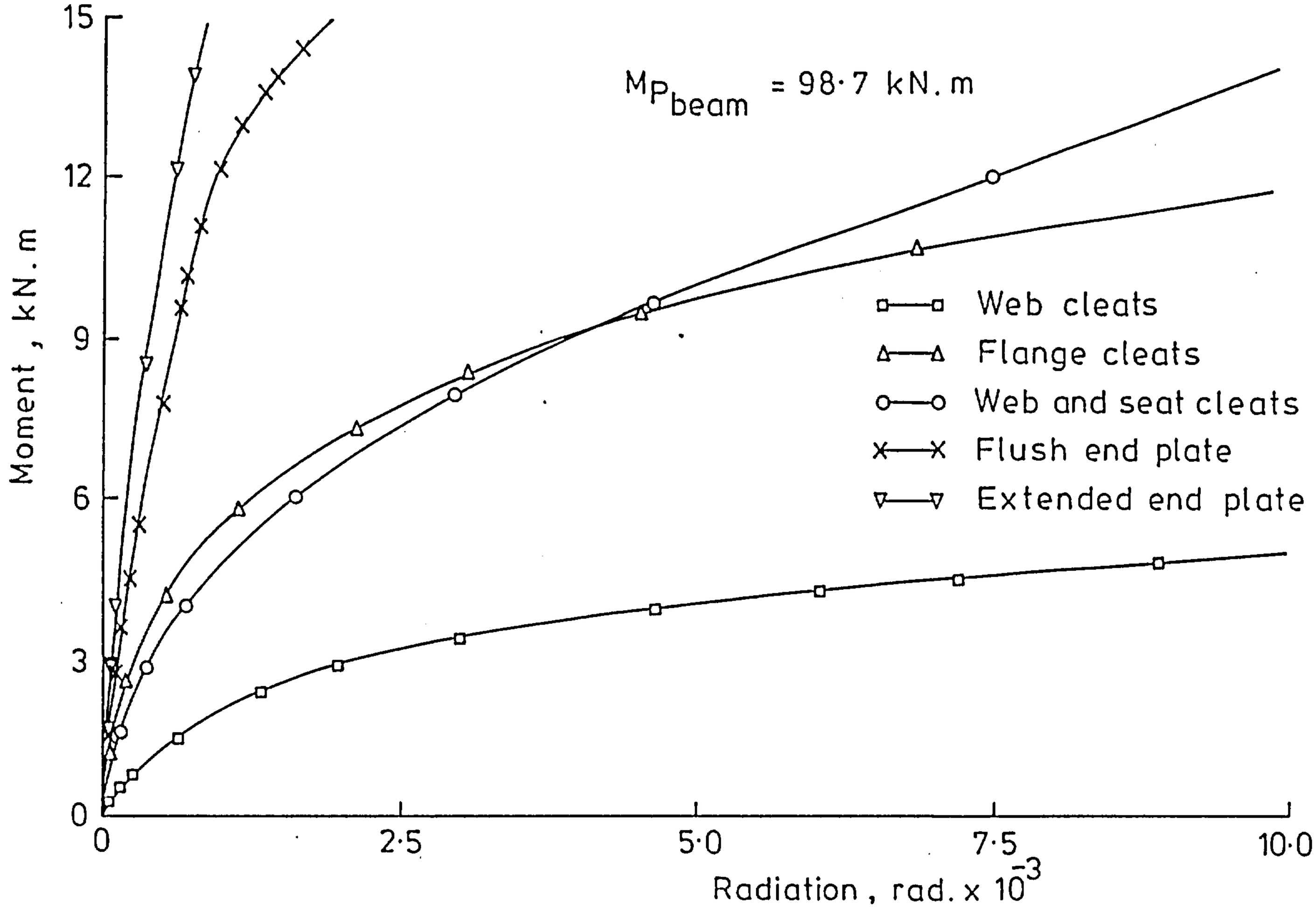

FIG. 6·13 MOMENT-ROTATION CURVES (MAJOR AXIS) : ENLARGEMENT OF THE EARLY PARTS

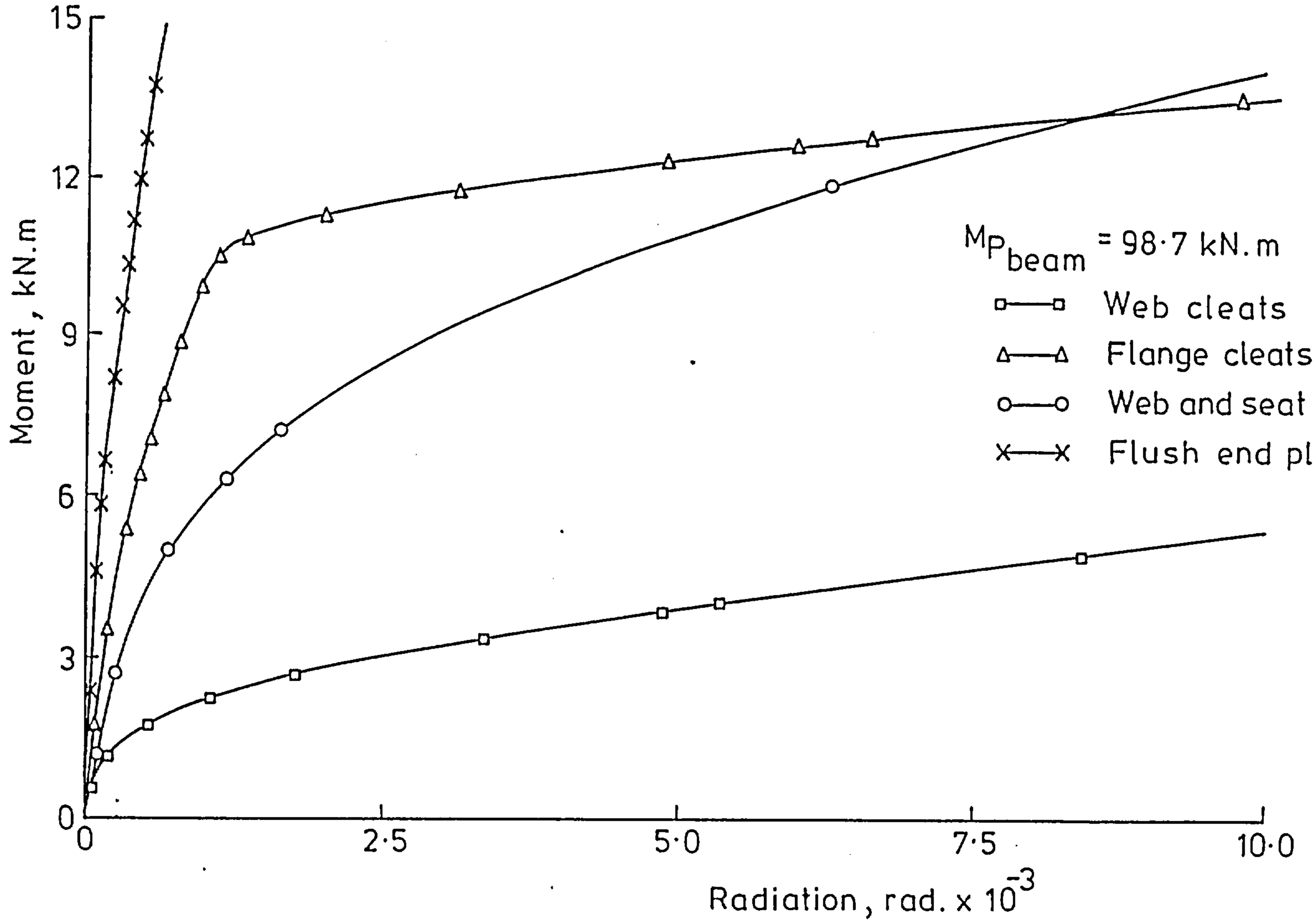

FIG. 6·14 MOMENT-ROTATION CURVES (MINOR AXIS) : ENLARGEMENT OF THE EARLY PARTS

ranged from that of a very stiff one in the case of an extended end plate connection to that of a flexible web cleat one. Table 6.2 shows the initial stiffness for all the connections as obtained from the smooth M-ϕ curves. It is of interest to note that the connections are stiffer when connected to the column's web than when they are connected to the column flanges. This was also pointed out in ref 53. The reason behind this is the additional flexibility due to flange deformations present in the latter case.

6.2.3- Subassemblage Tests:

A series of nine tests on full scale subassemblages of the type shown in Fig-6.15 were conducted (47,48). The subassemblage consisted of four 1.5m long beams connected to a 6.5m long column by means of four nominally identical semi-rigid connections. The connections used in these tests were essentially the same as those tested in the first series. The beams were allowed to bend about their major axes while both major and minor axis bending was considered for the column, although for the former case bracing was employed to prevent out-of-plane deformation. The far ends of the beams were allowed to move vertically but were restrained against rotation; they therefore acted as one half of a beam of twice the span (47)

Cross-sectional dimensions of each member were taken from measurements on specimens cut for each test. Table-6.3 presents the average cross-sectional dimensions as well as the static yield stress for the sections used in each test. All sections were thought to be cold-straightened since very low amounts of residual stress (less than 30N/mm^2 at the flange tips) were measured (47). This is also supported by the evidence of marks made by cold straightening rollers. Initial

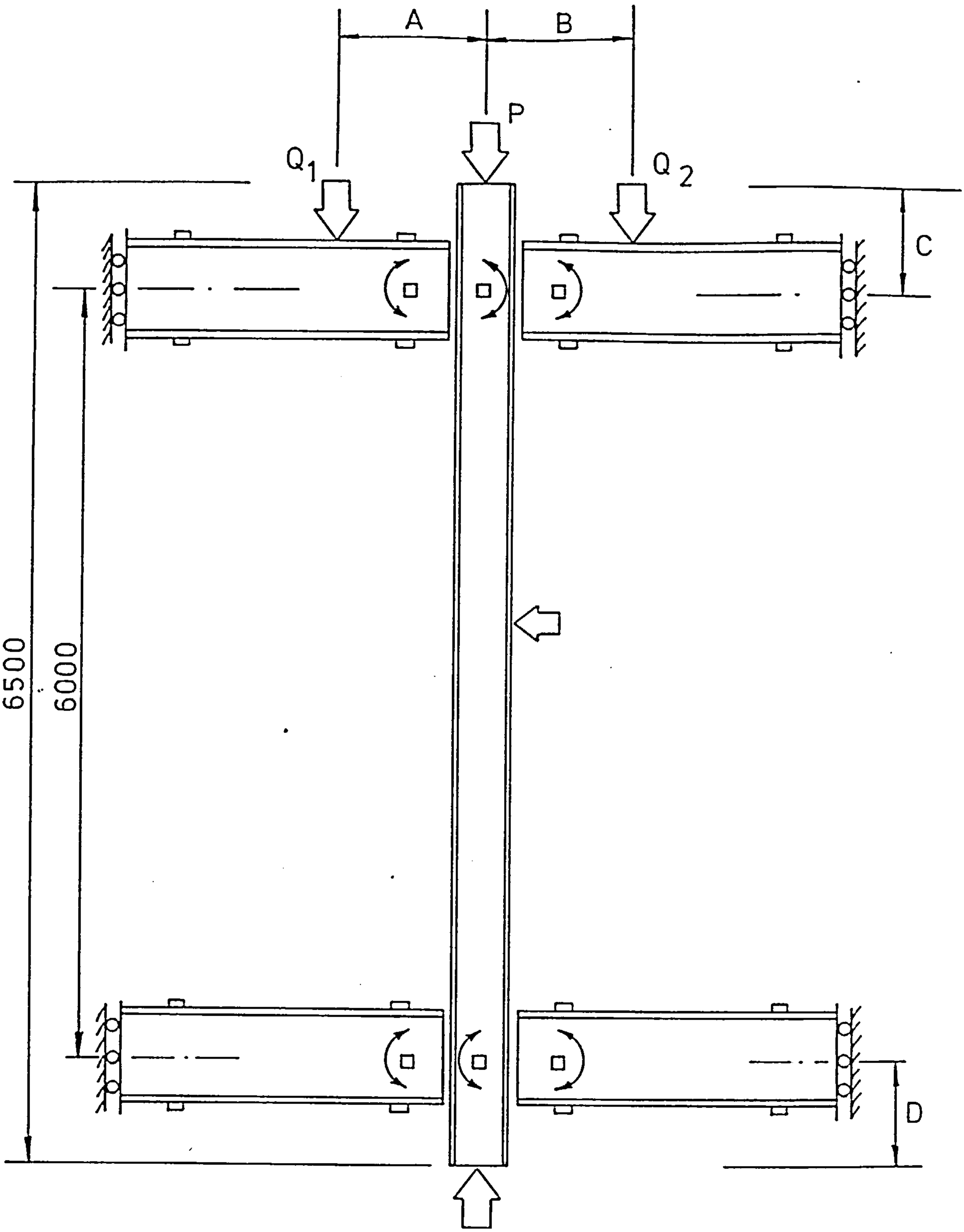

FIG. 6·15 THE TEST SUBASSEMBLAGE

Table-6.3*: Cross-sectional Dimensions and Tensile Strength of Test Specimens

Test	Sectional Dimensions**				Static Yield Stress (N/mm²)**
	D	B	t_w	t_f	
ST2	151.51	152.34	6.08	6.27	290.0
ST3	152.94	152.86	6.29	6.45	265.0
ST4	153.16	152.62	6.46	6.61	273.0
ST6	152.78	152.59	6.08	6.43	288.0
ST7	152.28	152.24	6.07	6.29	278.0
ST8	152.18	152.19	6.21	6.27	279.0
ST9	152.37	152.03	6.27	6.21	271.0
ST10	152.41	152.22	6.28	6.26	272.0

* from ref 2

** from column specimens only

Table-6.4 : Subassemblage Test Series

Test	Connection Connection Type	Column's axis Column's axis of bending	Applied Loads			
			P	Q_1	Q_2	Q_3
ST2	Web Cleats	Major	X		X	
ST3	Web Cleats	Minor	X	X	X	
ST4	Flange Cleats	Major	X	X	X	X
ST6	Flange Cleats	Minor	X	X	X	
ST7	Flange Cleats	Minor	X		X	
ST8	Web and Seat Cleats	Minor	X	X	X	X
ST9	Flush End Plate	Minor	X	X	X	X
ST10	Extended End Plate	Major	X	X	X	X

out-of-straightness was very small (2mm or less).

Table-6.4 lists the series of tests that were conducted. Also shown in this table are the type of connections used, the axis of bending of the column and the set of applied loads that were considered in each test. The general test procedure was to introduce a small column load of about 25 kN before the beam loads were applied in increments up to prescribed maximum values after which they were held constant while the column load was increased up to failure. Due to the very high degree of straightness of some columns coupled with symmetric beam loads, a small lateral load was applied at the centre of the column using a screw jack to produce initial deflections in the column. This load was maintained until the deflections in the column were large enough to permit to increase when the jack to be removed without retraction.

Tests ST2 and ST3 were conducted on subassemblages with web cleat connections. The column was bent about its major axis in test ST2. Load was applied to the right hand beam gradually up to a maximum of 45kN. The column load was then applied while keeping the beam load approximately constant. A maximum column load of 631kN was reached when it was decided that the beam load should be increased again to bring the column to failure(47). As the column load was applied via a screw jack this resulted in a modest reduction in the axially applied column load. The total load for this case was 682kN. In test ST3 minor axis bending was considered for the column. Equal beam loads were applied in the same manner as in test ST2. After the attainment of 43kN on each beam, the column load was increased up to failure. The total failure load (including beam loads) was 520kN.

Tests ST4 and ST5 were conducted allowing the column to bend

about its major axis using flange cleat beam to column connections. After the application of 25kN axial load, initial deflections were applied to the column of test ST4 using a screw jack. The maximum initial deflection at the centre of the column was 6.25mm. Two beam loads were then applied to a maximum of 110kN per beam. The last stage was to increase the column load to bring the column to failure at a total load of 762kN. In the pilot test ST5, lateral- torsional buckling was observed (47). For this reason, it will not be used herein.

Two further tests were conducted using flange cleat connections. These are tests ST6 and ST7. In both these tests, the column was caused to bend about its minor axis. In test ST6, two beam loads of 41 and 44kN were applied to the top-left and top-right beams respectively after the application of the 25kN axial load. On the other hand, only one 40kN load.was applied to the top-right beam of test ST7. The column load was then increased to bring the column to failure in both tests. Total failure load for test ST6 was 518kN while that for test ST7 was 526kN.

In tests ST8,ST9 and ST10 , web and seat cleats, flush end plate and extended end plate connections were used respectively. Minor axis bending was considered for the column of tests ST8 and ST9. On the other hand, the column of test ST10 was bent about its major axis. In all these tests initial deflections were artificially induced in the same manner as in test ST4. In test ST8, the maximum initial deflection was 12.5mm. Two beam loads of maximum values of 67kN and 70kN were applied to the beams. The total failure load was 518kN. In test ST9, the initial central deflection was 5mm. Nearly symmetric beam loads with upper limits of 83kN and 85kN were applied. The maximum failure load in this case was 485kN. The central initial deflection in test

ST10 was 7.5mm. Two almost symmetrical beam loads of 120kN each were used. The column load was then increased while keeping the beam loads at the same levels for sometime. The beam loads were then reduced -to almost zero values- (at slightly different rates) while still increasing the column load. The maximum total load attained was 743kN.

6.3- Comparisons of analysis with experimental results:-

6.3.1- Load-Deflection Curves:-

The subassemblage of Fig-6.15 was analysed by the computer program described in chapter 4 at least once for each of the tests ST2 to ST10. The M-ϕ curves used in these analyses were the smooth curves based on data obtained from the experimental joint tests as described in Sec-6.1.2. The same M-ϕ curves were used for all the connections in any one subassemblage. even though the behaviour of the individual connections may differ slightly. The column and beam cross-sectional dimensions used in the analyses are shown in Table-6.3 and were obtained from measurements on a number of offcuts from the test specimens. Also shown in Table-6.3, is the static yield stress for each test. Although the beam sections may have different yield stresses (47), only that of the column section was used for the whole subassemblage. In all the experimental tests, the beam loads were applied in such a way that all beams remained well in the elastic region. Consequently, it was not important to use the measured yield stress for each beam. All sections were assumed to be initially stress-free. The distances from the column ends to the points where the connections were made are shown in Table-6.5. These distances vary slightly from test to test. In addition, the lever arms of the applied beam loads are shown in this table.

Table-6.5: Beam loads lever arms and locations of beam-to-column connections

Test	Dimensions * (mm)			
	A	B	C	D
ST2	-	346	251	249
ST3	333	343	250	250
ST4	338	353	204	296
ST6	335	335	210	290
ST7	-	328	217	283
ST8	342	348	217	283
ST9	343	428	247	253
ST10	336	431	220	280

* See Fig-6.15

Table-6.6 : Results of Subassemblage Analyses

Case	Applied Loads at Failure (kN)					
	P	Q_1	Q_2	Q_3	Total Column Load	
					Analysis	Experiment
ST2	597.5	-	73.3	-	670.8	682.0
ST3	452.5	41.0	44.0	-	537.5	520.0
ST4	463.3	110.0	110.0	3.35	683.3	762.0
ST6	510.0	41.4	43.0	-	594.4	518.0
ST7	484.0	-	40.0	-	524.0	526.0
ST8	362.0	67.0	70.0	1.50	499.0	518.0
ST9	343.0	83.0	85.0	1.54	511.0	485.0
ST10	403.0	93.0	100.6	7.74	596.6	743.0

Due to the adopted arrangement for the application of the axial column load in the experimental tests, a small amount of axial load eccentricity may be expected. For this reason, the column load was assumed to act at a small eccentricity of 2mm. The accuracy to which the initial out-of-straightness were measured in the columns also allowed for a reasonable estimate of the initial deflections to be accepted. Consequently, initial deflections with a sinusoidal shape and a maximum central deflection of 2mm were assumed.

The load patterns assumed for the analysis of the above mentioned cases are shown in Fig-6.16. They closely simulate the actual loading patterns adopted in the tests. However, there was no information on the actual magnitude of the lateral load which was applied to the column in cases ST4,ST6,ST8,ST9 and ST10. Therefore a small variable lateral load was assumed for this form of loading which in each individual case gave a lateral displacement of the column at midheight corresponding to that measured in the test during the application of the jack force. The magnitude of this load was allowed to fall as axial loading proceeded. It could be seen from these patterns that, a small portion of this load was still present at the end of the analysis of each of these tests. This is in contrast to the experiments, in which the lateral load was removed before the attainment of the column maximum load.

The analytical and experimental P-Δ curves for all of the cases are shown in Figs-6.17 to 6.24. Table 6.6 compares the maximum loads obtained from the analysis with those of the experiments for all these cases. It can be seen from these figures that the analytical P-Δ curves compare very well with the experimental curves in cases ST2,ST3,ST8 and ST9. The maximum loads were also satisfactorily

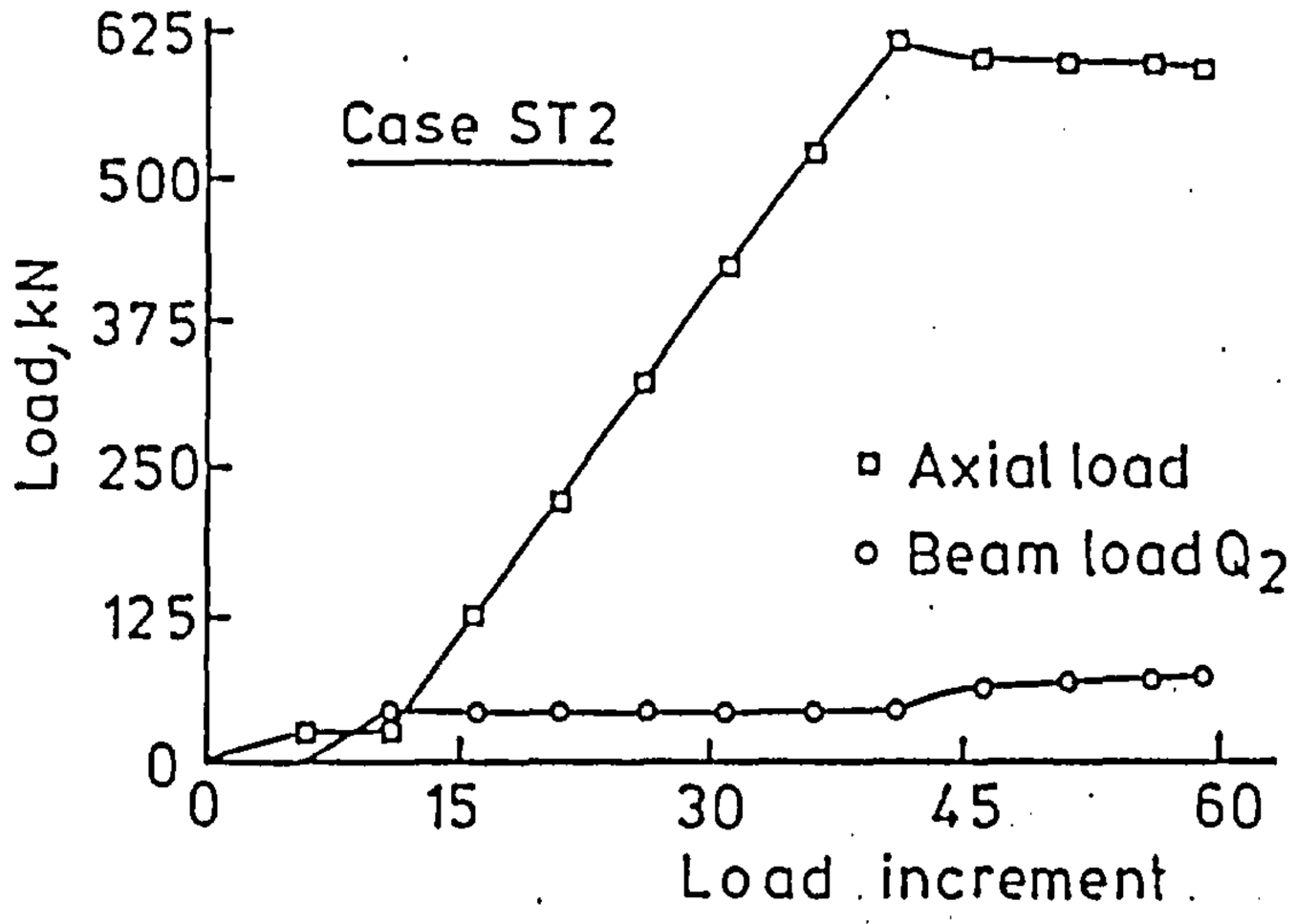

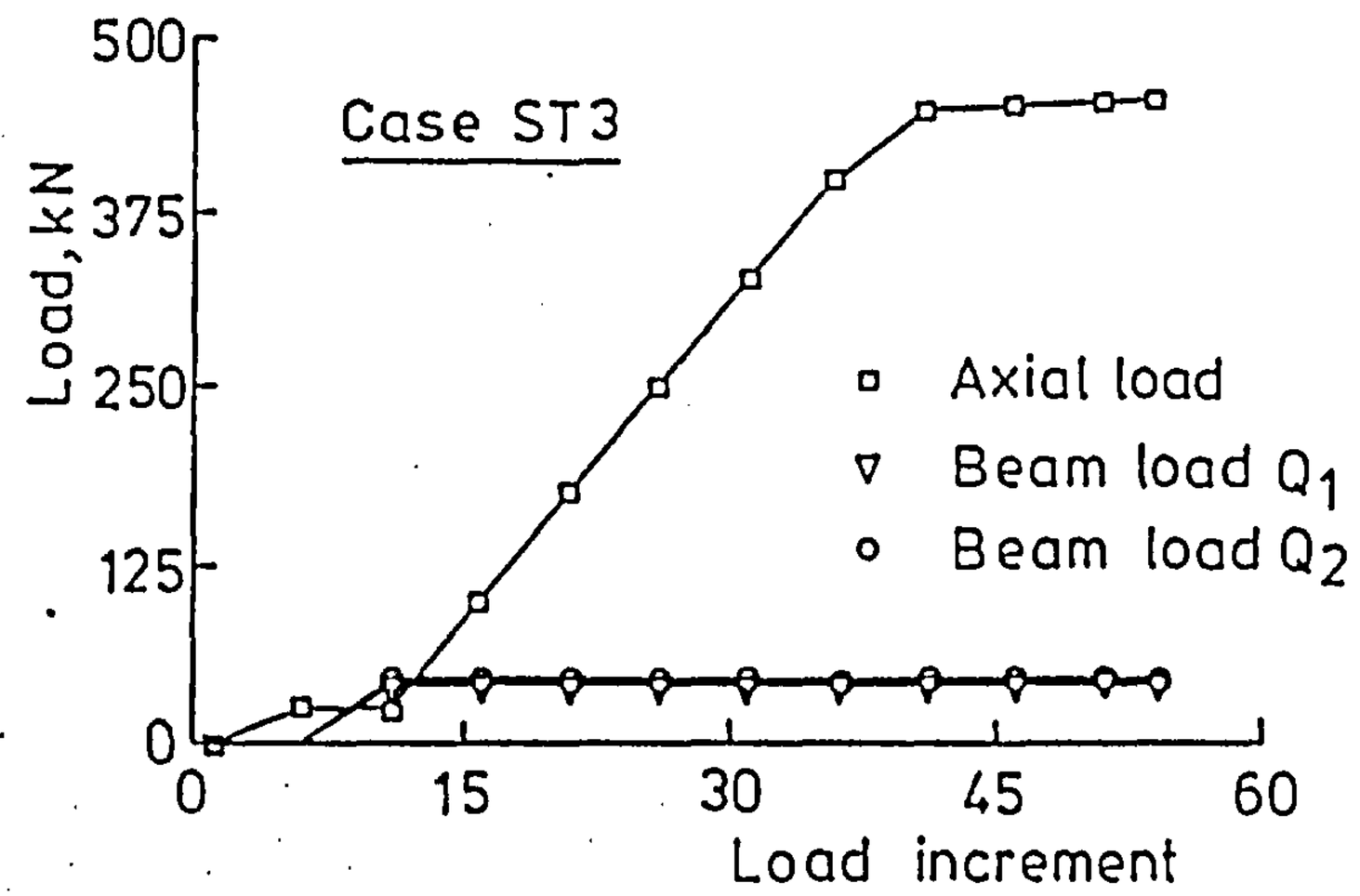

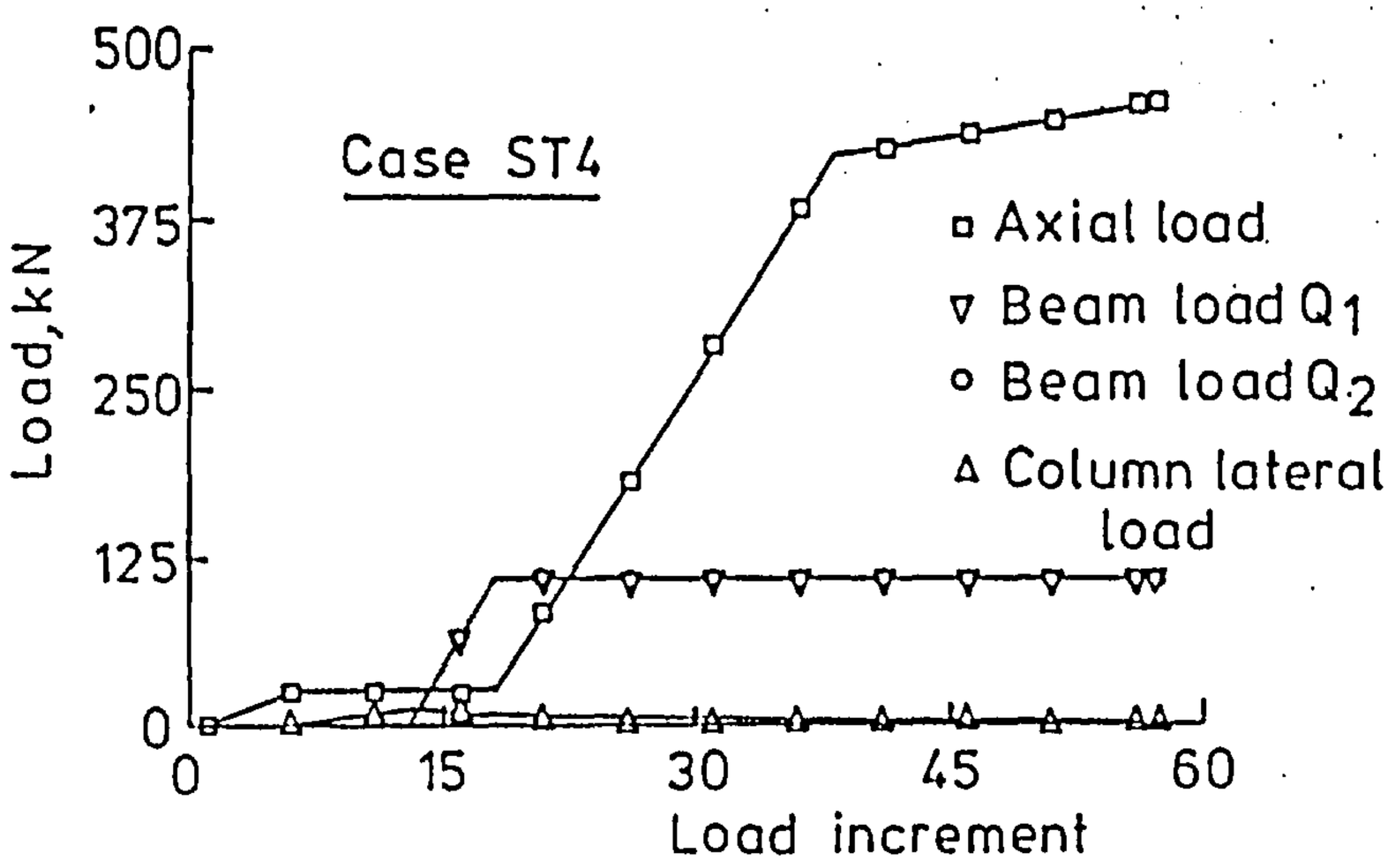

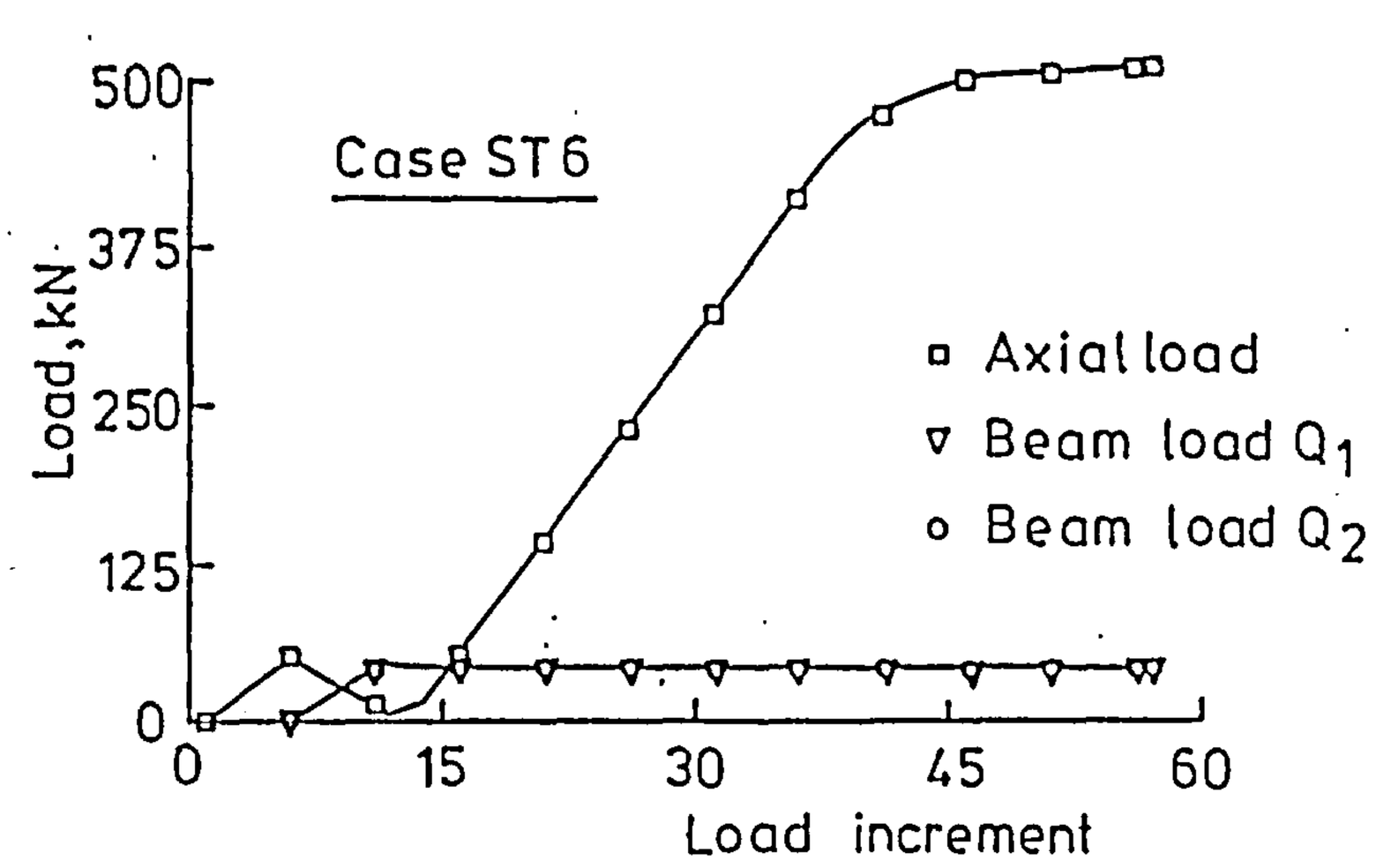

FIG. 6·16(a) LOAD PATTERNS FOR CASES ST2 , ST3 , ST4 AND ST6

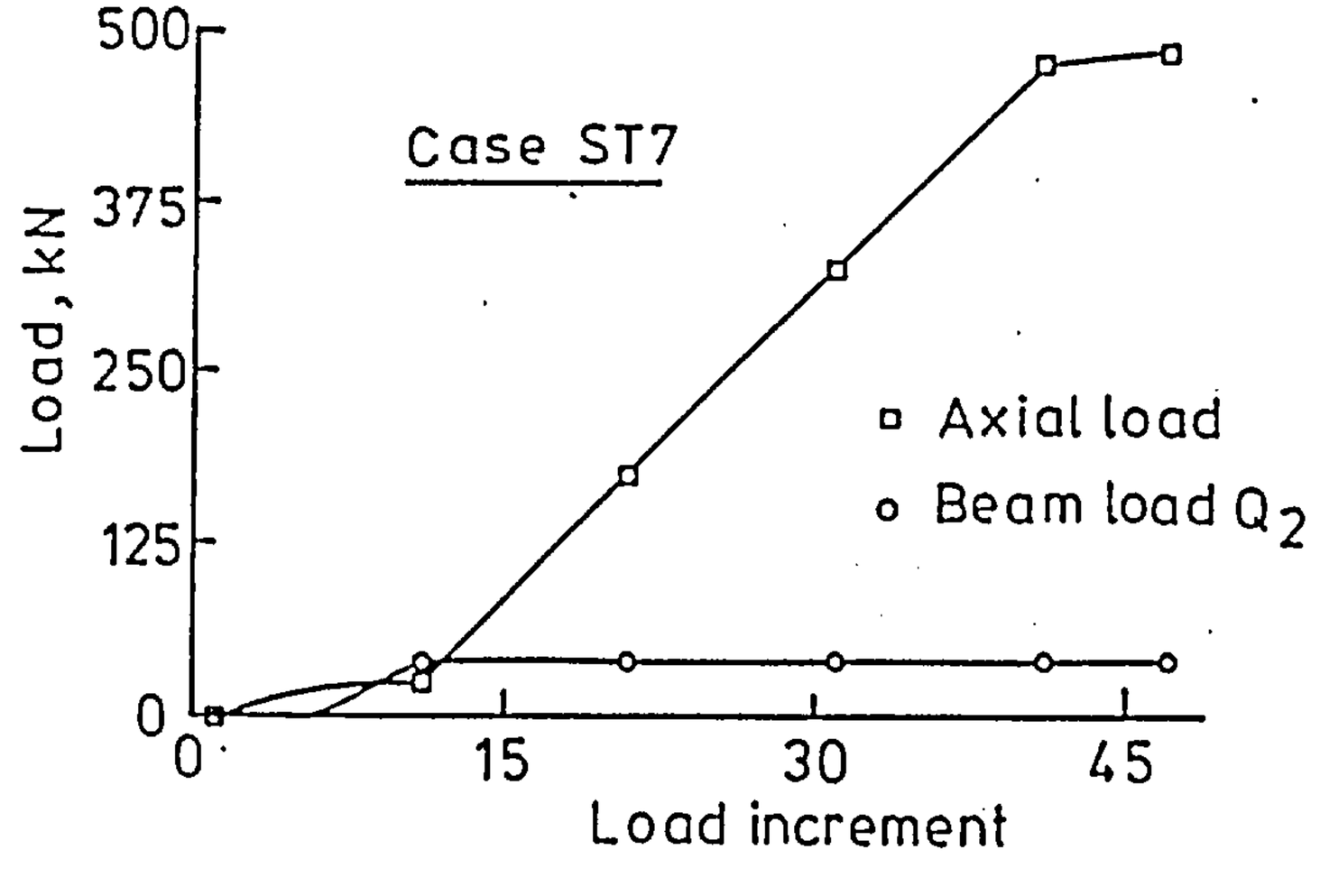

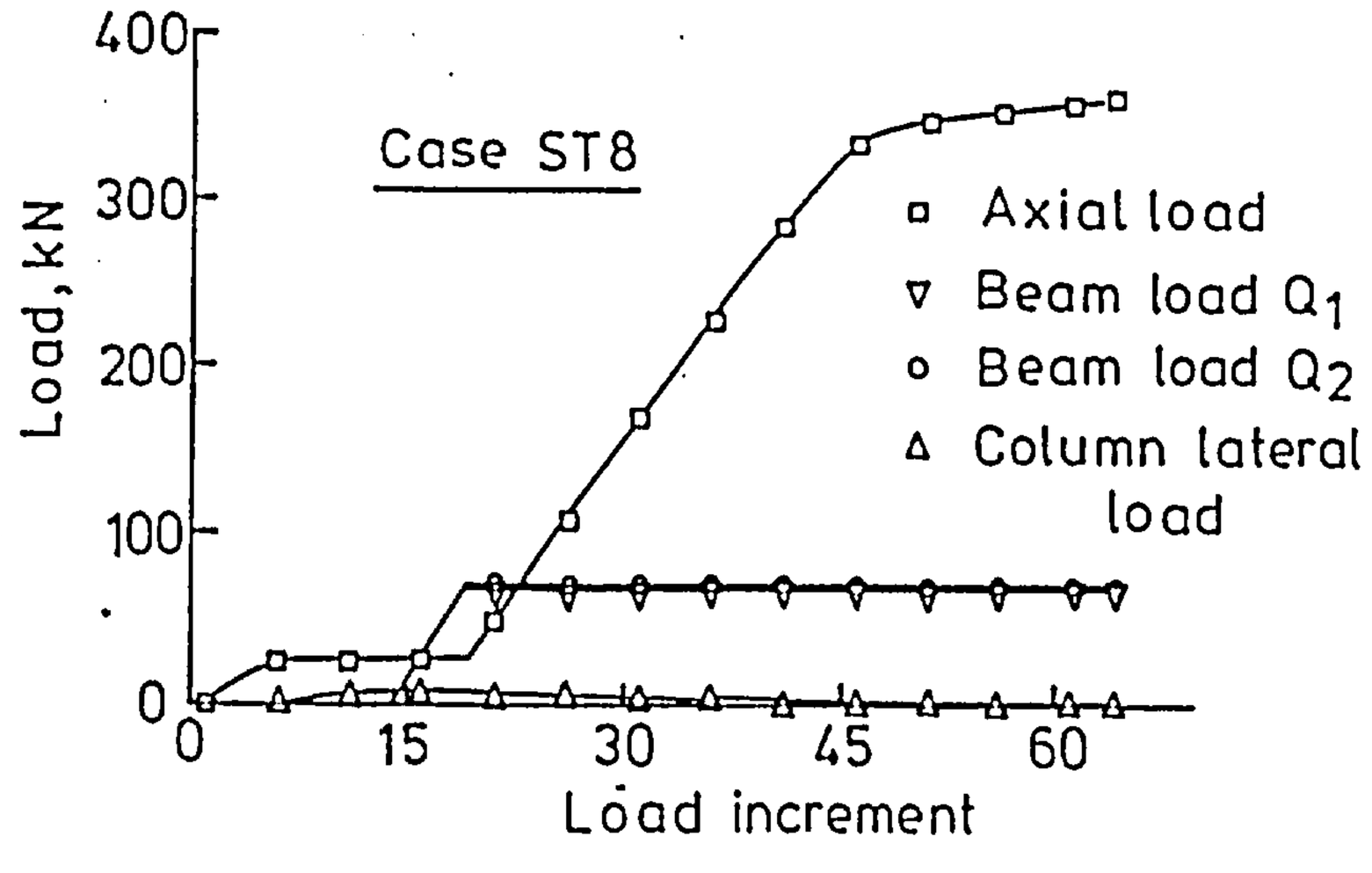

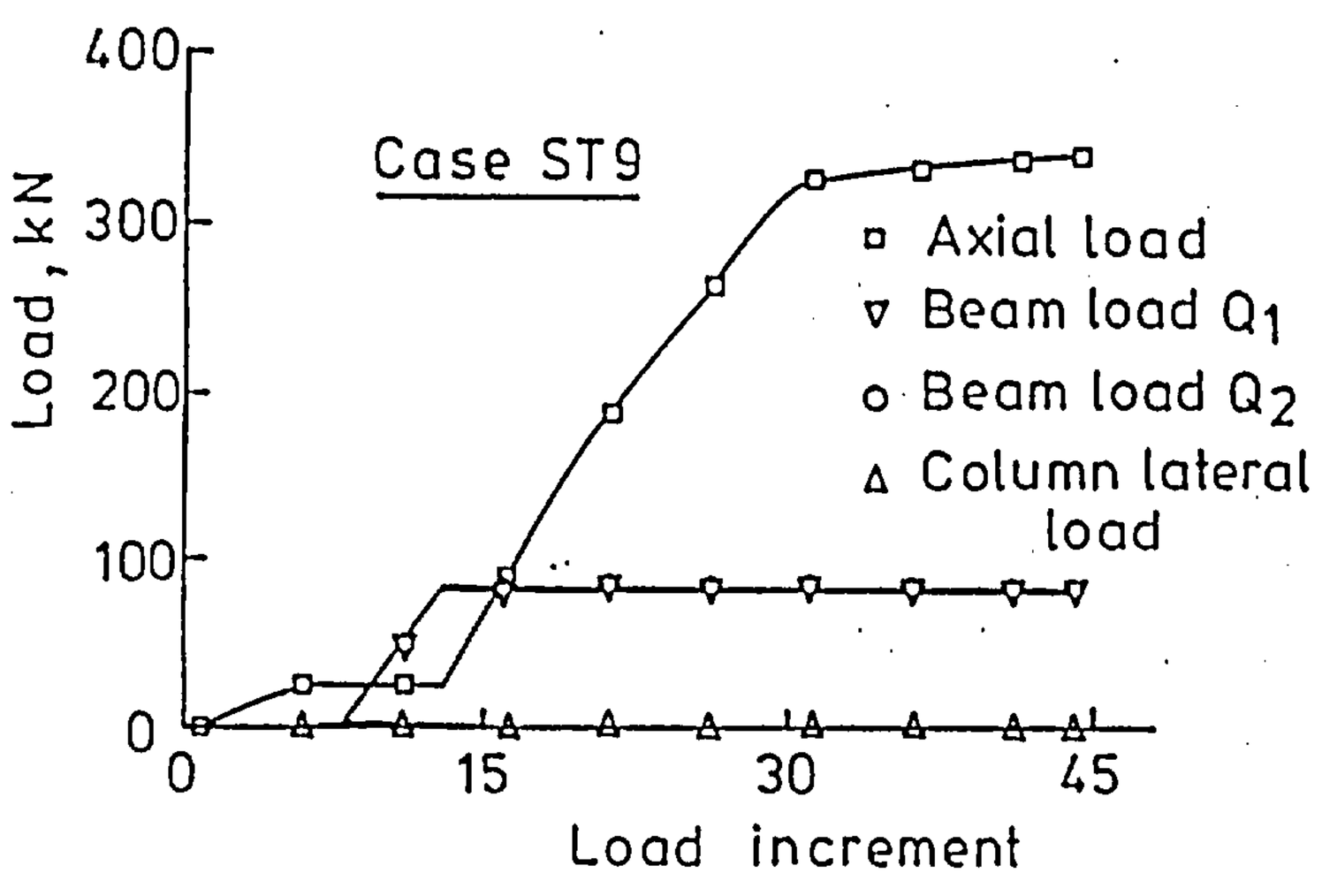

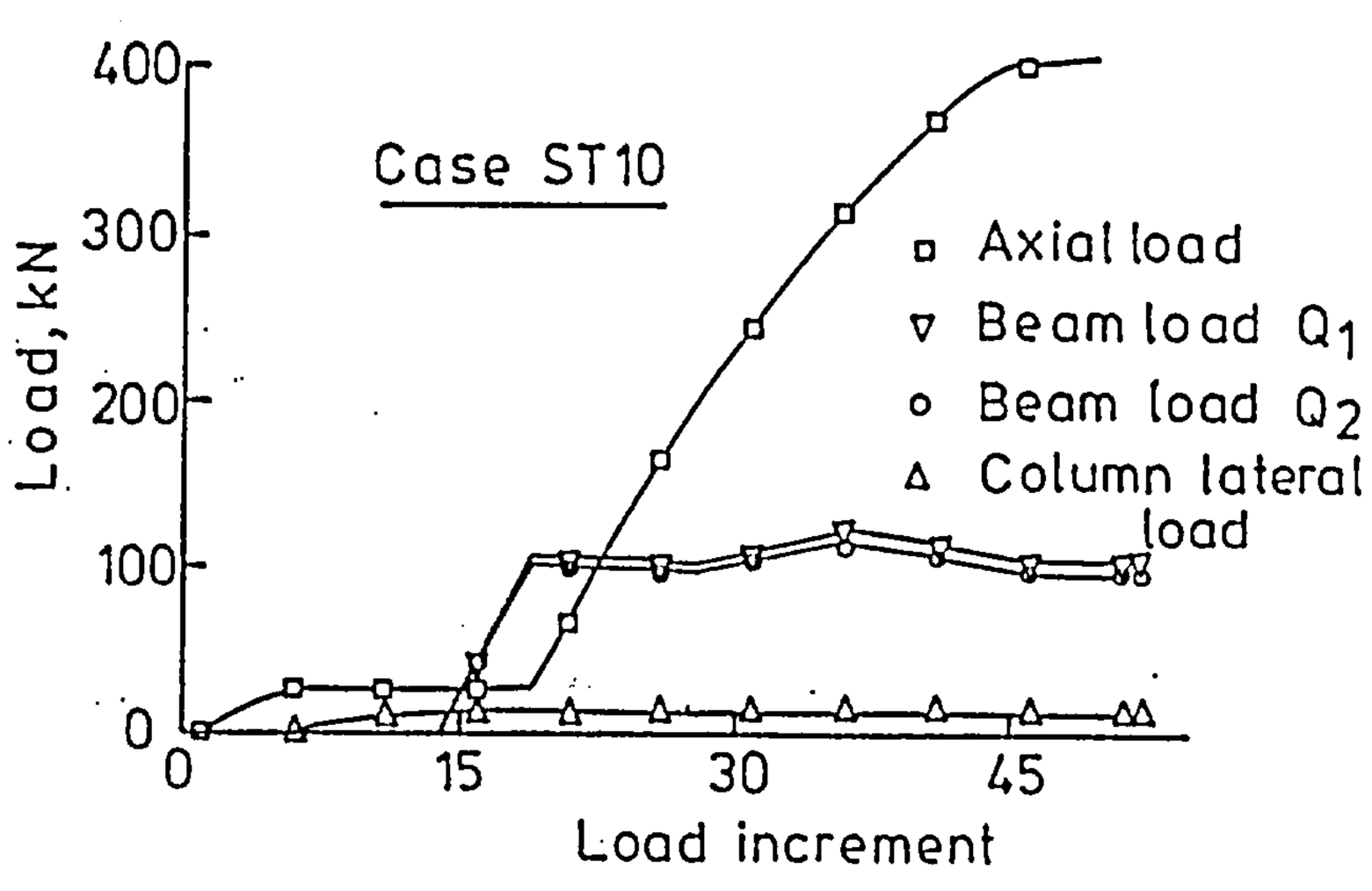

FIG. 6·16(b) LOAD PATTERNS FOR CASES ST7, ST8, ST9 AND ST10

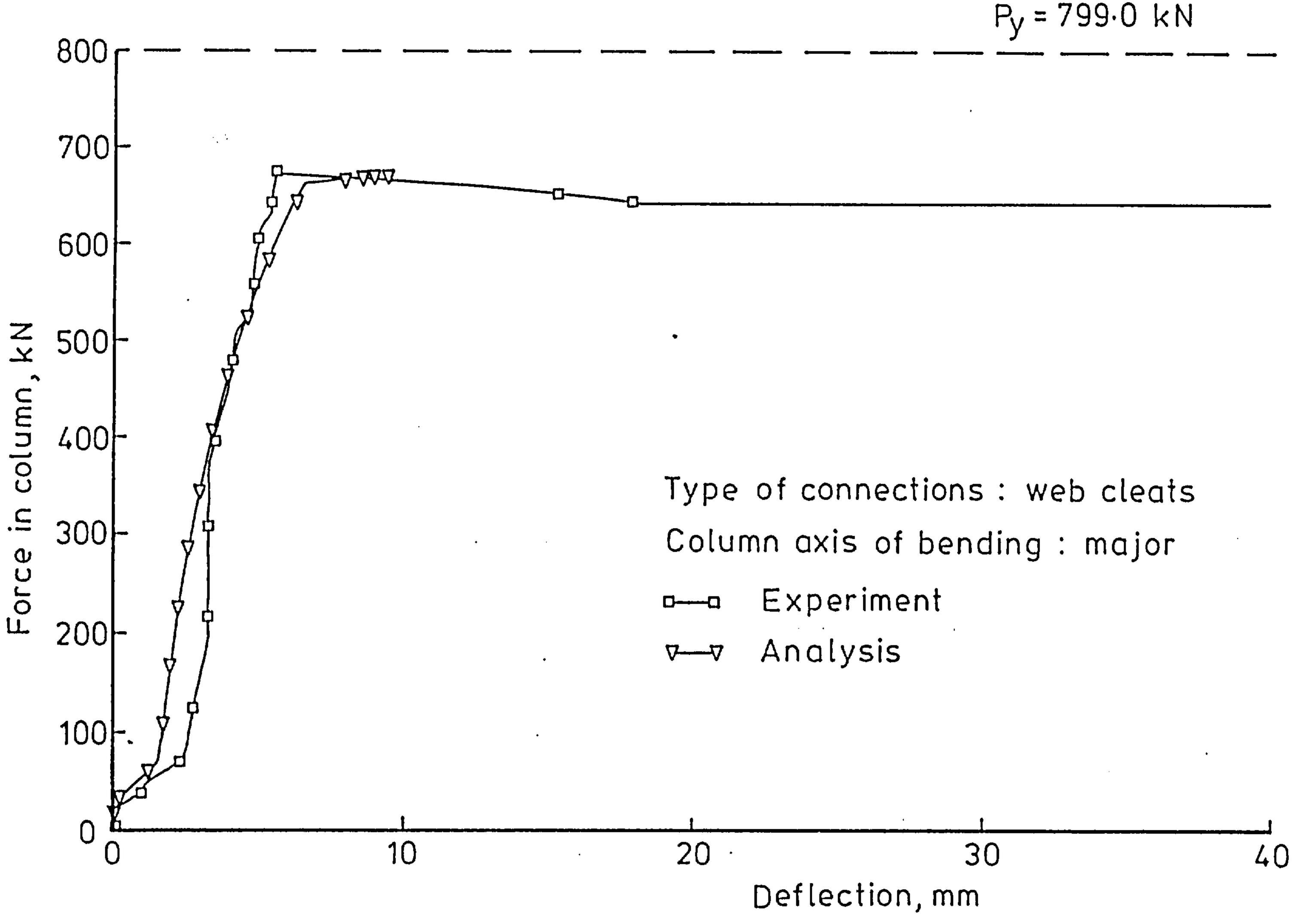

FIG. 6·17 LOAD–DEFLECTION CURVES FOR CASE ST2

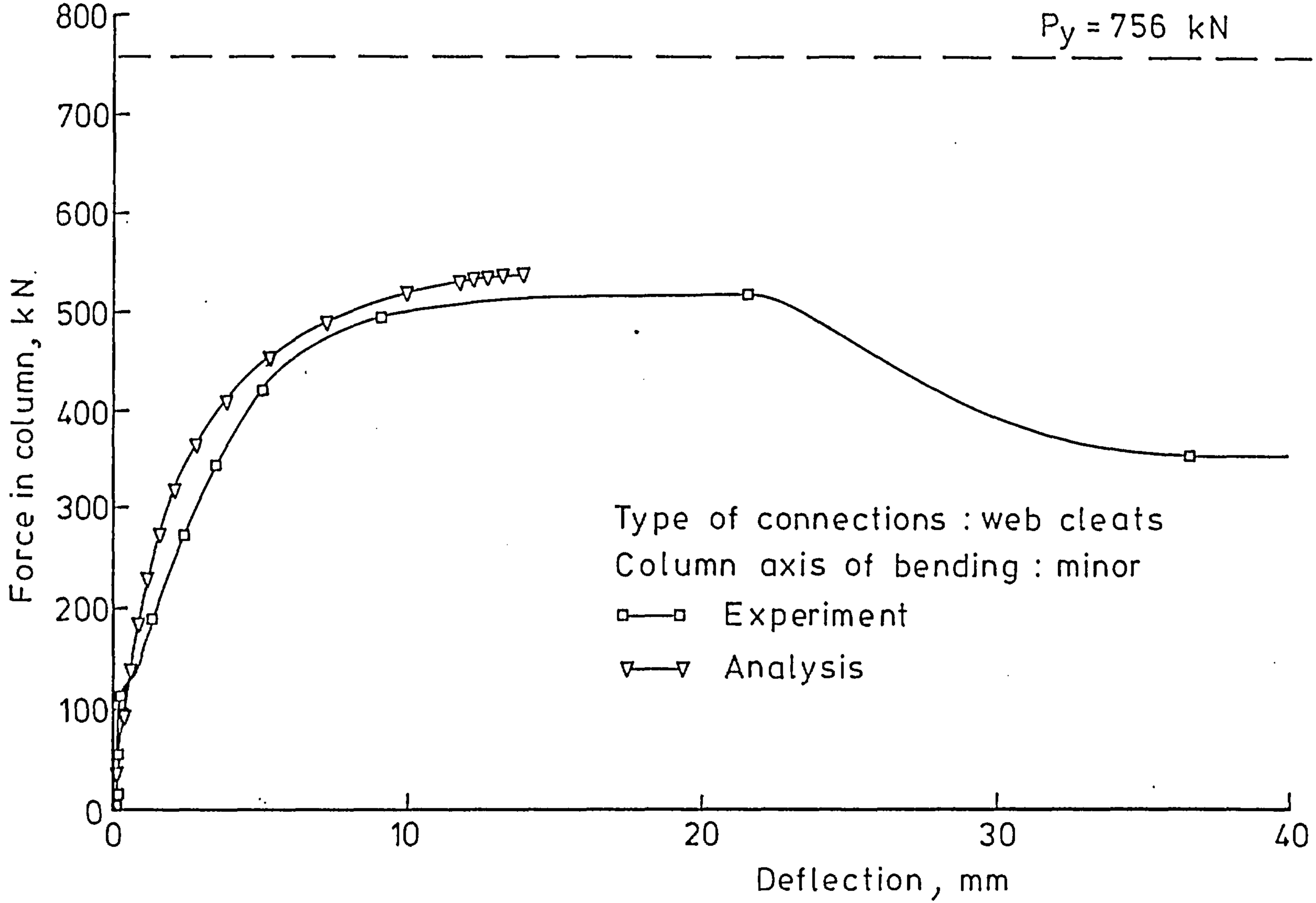

FIG. 6·18 LOAD–DEFLECTION CURVES FOR CASE ST3

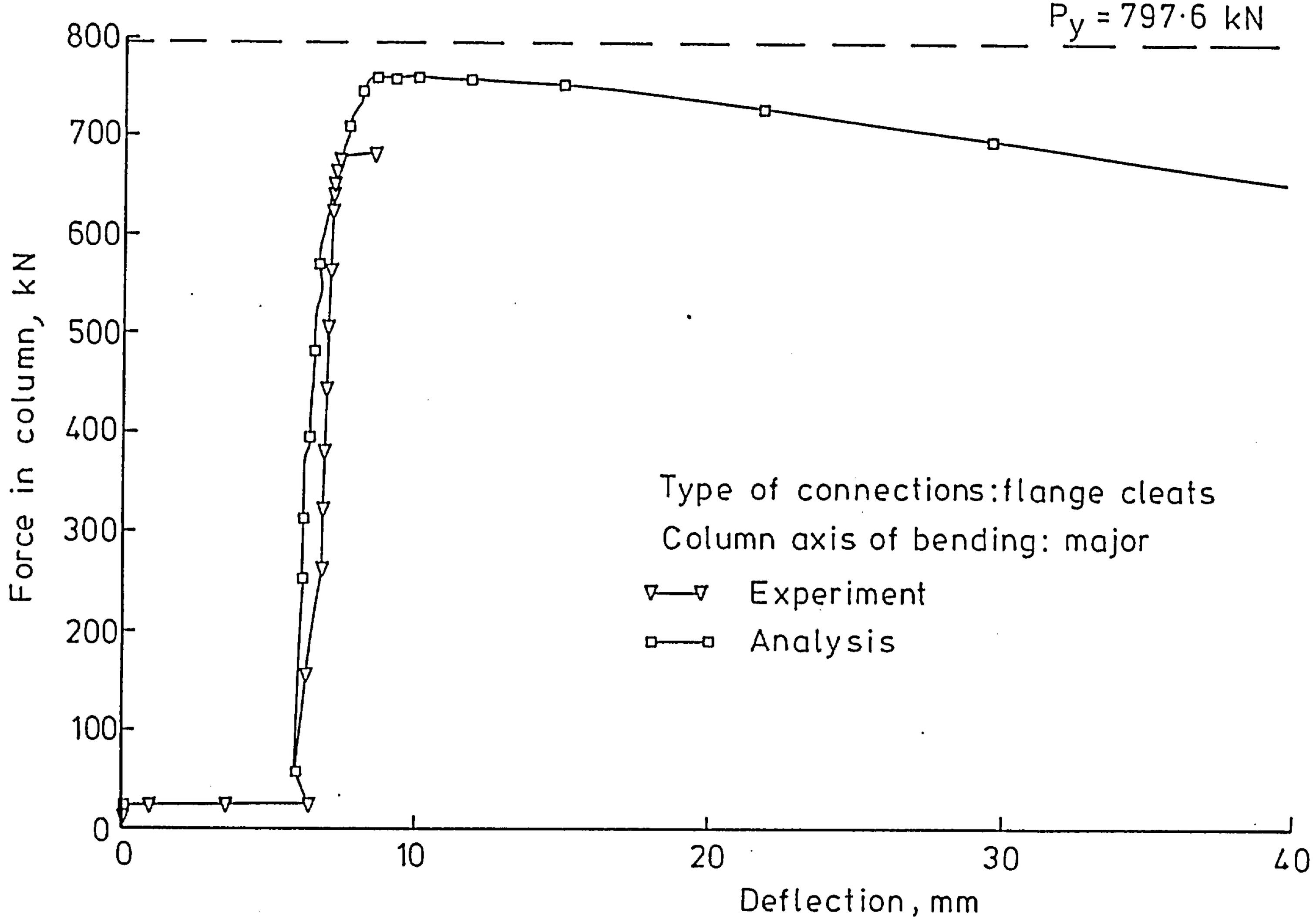

FIG. 6·19 LOAD – DEFLECTION CURVES FOR CASE ST4

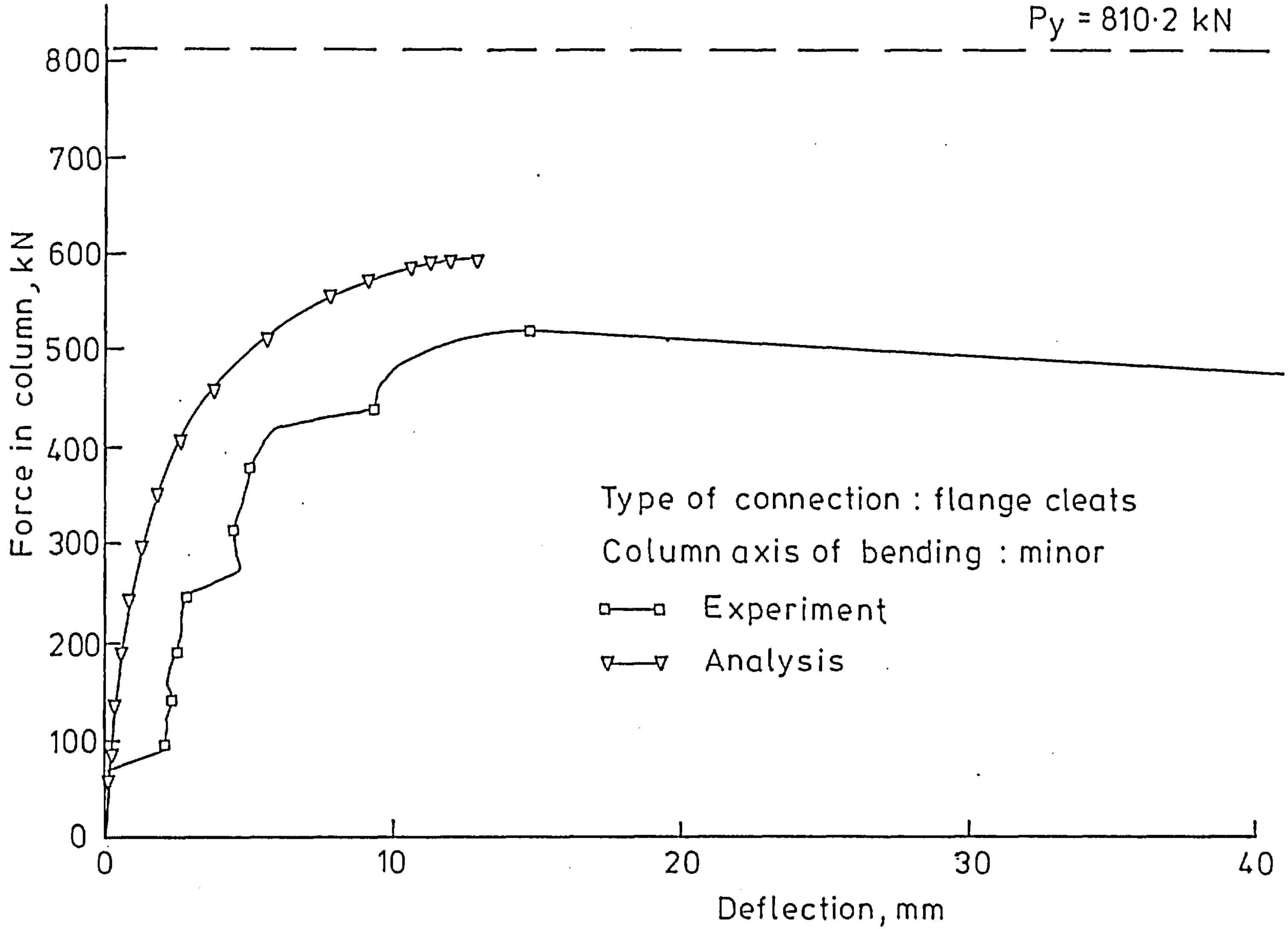

FIG. 6·20 LOAD – DEFLECTION CURVES FOR CASE ST6

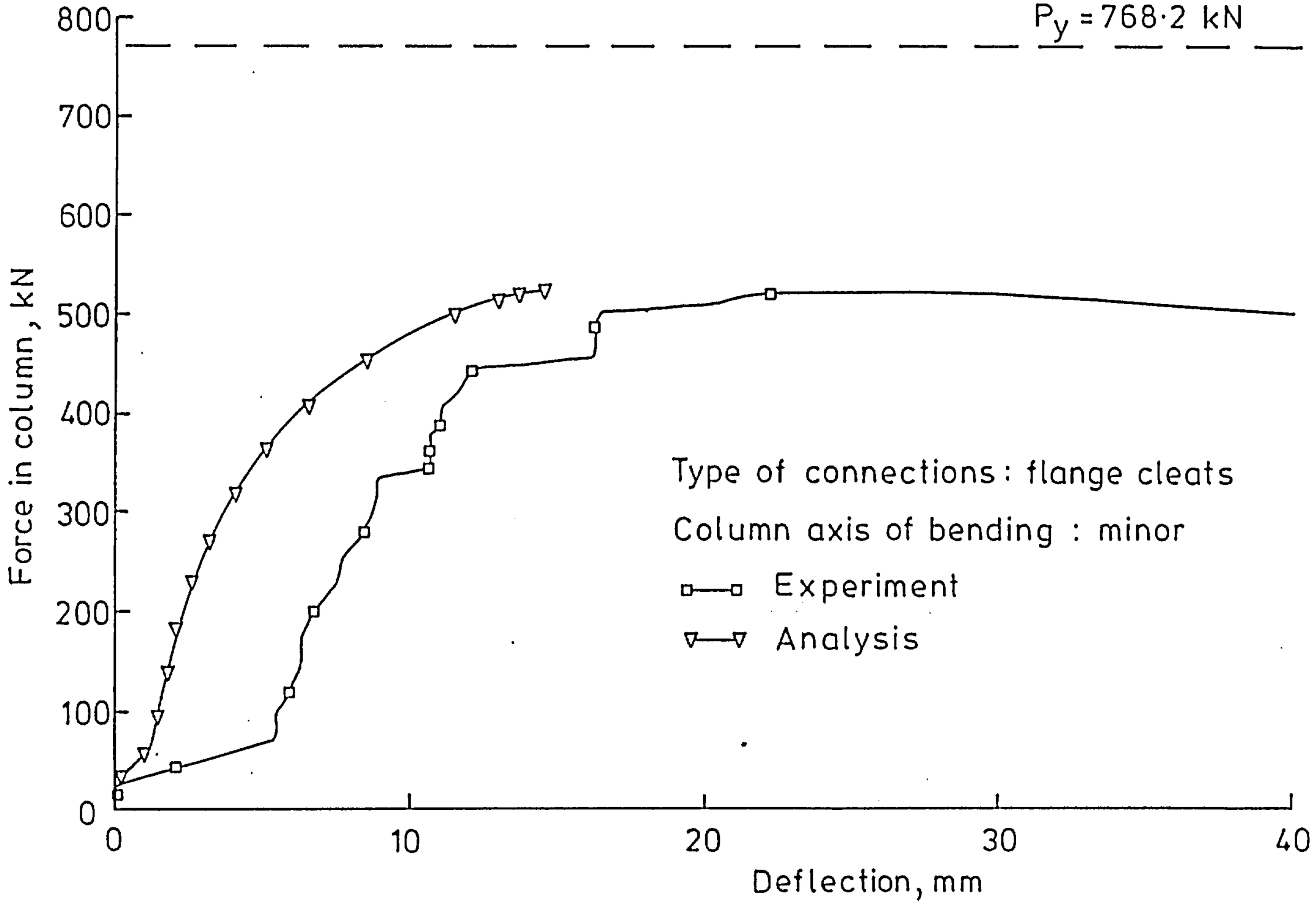

FIG. 6·21 LOAD – DEFLECTION CURVES FOR CASE ST7

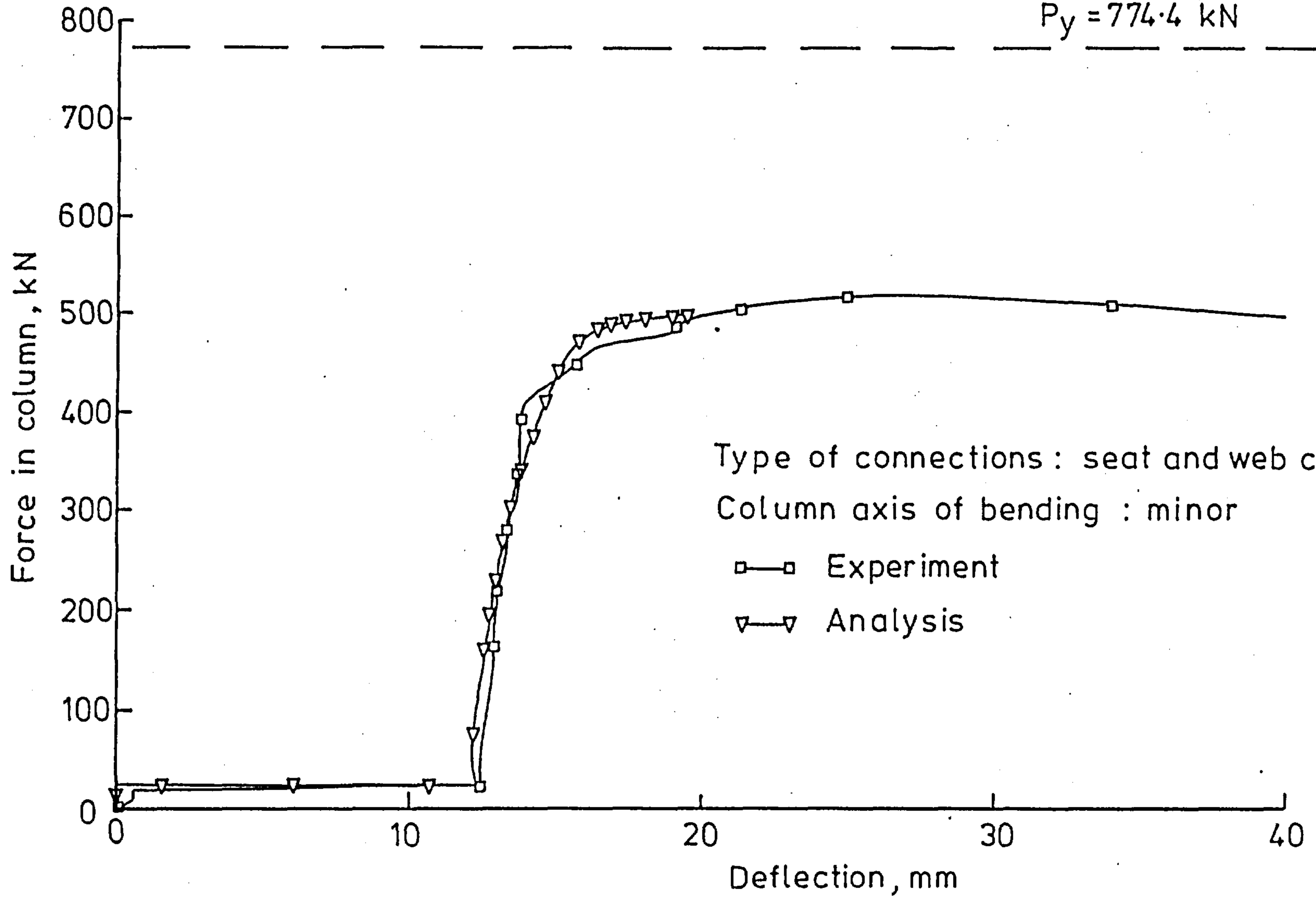

FIG. 6·22 LOAD - DEFLECTION CURVES FOR CASE ST8

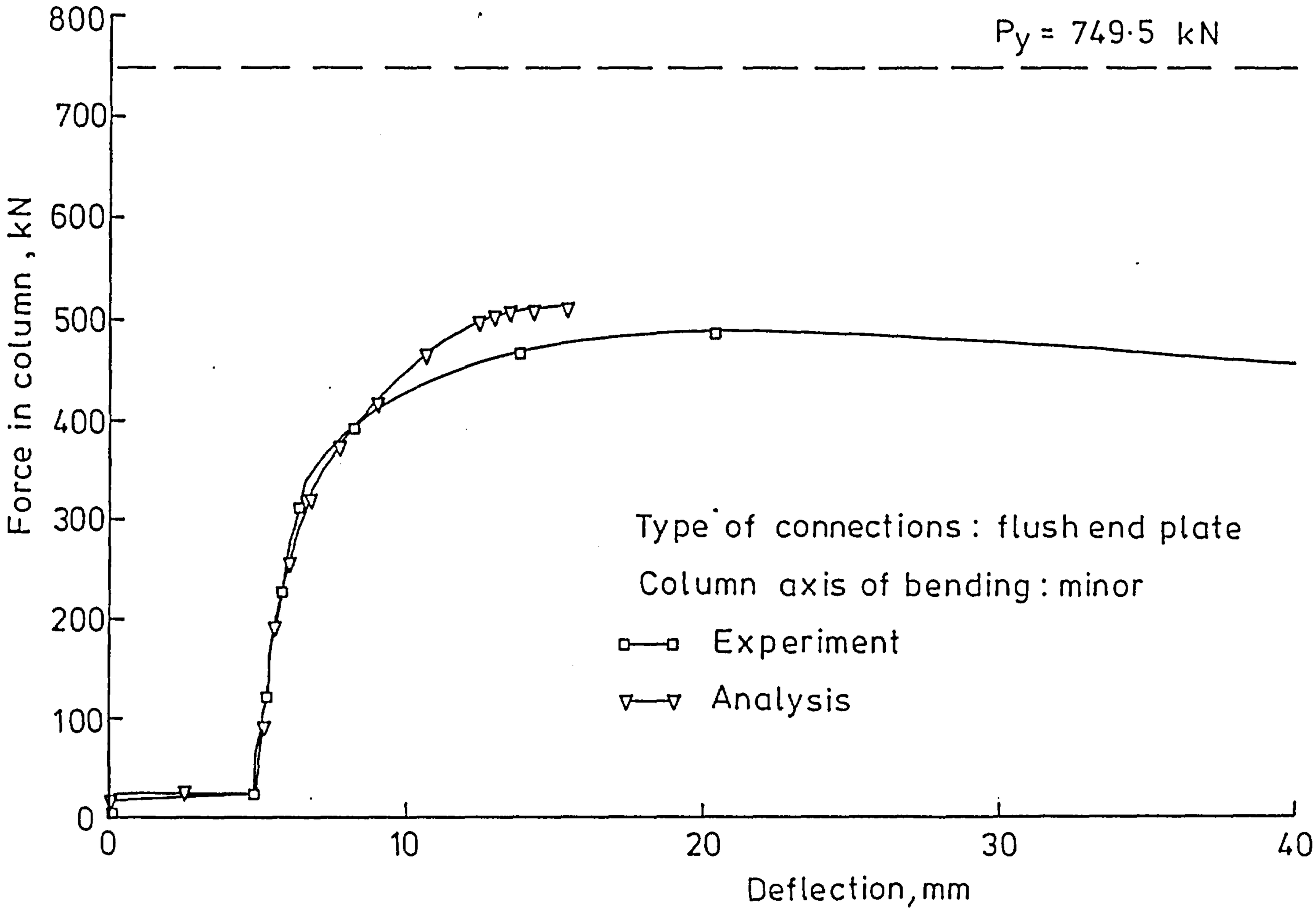

FIG. 6·23 LOAD – DEFLECTION CURVES FOR CASE ST9

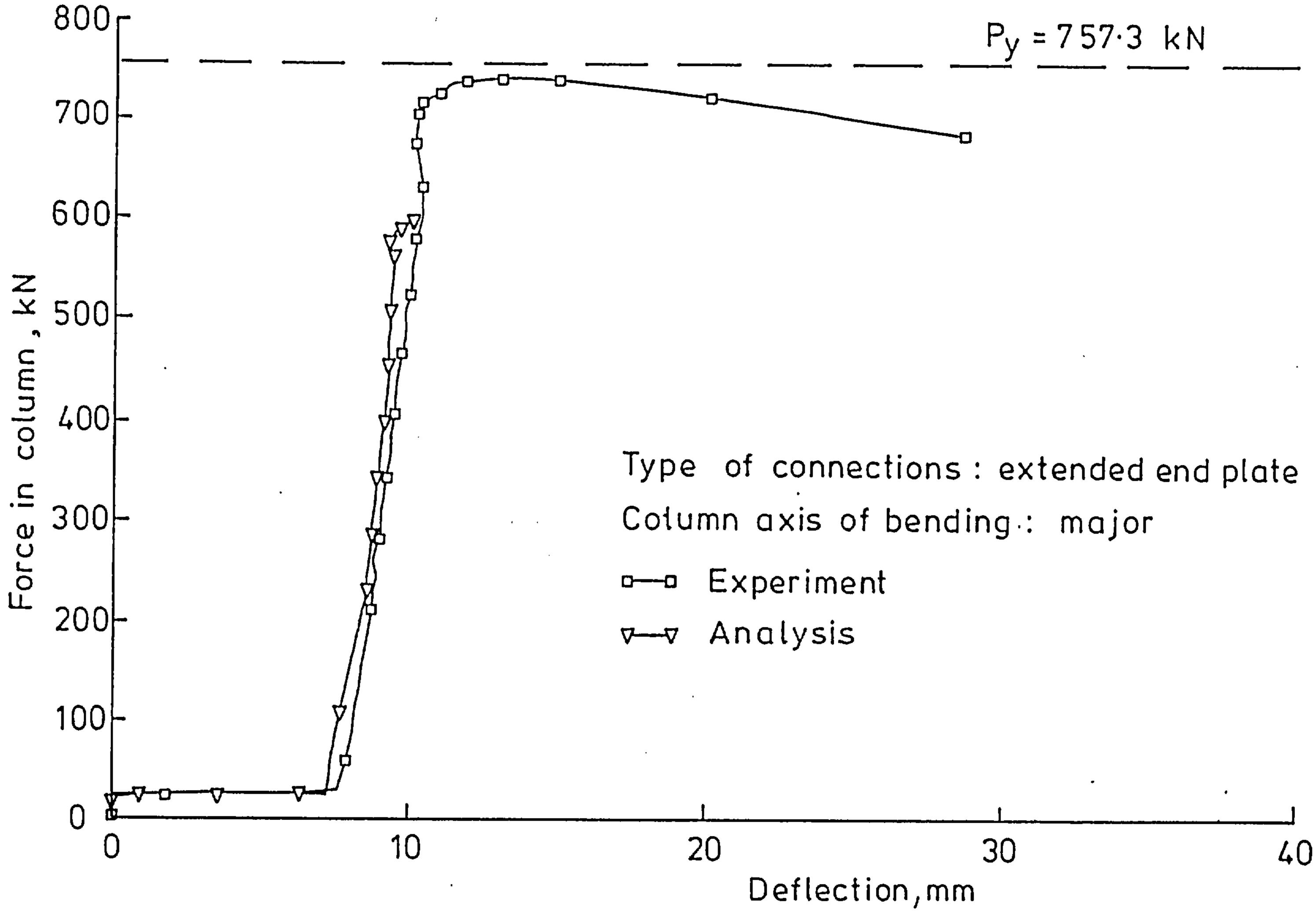

FIG. 6·24 LOAD – DEFLECTION CURVES FOR CASE ST10

predicted by the program. The agreement was acceptable for cases ST4 and ST10, although the maximum loads were not correctly predicted for these cases. The calculated failure loads for these two cases were found to be a result of numerical divergencies rather than true instability conditions. Although the maximum load was predicted with a good degree of accuracy in case ST7, the analytical P-Δ curve was not so good when compared with the experimental one. Perhaps, the worst comparison is that of case ST6. In this case, neither the maximum load nor the P-Δ curve was correctly predicted.

The beam loads used in the analysis of case ST6 were almost symmetrical. The lever arms were nominally the same and the maximum levels for these loads differed by only 3kN(less than 8%). It was expected, therefore, that there would be very small lateral deflections in the column. The relatively small lateral deflections observed in Fig-6.20 are , in fact, due to the assumed initial imperfections and the column load eccentricity. Some of the reasons for the discrepancy between the analytical and the experimental results in this case and in case ST7 might be:

1- The depth of the connection is comparable to the beam load lever arm. This may result in part of the beam load by-passing the connection and acting as a direct axial load on the column. This behaviour is illustrated in Fig-6.25. It is most pronounced in the cases in which flange cleats are used.

2- The use of the same M-Φ curves for both left and right connections. This would lead to reducing the bending moment transmitted to the column as compared with any assumption of unbalanced connection behaviour.

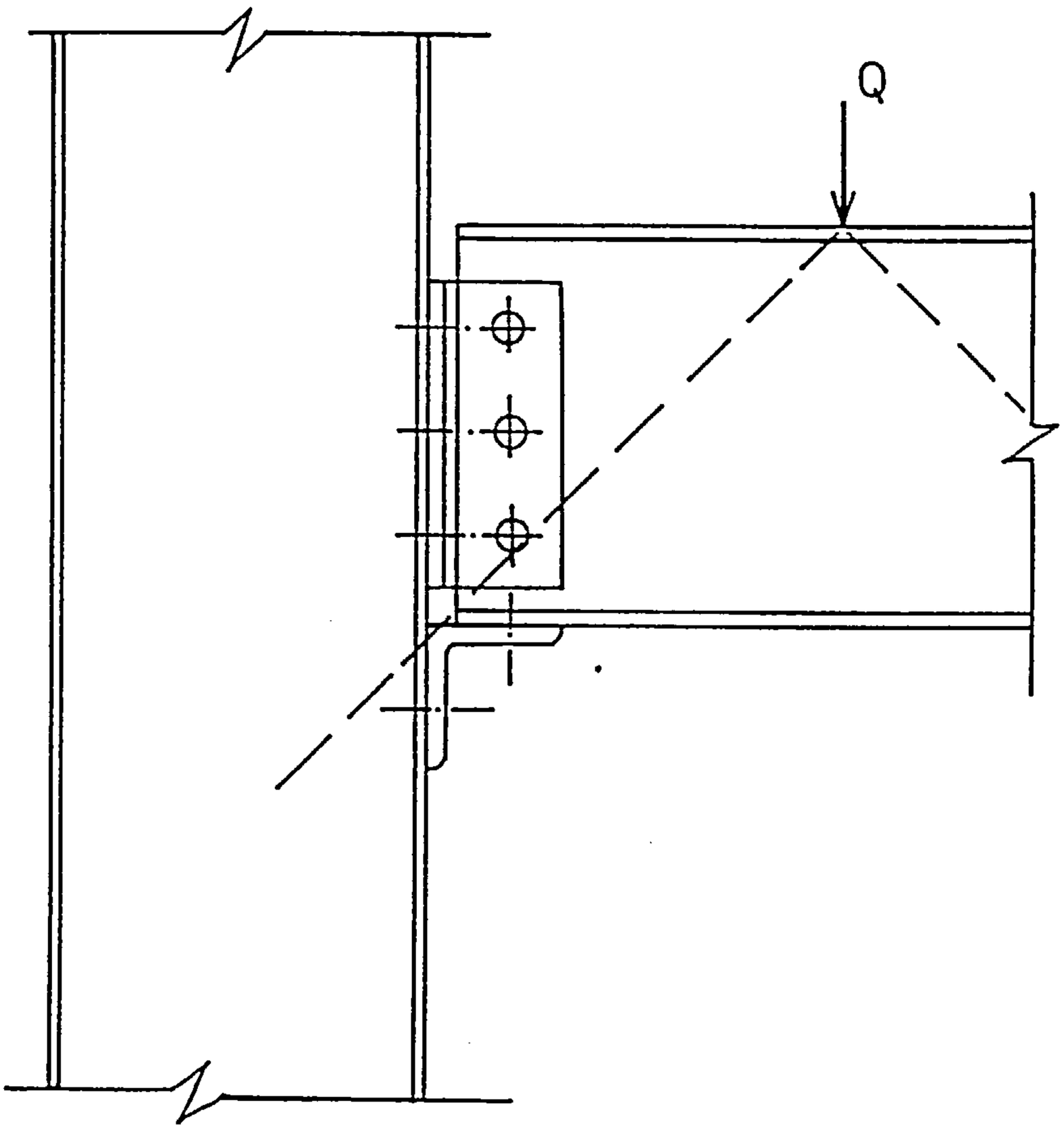

FIG. 6·25 BRIDGING EFFECT ON THE TRANSFER OF THE BEAM LOAD TO THE COLUMN

3- The residual stress state in the column may not be the same as assumed (stress-free). Ref 47 reported that some cross-sections did have some degree of residual stress, but that the overall tendency seemed to be that negligible residual stresses were present. Cold straightening may not have removed all the hot rolling-type residual stresses.

4- The actual connections used may be more flexible than those used in the joint tests- some (small) degree of variability is inevitable.

The subassemblage of case ST6 was re-analysed several times. In the first of these analyses, a small lateral load was applied at the centre of the column. The load was applied in a gradual manner in phases after the application of the 25kN column load. All other parameters were kept the same as described above. The effect of this load is to introduce more bending to the column to compensate for some of the above mentioned reasons. The P-Δ curve for this case is shown in Fig-6.26 along with the experimental curve and the curve obtained from the original analysis of ST6. The maximum load has now dropped to about 566kN, which is 9.3% in excess of the experimental load. The load-deflection curve is closer to the experimental one.

In order to explore the effect of different M-Φ curves on the behaviour of the subassemblage of test ST6, the subassemblage was analysed with two M-Φ curves. The M-Φ relationship that was measured in the experimental test of ST6 for the top left and top-right connections were used to obtain two smooth curves for the two connections. The experimental points were plotted and a smooth curve was drawn so that it passes through one set of data. Particular consideration was given to make the slopes of the curves always descending. Again any

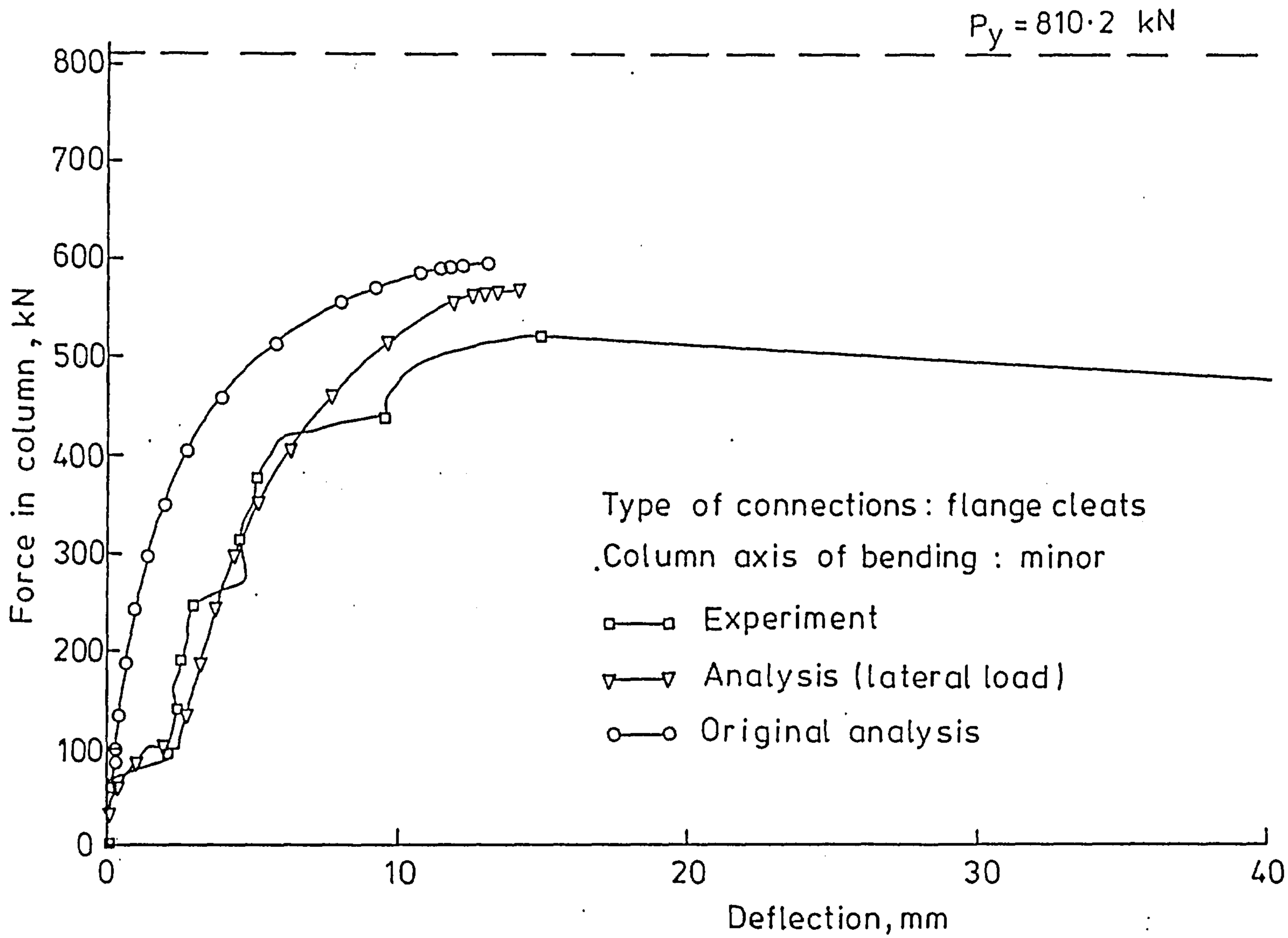

FIG.6·26 LOAD-DEFLECTION CURVES FOR CASE ST6. (RERUN: EXTRA PARAMETERS : A LATERAL COLUMN LOAD)

irregularities or unloading behaviour was not taken into consideration. Fig-6.27 show the experimental M-Φ relationships as well as the smooth curves for the two connections. In addition, the smooth curve used for the original analysis of case ST6 is shown on the same figure. Clearly, the two curves inferred from the subassemblage test departed from each other at a rather low rotation levels. This would have the effect that, in an actual analysis, an amount of bending moment would transfer to the column forcing it to deflect more. It can also be seen from Fig-6.27 that both curves lie below the curve used for the original analysis of case ST6. This means that the two connections are weaker than those tested in the joint tests. This difference in strength, however, may be partly due to the fact that the connections are part of a flexible subassemblage as opposed to the joint test arrangement. All other parameters were assumed to be the same as those assumed for the original analysis of case ST6. The maximum load for this case was about 570kN. Another analysis was performed on the same subassemblage but with residual stresses assumed present in the column. A parabolic variation was assumed for these stresses with a maximum compressive stress at the flange tips of $0.3\sigma_y$. This pattern of residual stresses is similar to that suggested by Young (57), but is slightly less severe. The maximum load dropped to about 530kN, which is in excess of the experimental load by less than 2.5%. The P-Δ curves for this last analysis as well as the experimental one are shown in Fig-6.28.

It is evident from the above analyses on case ST6 that the level of uncertainty in the input data to the subassemblage analysis is sufficient for it to have a significant result on the behaviour of the subassemblage. These results also show that it is not always possible to exactly simulate experimental tests.

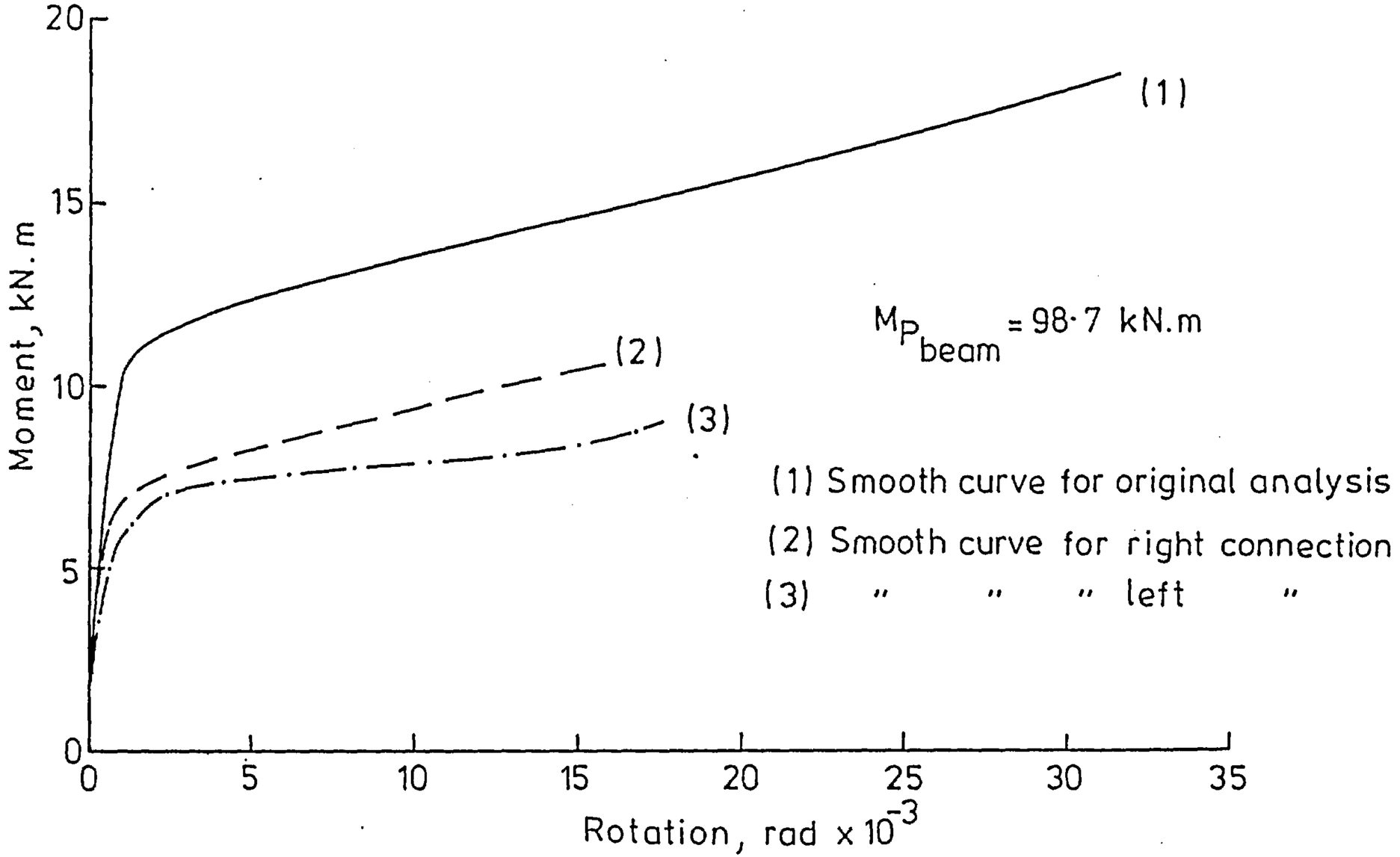

FIG.6·27 M– ϕ CURVES FOR A FLANGE CLEAT CONNECTION
(CURVES 1 AND 2 INFERRED FROM TEST ST6)

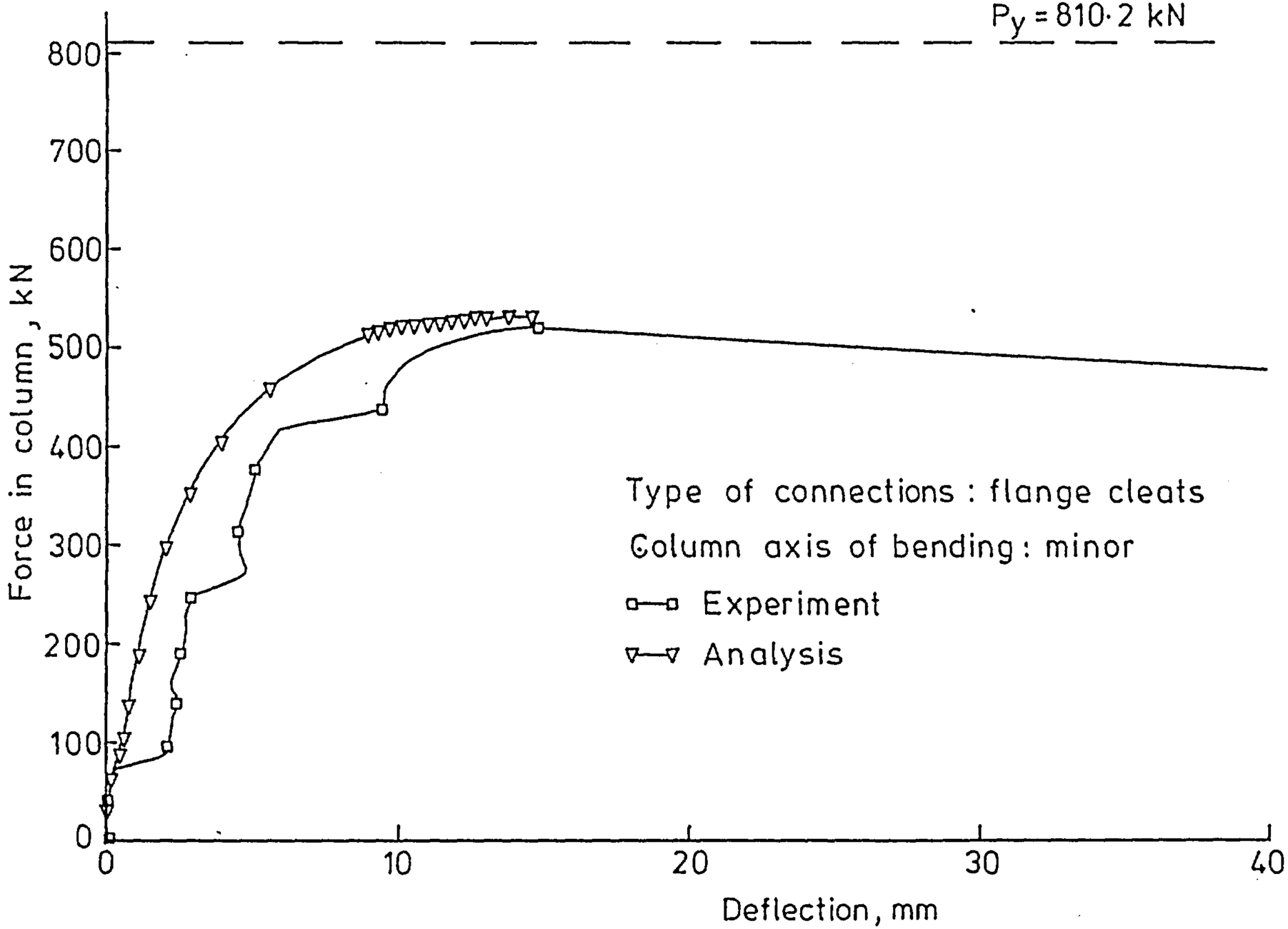

FIG. 6·28 LOAD - DEFLECTION CURVES FOR CASE ST6 (RERUN)
EXTRA PARAMETERS (1) A PARABOLIC RESIDUAL STRESS PATERN
(2) TWO DIFFERENT M - ϕ CURVES FOR LEFT & RIGHT CONNECTIONS

A further analysis was carried out on the subassemblage of test ST7. In the same way as was done for case ST6, a small lateral load was applied to the column. All other parameters were the same as for the original analysis. The P-Δ curve for this case is shown in Fig-6.29. The comparison with the experimental curve was quite satisfactory. The maximum load was about 3.5% below that obtained experimentally.

6.3.2- Column axial load - column moment (P-M) Curves

It is of interest to study the distribution of moments at the top end of the column at various stages during the loading sequence. Such a study should assist in understanding how much moment is transfered to the column during the loading process. The most important load level at which this distribution is needed, is clearly immediately prior to failure of the column. For simple construction, BS5950 (1) requires that the column be designed for the maximum axial load together with a moment given by the product of the beam reaction and an eccentricity of 100mm measured from the face of the column flange or the column web depending on whether major or minor column bending is being considered. Another reason for the importance of studying the beam P-M curves is that with these curves it is possible to know when the connections unload or reload. This is because the variation of a beam moment dictates the behaviour of the connection which is connected to the beam since the moment in the connection must be equal in magnitude and opposite in sign to the beam moment. A connection would either load, unload or reload depending on the variation of the joint moment.

Figs-6.30, 6.31, and 6.32 show the P-M curves for the top

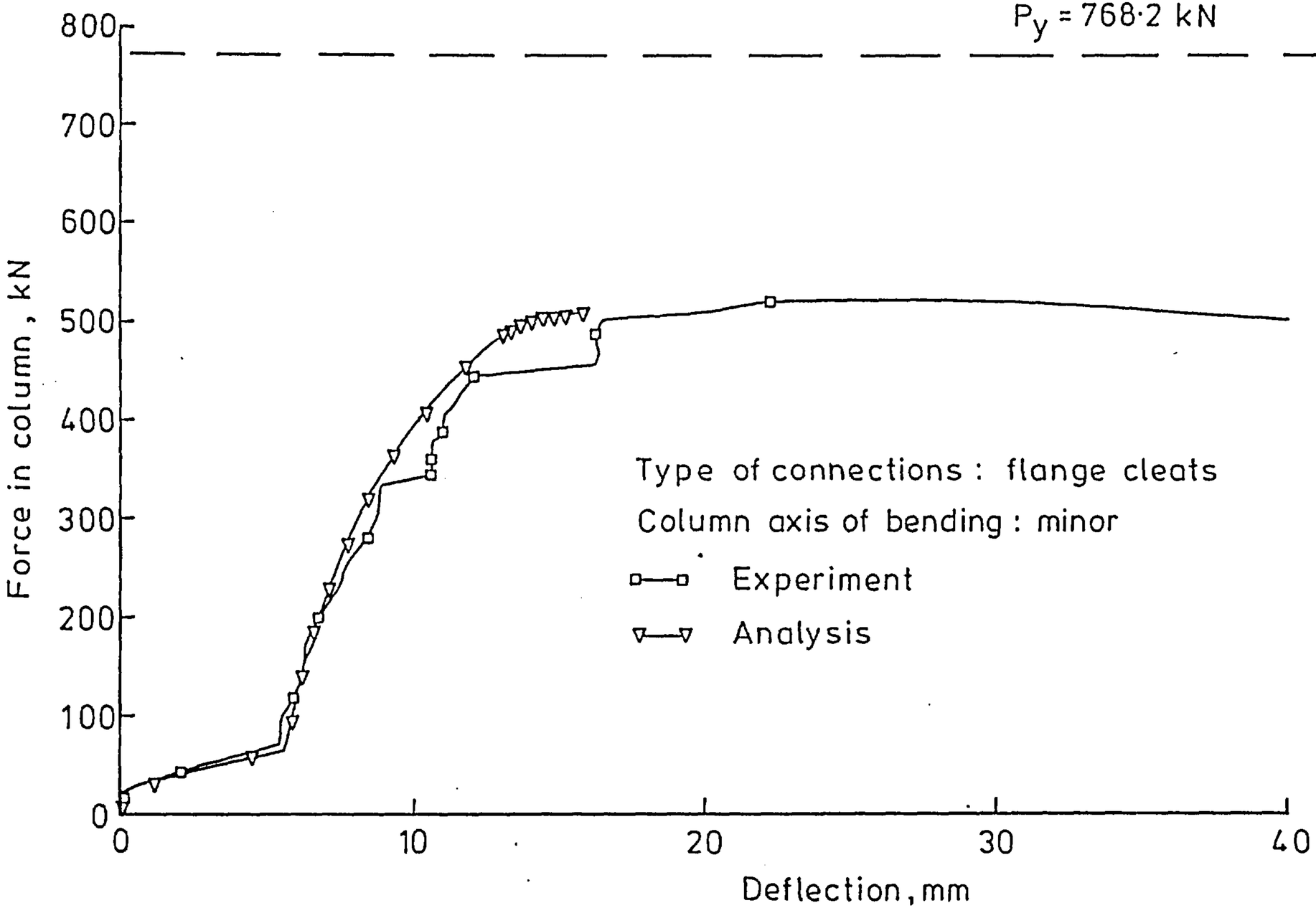

FIG.6·29 LOAD-DEFLECTION CURVES FOR CASE ST7 (RERUN)
EXTRA PARAMETERS : A LATERAL COLUMN LOAD

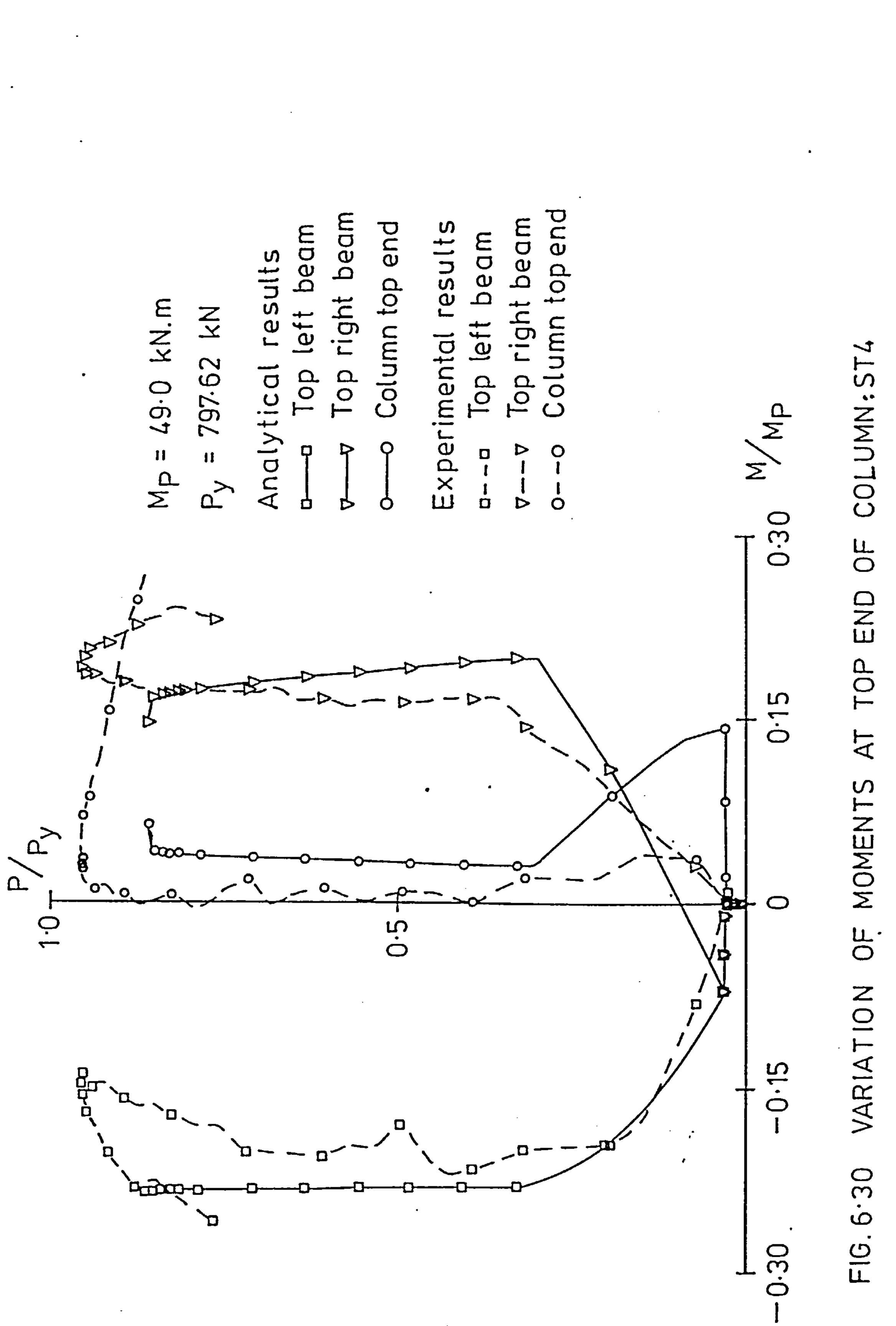

FIG. 6·30 VARIATION OF MOMENTS AT TOP END OF COLUMN: ST4

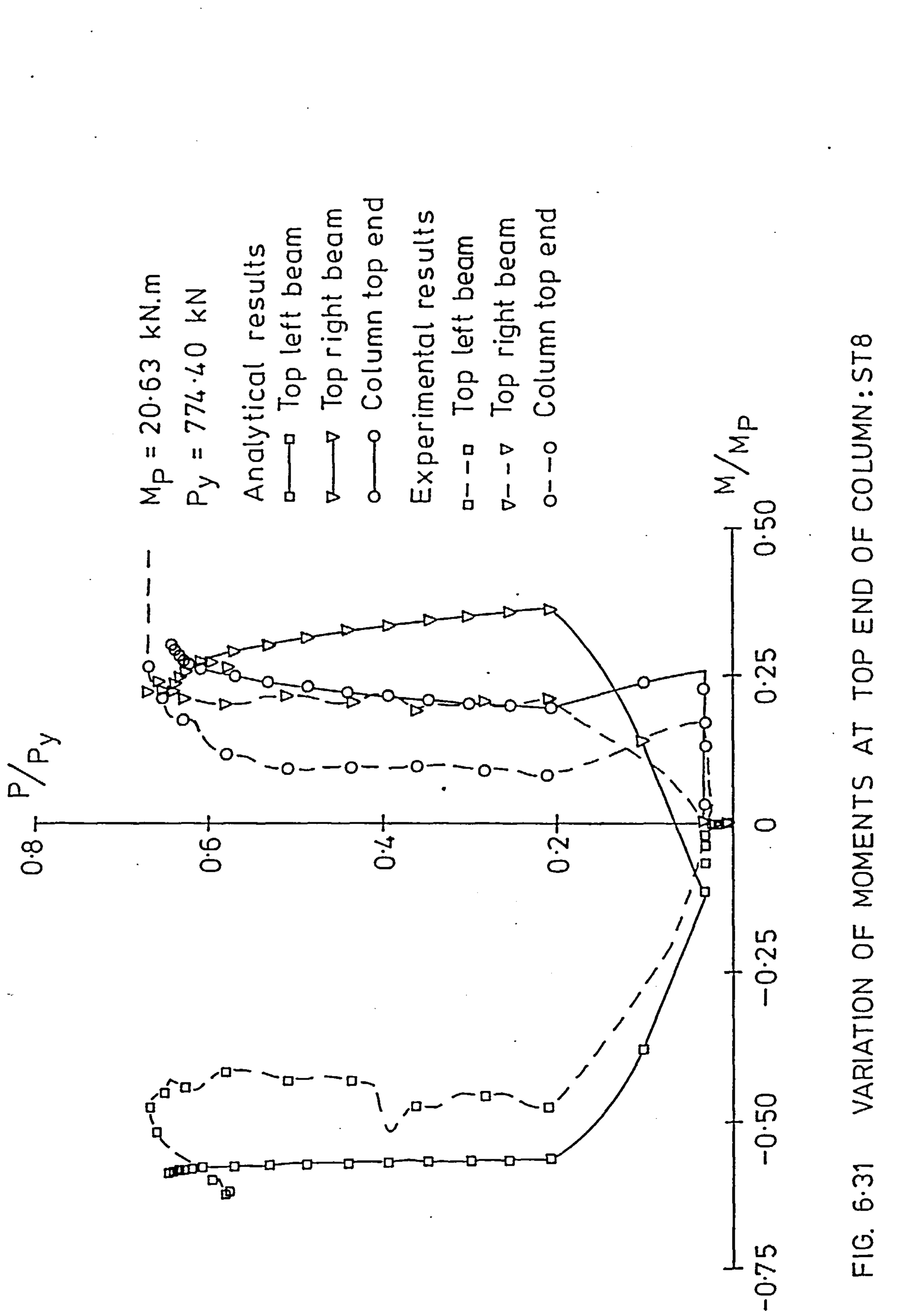

FIG. 6·31 VARIATION OF MOMENTS AT TOP END OF COLUMN: ST8

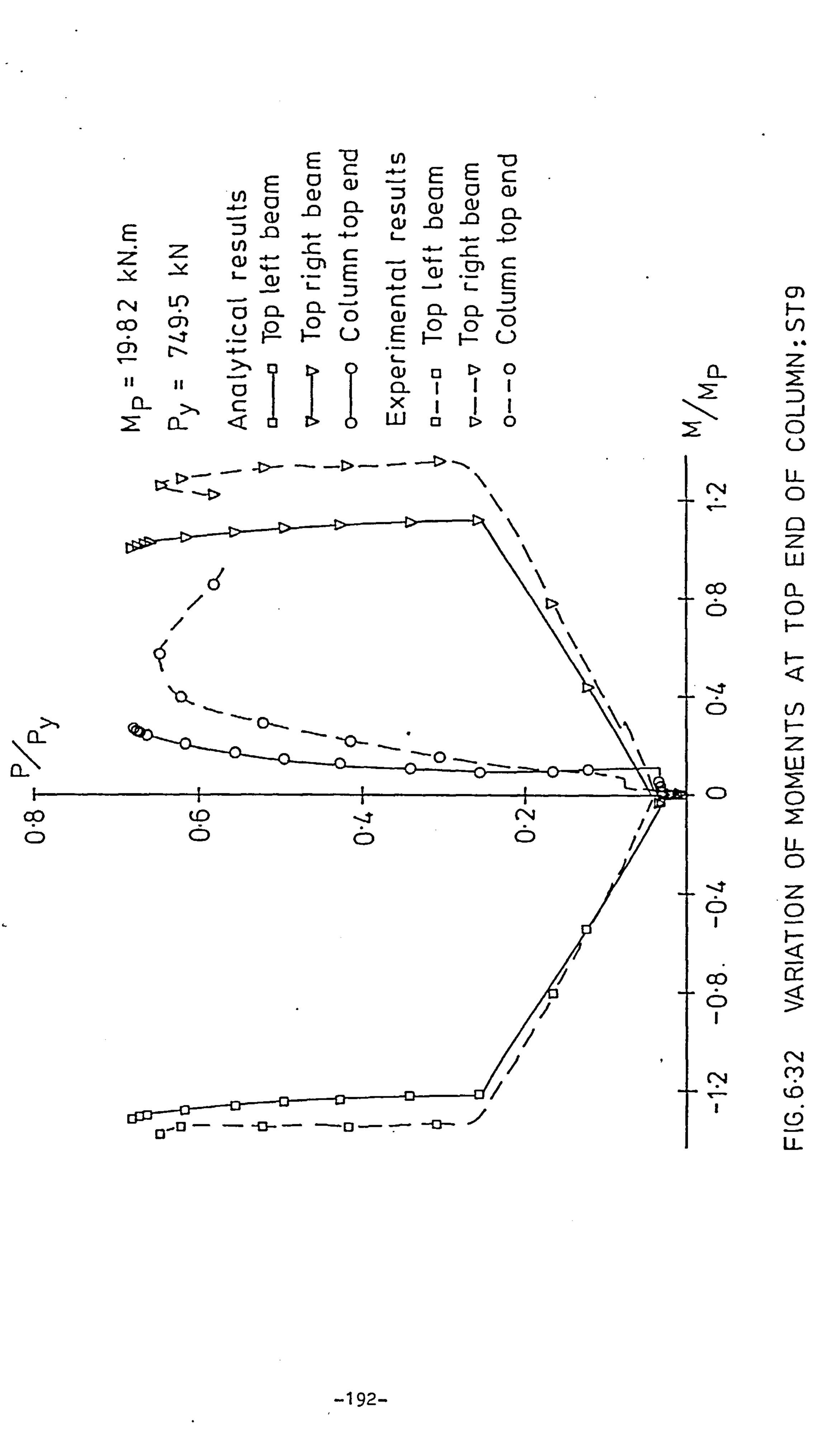

FIG.6.32 VARIATION OF MOMENTS AT TOP END OF COLUMN N:ST9

left beam, top right beam and the top column moments of the subassemblages of tests ST4, ST8 and ST9. Both the analytical and experimental curves are shown in these figures. Very good agreement between the two sets may be observed in each case. The general trend of the curves was correctly predicted by the analysis. It should be noted that the experimental column moments correspond to points situated about 250mm below the connection level. The P-M curves for most of the other cases also have acceptable comparisons for the moment variation in at least one of the three components. For example, the P-M curves for the left and right beams compared well with those obtained from the experimental results of test ST6 (Fig-6.33). The column moment, however, seems to reverse in direction as failure is approached. Similar observations are noticed for case ST7 (Fig-6.34) in which the column moment changed sign as the column load increased. The magnitudes of the predicted and measured moments are not satisfactorily close.

Returning to Fig-6.33, it may be noticed that the experimental column moment fluctuated about zero up to a column force of 400kN. The maximum moment in the column in this region was not more than 0.5kN-m. This is due to the approximately symmetrical beam load which should not produce any moment in the column. The small moments in this region are probably the result of the slightly different behaviour of the left and right connections and initial imperfections e.g. lack of straightness of column. This observation raises a question as to whether the sudden increases in the lateral deflections in the column (Fig-6.19) are genuine or not. If it is accepted that these increases are not true, then they should be omitted. Probably, these sudden increases are caused by a slight tendency to move laterally, restrained by small frictional forces in the bracing system etc. resulting in

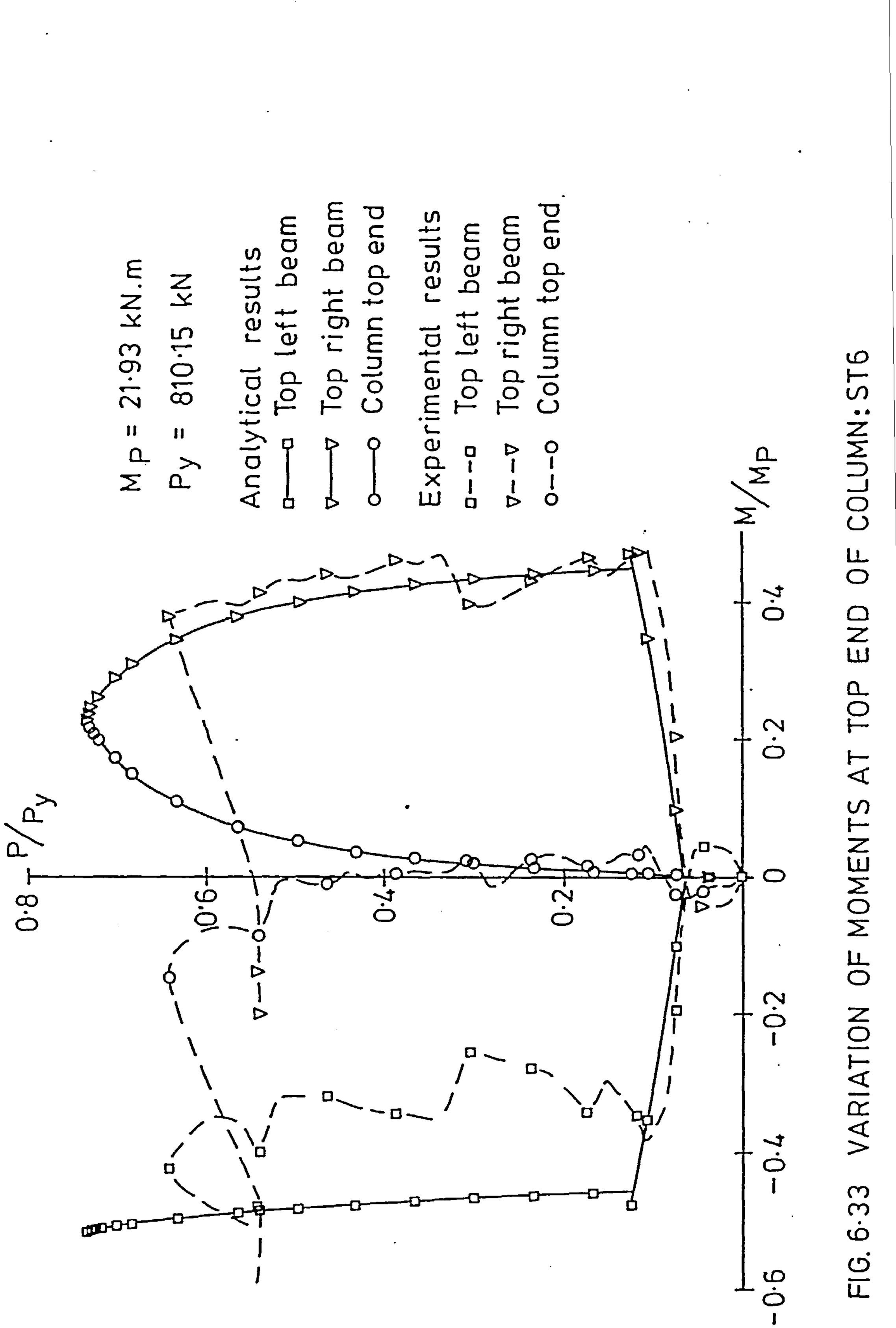

FIG. 6·33 VARIATION OF MOMENTS AT TOP END OF COLUMN: ST6

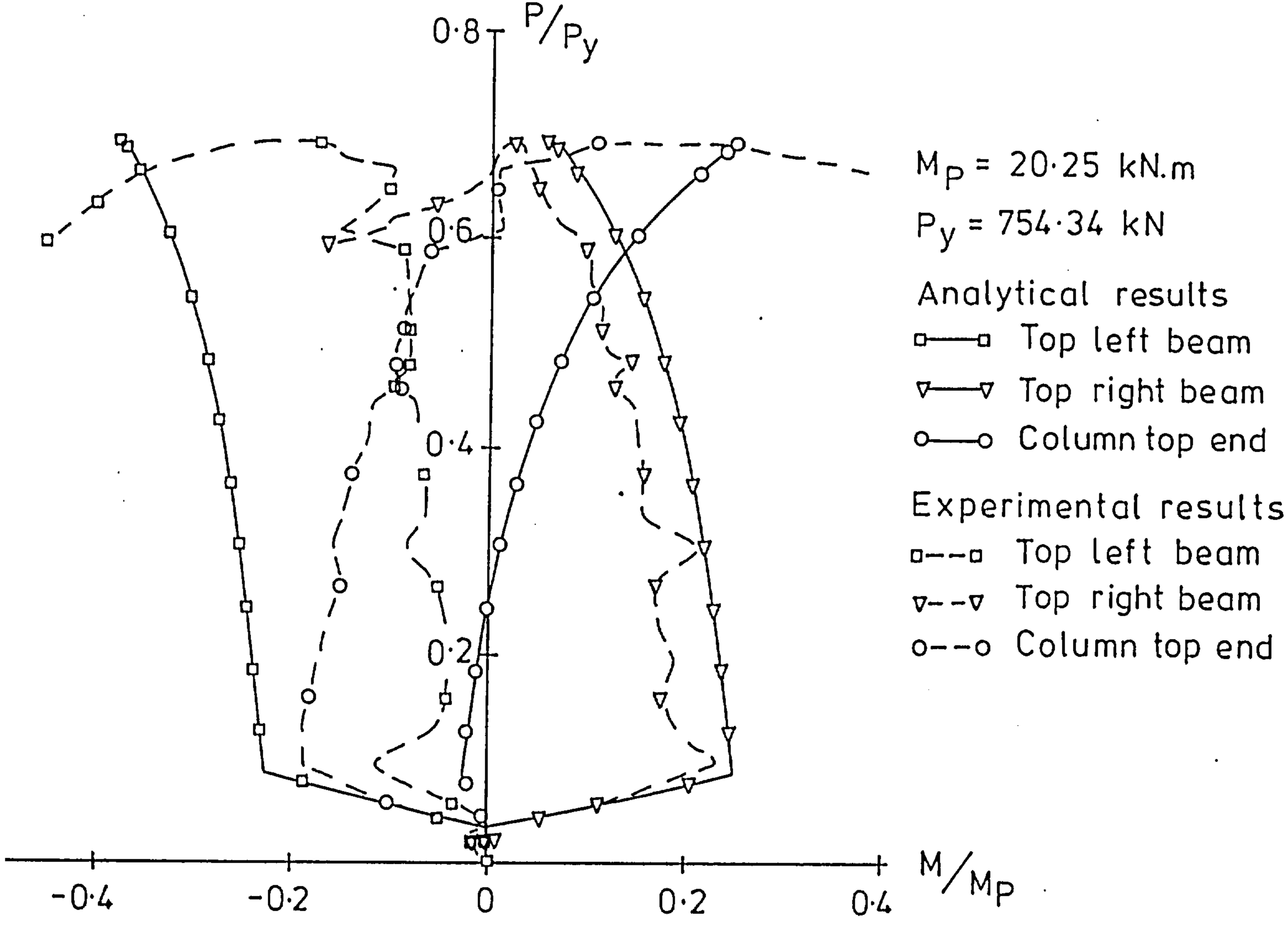

FIG. 6·34 VARIATION OF MOMENTS AT TOP END OF COLUMN: ST 7

jerky movements as frictional resistance builds up and is then overcome. Consequently, the analytical P-Δ curve of case ST6 (Fig-6.28) in which residual stresses were assumed to be present, may readily be accepted.

Fig-6.35 shows the P-M curves for case ST7 in which a lateral load was applied to the column. It is readily seen that the column moment has a completely different pattern from that of the experimental one. This suggests that in this instance the application of a lateral load to the column is not the solution for the discrepancy encountered in Fig-6.20. Once more, the same explanation that was suggested for the sudden movements in test ST6 may be offered here, since both the P-Δ curves for the two cases contain sudden movements. As the maximum load for this case was predicted with a good accuracy, it seems that the assumption of no residual stresses was correct.

Table-6.7 shows for each of the cases ST2 to ST10, the maximum load (including beam loads) and the corresponding column moment obtained from the analysis and the experimental test. In addition, the column moments recommended by BS5950 are shown in this table. According to this latter source, the column moment is taken as the result of multiplying the beam reaction and an eccentricity e given in mm by

$$e = \frac{D}{2} + 100 \quad \text{for major axis column bending} \qquad (6.1a)$$

$$= 100 + \frac{t_w}{2} \quad \text{for minor axis column bending} \qquad (6.1b)$$

for the cases in which other than cap plates are used. In the case of plate connections such as flush or extended end plates, the eccentricity e is given by

$$e = \frac{D}{2} + t_p \quad \text{for major column bending} \qquad (6.2a)$$

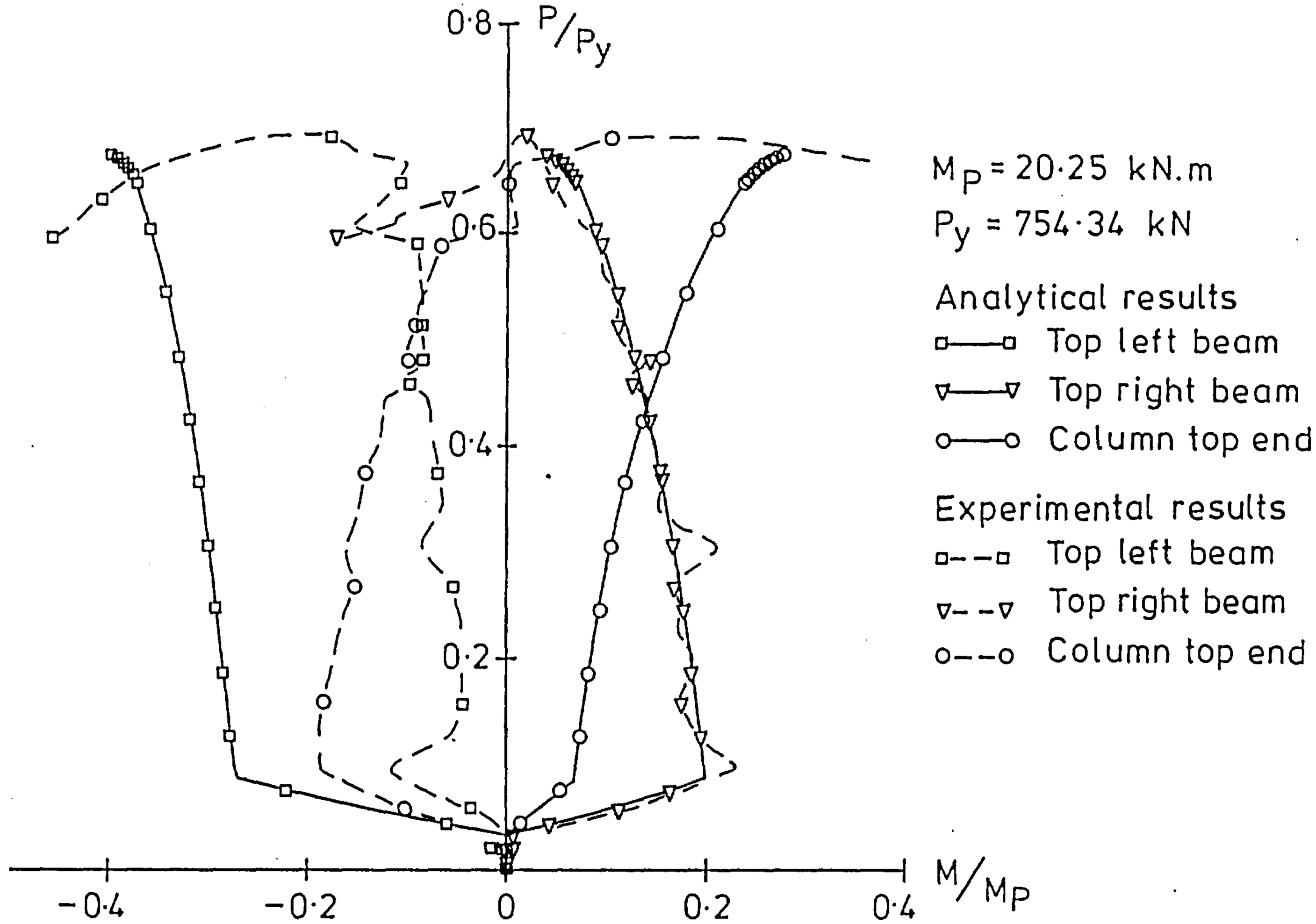

FIG. 6·35 VARIATION OF MOMENTS AT TOP END OF COLUMN: ST7 (RERUN)

Table-6.7: Total Column Loads and Column Moments at the Maximum Load

Case	Analysis		Experiment		BS5950*	
	P (kN)	M (N-m)	P (kN)	M (N-m)	P (kN)	M (N-m)**
ST2	670.5	736.0	675.6	-	670.5	14069.0
ST3	537.5	4980.0	519.9	4363.0	537.5	1205.0
ST4	683.3	3041.0	762.0	802.0	683.3	927.0
ST6	594.4	4992.0	520.3	3233.0	594.4	1180.0
ST7	524.0	5275.0	526.4	2298.0	524.0	4968.0
ST8	498.7	6353.0	518.3	5415.0	498.7	1024.0
ST9	511.0	5586.0	486.5	11286.0	511.0	686.0
ST10	596.5	8185.0	742.8	26955.0	596.5	1385.0

* moments are based on beam loads used in the analysis

** including an axial load eccentricity of 2mm

$$= t_p + \frac{t_w}{2} \qquad \text{for minor column bending} \qquad (6.2b)$$

In the above equations, D is the depth of the cross-section of the column, t_w is the thickness of the web of the section and t_p is the thickness of the packing material if used. In the calculations leading to the values reported in Table-6.7, t_p and t_w were neglected. A column load eccentricity of 2mm was used. It has to be noted that experimental column moments correspond to points which are slightly offset from the beam and column intersection.

It is seen from Table-6.7 that the recommended values of the column moments in the case of nearly balanced beam loads were grossly under-estimated. The analytical moments are, in general, higher than the experimental ones. All of the results shown in Table-6.7 correspond to the maximum loads for which there may be some difference between the analysis and the tests. Fig-6.36 shows the interaction between the nondimensionalized total column load and the nondimensionalized column moment for the cases considered. The nondimensionalized column load was obtained by dividing the total load by the critical load defined as the less of the squash load and the Euler load for the column in consideration. The plastic moment of the column's section was used to nondimensionalize the column moments. It is clear that the experimental results are more scattered than the analytical ones.

Although it is difficult to draw reasonable conclusions from this figure, since the number of cases is small, a few points may be made:

1- The BS5950 recommendations seem to be too conservative for cases where there is load on one beam only but may be unconservative in cases where balanced beam loads are used, regardless of the

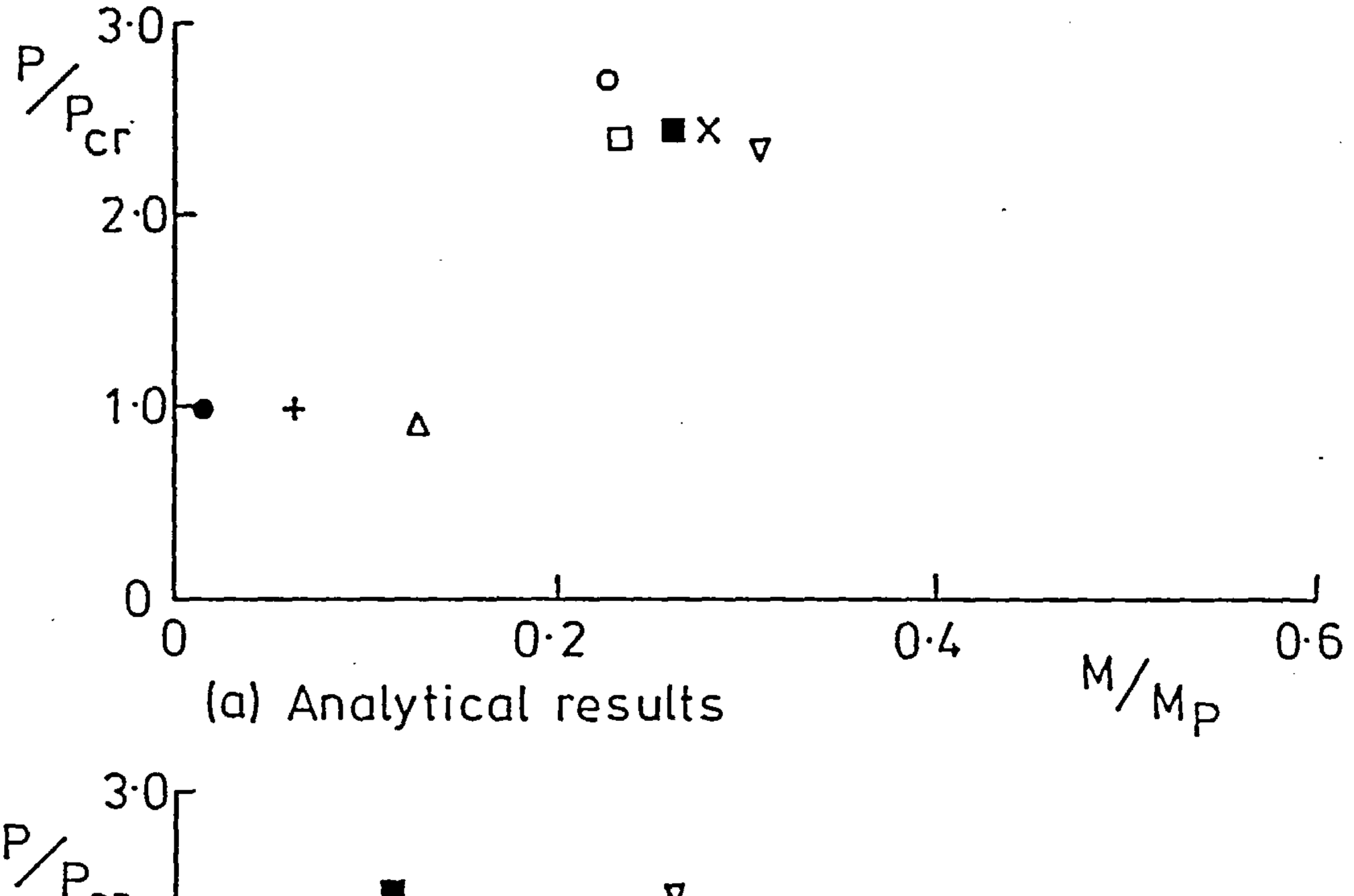

(a) Analytical results

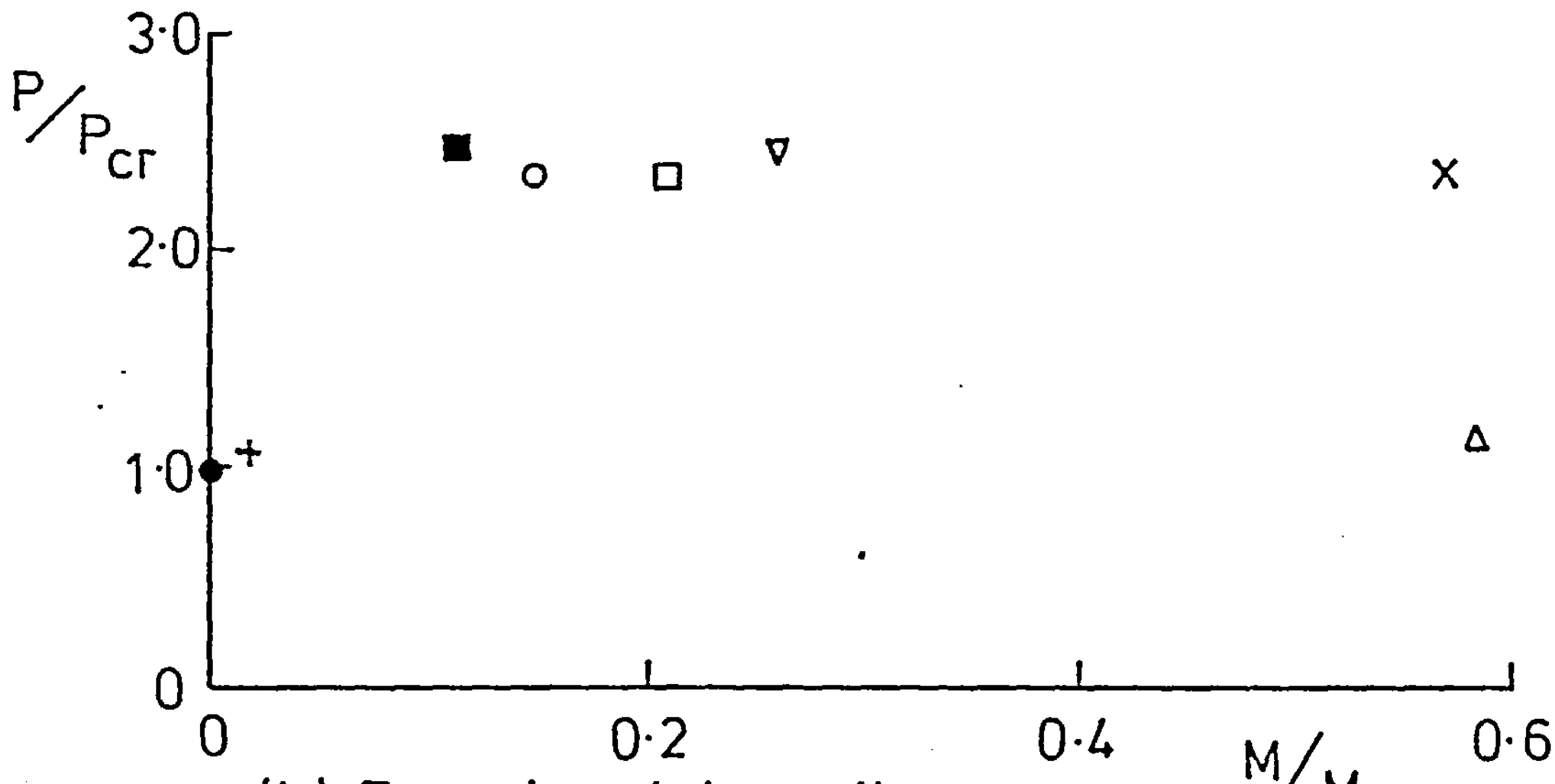

(b) Experimental results

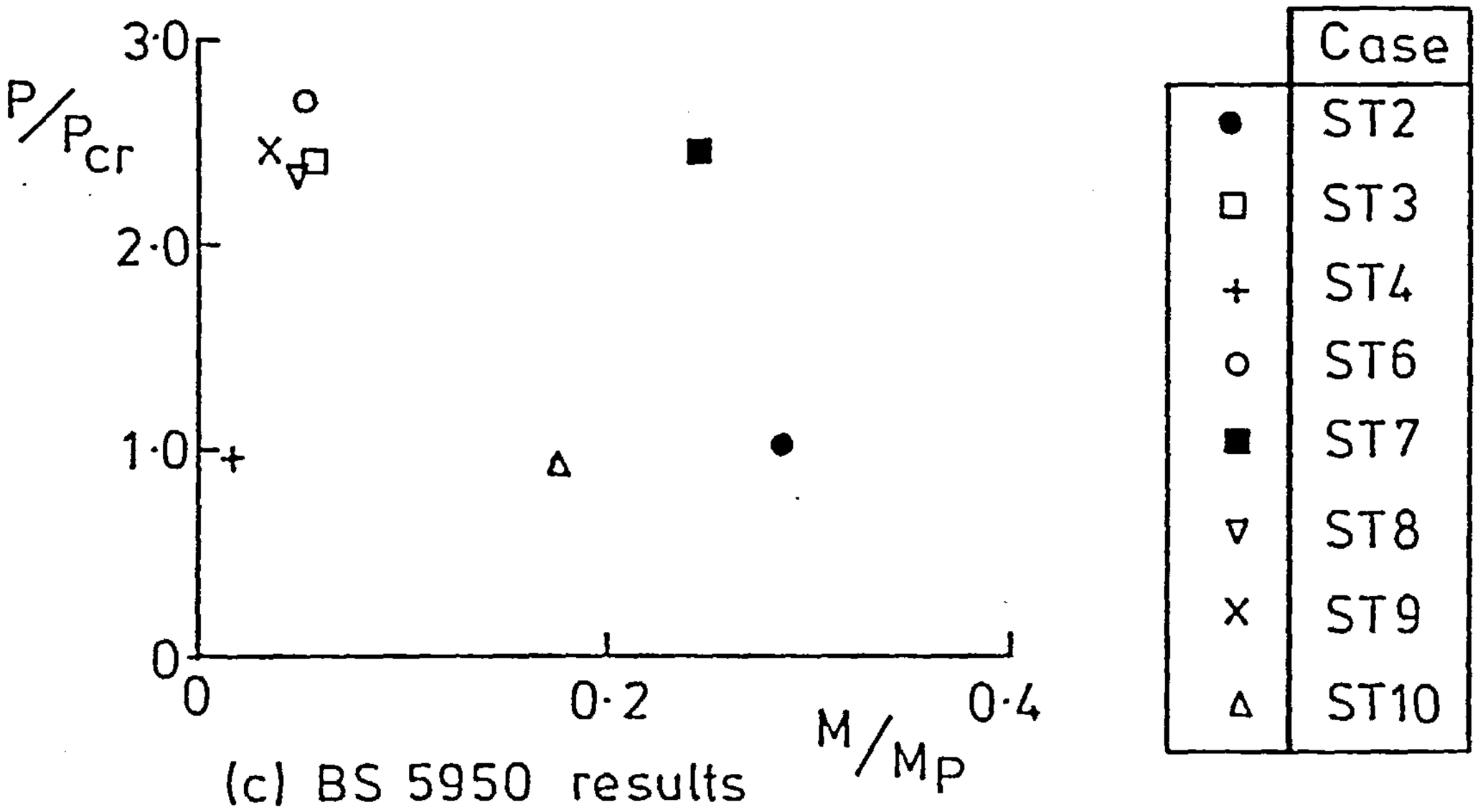

(c) BS 5950 results

FIG.6·36 INTERACTION PLOT FOR SUBASSEMBLAGE SERIES

actual moment arms. For the cases considered above, BS5950 ignores the actual lever arms of the beam load. In cases of one beam load only, BS5950 seems to ignore the fact that some of the moment produced by the beam load is shared between the two connections meeting at the column. Only the difference between these moments transfers to the column end.

2- The theoretical and test column moments are more consistent for most of the cases. It can be seen from the P-M curves that the test moments change very rapidly near the maximum load. This explains the difference in moment in some cases.

3- The allowance for the beam reaction suggested in BS5950 is oversimplified. As mentioned above, load lever arms and connection stiffness were not taken into account.

4- A more comperhensive study covering the main parameters is needed as a basis for a more realistic design allowance for the moments transferred from beams into column by semi-rigid connections.

6.4- Conclusions:-

The computer program described in chapter 4 was used to simulate a series of I-shaped subassemblages that were tested at the University of Sheffield. Most of the parameters describing the experiments were accurately known. If insufficient information was available on a parameter, a judgement was made for the most appropriate value. Comparisons were made between the analytical and experimental results characterized by the maximum loads, load-deflection curves and load-moment curves. Good agreement was obtained between the analytical and the experimental load-deflection curves for all of the cases

considered. The general trends of the measured and calculated load-moment curves for most cases were found to be comparable.

It was pointed out that it is difficult to exactly simulate an experimental result. This leads to some disagreement in certain the cases. However, by changing selected input parameters (whose values were known precisely) such as residual stresses, it was possible to arrive at better agreements.

The recommendations given in BS5950 for the design of columns in simple construction were applied to all the cases under consideration. It was found that these were unconservative in the cases of balanced loading and conservative in the cases of unbalanced loads. However, more cases should be considered to verify this finding. A parametric study is to be presented in chapter 7 and further comparisons with the BS5950 recommendations will be made therein.

CHAPTER-7

PARAMETRIC STUDY

7.1- Introduction:-

In chapters 5 and 6, the computer program described in chapter 4 was used to simulate some tests in which the behaviour of a variety of frames was determined experimentally. Frames with both flexible and rigid beam to column connections were considered in the simulations. The results obtained by the program were found to be reasonably close to the experimental results. It was also noticed that the presence of semi-rigid joints has an important influence on the behaviour of the flexible frames. Some of the design recommendations for including the effect of semi-rigid joints were checked against the analytical and experimental results. It was concluded in chapter 6 that the behaviour of flexible frames should be investigated more thoroughly in order to be able to assess the recommendations given in the BS5950 for the design of columns which are part of flexible frames.

In this chapter, a limited parametric study of the behaviour of subassemblages with semi-rigid joints is presented together with a discussion of the results obtained from this study. The computer program mentioned above was used to produce these results. The three most important parameters considered in this study are:

(1) presence of semi-rigid beam-to-column connections;

(2) presence of flexible beams; and

(3) type of applied loads.

A description of the parametric study is presented in the next section. The results obtained from the study are then discussed in Sec-7.3. Finally, an attempt to incorporate the findings from the study in design recommendations is given in Sec-7.4.

7.2- Description of Parametric Study:-

The parametric study involves the analysis of the subassemblage shown in Fig-7.1 It consists of a column and four beams connected to the column by means of four identical connections. Major axis bending was considered for all members of the subassemblage. The column was a 152x152x23UC section while the beams were 254x151x22UB sections. The material of all members of the subassemblage was assumed to possess an elastic-plastic stress-strain relationship with strain hardening as shown in Fig-7.2a. This type of behaviour is generally acceptable for most steels. The yield stress, σ_y was taken to be 285N/mm^2. A value of 210kN/mm^2 was assumed for the modulus of elasticity, E and the yield strain, ε_y was therefore $\sigma_y/E = 0.00136$. Strain hardening was assumed to start at a strain, $\varepsilon_{sh} = 10\varepsilon_y$ with a strain-hardening modulus, E_{sh} of 10kN/mm^2. A residual stress pattern of the type suggested by Young (57) and shown in Fig-7.2b was assumed for all sections. A half sine wave with an amplitude of L/1000 was assumed for the initial deflections in the column.

Three types of semi-rigid connection were considered and these are

(a) extended end plate connections;

(b) flange cleat connections; and

(c) web cleat connections.

The M-Φ characteristics for these types of connections were based on tests made on similar connections at the University of Sheffield shown in Fig-6.11 and described fully in Sec-6.2. In addition to the above types of connections, rigid and pin joints were considered as they represent the extreme boundaries for connection stiffness. To study the effect of beam flexibility, beams with spans of 1.5m, 3.0m and 4.5m

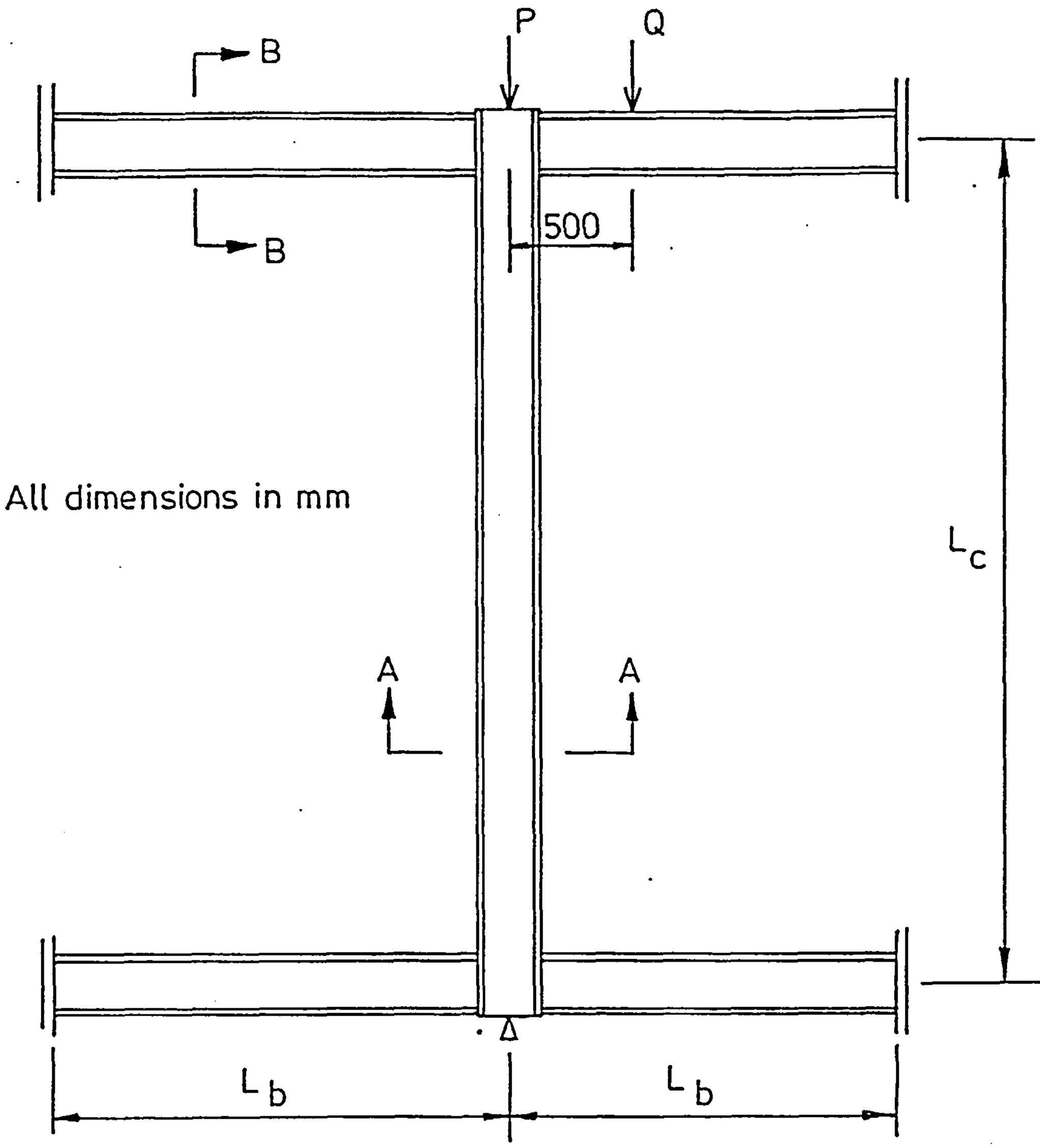

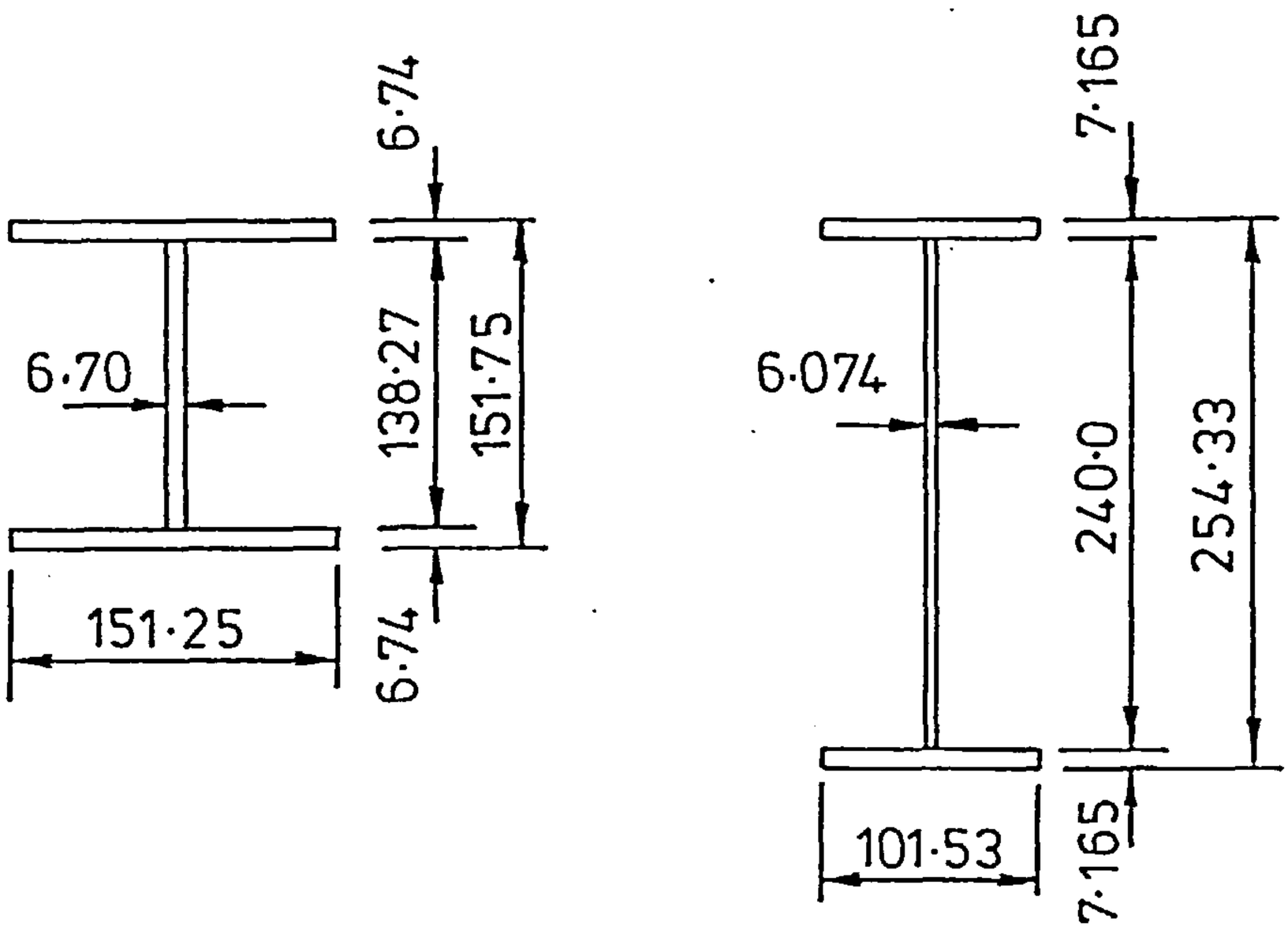

Section AA Section B B

FIG. 7·1 STANDARD SUBASSEMBLAGE

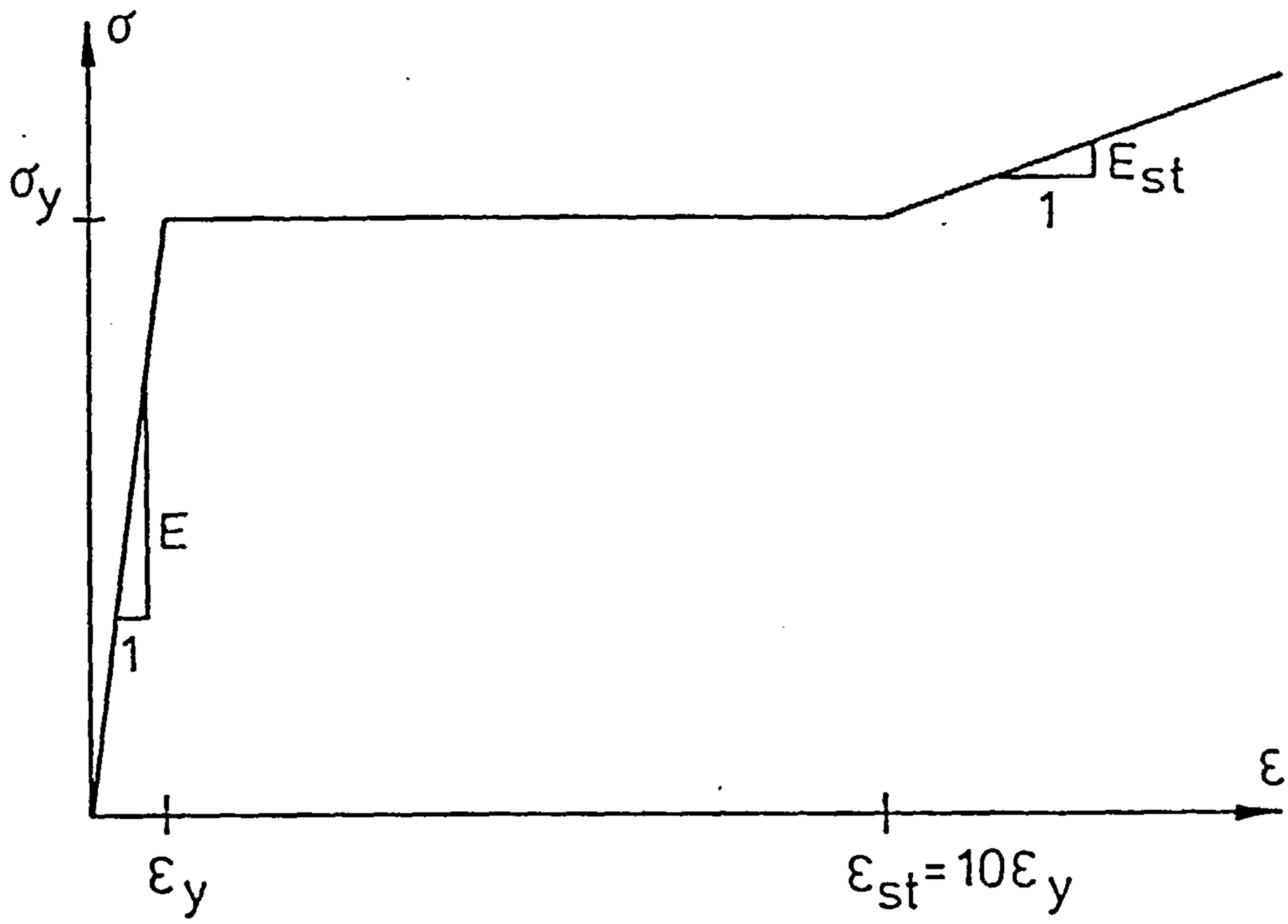

FIG. 7·2 a IDEALIZED STRESS-STRAIN CURVE

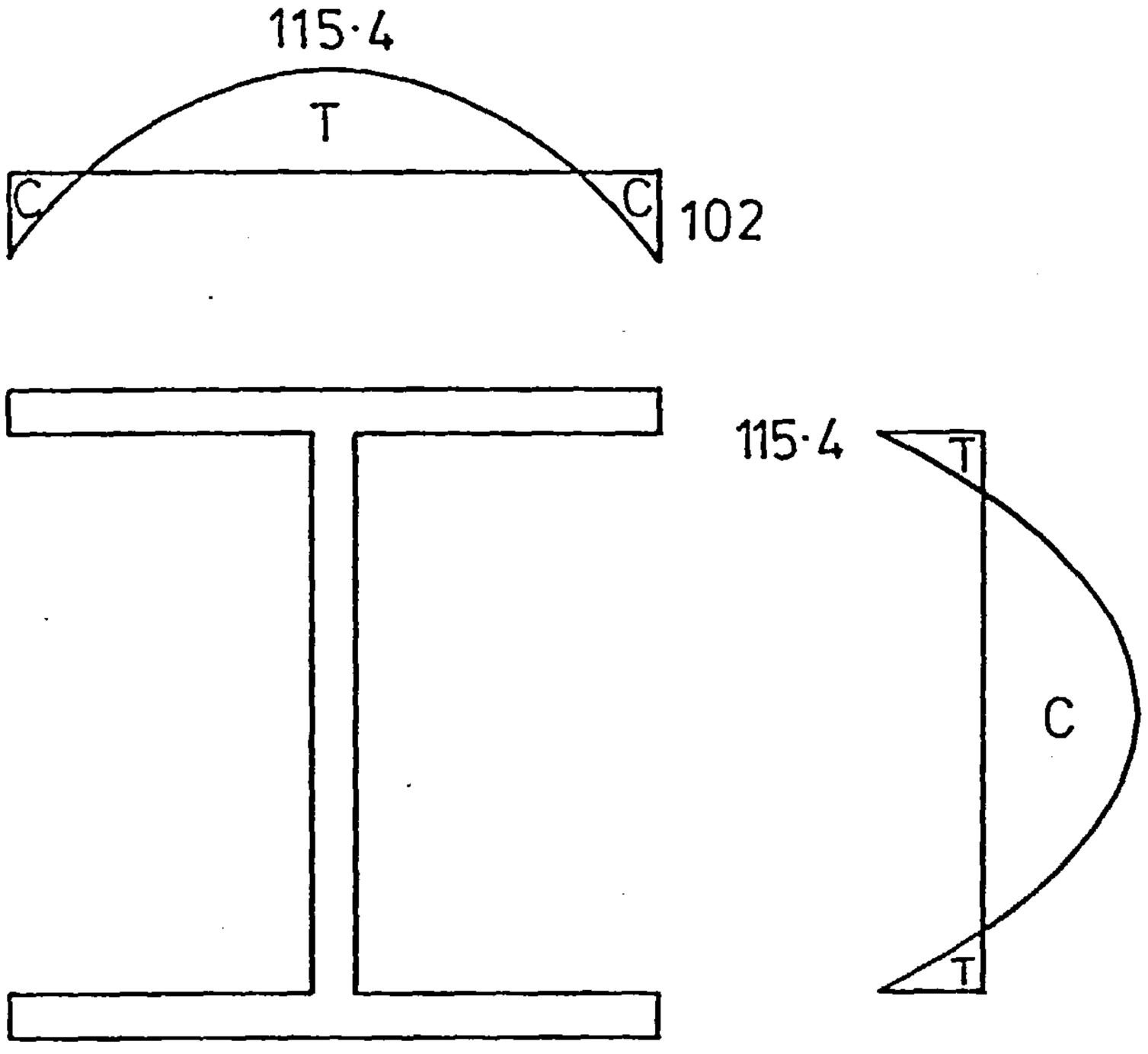

FIG. 7·2 b RESIDUAL STRESS PATTERN ADOPTED FOR THE PARAMETRIC STUDY

were considered. All beams in any one subassemblage have the same span. In addition, an isolated column (with connections made to infinitely rigid beams) was considered for comparison.

The present study consists of two series of analyses. Table-7.1 summarizes the variations of the main parameters in these series. The first series was intended to study the behaviour of columns as part of a frame under the action of column loads only. Column strength curves were constructed and used to study the effect of the main parameters such as the type of connections used. Only column load was applied up to failure of the structure. Column height was varied between 2m and 14m giving slenderness ratios between 30 and 220. A total of 102 analyses were performed. Thirty analyses (five for every column slenderness ratio) correspond to an isolated column. All five types of end restraints mentioned above (i.e. rigid, extended end plate, flange cleat, web cleat and pin joints) were considered in this series. In these analyses, two beams with very large sections and relatively small span were assumed to be attached to each column by the connections under consideration (see Fig-7.3). Corresponding to subassemblages with each of the beam spans mentioned above, 24 analyses (four for each column slenderness) were performed. In this way, it is possible to differentiate between the effects of the connection type and the beam flexibility on the behaviour of the column.

The second series of analyses studied the behaviour of subassemblages under the action of column and beam loads. The presence of beam loads introduces primary bending action into the column. One of the most important problems raised by this type of loading is the transfer of moments from the beams to the column. This is particularly true if flexible connections are used since the M-Φ characteristics of

Table-7.1: Main Parameters in the Parametric Study

Parameter	Series of Analysis	
	"Column Load Only"	"Column and Beam Loads"
Connection Type	Rigid Extended End Plate Flange Cleats Web Cleats Pins	Rigid Extended End Plate Flange Cleats Web Cleats -
Beam Span (m)	0.0, 1.5, 3.0, 4.5	1.5, 3.0, 4.5
Applied Loads	Column Load Only	(1)Beam load Q: Q= 0, 30, 60, 90 and 120 kN (2)Column Load P
Column Slenderness ratio	31, 62, 103, 140, 180 and 218	78 and 140

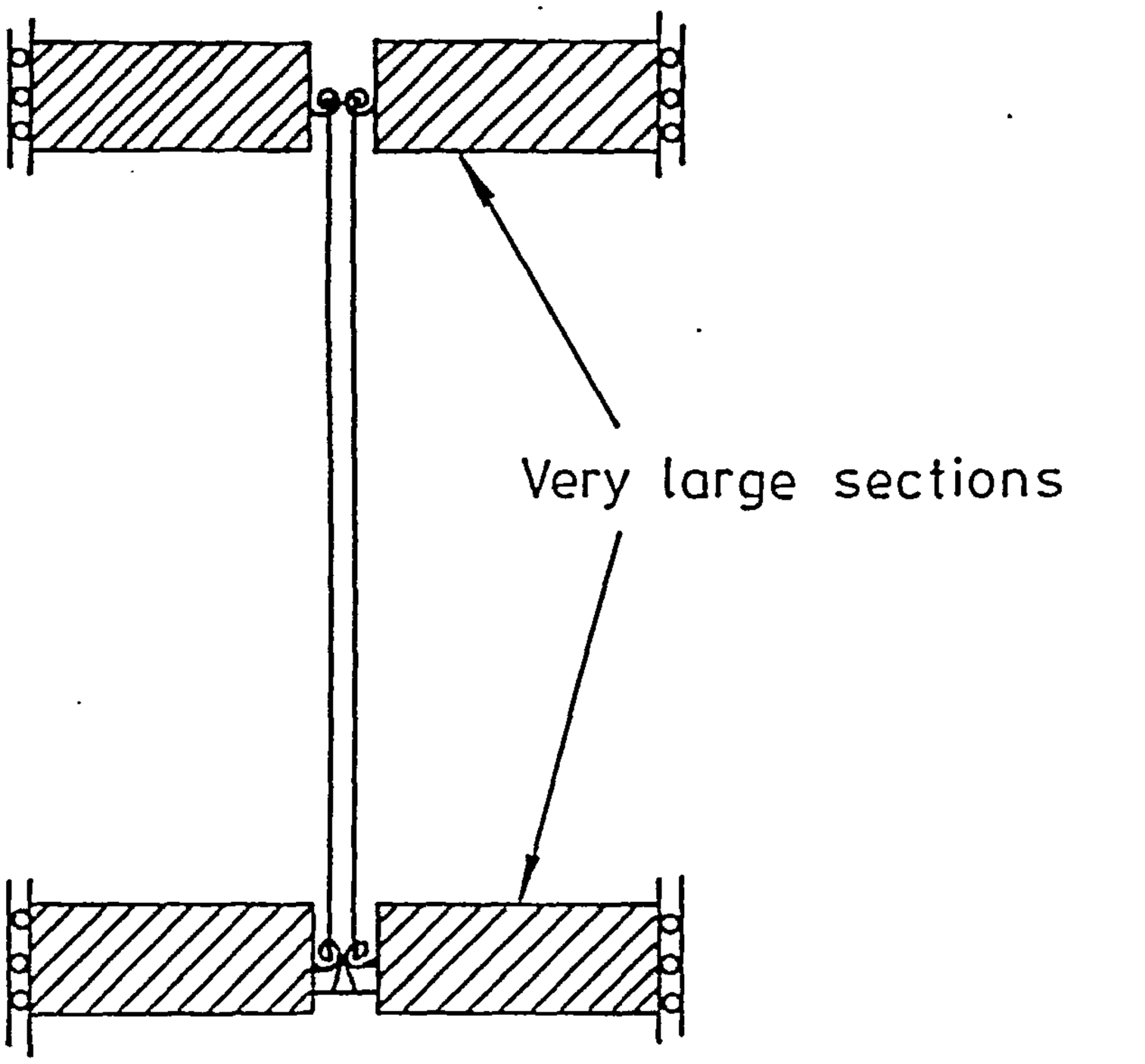

FIG.7·3 MODEL FOR THE ISOLATED COLUMN WITH FOUR SEMI-RIGID CONNECTIONS

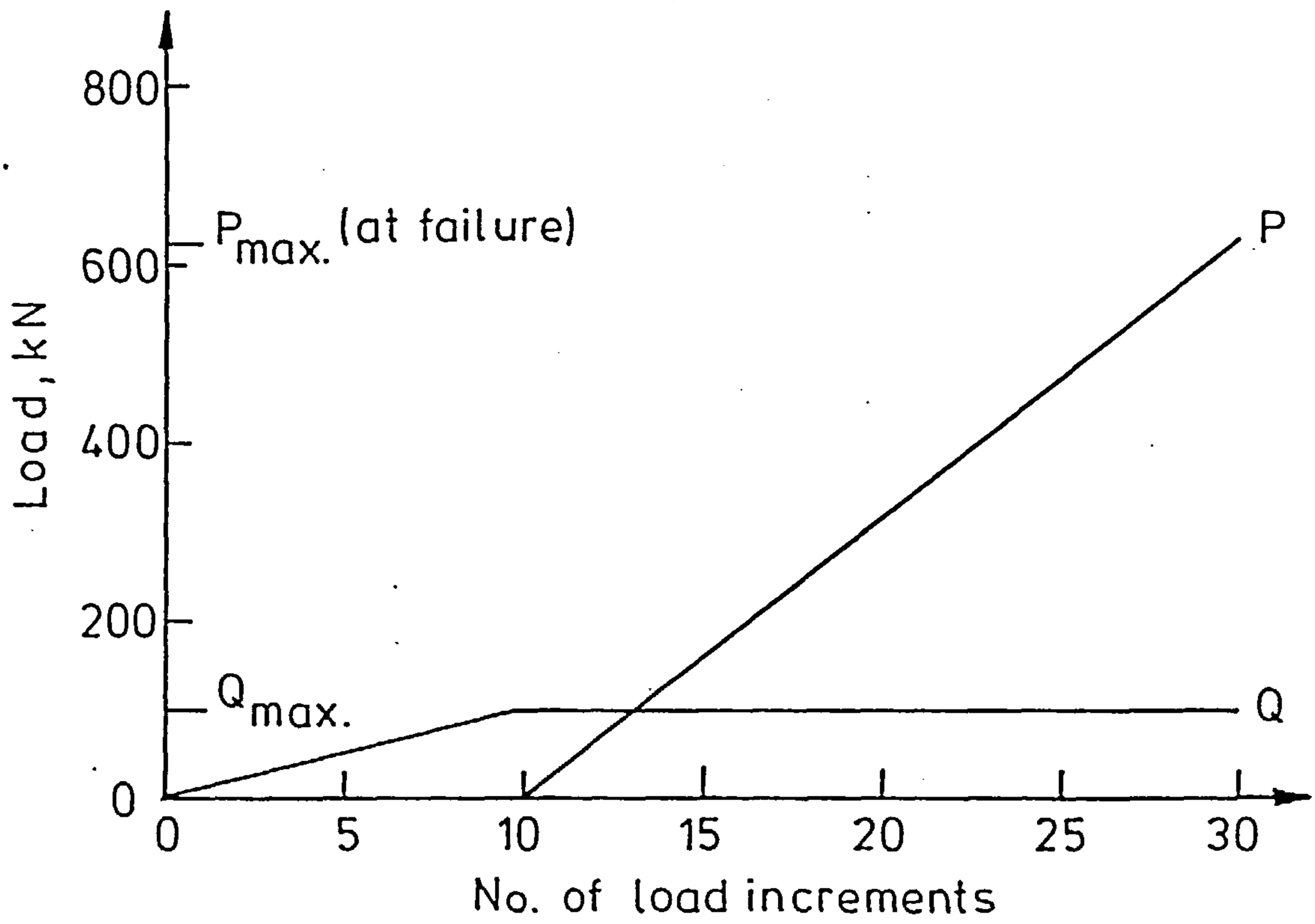

FIG.7·4 LOAD PATTERN USED IN THE PARAMETRIC STUDY

these connections dictate this sort of moment transfer. The importance of moment transfer lies in the fact that it is essential to know the moment for which the column should be proportioned; this is probably the moment coexistant with the axial load at collapse. As may be seen from Table-7.1, four types of beam-to-column connections were used. Column heights were restricted to 5m and 9m. All beams were assumed to have a span of 4.5m. The loading pattern (Fig-7.4) is divided into two stages:

(i) in the first stage, the beam load was increased from 0 to a maximum value of either 0, 30kN, 60kN, 90kN or 120kN.

(ii) in the second stage, the column load was increased up to failure of the subassemblage.

7.3- Discussion of Results:-

7.3.1- Column Strength Due to Axial Load Only:-

7.3.1.1- Column Strength Curves:-

Column strength curves were constructed from the results of the analyses of the first series and provide a means for understanding the effects of different parameters on the ultimate strength of axially loaded columns. Fig-7.5 shows the column strength curves for the isolated column. The effect of end restraint may readily be seen. A rather wide band of curves is noticed in this figure suggesting that there is a pronounced difference between the strengths of a pin-ended column and a restrained one. Even for the most flexible web cleat connection, the column curve is much higher than that corresponding to a pin-ended column. It can be seen from Fig-7.5 that the column strength curves for extended end plate connections and rigid joints are very close. Thus it would appear that extended end plate connections

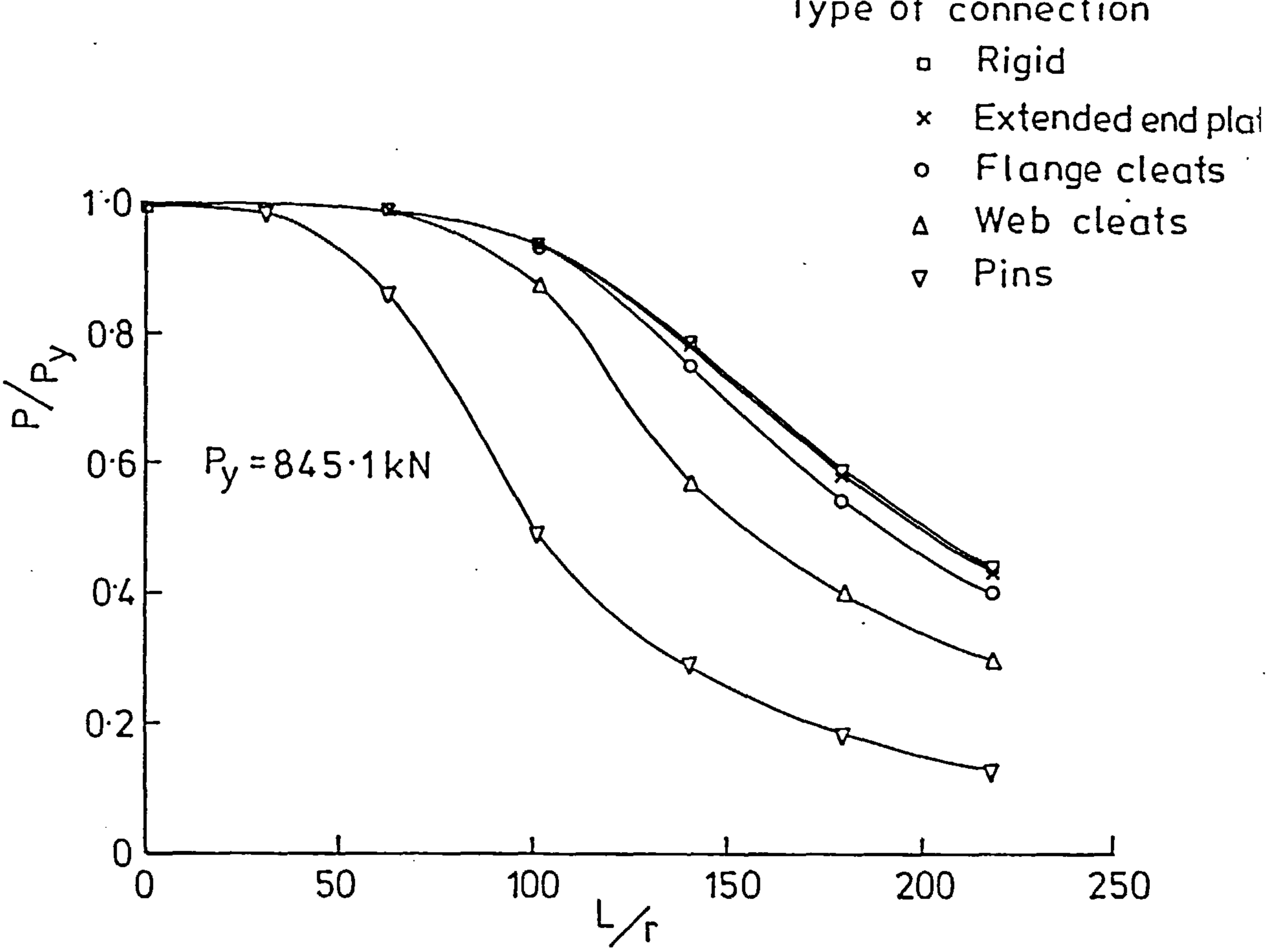

FIG. 7·5 COLUMN STRENGTH CURVES FOR AN ISOLATED COLUMN

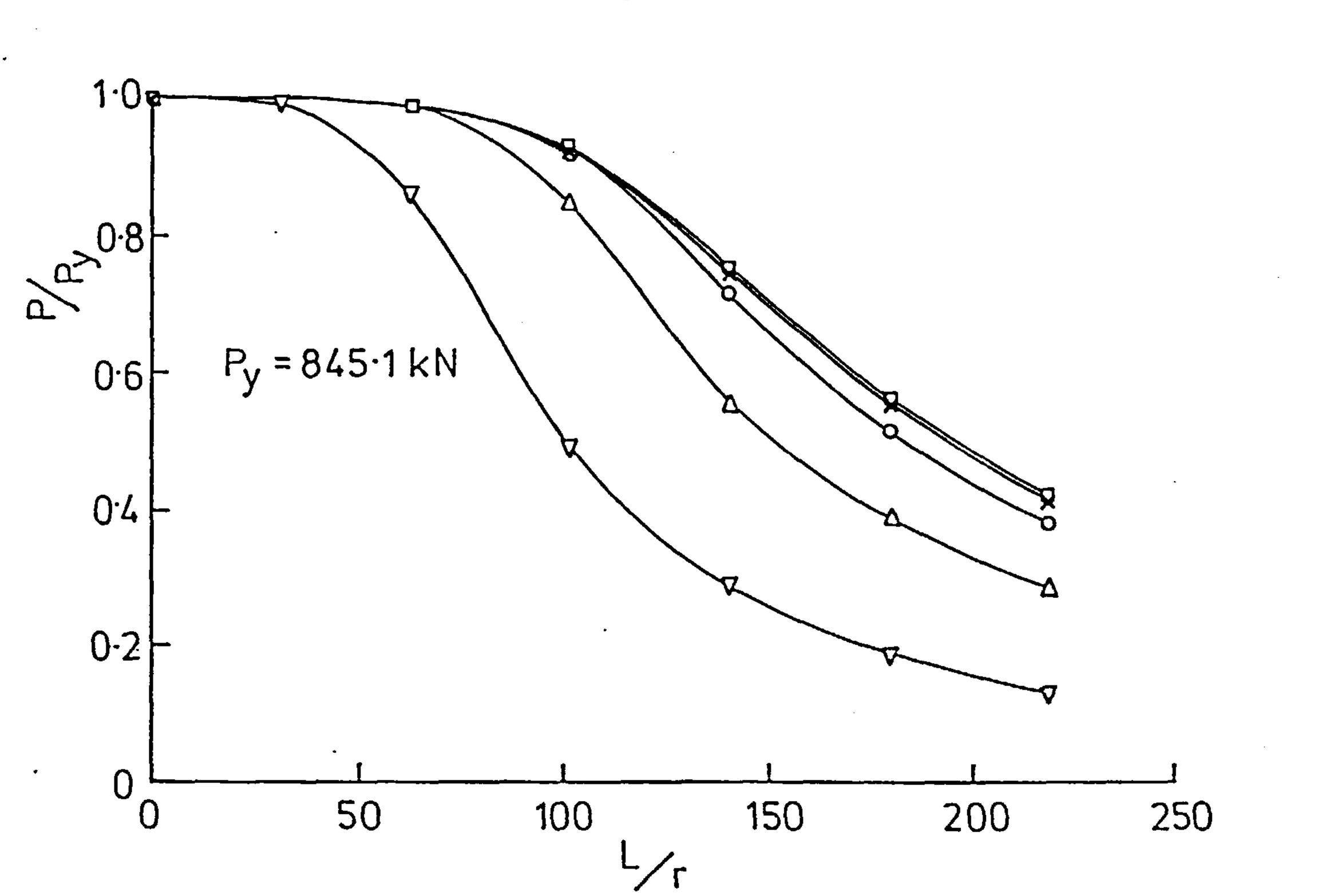

FIG. 7·6 COLUMN STRENGTH CURVES FOR A SUBASSEMBLAGE WITH 1·5m BEAMS

may be considered to be fully rigid. Figs-7.6 to 7.8 show the column strength curves for the subassemblage with beams of different beam spans together with the column strength curve for a pin-ended column for comparison. Similar observations may be made from these figures. In general, the rate of increase in column strength tends to decrease with increasing connection stiffness. Flat portions extending up to a slenderness ratio of about 40 are recognized in all curves which correspond to cases in which the column was not pin-ended. A shorter plateau is recognized for the pin-ended column. These portions indicate that the full squash load was obtainable before a condition of instability occurred. The effect of end restraints is to make these plateaus longer i.e. it extends the range of slenderness ratios for which the column may sustain the full squash load.

Shown in each of Figs-7.9 to 7.12 are the column strength curves for subassemblages with different beam spans. These figures correspond to rigid, extended end plate, flange cleat and web cleat connections respectively. For comparison, the column strength curve for the column connected to infinitely rigid beams is also shown in each of these figures. A few observations may be made from these figures:

(i) in the cases where rigid or extended end plate connections were used, there seems to exist a linear relationship (i.e. constant rate) between the beam span and the ultimate strength of the structure.

(ii) in the cases where more flexible connections were used, the effect of beam flexibility seems to decrease as beam span increases.

(iii) the band width of the set of curves corresponding to the various beam spans decreases when using more flexible

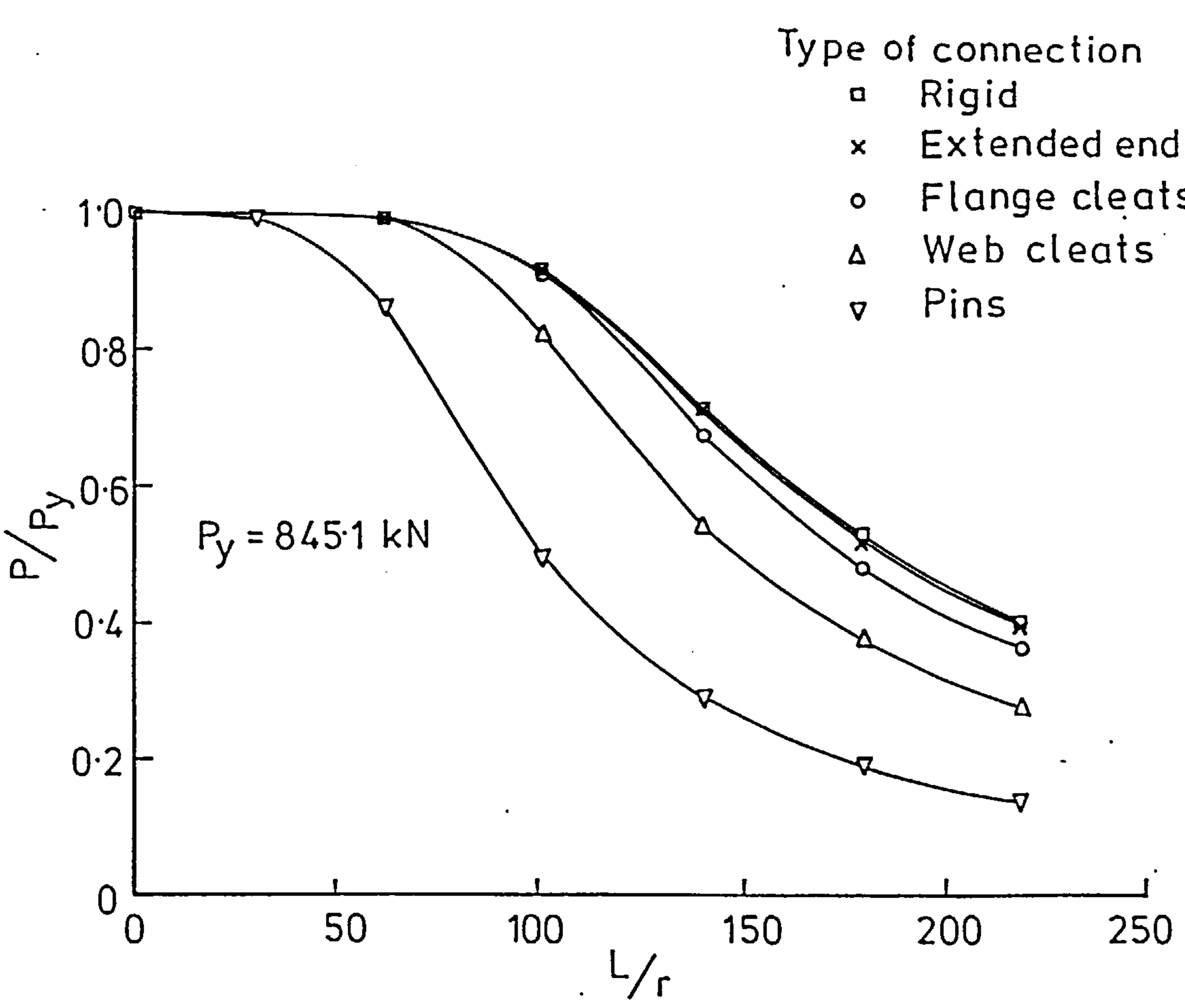

FIG. 7·7 COLUMN STRENGTH CURVES FOR A SUBASSEMBLAGE WITH 3·0m BEAMS

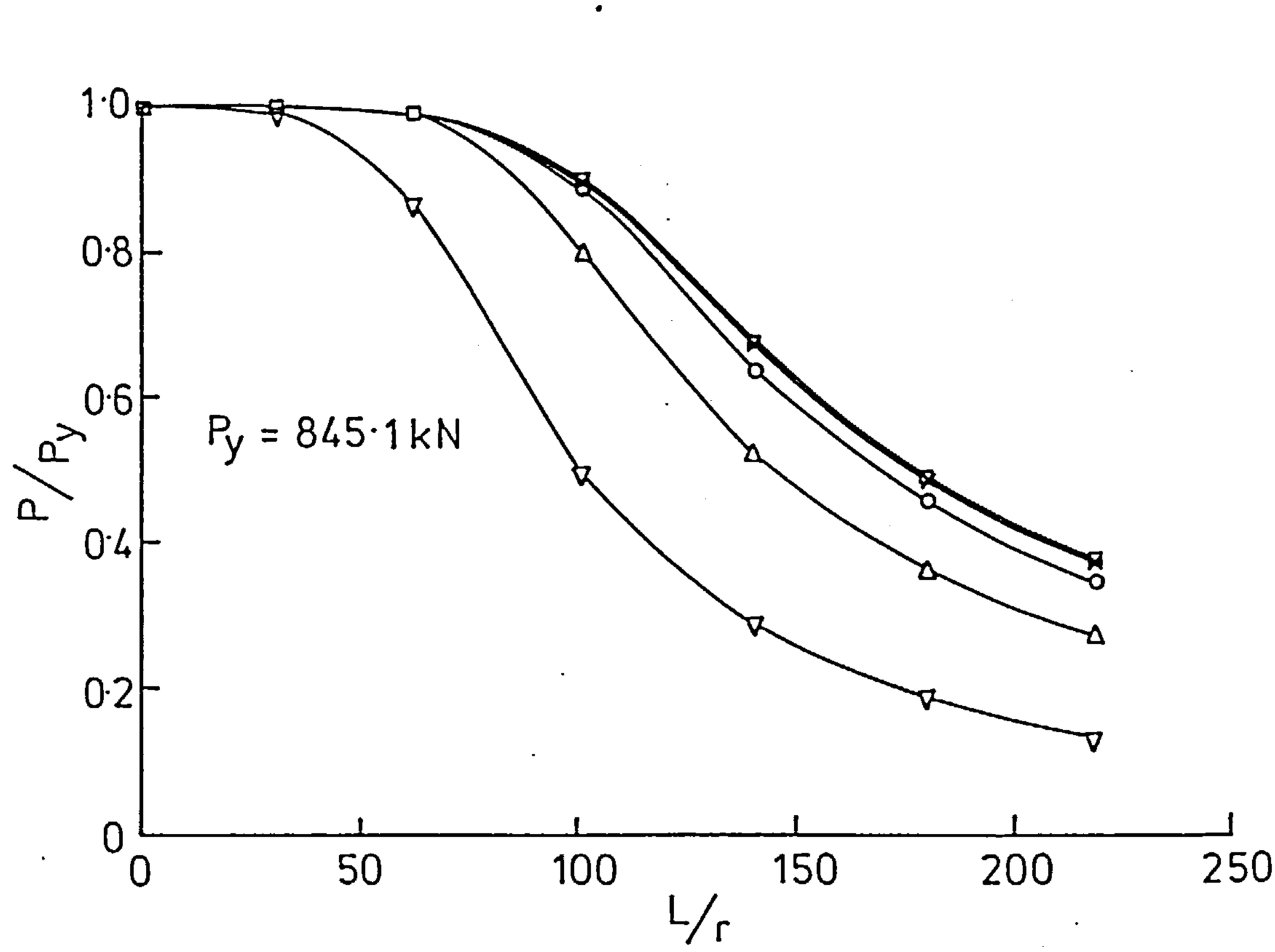

FIG. 7·8 COLUMN STRENGTH CURVES FOR A SUBASSEMBLAGE WITH 4·5m BEAMS

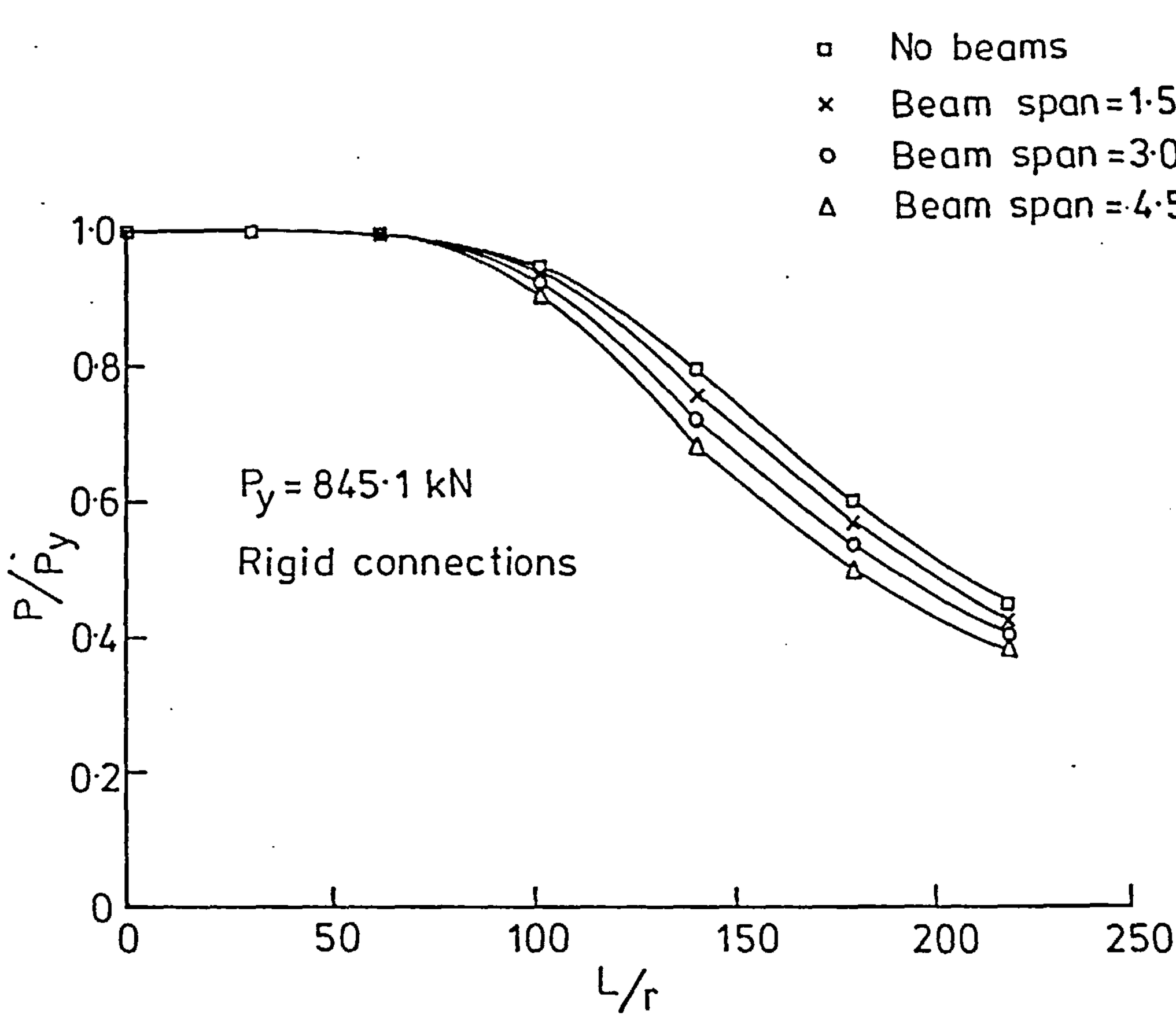

FIG. 7·9 COLUMN STRENGTH CURVES FOR A RIGID JOINTED SUBASSEMBLAGE

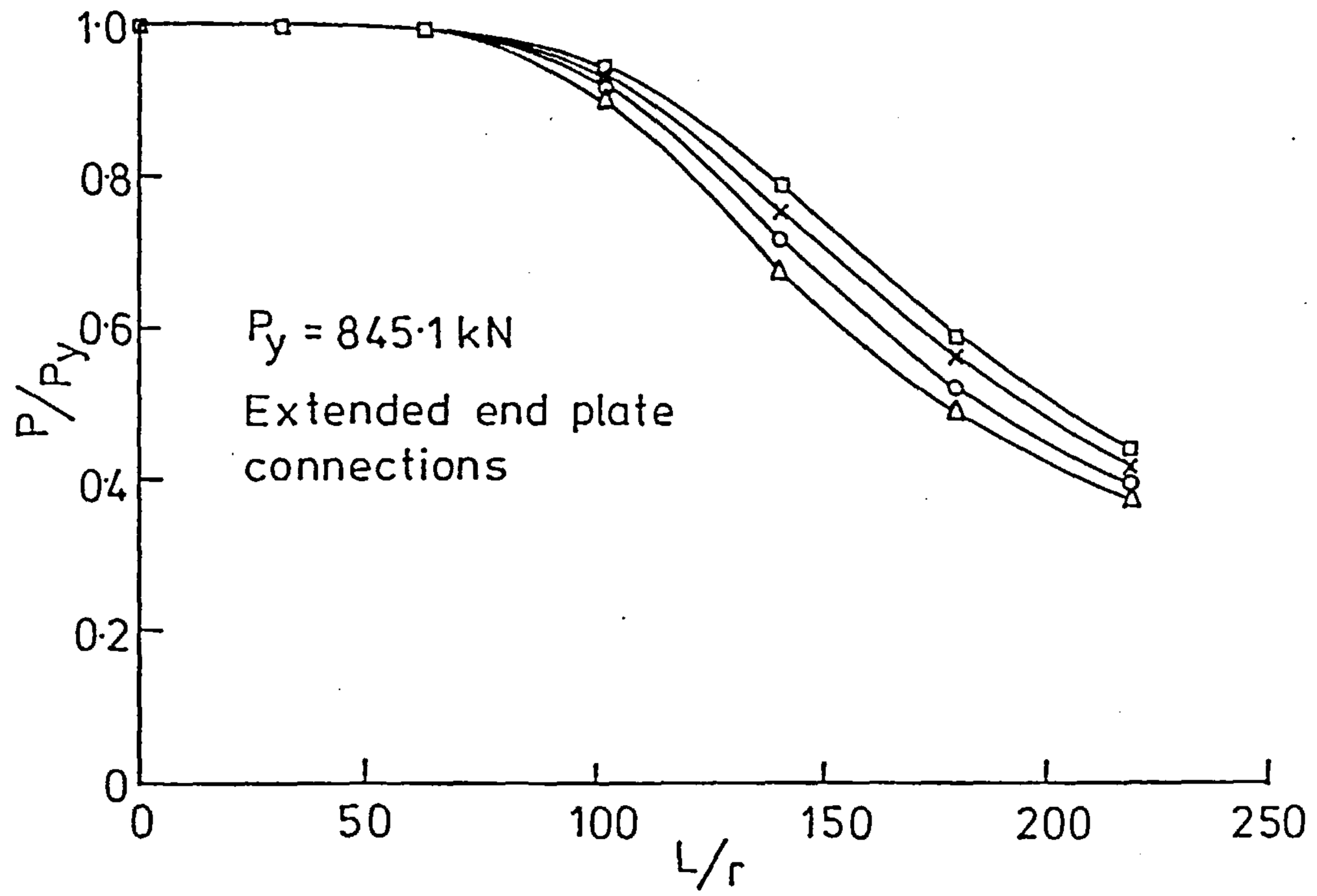

FIG. 7·10 COLUMN STRENGTH CURVES FOR A FLEXIBLY CONNECTED SUBASSEMBLAGE

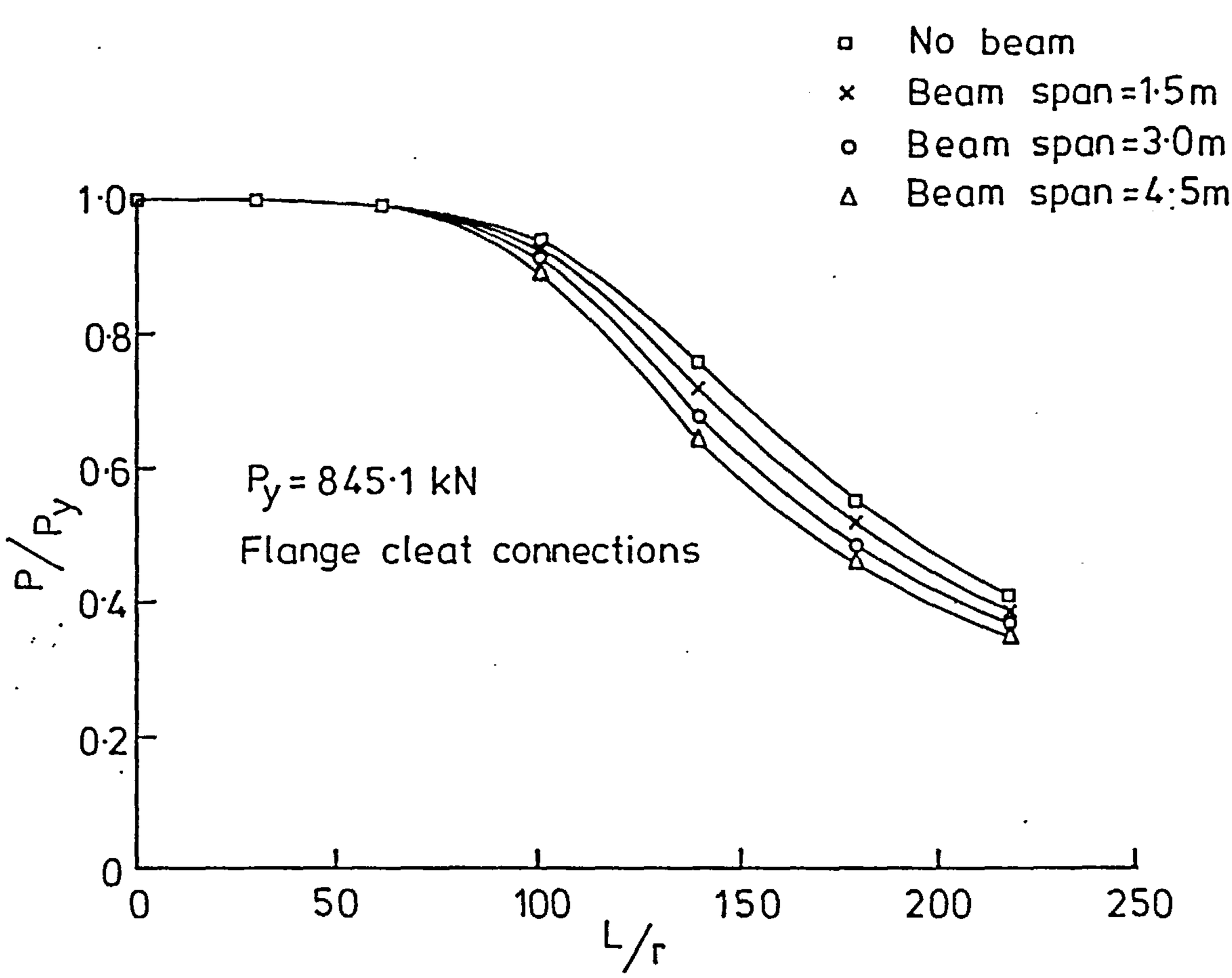

FIG. 7·11 COLUMN STRENGTH CURVES FOR A FLEXIBLY CONNECTED SUBASSEMBLAGE

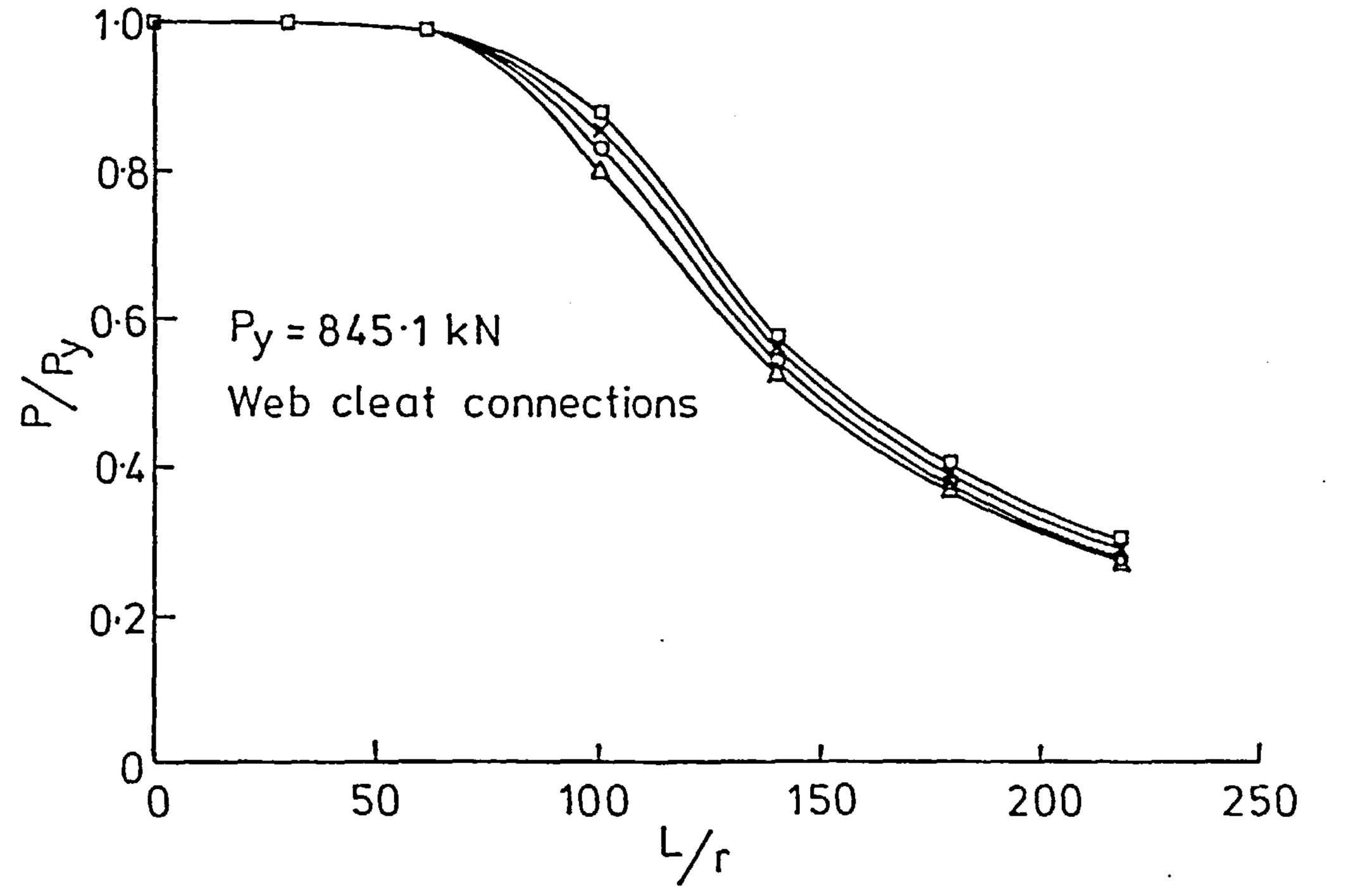

FIG. 7·12 COLUMN STRENGTH CURVES FOR A FLEXIBLY CONNECTED SUBASSEMBLAGE

connections.

These observations may be explained on the basis of Table-7.2. In this table, the combined beam and connection restraint , C^*, for all types of connection and beam span used are given, where

$$C^* = \frac{EI_b}{l_b}\left[\frac{1}{1 + \frac{EI_b}{l_b C_j}}\right] \qquad (7.1)$$

in which l_b is the clear span of the beam (hence in the case of the column bending about major axis, l_b is equal to the beam span less half the depth of the column section). The derivation of this expression may be found in Appendix A. The initial stiffness, C_j, of the connections was used in eqn-7.1.

To explain the first and second observations, attention may be directed to the values of the ratio, R, given by

$$R = \frac{C^* L_b}{EI_b} \qquad (7.2)$$

This ratio, which is a measure of the effectiveness of the continuity of the connection, varies between 0.92 to 0.97 for the extended end plate connections and between 0.67 to 0.86 for web cleat connections. In the case of the former, almost the full beam stiffness is used in all cases. Consequently, for the same column height, the ultimate strength is controlled by the beam span since the the beam rigidity, EI, is constant (assuming that the beams do not yield which is a valid assumption for the cases of axial load only). In other words, the column strength is mainly controlled by the beam span. In the second type of connections, the ratio R is much lower than unity and the range

Table-7.2: Initial Stiffness for the Connections

Used in the Parametric Study

Connection Type	C_j $x10^5$ N.m/rad	L_b (m)	$\frac{EI_b}{L_b}$ $x10^5$ N.M	C^* $x10^5$ N.m	R
Rigid	∞	0.0	∞	∞	1.0
		1.5	40.9	40.9	0.0
		3.0	20.45	20.45	0.0
		4.5	13.63	13.63	0.0
Extended End Plate	491.0	0.0	∞	491.0	0.0
		1.5	40.9	37.75	0.923
		3.0	20.45	19.63	0.960
		4.5	13.63	13.26	0.973
Flange Cleats	207.0	0.0	∞	207.0	0.0
		1.5	40.9	34.15	0.835
		3.0	20.45	18.61	0.910
		4.5	13.63	12.79	0.938
Web Cleats	84.4	0.0	∞	84.4	0.0
		1.5	40.9	27.55	0.674
		3.0	20.45	16.45	0.804
		4.5	13.63	11.73	0.861
Pins	0.0	0.0	∞	0.0	0.0

is much greater. The effect of connection flexibility is pronounced in this case. Comparing the ratios for this case, it is seen that the difference between successive values tends to be smaller. Hence the effect of the beam stiffness decreases with increasing beam span when using flexible connections.

It is seen from Table-7.2 that the C^* values range from 13.63 to infinity for the rigid connections while those for web cleat connections fall between 11.73 and 84.4. This means that the range of effective end restraint is much narrower in the case of web cleat connections. Consequently, a narrower band width is obtained.

7.3.1.2- Effective Length Factor:-

When designing a column which is either restrained or is a part of a frame, it is common to modify this column to an equivalent pin-ended one with an "effective length" (1,2). The ratio of the effective length to the original length is the effective length factor. Following is a description of four methods for evaluating the effective length factors for restrained columns. These methods will be referred to as:

Modified AISC approach: which is based on the use of alignment charts in conjunction with special distribution factors.

Modified BS5950 approach: which is similar to "the modified AISC Approach" in that special charts are used in conjunction with special stiffness distribution factors.

Chen and Lui approach: in which the effective length factor is calculated using an empirical formula

suggested by Chen and Lui; and

Proposed approach: which is based on the present series of analyses and is outlined below and explained in more detail in Appendix B.

The Modified AISC Approach:-

The AISC specifications (2) recommends that the effective length factor for a column in a rigid frame be determined from alignment charts if the stiffness distribution factors, G_{top} and G_{bottom}, for the specific column under consideration are known. The G factors are calculated as

$$G = \frac{\sum \frac{EI_c}{L_c}}{\sum \alpha \frac{EI_b}{L_b}} \qquad (7.3)$$

where

E = modulus of elasticity of the material

I = second moment of area of cross section

α = a factor depending on the restraint at the far ends of the beams; and

b and c are suffices which refer to beam and column respectively.

Eqn-7.3 is valid for elastic rigid frames. Yura (67) proposed a method for including column inelasticity in eq-7.3. An effective column stiffness, which corresponds to the failure load is used instead of the elastic value. Consequently, eq-7.3 may be rewritten as

$$G_{inel} = \frac{\sum \frac{(EI_c)_{eff}}{L_c}}{\sum_{\alpha} \frac{EI_b}{L_b}} \qquad (7.4)$$

where $(EI_c)_{eff}$ is the effective flexural rigidity of the column.

Yura suggested that the effective column stiffness be calculated as

$$(EI_c)_{eff} = I_c . E_t \qquad (7.5)$$

in which I_c and E_t are the moment of inertia of the column's cross section and the tangent modulus respectively. He pointed out that the tangent modulus may approximately be given by

$$E_t = E . \frac{F_a}{F_e'} \qquad (7.6)$$

where F_a is the allowable compressive stress for the column and F_e' is the Euler critical stress calculated as the Euler load P_e divided by the cross sectional area for the column A. It follows from eqns-7.5 and 7.6 that

$$(EI_c)_{eff} = EI_c . \frac{F_a}{F_e'} \qquad (7.7)$$

The procedure just outlined is related to the working stress design. As the current generation of steelwork codes are in limit state and the ultimate load conditions are more relevant, the term F_a/F_e' in eqn-7.7 may be replaced by P_u/P_e where P_u is the ultimate load for the column under consideration. Hence eqn-7.4 may be rewritten as

$$G_{inel} = \frac{\sum \frac{EI_c}{L_c} \cdot \frac{P_u}{P_e}}{\sum \alpha \frac{EI_b}{L_b}} \qquad (7.8)$$

$$= G \cdot \frac{P_u}{P_e}$$

Both eqs-7.3 and 7.8 are applicable to rigid frames only. Chen and Lui (66) proposed a procedure for incorporating the effect of flexible connections. He derived an expression for a combined beam and connection stiffness, C^*, for a rectangular closed frame. The expression for C^* is

$$C^* = 2 \frac{EI_b}{L_b} \left[\frac{1}{1 + 2 \frac{EI_b}{C_j L_b}} \right] \qquad (7.9)$$

in which C_j is the stiffness of the connection. This expression may vary slightly for other types of frames. For the subassemblage of Fig-7.1, the expression for C^* is given by eqn-7.1. This equation is the same as eqn-7.9 except for the absence of the factor 2. The C^* values may be used instead of the beam stiffness in eqns-7.3 or 7.8. Hence, eqn-7.8 may be written as

$$G_{inel} = \frac{\sum \frac{EI_c}{L_c} \cdot \frac{P_u}{P_e}}{\sum C^*} \qquad (7.10)$$

The Modified BS5950 Approach:-

BS5950 (1) recommends some values for the effective length

factors for columns in some single storey non sway structures which are considered to be of "simple construction". It recommends the use of an effective length factor of unity for the simple structures not covered in these cases. The standard also recommends an approach in which the effective length factors may be determined for columns in rigid frames. The approach involves the calculation of stiffness distribution factors, k_{top} and k_{bottom} given by

$$k_i = \frac{\sum k_c}{\sum k_c + \sum k_b} \qquad (7.11)$$

where

i = end number (1 for top and 2 for bottom)

k_c = column stiffness, $\frac{I_c}{L_c}$

k_b = beam stiffness, $\frac{I_b}{L_b}$

and the summation means that contribution of similar elements meeting at the joint in consideration are added. With the values for k_{top} and k_{bottom} in hand, the effective length factor may be determined from specially prepared charts (1).

In line with the modifications made on eq-7.3 for the inclusion of connection flexibility and inelastic behaviour of the column, eq.7.11 may be modified to the following form

$$k_i = \frac{\sum EI_c . \frac{P_u}{P_e}}{\sum \frac{EI_c}{L_c} . \frac{P_u}{P_e} + \sum C^*} \qquad (7.12)$$

where C^* is given by eq.7.1.

The Chen and Lui Approach:-

Based on analytical results, Chen and Lui (66) proposed a formula for calculating the effective length factors for inelastic isolated columns with semi-rigid joints. The proposed formula is

$$k = 1.0 - 0.017\,\beta \qquad \text{for } \beta < 23 \qquad (7.13)$$

$$= 0.6 \qquad \text{for } \beta > 23$$

where β is given by

$$\beta = \frac{C_j}{M_{pc}} \qquad (7.14)$$

in which M_{pc} is the plastic moment for the column cross section. Once again, beam flexibility may be accounted for by the use of C^* instead of C_j in eqn-7.14(66,68), otherwise applying eqn-7.13 in the same manner as before.

In arriving at eqn-7.14, Chen and Lui defined the effective length as that length (slenderness) which gives, on the basic column curve for pinned ends, the same strength as the failure load for the actual column with its actual end restraints (66,68). Hence, referring to Fig-7.12, the effective length factor is expressed as

$$k = \frac{\lambda_p}{\lambda_r} \qquad (7.15)$$

where λ_p and λ_r are the slenderness ratios corresponding to pinned ends and restrained columns respectively.

The Proposed Approach:-

The effective length factors for the cases considered in the present study were calculated in a manner similar to that used by Chen

and Lui in their studies which led to eqn-7.13 but using the column strength curves shown in Figs-7.5 to 7.8. A typical example of the procedure may be found in Appendix B.

Comparison of the Effective Length Factors Computed by the Above Approaches:-

Table-7.3 shows the effective length factors calculated by the four methods described above. The ultimate strengths for the sixteen columns considered in the present study were calculated using each of the four approaches mentioned above. Figs-7.13 to 7.16 show the correlation between the actual and the estimated column strengths for the columns considered in the present study for the four methods described above. It is clear from these figures that the ultimate strength estimations using the "proposed approach" seem to be the most reliable. All other approaches seem to be less satisfactory.

Returning to Table-7.3, and assuming that the values given by the proposed approach are correct, it may be observed that both the "modified AISC approach" and the "modified BS5950 approach" seem to give rather unconservative values for the effective length factor although the former one seems to give acceptable estimates for the subassemblages and the isolated columns with rigid joints. The "Chen and Lui approach" produced conservative values for k for the stiffer connections (too conservative in many cases). On the other hand, it produced unconservative estimates for k for the cases where web cleat connections were used. It must be noted that both the "modified AISC approach" and "modified BS5950 approach" are based on the initial joint stiffness and hence ignore the reduction in joint stiffness at higher load values. Although the "Chen and Lui approach" is based on column strength curves based on analytical results in which bi-linear

Table-7.3: Comparison of Effective Length Factors Calculated by Different Methods

C^* $x10^5$ N.m/rad	Procedure			
	Proposed Approach	Modified AISC Approach	Modified BS5950 Approach	Chen and Lui Approach
∞	0.5	0.5	0.5	-
491.0	0.5	0.5	0.5	0.6
207.0	0.519	0.503	0.5	0.6
84.4	0.627	0.507	0.502	0.6
40.9	0.517	0.514	0.506	-
37.75	0.52	0.514	0.507	0.6
34.15	0.542	0.516	0.508	0.6
27.55	0.645	0.52	0.51	0.6
20.45	0.542	0.526	0.513	-
19.63	0.546	0.527	0.514	0.6
18.61	0.568	0.529	0.515	0.6
16.45	0.664	0.533	0.517	0.6
13.63	0.57	0.539	0.52	-
13.26	0.574	0.54	0.521	0.6
12.79	0.593	0.542	0.522	0.6
11.73	0.681	0.545	0.523	0.613

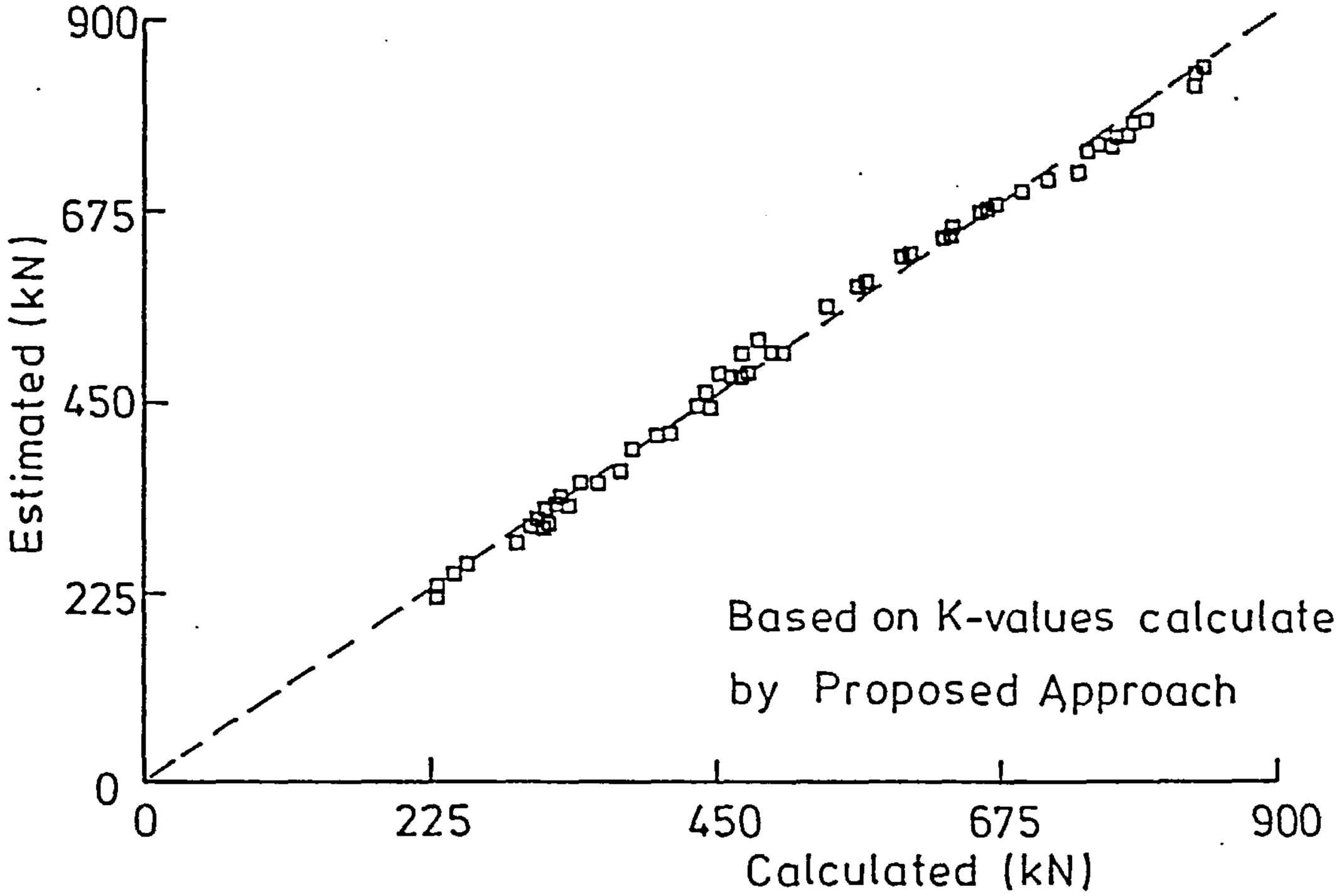

FIG. 7·13 COMPARISON BETWEEN ESTIMATED AND CALCULATED ULTIMATE LOADS

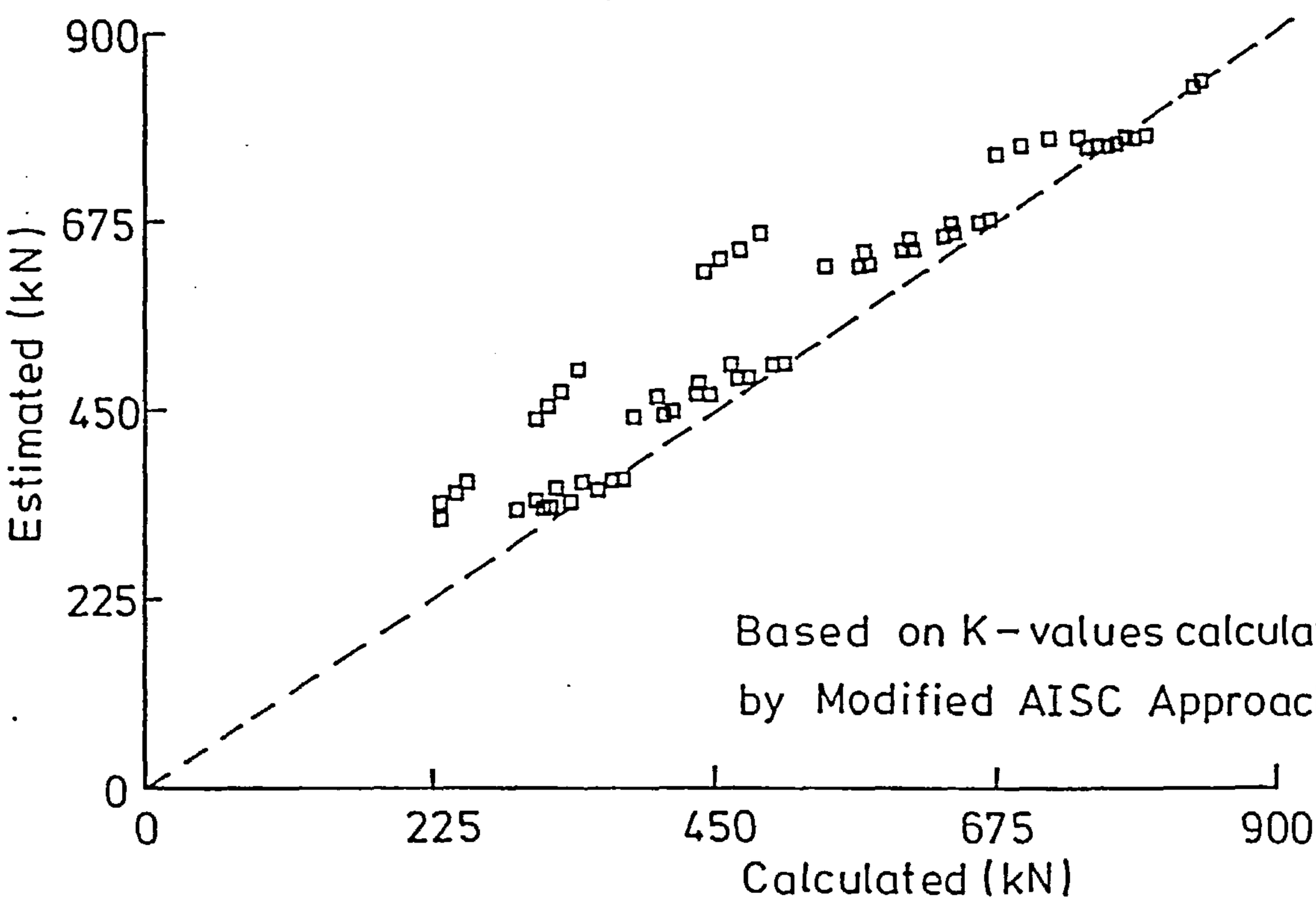

FIG. 7·14 COMPARISON BETWEEN ESTIMATED AND CALCULATED ULTIMATE LOADS

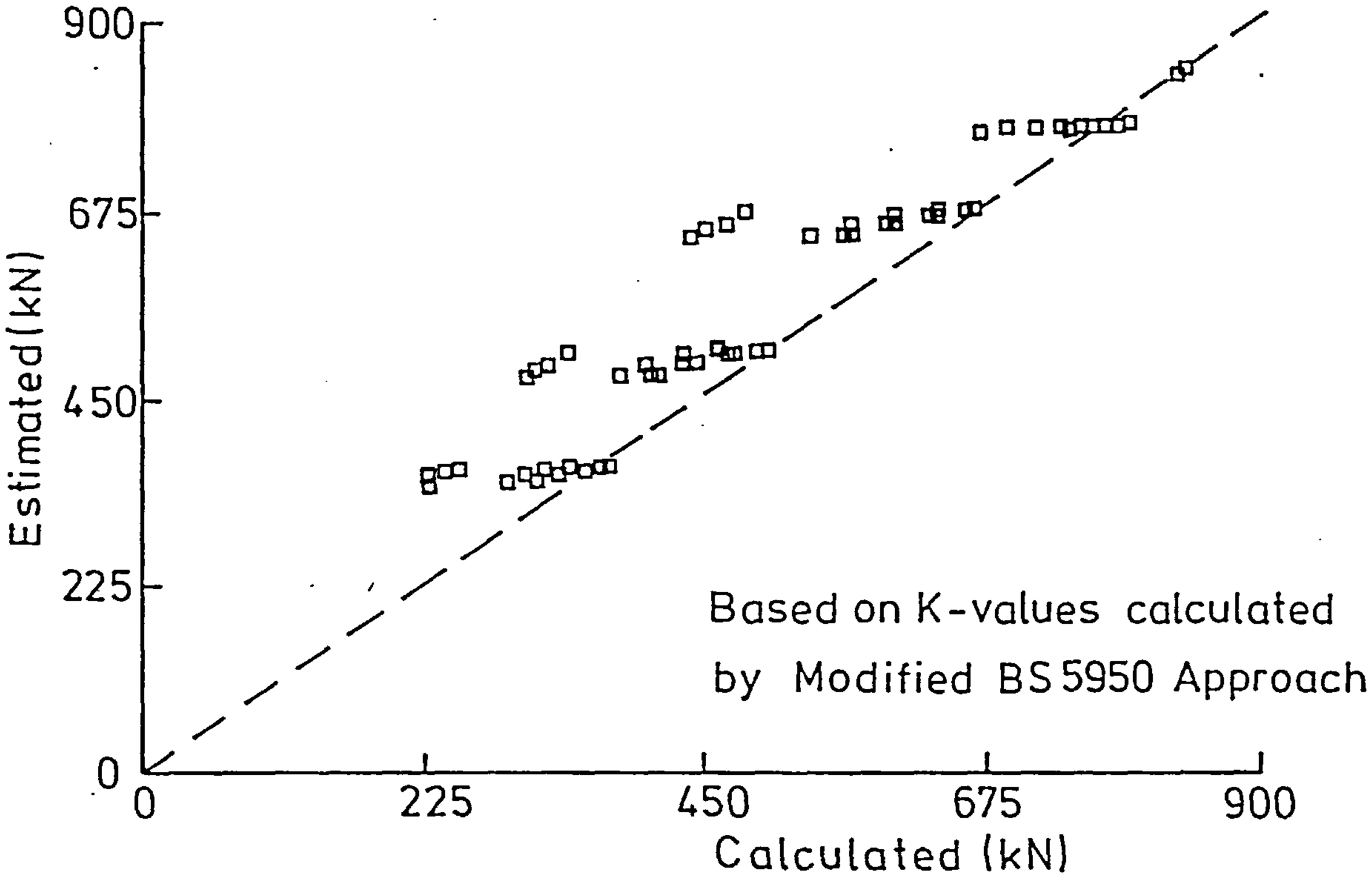

FIG.7-15 COMPARISON BETWEEN ESTIMATED AND CALCULATED ULTIMATE LOADS

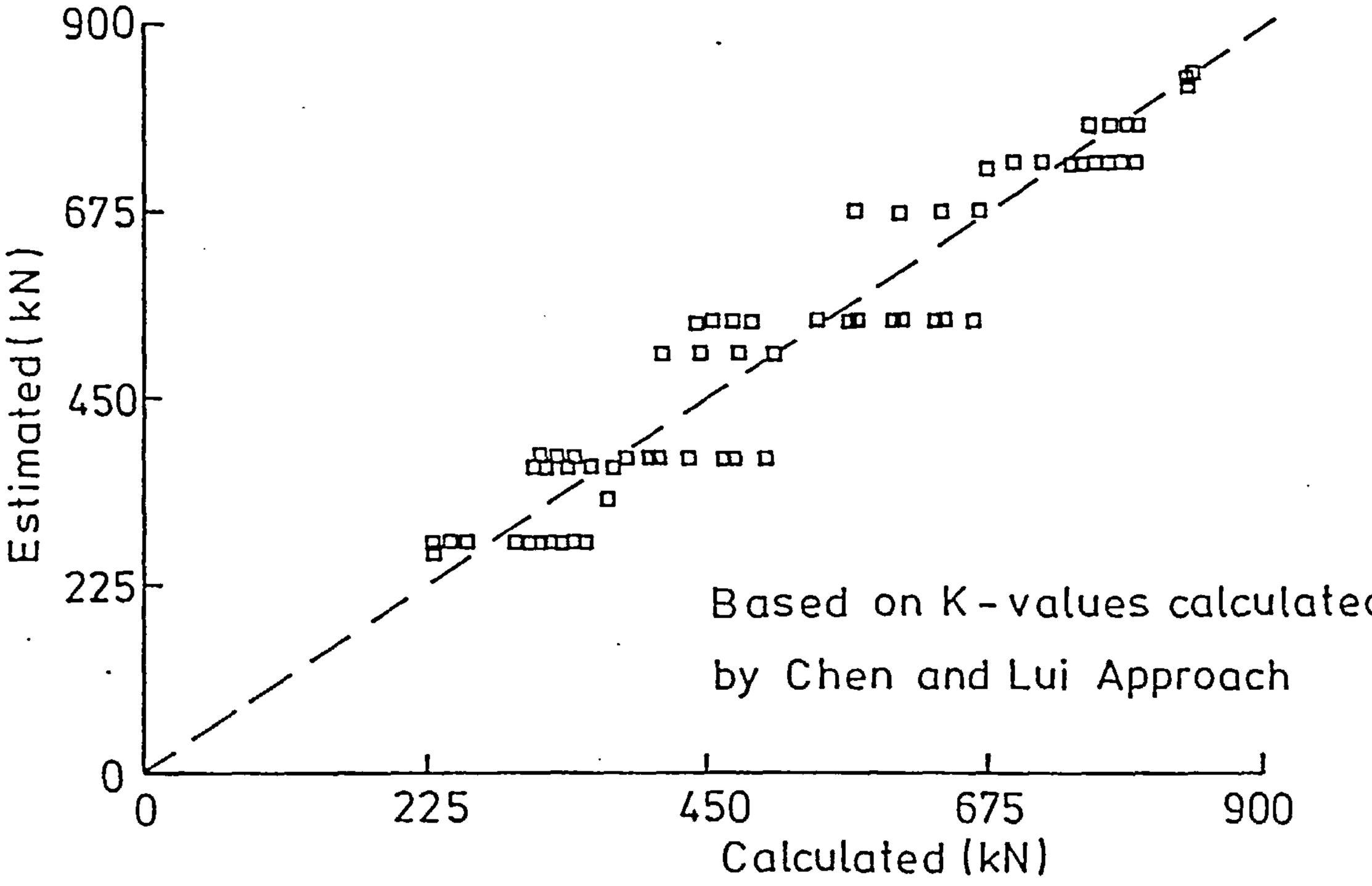

FIG.7-16 COMPARISON BETWEEN ESTIMATED AND CALCULATED ULTIMATE LOADS

representation for the connection behaviour was used, column failure usually corresponded to the first part of the M-Φ curve for the considered connection. The "proposed approach", on the other hand is based on actual column curves which were based on analyses in which the reduction in joint stiffness was taken into account.

The variation of the estimated k-values using the "proposed approach" with the combined beam and connection stiffness, C^*, is shown in Fig-7.17. The effect of the beam to column connections may readily be seen from this figure. Careful consideration of the figure may also reveal the effect of beams on the effective length factor. All points which were made in the previous section may be observed from this figure.

Fig-7.18 shows a plot between the the estimated effective length factor and the non-dimensional quantity, C^*/C_j for the same cases of Fig-7.17. The isolated column cases were not shown in Fig-7.18 as the quantity C^*/C_j would always be equal to one no matter what type of connection is used. The relation between k and C^*/C_j seems to be of a smooth nature. It was found that these relations may be closely approximated by quadratic equations in C^*/C_j of the form

$$k = a + b\left(\frac{C^*}{C_j}\right) + c\left(\frac{C^*}{C_j}\right)^2 \qquad (7.16)$$

where a, b and c are constant which seem to depend on the beam span. The constant a was found to be the effective length factor for the columns in rigid subassemblages. Constant b was found to vary from a negative value of -0.09 for a beam span of 1.5m to a positive value of 0.02 for a beam span of 4.5m. The second term was found to be reasonably small in all cases and could be neglected. The third constant c was found to vary non-linearly with the beam span. The

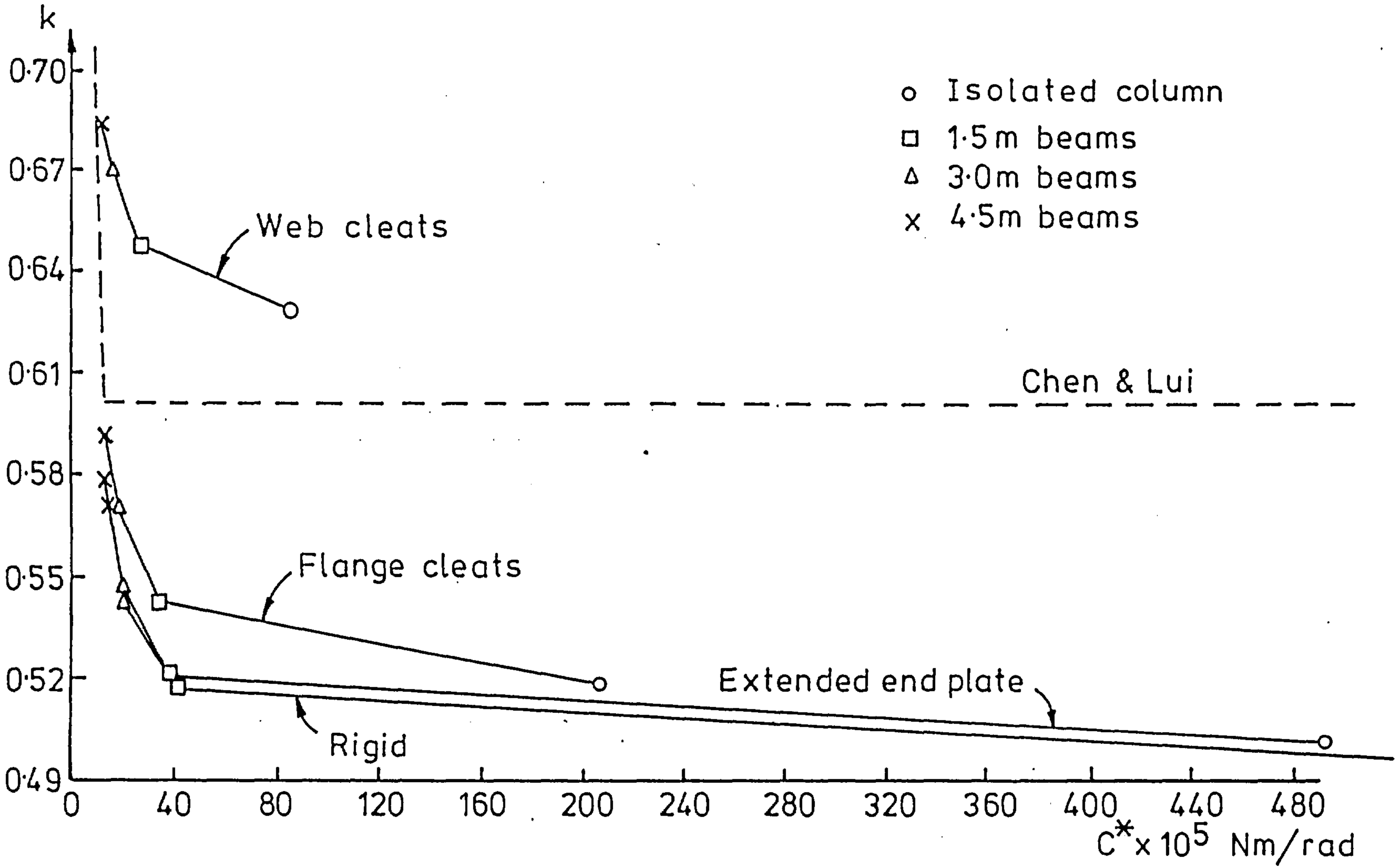

FIG. 7·17 VARIATION OF ESTIMATED EFFECTIVE LENGTH FACTORS k WITH COMBINED BEAM AND CONNECTION STIFFNESS, C^*

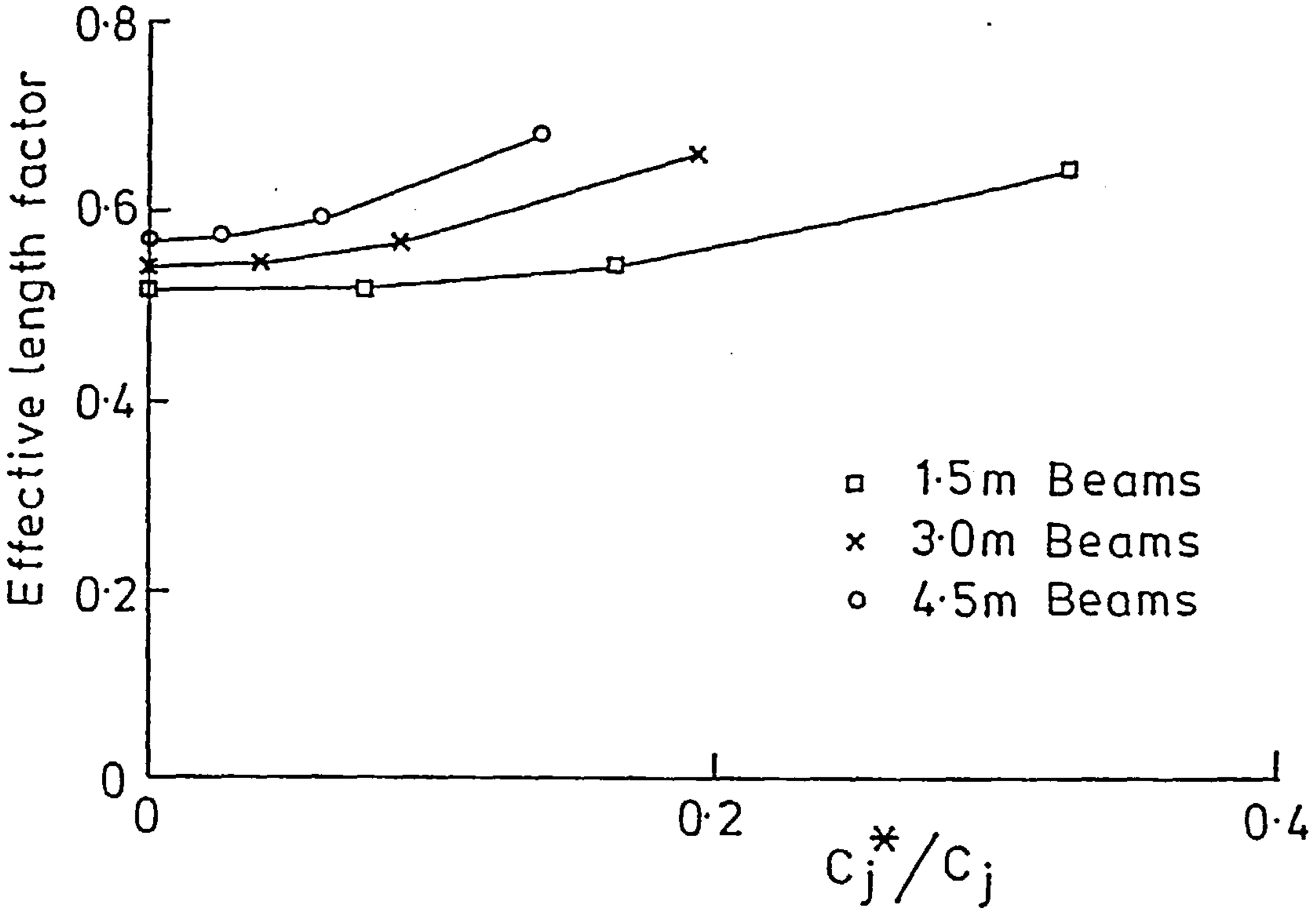

FIG. 7·18 EFFECTIVE LENGTH FACTORS Vs C_j^*/C_j

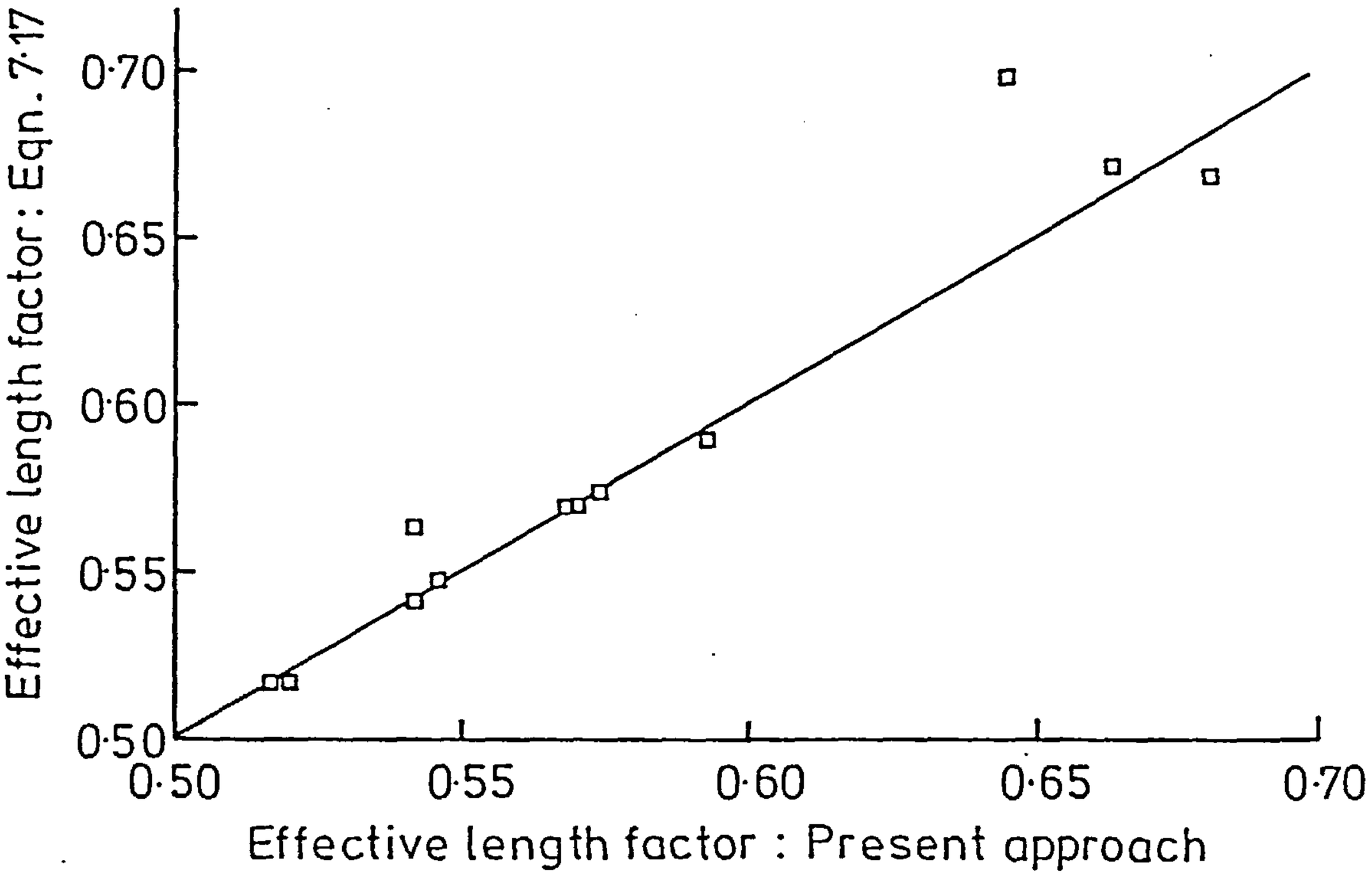

FIG. 7·19 CORRELATION BETWEEN EFFECTIVE LENGTH FACTORS

relation, however, was found to be close to a straight line. A linear relationship of the form

$$c = 1.1333\ L_b \qquad (7.17)$$

was found to approximate the c vs. L_b relationship in which L_b is the beam span in metres. From eqns-7.16 and 7.17, the effective length factor for the column in the subassemblage of Fig-7.1 may be approximated by

$$k = k_{rigid} + 1.1333\ L_b\ (\frac{C^*}{C_j})^2 \qquad (7.18)$$

Fig-7.19 shows the correlation between the estimated effective length factors shown in Table-7.3 (proposed approach) and those calculated from eqn-7.18. There seems to be a good correlation between the two sets of values. Eqn-7.18 may thus be accepted for calculating the effective length factors for columns in 'flexibly connected subassemblages. The effective length factors for columns in rigid subassemblages may be calculated by the "modified AISC Approach". It must be noted, however, that the present study is rather limited both in the variety of parameters that may affect the behaviour of subassemblages and in the variations in the parameters considered. For instance, minor axis bending for the column may be an extra parameter that may be included in a more comprehensive study. More connection types, especially flexible ones should be included to confirm the validity of eqn-7.18.

7.3.2- Subassemblage Strength Due to Combined Column and Beam Loads:-

7.3.2.1- Interaction Curves:-

It is common to illustrate the failure conditions of a subassemblage due to combined beam and column loads in the form of interaction curves. The interaction curves for the subassemblage of Fig-7.1 are shown in Fig-7.20 for the different connection types and column lengths considered in the present study. These curves describe the relation between the total force in the column and the column end moment at the failure condition. The points on each curve (which correspond to a specific connection type) relate to a certain maximum value for the beam load and each is representeed by a different symbol as indicated in the legend of Fig-7.20. For instance, the case corresponding to a beam load of 30kN and rigid beam to column connections represented by *. Solid lines correspond to 5m columns while broken lines correspond to 9m columns.

The following observations may be made from this figure:

(i) The moment at the column's end at the failure condition due to column load only is substantial. This is in contrast with the isolated pin-ended column cases in which the interaction curve starts from the vertical axis (i.e zero moment condition). The presence of end restraint offered by the beams and the connections is responsible for this behaviour.

(ii) The interaction curves corresponding to the 5m long column are less scattered than those corresponding to the 9m long column. Excessive yielding in the 5m column may be regarded as being the reason behind this behaviour. As there is a large axial force in the column, the plastic moment is reduced. Hence there

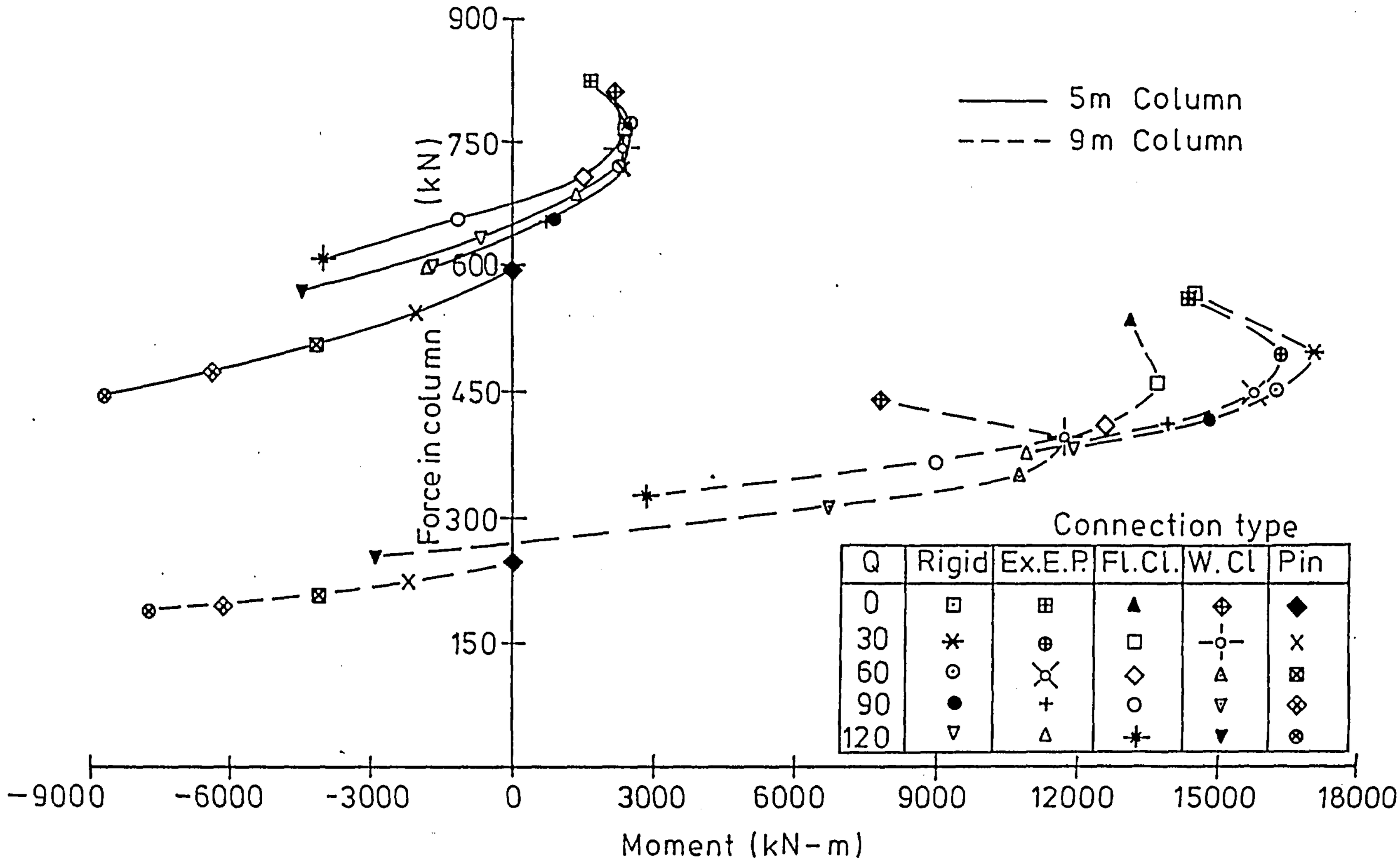

FIG. 7·20 INTERACTION CURVES FOR THE SUBASSEMBLAGE OF FIG. 7·1

is a narrower range for the moment that develops in the column.

(iii) As expected, the total axial force in the column at failure decreases as the beam load increases due to the larger applied primary moment.

(iv) The moment at the column's end, on the other hand, increases up to a certain maximum value after which it starts to reduce. This point of maximum moment corresponds to a beam load in the range of 30 to 40kN.

To understand this last observation, consider the deflection modes of the subassemblage of Fig-7.1 under the action of beam load only, column load only and combined beam and column loads. If there is only a beam load acting on the top-right beam of the subassemblage shown in Fig-7.21a, the left beam and the column share the resistance of the moment transmitted through the right connection and that produced by the beam reaction through the joint offset distance, D/2. The directions of the moments developed at the beam-column-beam junction are shown in the inset of Fig-7.21a. A clockwise moment is developed at the column's end. The connections, if flexible, are assumed to follow the loading path on their corresponding M-Φ curves which are schematically shown in Fig-7.21b. If the beam-to-column connections were rigid, these paths, of course, would correspond to the vertical axes on these curves. On the basis of Fig-7.21a, the column moment, M_c, may be expressed as

$$M_c = M_r - M_l + Q \frac{D}{2} \qquad (7.19)$$

Where M_l and M_r are the moments transmitted from the left and right beam ends through the beam-to-column connections. In flexible connections, both M_l and M_r are controlled by the M-Φ curves for the

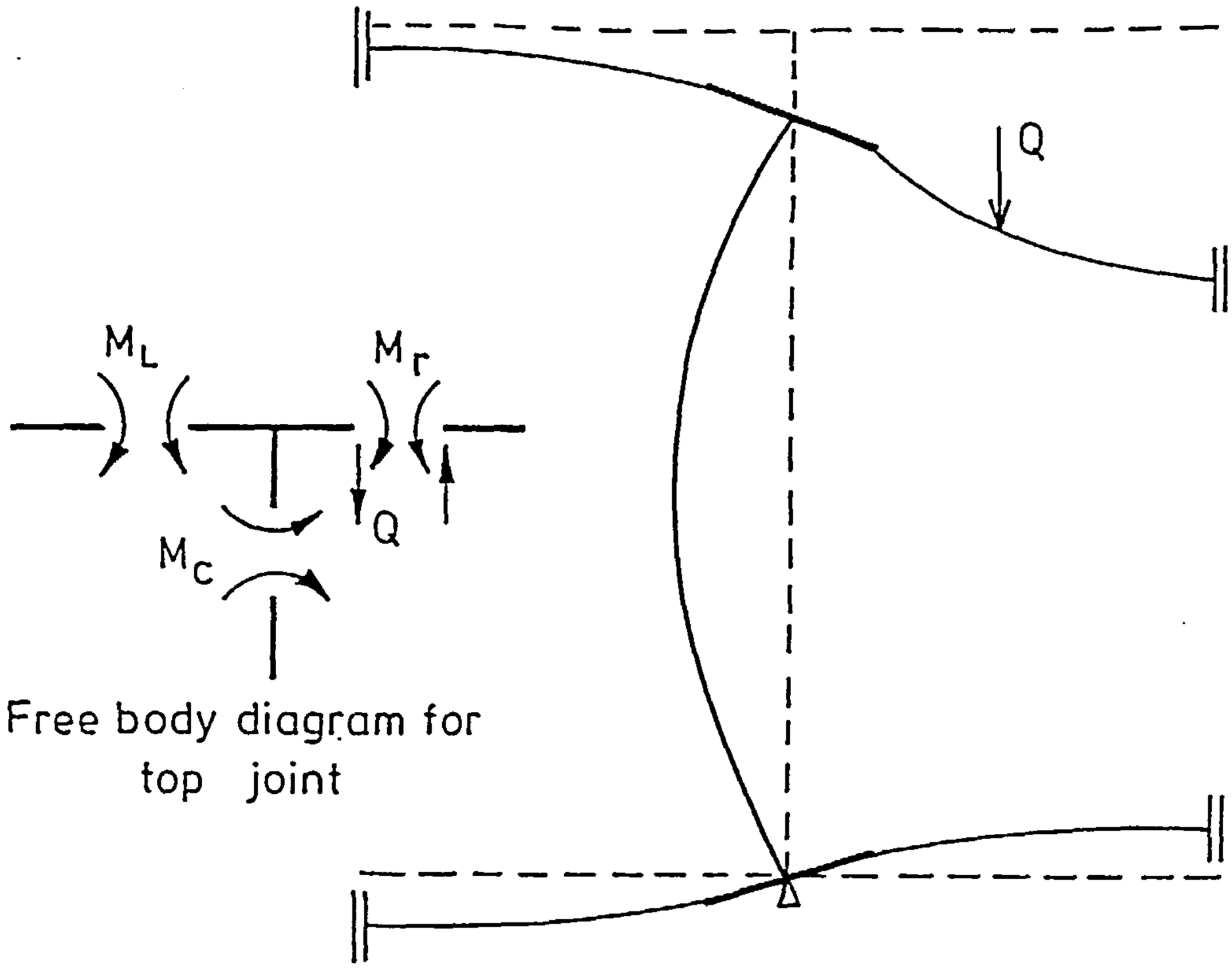

(a) Deflection mode

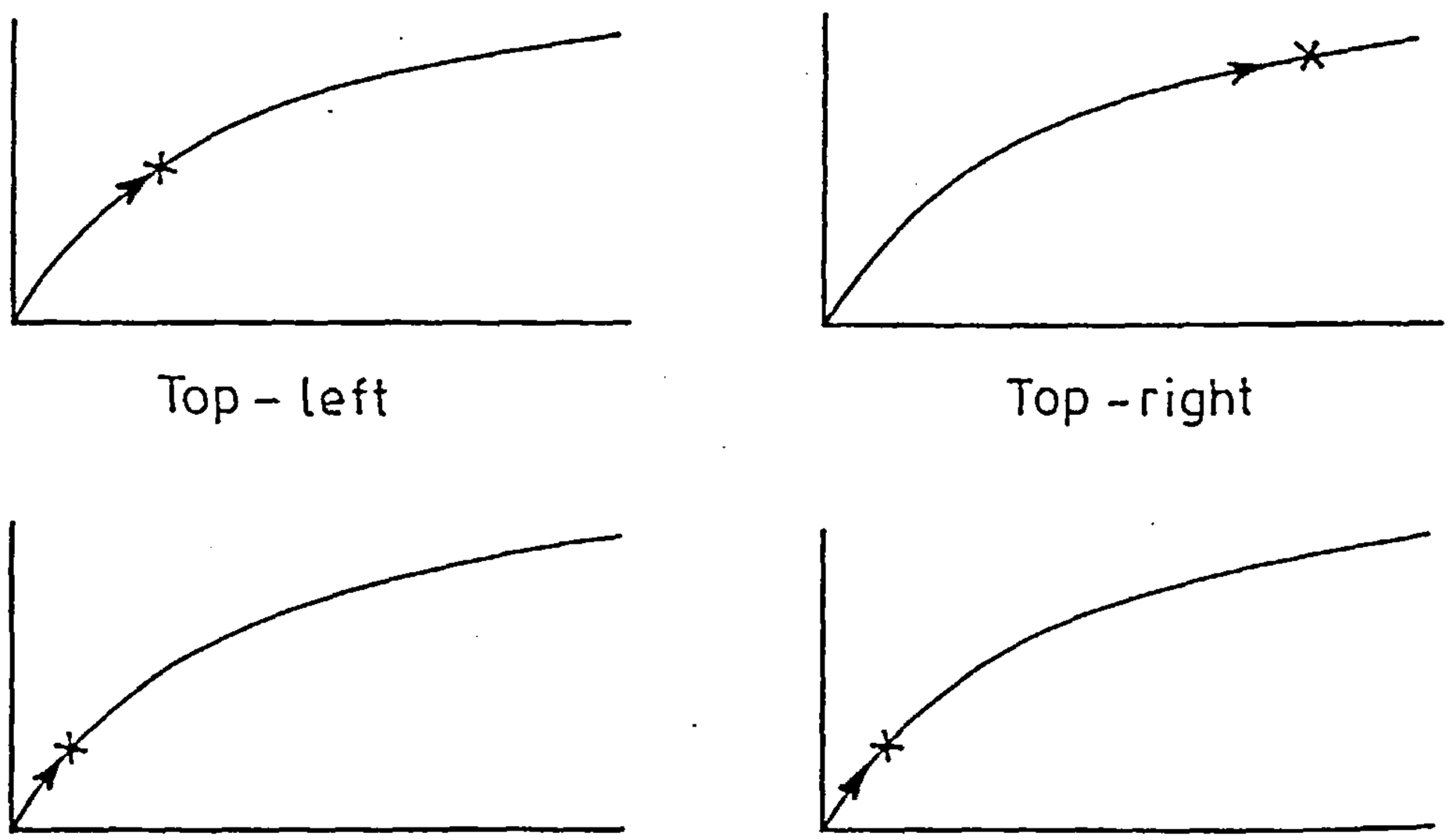

(b) Qualitative M - ϕ curves

FIG. 7·21 BEHAVIOUR OF SUBASSEMBLAGE UNDER BEAM LOAD ONLY

connections used.

Fig-7.22a shows the deflected shape of the subassemblage under the action of column load only. Once again, the moments induced in the beam-column-beam junction are shown in the inset of Fig-7.22a. directions of the column moment and the right beam are opposite to those shown in Fig-7.21a. Hence, the cases just described may be considered as the extremes. The M-ϕ curves for the beam-to-column connections are shown in Fig-7.22b. Both connections are assumed to be in the loading condition. Unlike the beam load case, both connections here possess nearly equal rotations in the same sense due to symmetry provided that both connections are of similar M-ϕ characteristics.

The third case is a combination of those described above. Assuming that a beam load is applied to the subassemblage in the first load stage, then, while the beam load is held constant, a column load is applied. At the end of the first load stage, the deflected shape of the subassemblage is shown in Fig-7.23a (dotted lines). As the column load is applied, the deflected shape of the subassemblage will change to that shown by the continuous lines in Fig-7.23a. Although the column's lateral deflections and the beam lateral deflections are still increasing, this increase is not as it was when the beam load was increasing. The right beam joins the left one in assisting the column to resist the applied load. The relation between the moments in the beam-column-beam junction are as expressed by eqn-7.19. However, the increments of moments would correspond to a case in which only the column load is applied. In other words, by inspecting Figs-7.21a and 7.22a, the moment in the column reduces from that reached at the end of the beam load stage. In Fig-7.23b, the M-ϕ curves for the beam-to-column connections are shown. The right connections now unload

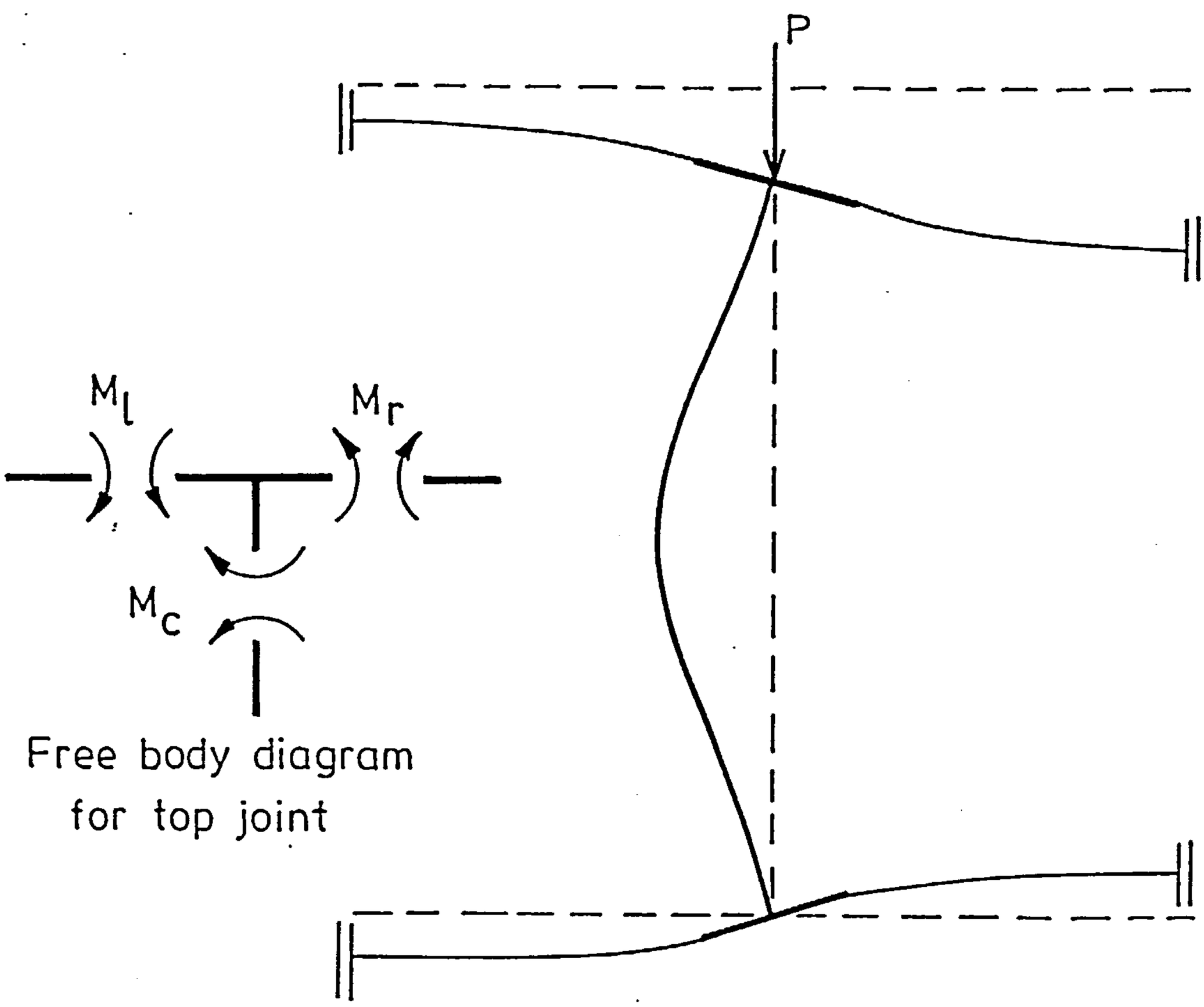

(a) Deflection mode

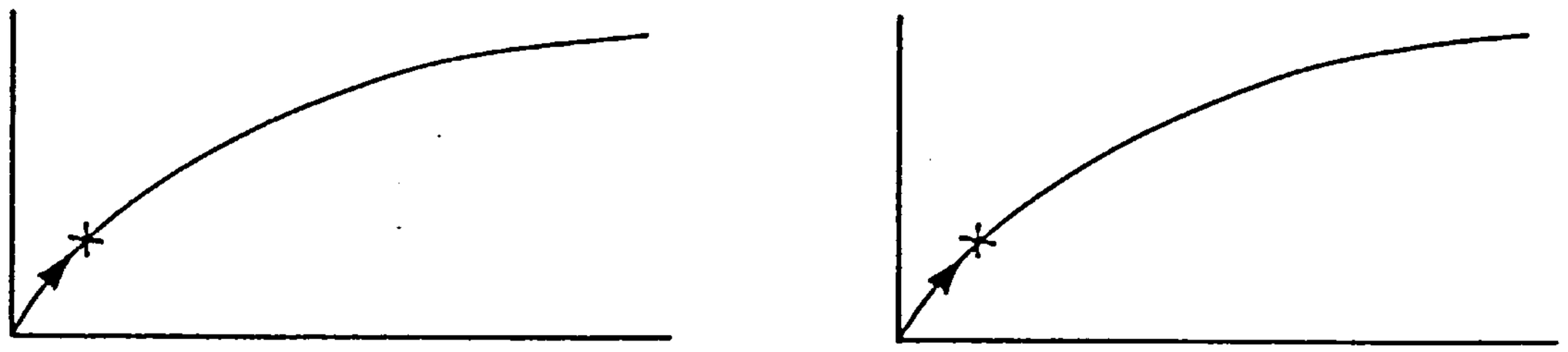

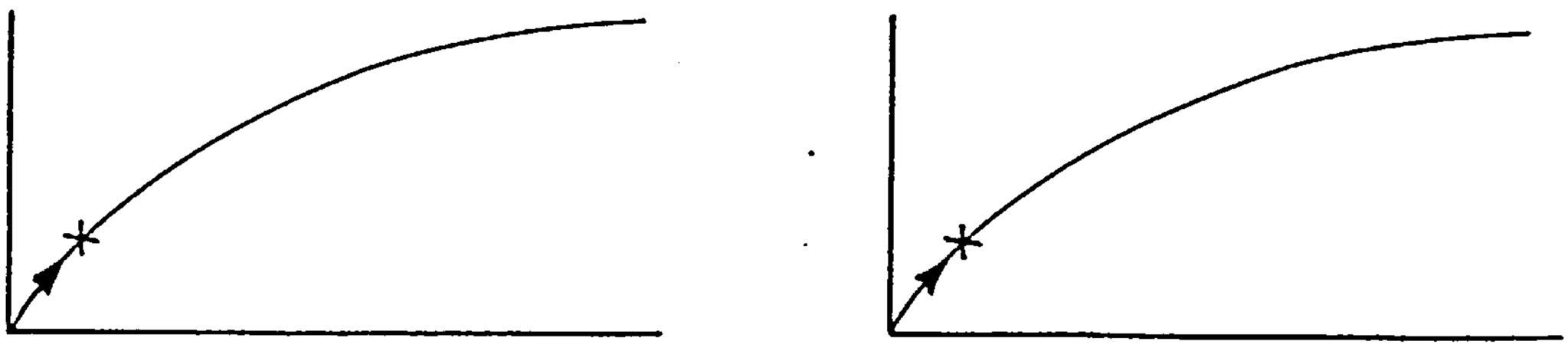

(b) Qualitative M − ϕ curves

FIG. 7·22 BEHAVIOUR OF SUBASSEMBLAGE UNDER COLUMN LOAD ONLY

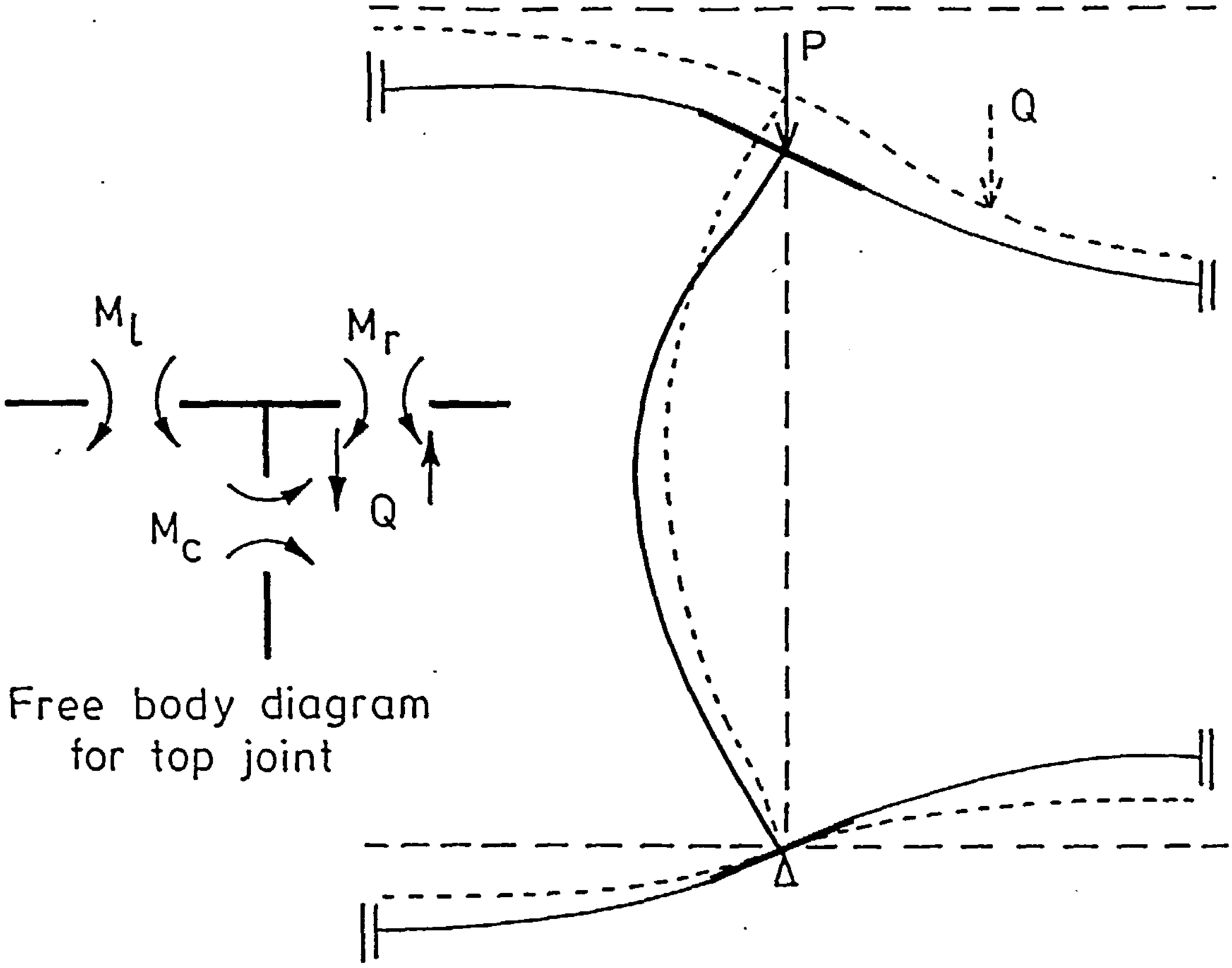

(a) Deflection mode

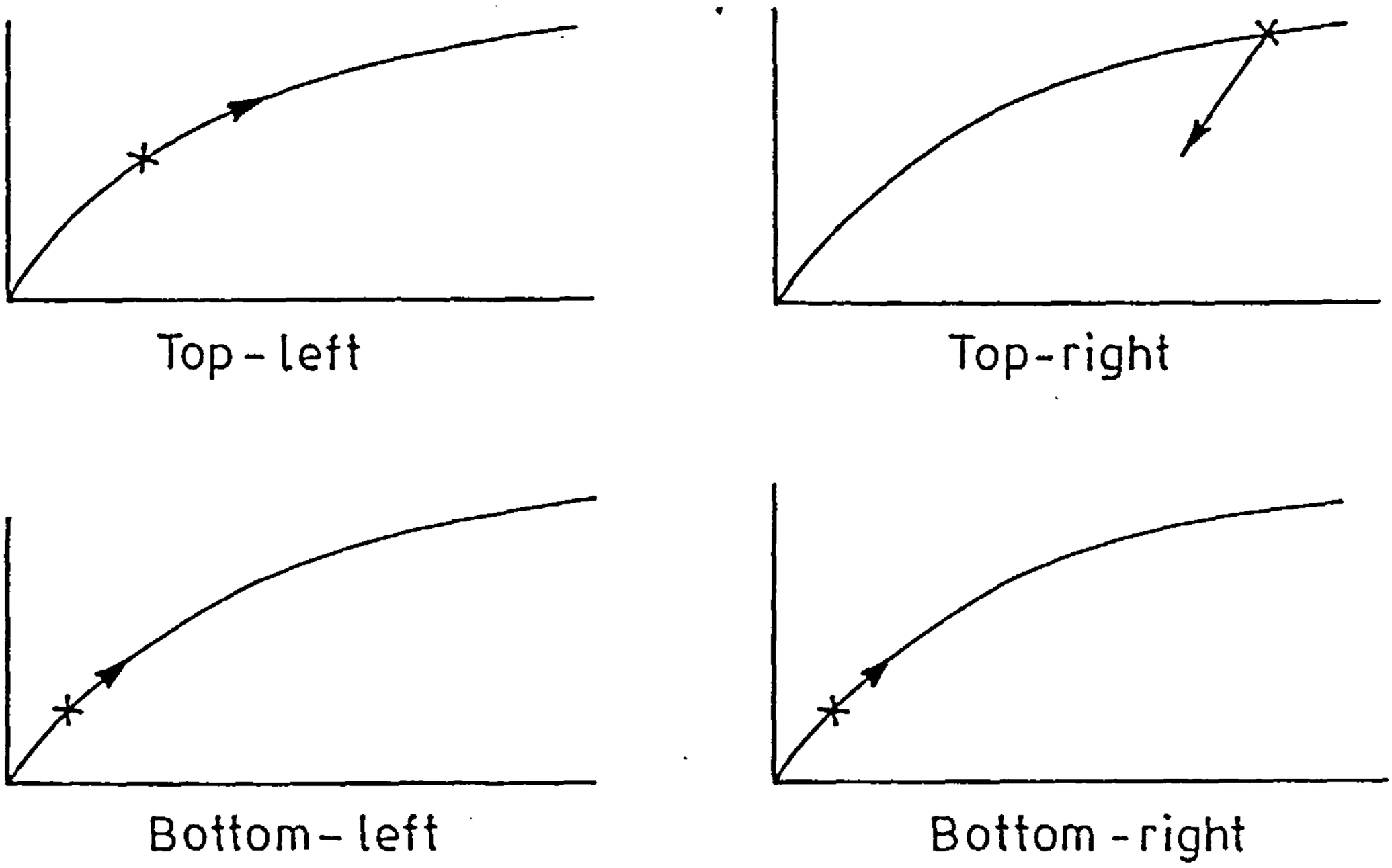

(b) Qualitative method M - ϕ curves

FIG. 7-23 BEHAVIOUR OF SUBASSEMBLAGE UNDER COMBINED BEAM AND COLUMN LOADS

while the left one still continues to load. In all of the above cases, the lower connections continue to load throughout the loading process. As they undergo relatively smaller rotations, their stiffnesses would generally be greater than those for the upper connections when in loading condition.

Figs-7.24 and 7.25 show the variation of column end moment with the total force in the column for the columns in the subassemblages with rigid and web cleat connections respectively. The curves in these figures correspond to the beam loads considered in this study (i.e. in 30kN increments from 0 to 120kN.) All curves of Figs-7.24 and 7.25 have the feature that the moment increases in one direction, then starts to reverse back as the column load increases. In almost all of the curves the moment actually reversed its sign. The end points of these figures correspond to failure on the envelopes that appear in the interaction curves of Fig-7.20 for the rigid and web cleat connection cases.

It is of interest to point out that the slope of these curves at the start of the column load stage reduces when greater beam load is applied. This may be attributed to the fact that the application of beam loads results in rather large lateral deflections in the column hence increasing the effect of the end restraint in reducing the end moment in the column. In other words,the effect of a beam load is analogous to the presence of initial imperfections. This was also pointed out by Gent and Miller (42).

Figs-7.26 and 7.27 show the variation of the flexural rigidity, EI, for the column at the failure load for the cases with rigid and web cleat connections respectively. It can be noticed from these figures that the amount of yield in the column is much larger (as

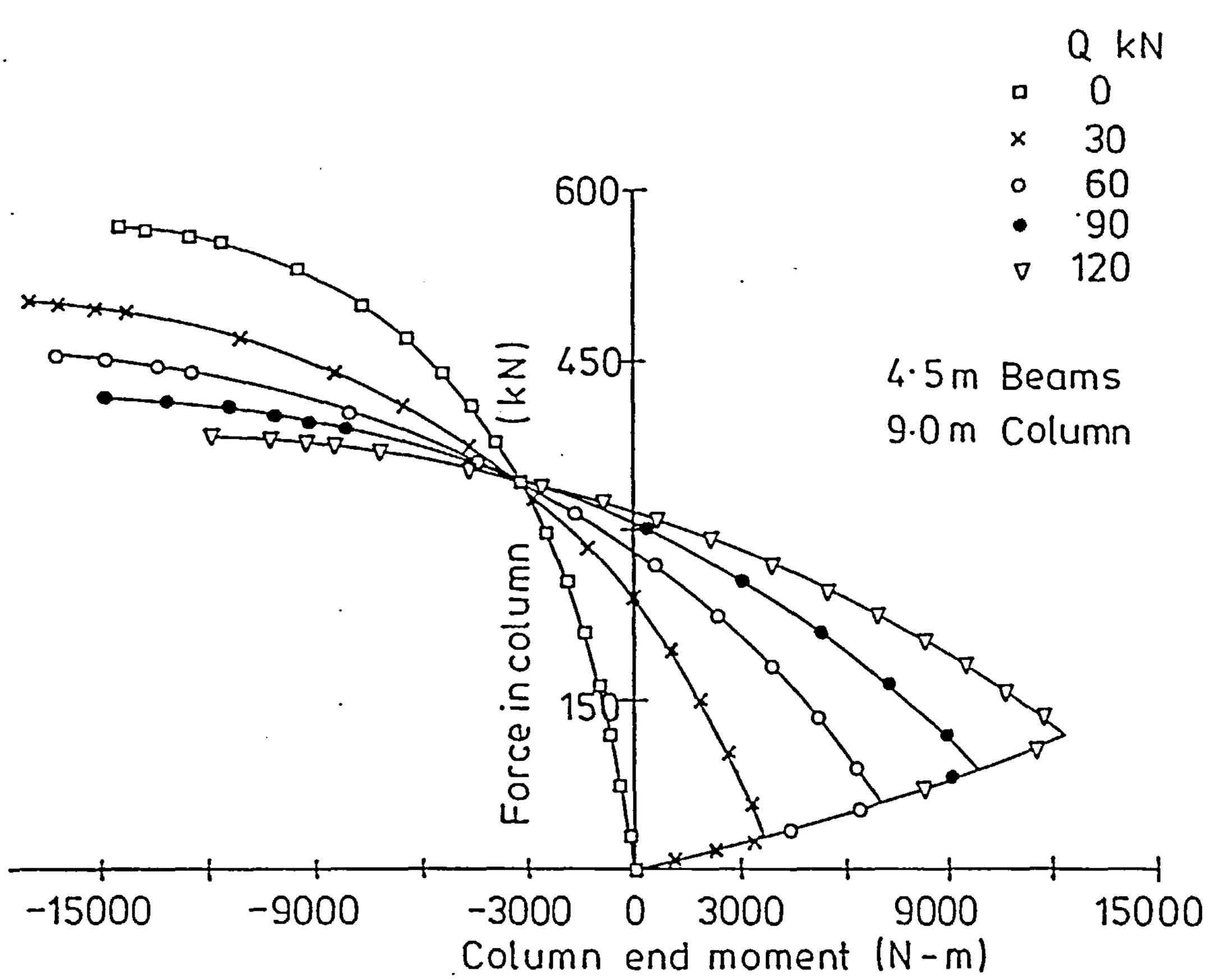

FIG.7·24 FORCE-MOMENT CURVES FOR DIFFERENT BEAM LOADS (RIGID JOINTS)

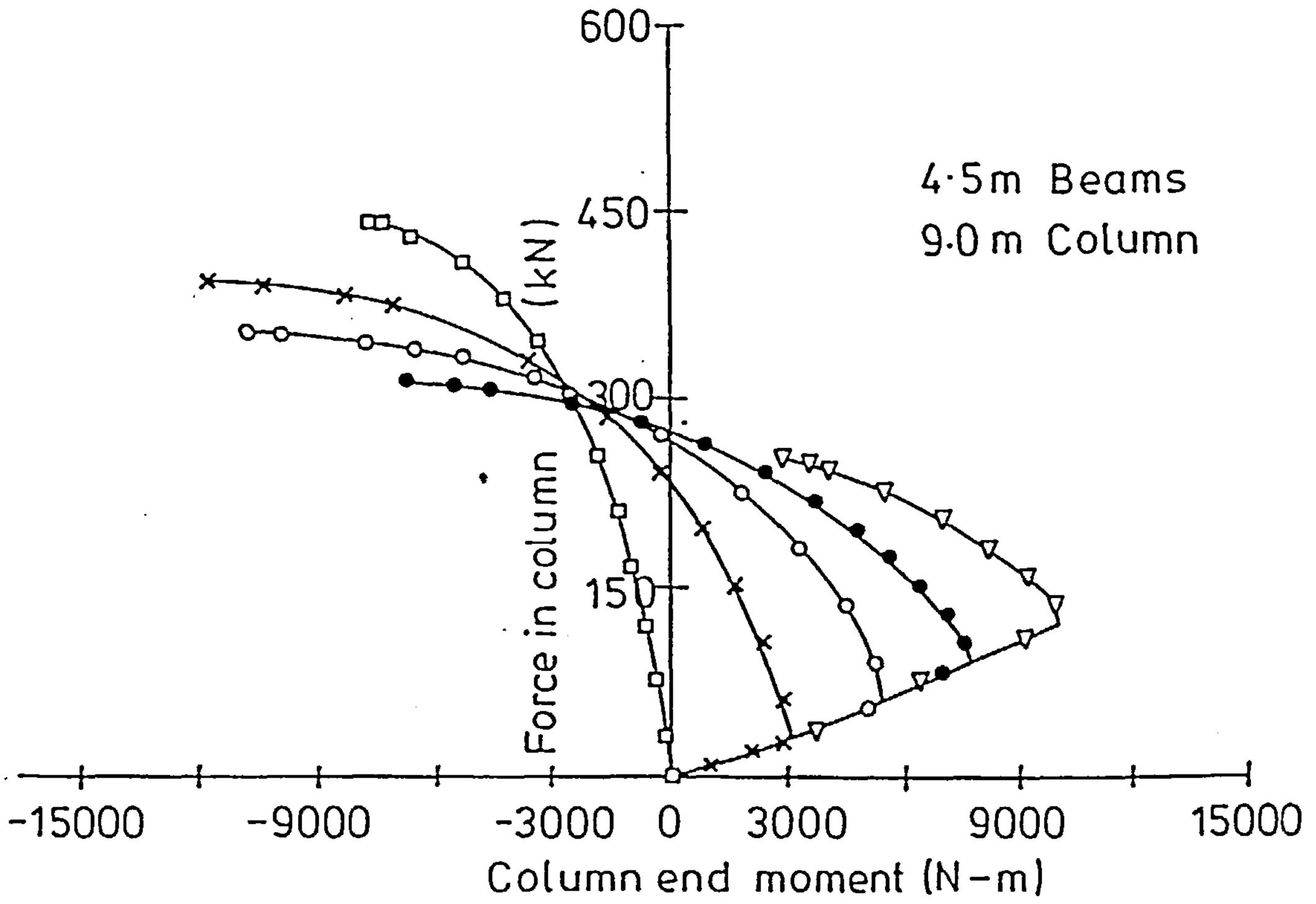

FIG.7·25 FORCE-MOMENT CURVES FOR DIFFERENT BEAM LOADS (WEB CLEATS)

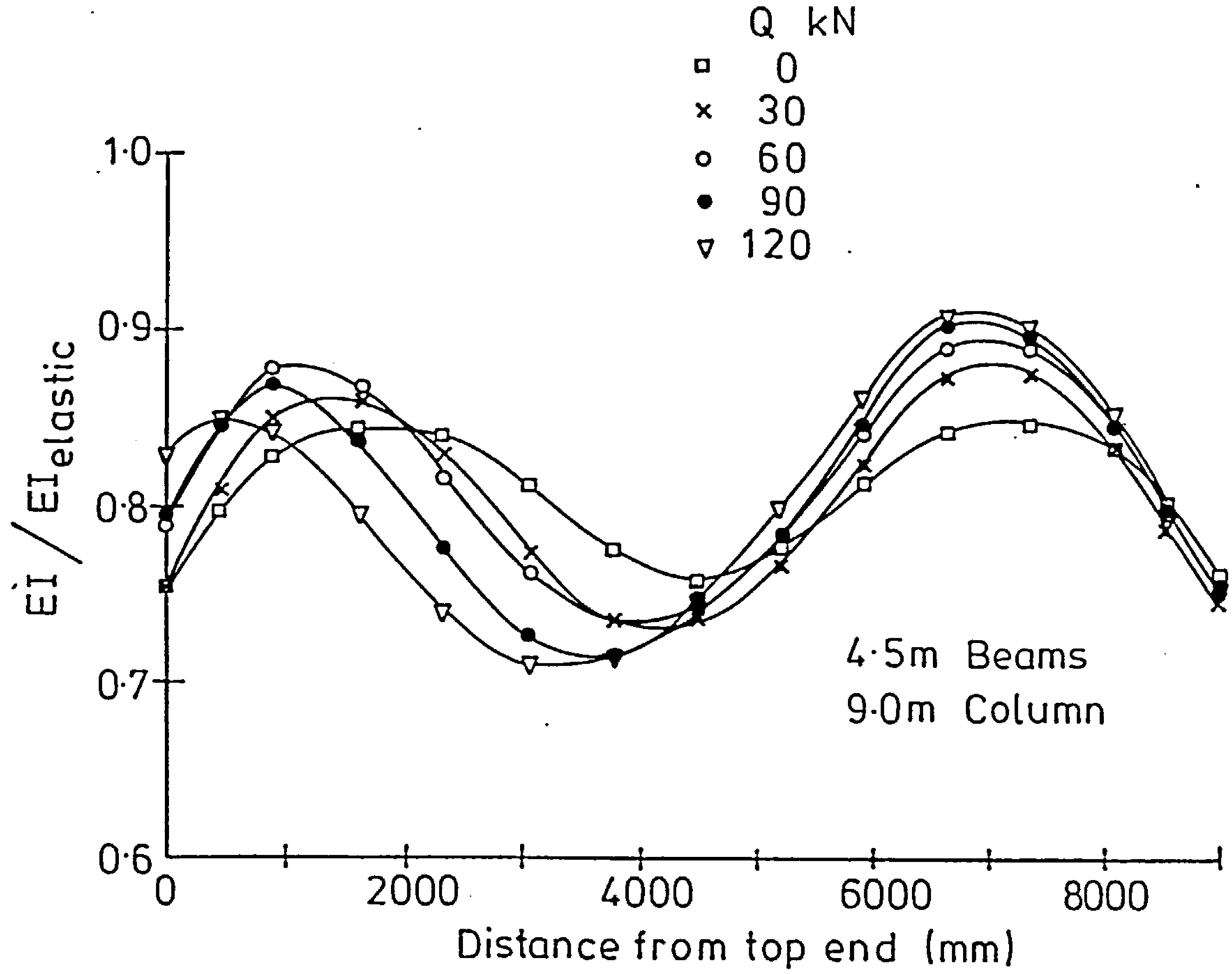

FIG. 7·26 SPREAD OF YIELD (RIGID JOINTS)

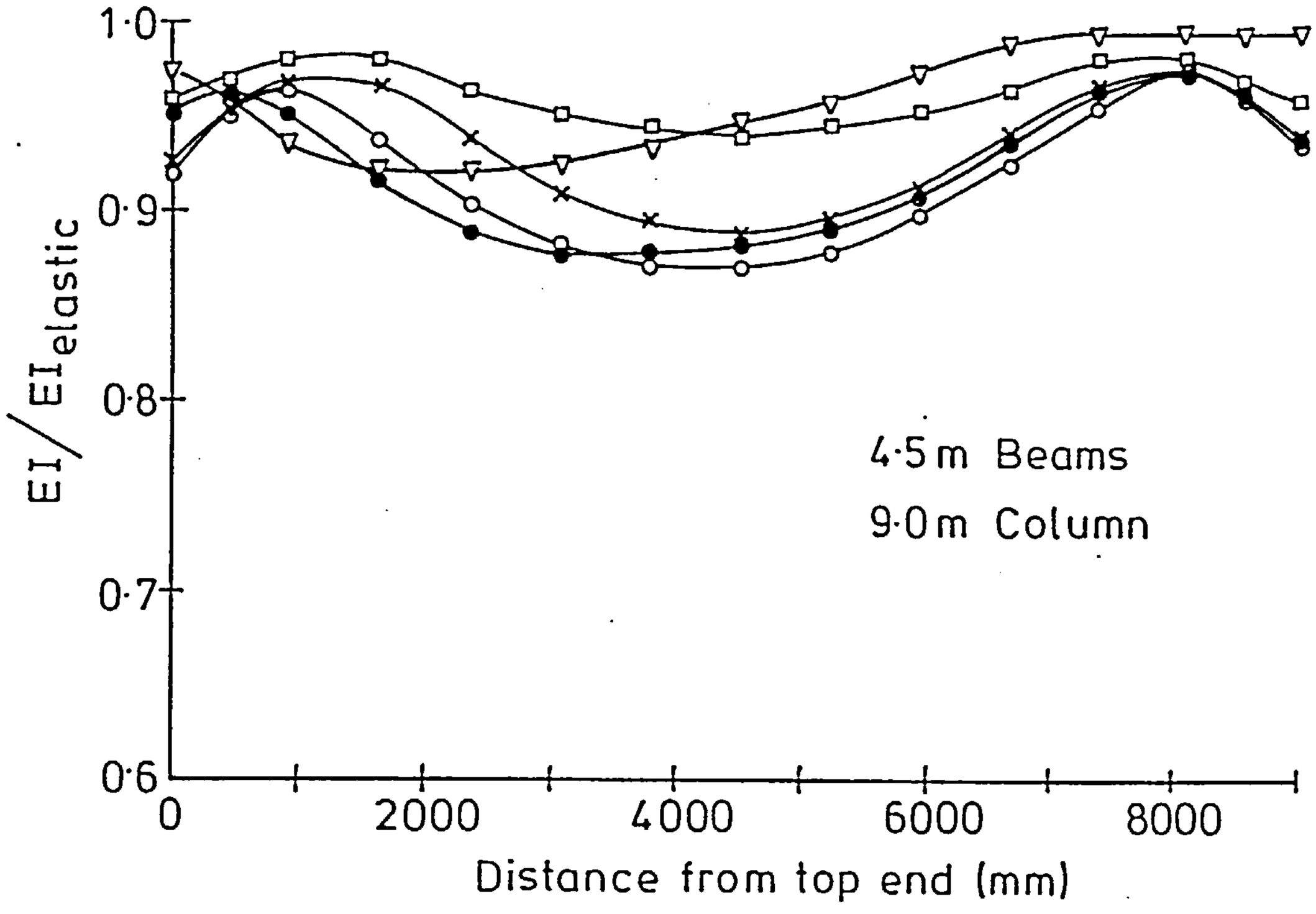

FIG. 7·27 SPREAD OF YIELD (WEB CLEAT CONNECTIONS)

shown by a decrease in EI value) in the case of a rigid subassemblage than it is in the subassemblage with web cleat connections. This is because the former can sustain more column load and hence a larger force in the column. It can be seen that the critical section in all of the cases considered is somewhere along the length of the column (i.e. not at the column's end). The section at the centre of the column is critical for the cases of column load only. In the cases where a beam load was applied, the critical section moves towards the top end of the column as a larger beam load was used hence approaching a case of an eccentrically loaded column.

The maximum column load at which the subassemblage fails depends on three factors:

(i) as was pointed out earlier, the presence of beam load reduces the axial stiffness of the column due to the presence of large lateral deflections. In other words it is easier to fail a laterally deflected column than a straight one.

(ii) in flexible subassemblages, the beam load results in substantially reduced stiffness of the connections (Fig-7.21b) hence reducing the end restraint offered by these connections.

(iii) if the beams become inelastic, their stiffness, which assists the column in the column load stage, becomes less resulting in a lower assistance offered to the column.

From the above discussion, two points emerge:

(a) On one hand, the column fails in a combined mode due to bending and column actions which separately result in column moments of opposite signs. This means that as more bending is introduced into the column, the ultimate moment at the column's end must gradually change from a moment in one sense say anti-clockwise

(Fig-7.22a) corresponding to a 'column load only' case to a clockwise one (Fig-7.21a) which corresponds to a 'beam load only' case.

(b) On the other hand, the rate of change of column moment during the column load stage increases as a larger beam load is used. Hence the total change in the column load within each case increases with the increase of the beam load.

These two points have opposite effects. As long as the beam load is small, the second criterion prevails, hence the moment tends to increase in the same direction as in the case of no beam load. However, as more beam load is applied, the first criterion becomes more prominent and hence the ultimate moment in the column reverses its direction to ultimately that of a 'beam load only' case. Hence, there must be a beam load for which the moment in the column at failure is maximum. This in fact explains the fourth observation on Fig-7.20.

7.3.2.2- Effect of Beam to Column Connections on the Failure Load:-

The effect of beam-to-column connections may be easily demonstrated if the relation between the failure load (total force in the column at failure) and the initial stiffness of the connection is examined. Figs-7.28 shows such relations for the beam loads considered. The first observation which may be made is that, in the case of the shorter column, there seems to be little difference in the axial capacity of the column when using medium and stiff connections. This is irrespective of the level of beam load used. On the other hand, in the case of the more slender column, the effect of different connections is more appreciable, although this effect tends to diminish as stiffer connections are used. Again, this observation holds for all values of

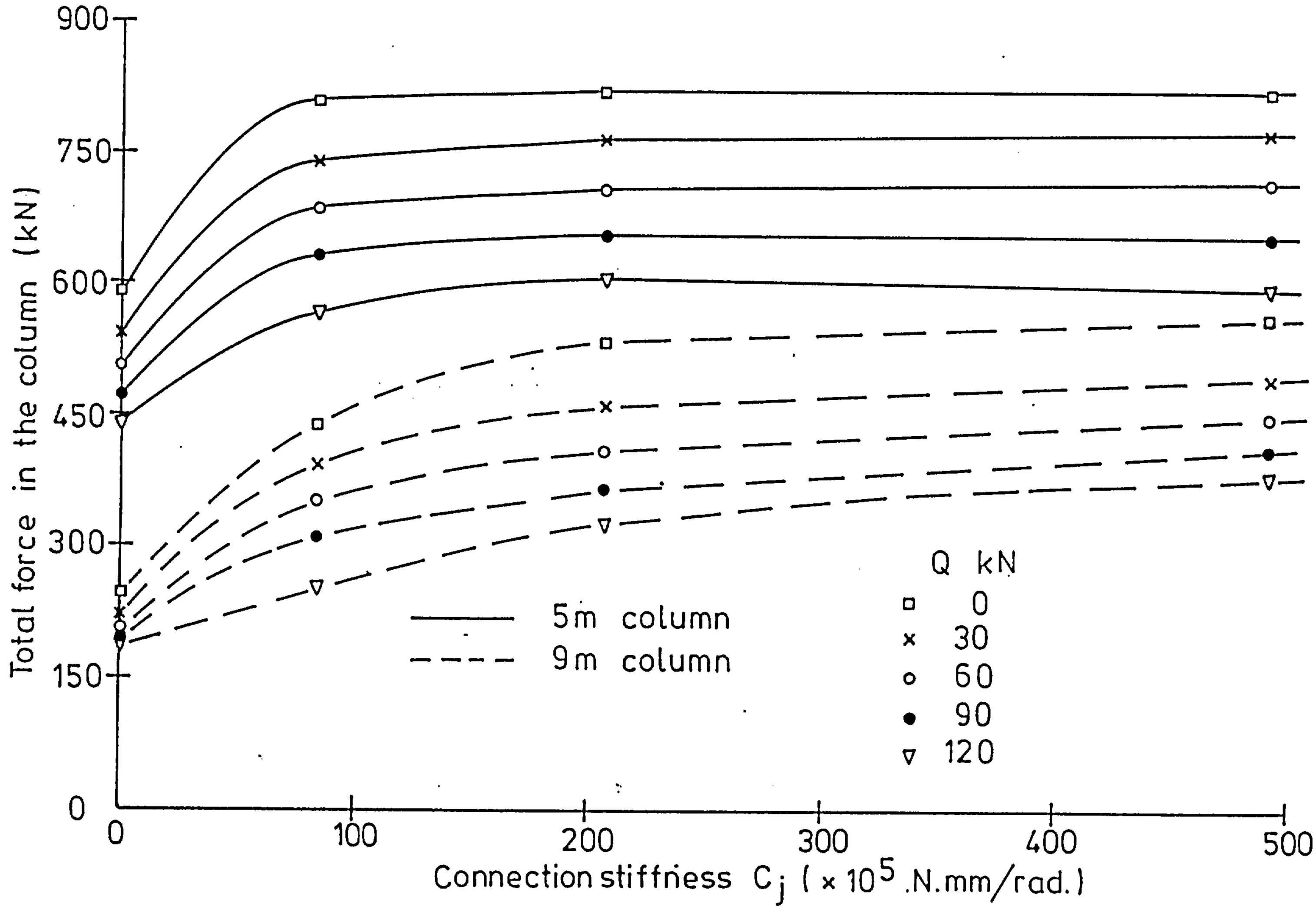

FIG.7·28 COLUMN LOAD Vs CONNECTION STIFFNESS

the beam load. The axial capacity for the column in subassemblages with pin connections is generally less than that for a pin ended column with the same height as the beam load is applied eccentrically. The failure load reduces when using higher beam loads. This could be explained on the basis of eqn-7.19. In the beam load stage, both M_l and M_r are identical to zero. Hence, the problem becomes one of an eccentrically loaded column in which the eccentricity is D/2. This in fact results in a reduced axial capacity for the column. A final observation is that the difference in column capacity, for any particular connection- especially medium and stiff ones- is slightly increasing in the case of the 5m column and decreasing in the 9m one.

7.3.2.3- Effect of Beam Load on Column Load:-

As may be seen from Figs-7.20 and 7.28, the effect of the presence of beam load is to reduce the column load that is required to fail the subassemblage. The reasons for this have already been discussed in Sec-7.3.2.1. Fig-7.29 shows the variation of the column load required to fail the subassemblage with the applied beam load for all connection types used. Two groups of curves corresponding to column lengths of 5m and 9m are presented in this figure. The effect of semi-rigid joints is clearly demonstrated in this figure. In all the curves, an almost linear relationship seems to exist between the two types of loads. The slopes of these figures do not vary greatly with connection type or column length. Hence a linear relationship of the type

$$P = P_o - 1.88\ Q \qquad (7.20)$$

may be adopted. In eqn-7.20, P_o is the ultimate strength of the subassemblage when no beam load is applied and may be determined from

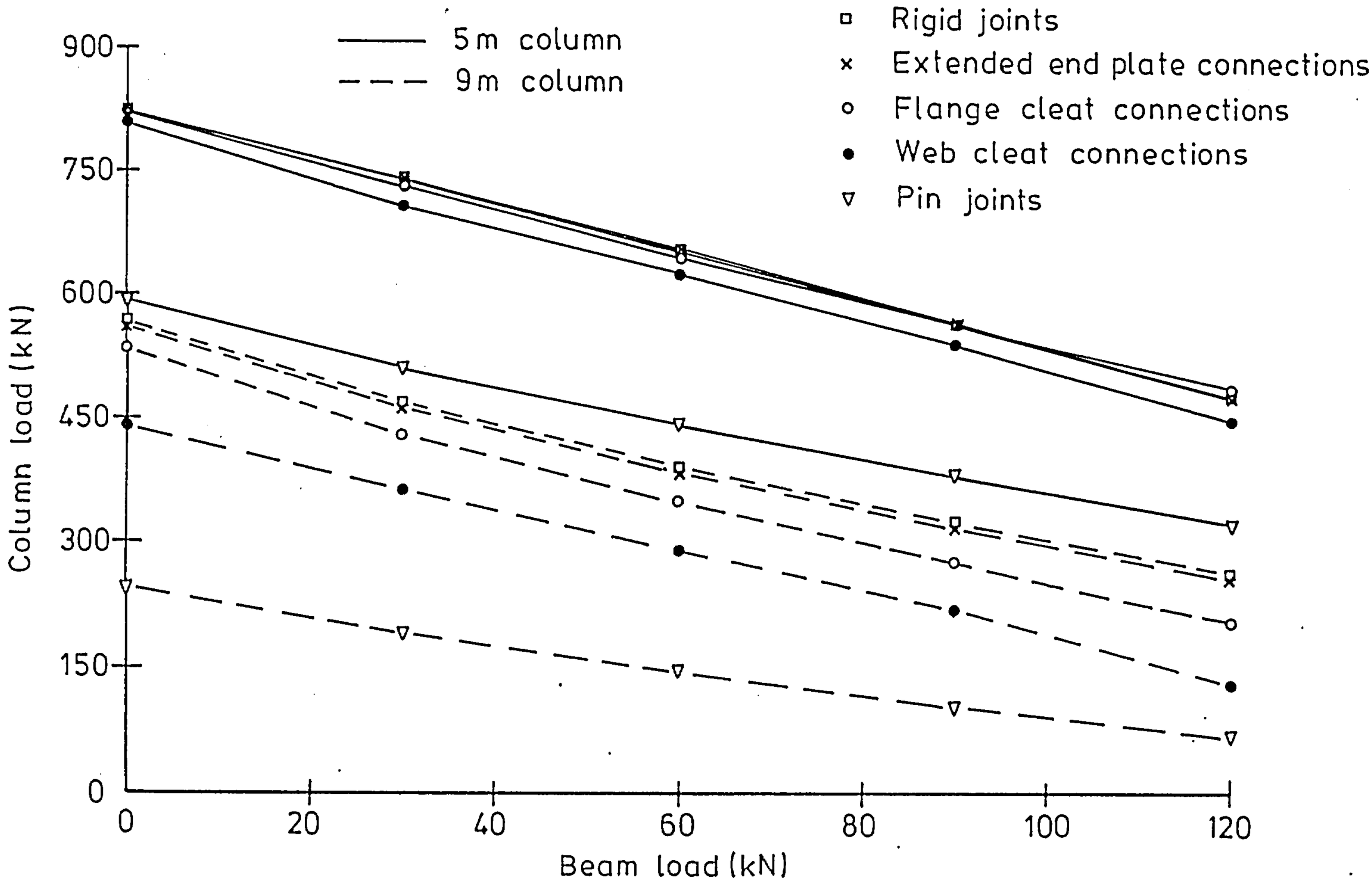

FIG. 7·29 INTERACTION CURVES (P Vs Q)

eqn-7.18 of the previous section. This is of course specifically related to the particular case considered but indicates the form of relationship which may be more generally applicable.

7.3.2.4- Maximum Moment at the Column End:-

It has already been pointed out that while the interaction curves of Fig-7.20 are of peculiar shapes, a point of maximum moment seems to exist for all connections other than pins. It would be interesting to examine such maximum moments in detail. Fig-7.30 shows the relation between the maximum moment that may develop at the column end and the initial connection stiffness. In the case of pin joints, there is no limit to the moment. This may be concluded from eqn-7.19 since both M_l and M_r are identical to zero. The column moment is therefore equal to QD/2 and is increasing with increasing Q. In the case of the 5m long column the maximum moment for all connections but pin joints seems to be constant. It may be argued, however, that if very flexible connections were used, the maximum moment must approach that of a pin joint (i.e. undefined).

Shown in Fig-7.31 is the relation between the maximum moment and the ratio R given by eqn-7.2 for all connections other than pins. An almost linear relationship is recognized for both the 5m and the 9m columns. The linear relationships may hence be assumed for both column lengths. The slope for the 5m column may be assumed to be zero while that corresponding to the 9m column may be assumed to be 42650.0 N.m. The linear relationship for the 9m column may be expressed as

$$M_{max} = M_{rigid} - S\ (1.0-R) \qquad (7.21)$$

in which M_{rigid} is the maximum moment that occurs at the column end when rigid connections are used and a beam load of 30kN is applied, and

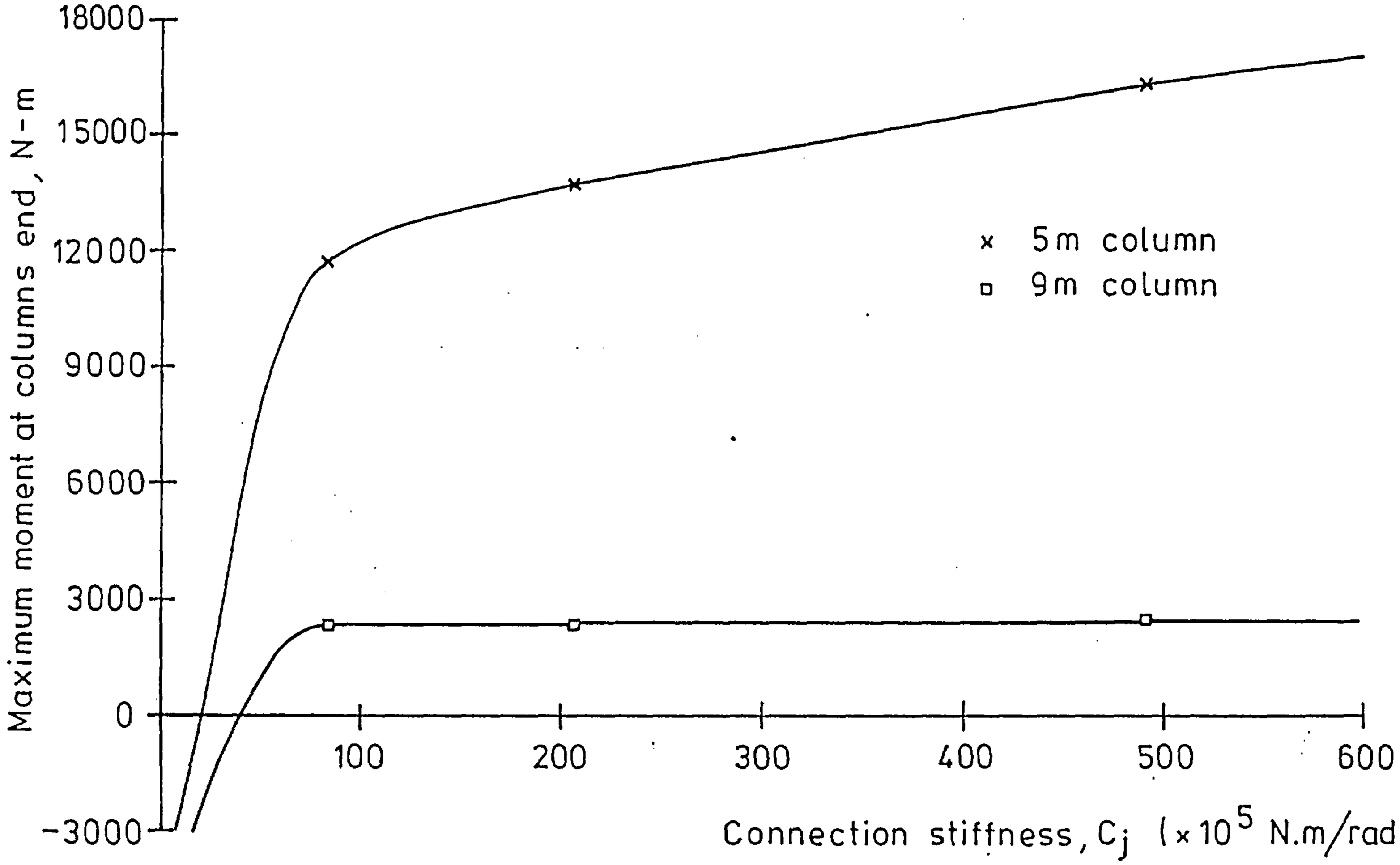

FIG.7·30 EFFECT OF CONNECTION TYPE ON MAXIMUM MOMENT AT THE COLUMN'S END

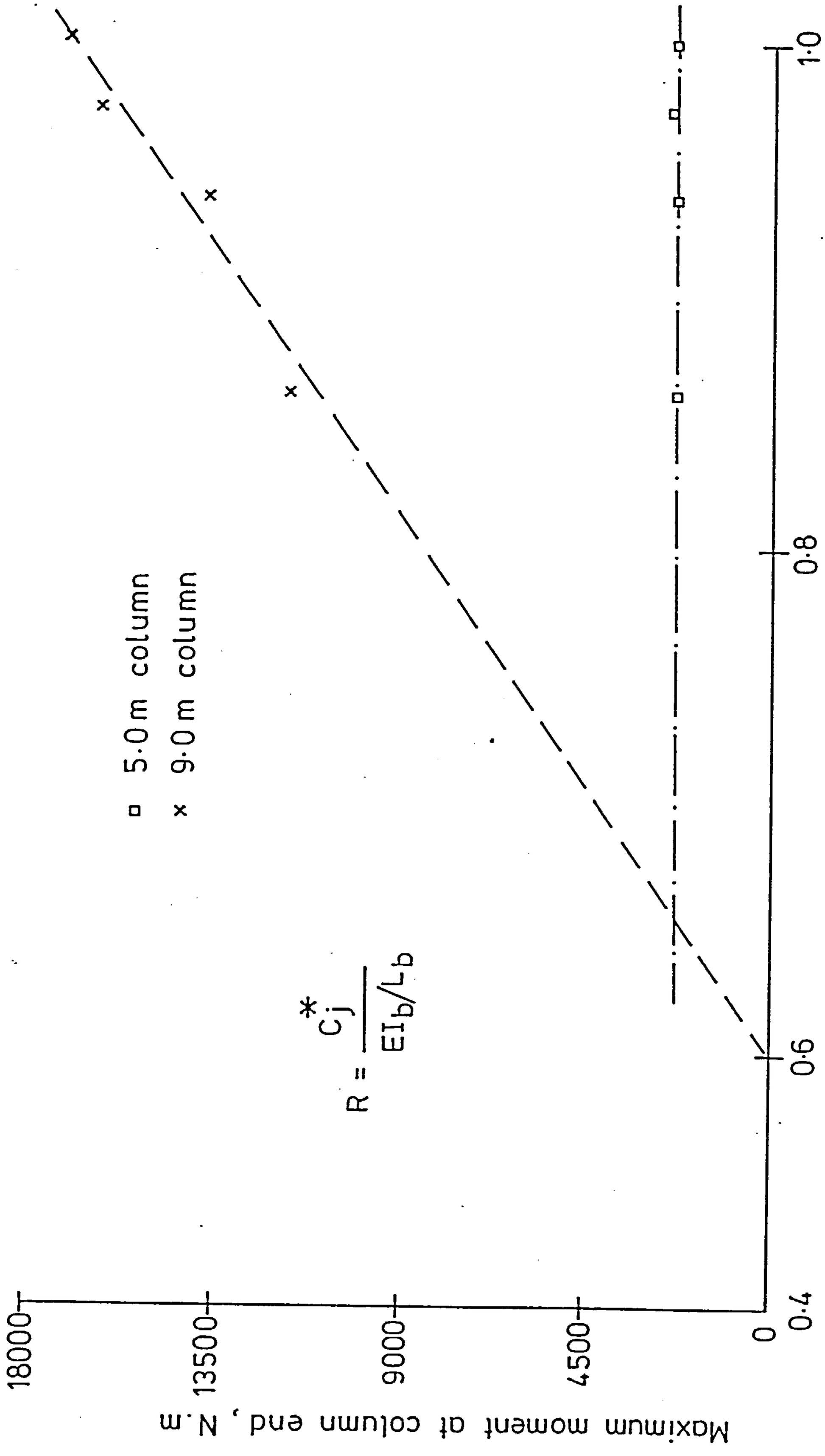

FIG.7.31 EFFECT OF CONNECTION TYPE ON MAXIMUM MOMENT AT THE COLUMN END

S and R are the slopes of the lines and the ratio given by eqn-7.2 respectively.

Eqn-7.21 is represented in Fig-7.31 by broken lines. It can be seen that this line meets the horizontal axis at a value of R equal to 0.6. This value corresponds to an initial connection stiffness of 8.18×10^5 N.m. which corresponds to a connection far more flexible than the web cleat connection used in the present study. Any connection with more flexibility than this one would result in a negative moment in the column and hense may conservatively be assumed to be a pin joint.

Eqn-7.21 may also be applied to the 5m column but with zero slope as mentioned above. Consequently the maximum moment may simply be taken to be that corresponding to rigid connections and a beam load of 30kN. It is very difficult to generalize eqn-7.21 to other column lengths. It is important that another curve similar to those of Fig-7.30 and 7.31 be constructed in order to speculate on the effect of column height.

In the case of pin joints, the moment at the column end may be taken as QD/2 in which Q is the beam load and D is the depth of the cross section of the column.

7.3.2.5- A Remark on the Recommendation of BS5950 for Designing Columns With Flexible Connections:-

BS5950 recommends that a column in a frame with flexible connections be designed on the basis of the overall reaction from the beams and the upper stories and a moment equal to the beam reaction times an eccentricity of (D/2+100) mm. Shown in Fig-7.32 is the interaction curve corresponding to web cleat connections for both the

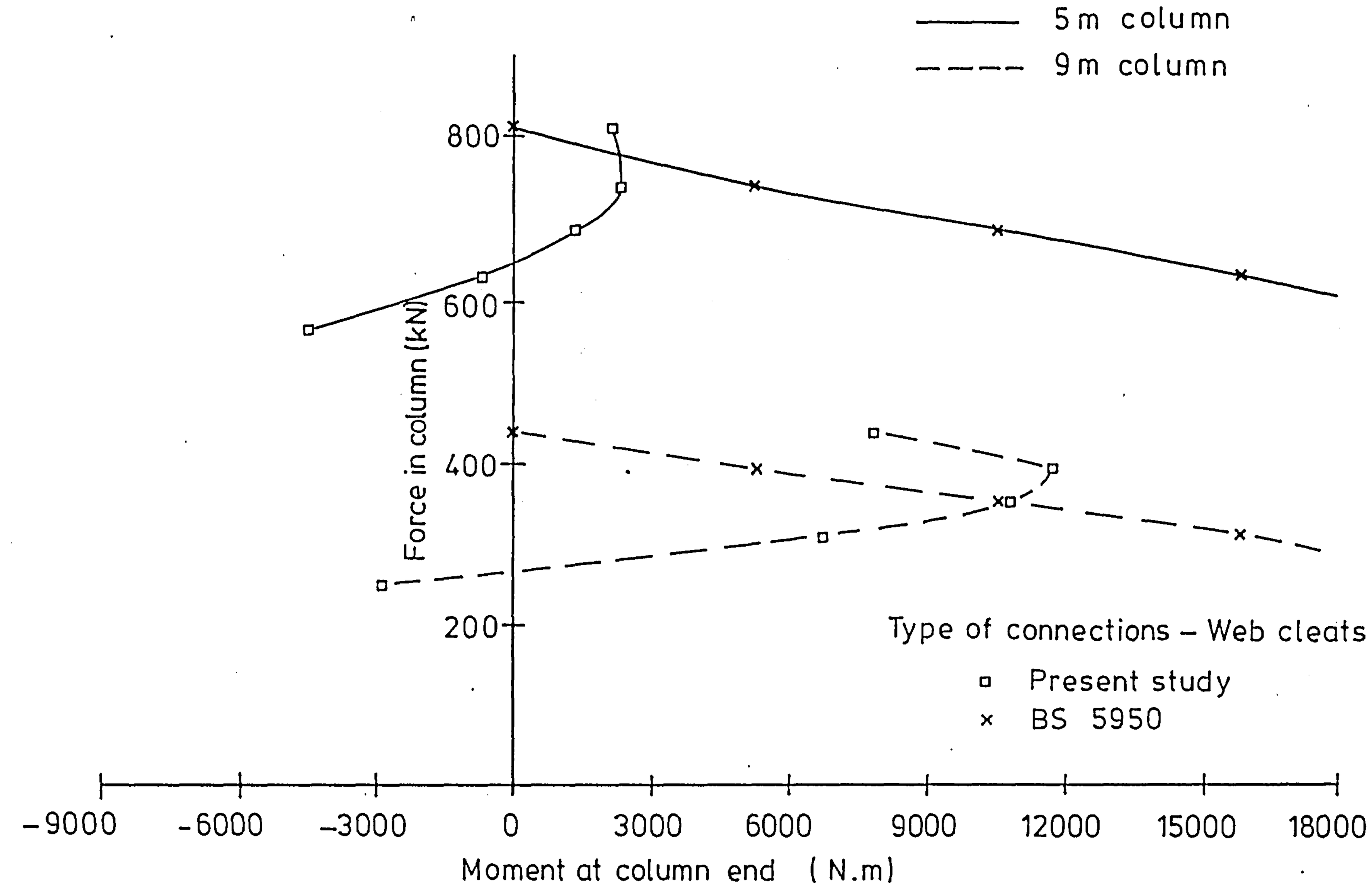

FIG. 7·32 INTERACTION CURVES

5m and 9m columns. In addition, the relationship between the failure load and the moment recommended by BS5950 is plotted for the two columns. It is clear that the two curves in each set intersect at a point corresponding to a certain value for the beam load. In the cases of beam loads less than this value, BS5950 seems to be on the unconservative side while it is conservative for higher beam loads. The simple criteria given by the specification, thus, seems to need more investigation.

7.4- Conclusions

The subassemblage of Fig-7.1 was analysed for different load types and different types of beam to column connections. A substantial effect was recognized for the presence of semi-rigid connections, whether or not a beam load was applied. Beam flexibility was also seen to affect the carrying capacity of the subassemblage under the action of column load only, although this effect is less noticable than that of the semi-rigid connections. A formula for the effective length factor is proposed.

The presence of beam load was found to result in an unexpected interaction curve which relates the total force in the column to the moment that is transmitted to the column's end. The column load was found to decrease with the increase of beam load. The relation seems to be an almost linear one. A linear relationship between the beam and column load was proposed. Another linear relationship between the ratio R and the maximum moment that might occur at the column end for any specific type of connection was also proposed.

It should be pointed out that all the findings of the present

study are limited to the cases considered but can serve as indicators of the behaviour of the subassemblage under axial load only and combined axial and beam loads. A much more comperhensive study is needed to verify, or otherwise, the findings of the present study. More parameters such as minor axis column bending should be included in both series of analyses. More types of connections, especially flexible ones, should be included. In the cases of combined column and beam loads, more column heights are also needed to be able to generalize the use of eqn-7.21.

CHAPTER-8

CONCLUSIONS

8.1- Summary:-

The work conducted by Jones on isolated columns with semi-rigid joints has been extended to cover the behaviour of limited subassemblages with flexible beams and semi-rigid beam to column connections. The theoretical background to the present computer program has been presented along with the program layout.

The program was used to simulate some of the experimental results obtained from tests on rigidly and flexibly connected frames. Both axial and lateral column loads were considered in the simulations of the rigidly connected frames. Beam loads and an axial column load were applied to the flexibly connected frames. The analytical results were found to compare reasonably well with the experimental results. The program may therefore be regarded as acceptable for analysing rigidly or flexibly connected frames

It was pointed out in Sec-5.4.2 that the boundary conditions adopted in any test must be well defined in order that analytical procedures be able to closely simulate test results.

The program was also used to simulate a series of I-shaped subassemblages that were tested at the University of Sheffield. Most of the parameters describing the experiments were accurately known. If insufficient information was available on a particular parameter, a judgement was made for the most appropriate value. Comparisons were made between the analytical and experimental results characterized by the maximum loads, load-deflection curves and load-moment curves. Good agreement was obtained between the analytical and the experimental load-deflection curves for all of the cases considered. The general trends of the measured and calculated load-moment curves for most cases were found to be comparable.

It was pointed out that it is difficult to exactly simulate an experimental result. This leads to some discrepancies in certain cases. However, by changing selected input parameters (whose values were not known precisely) such as residual stresses, it was possible to arrive at closer correspondance.

✓ The recommendations given in BS5950 for the design of columns in simple construction were applied to all the cases under consideration. It was found that these were unconservative in the cases of balanced loading and conservative in the cases of unbalanced loads.

A limited parametric study was conducted to study the effects of semi-rigid joints, beam flexibility and type of loading. In this study, an I-shaped subassemblage was analysed for different load types and different types of beam to column connections. A substantial effect was recognized due to the presence of semi-rigid connections whether or not a beam load was applied. Beam flexibility was also seen to affect the carrying capacity of the subassemblage under the action of column load only although this effect was less noticeable than that of the connection flexibility. A formula for the effective length factor is proposed.

The presence of beam load was found to result in an unexpected interaction curve which relates the total force in the column to the moment that is transmitted to the column's end. The column load was found to decrease with an increase of beam load. The relation seems to be an almost linear one and an empirical relationship between the beam and column load is proposed. A linear relationship between R, the ratio of the initial connection stiffness to the beam stiffness (EI/L), and the maximum moment that occurs at the column end for any specific type of connection is also proposed.

It is pointed out that all the findings of the present study are based on the range of cases considered in the prarametric study but it is suggested that they serve as indicators to the behaviour of any subassemblage under axial load only or axial load combined with beam loads. A much more comprehensive numerical study is needed to confirm the findings of the present study for all possible cases. More parameters such as minor axis column bending should be included in both series of analyses. More types of connection, especially the more flexible ones, should be investigated. In the cases of combined column and beam loads, more column heights are also needed to be able to generalize the use of eqn-7.20.

8.2- Recommendations for Future Work:-

The present work is restricted to the behaviour of limited subassemblages under the action of limited loading and boundary conditions. The following recommendations are thought to be important in developing more understanding of the behaviour of more realistic flexibly connected frames:

(1) As pointed out earlier, the parameters in any experimental study should be well defined in order to permit close simulation of the test results using theoretical procedures.

(2) Although provisions were made in the computer program for constructing the complete M-Φ envelope in which the connection may repeatedly load and unload, only the loading-unloading-reloading behaviour was considered in the present study. Full cyclic behaviour of connections should be considered since it is likely to occur in many realistic structures. In doing this, the program should be verified by

simulating results from tests in which a limited subassemblage is tested for cyclic loads.

(3) Joint offset was taken into account in the present program by modelling the panel zone by a rigid segment with a length equal to half the depth of the column cross section. A more realistic model should be included in such a way that panel zone deformation be taken into account. Such deformations may be non-negligible when very stiff connections are used.

(4) The present program is capable of tracing the load-deflection behaviour up to the maximum load only. Post-buckling behaviour is of great importance in structures in which more than one column is present. This is because if one column fails, some of its load would be redistributed to other columns. This redistribution is governed by the post-buckling behaviour of the column under consideration.

(5) In calculating the end forces due to loads applied within the length of the element, the effect of semi-rigid joints was not considered. The present work was, however, limited to concentrated nodal loads which are not affected by the presence of semi-rigid joints. It is desirable, however, to include the effect of semi-rigid joints on the element end forces. There should be no difficulty in fulfilling this recommendation.

(6) Once the last three recommendations have been fulfilled, the present work should be extended to include:

   (a) cyclic loads which may occur in realistic structures

   (b) larger frames which contain more than one column.

   (c) Element loads, particularly distributed loads.

(7) The findings of the limited parametric study serve as an

indicator to the effects of the parameters considered on the behaviour of limited subassemblages. A more comprehensive study is needed to confirm such findings. Both the range and the number of parameters should be increased; for instance, more types of semi-rigid connections should be included. The more flexible connections are particularly important. Other parameters such as column bending axis and type of cross section (i.e. whether rolled or welded) should be examined.

(8) The present work may be extended to cover sway frames. No difficulty should arise in such an extension as the present program is capable of accepting, in general, any type of boundary conditions.

(9) Finally, the present work may be extended to cover three dimensional behaviour. More information is needed, however, on the M-ϕ characteristics of semi-rigid joints in space.

APPENDICES

Appendix-A: Derivation of the Combined Beam and Beam-to-Column Connection Stiffness:-

Assume that the subassemblage of Fig-7.1 deforms in a symmetrical fashion as shown in Fig-A.1 as a result of the application of a column load P. The moments at the ends of the top-left beam may be found using the well known slope deflection equations (assuming that there is no axial force in the beam) as

$$M_{AB} = \frac{2EI_b}{L_b}\left[\ \theta_{BA} + 3\frac{\Delta_1}{L_b}\right] \qquad \text{(A-1a)}$$

and

$$M_{BA} = \frac{2EI_b}{L_b}\left[\ 2\ \theta_{BA} + 3\frac{\Delta_1}{L_b}\right] \qquad \text{(A-1b)}$$

Since the end A is free to move vertically, the shear force V_A at this end must equal zero. Hence

$$V_A = \frac{(M_{AB} + M_{BA})}{L_b} = 0 \qquad \text{(A.2)}$$

Substituting for the moments M_{AB} and M_{BA} from eqns-A.1 into eqn-A.2 and simplifying,

$$\theta_{BA} = -2\frac{\Delta_1}{L_b} \qquad \text{(A.3)}$$

Now, the moment M_{BA} must be equal in magnitude and opposite in direction to the moment in the joint M_j which is related to the joint rotation by

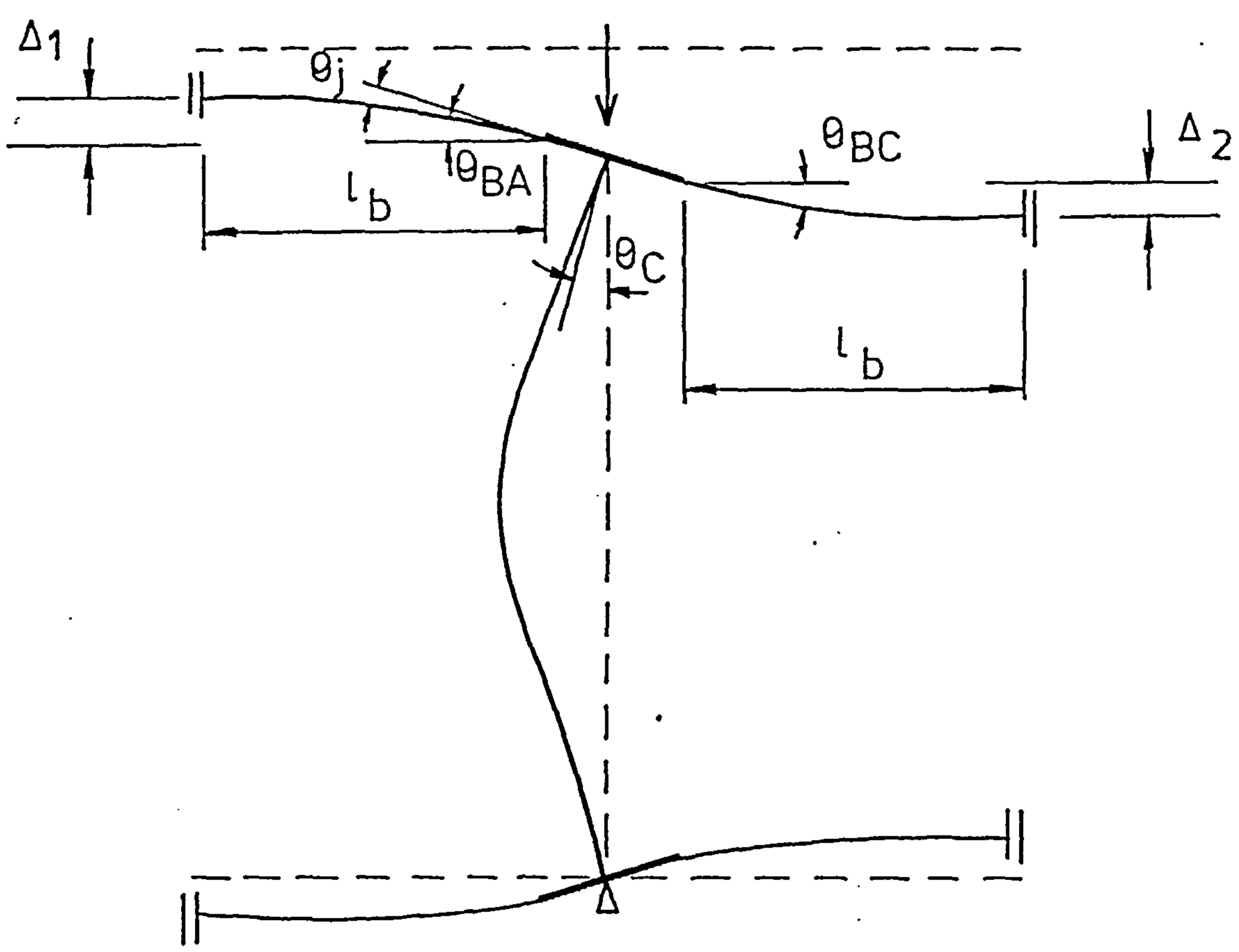

FIG.A-1 DEFLECTED SHAPE OF A SUBASSEMBLAGE UNDER THE ACTION OF COLUMN LOAD

$$M_j = - C_j \theta_j \qquad (A.4)$$

in which C_j is the joint stiffness. The beam rotation may now be expressed as (eqns-A.1b and A.4)

$$\theta_{BA} = \frac{C_j \theta_j}{\frac{EI_b}{L_b}} \qquad (A.5)$$

Now referring to Fig-A.1b the joint rotation may written as

$$\theta_j = -(\theta_c - \theta_{BA}) \qquad (A.6)$$

in which θ_c is the rotation of the column's end. Substituting for θ_j from eqn-A.6 and for θ_{BA} from eqn-A.5 into eqn-A.4 and simplifying the expression, we get

$$M_j = \frac{C_j}{1 + \frac{EI_b}{L_b}} \theta_c = C^* \cdot \theta_c$$

in which C^* is given by

$$C^* = \frac{C_j}{1 + C_j \frac{L_b}{EI_b}} = \frac{\frac{EI_b}{L_b}}{1 + \frac{EI_b}{C_j L_b}} \qquad (A.7)$$

L_b

Appendix-B: Calculation of the Effective Length Factor for a Restrained Column Using Column Strength Curves:-

Assume that it is required to calculate the effective length factor for a restrained column which has the column strength curve labelled 'restrained' in Fig-B.1. Also assume that a similar column but with pin ends has the column strength curve labelled 'pinned' in the same figure. Then for both columns to have the same ultimate strength, the length for the pin-ended column must be equal to

$$l = L \frac{\lambda_p}{\lambda_r} \qquad (B.1)$$

in which l, λ_p, L and λ_r are the lengths and slenderness ratios of the pin-ended and the restrained column respectively. Hence, the effective length factor is

$$k = \frac{\lambda_p}{\lambda_r} \qquad (B.2)$$

Eqn-B.1 was used to determine the effective length factor for an isolated column with web cleat connections at its ends. The column strength curves for this column and for the pin ended one are shown in Fig-B.1. The slenderness ratios corresponding to P_u/P_y values ranging from 0.3 to 0.95 (with 0.05 increments) were found from the restrained and pinned curves. The k-values corresponding to these P_u/P_y values were calculated using eqn-B.2. Table-B.1 lists λ_p, λ_r and k corresponding to the range of values for P_u/P_y mentioned above. An average value for all the k values was calculated and taken as the approperiate effective length factor for this column.

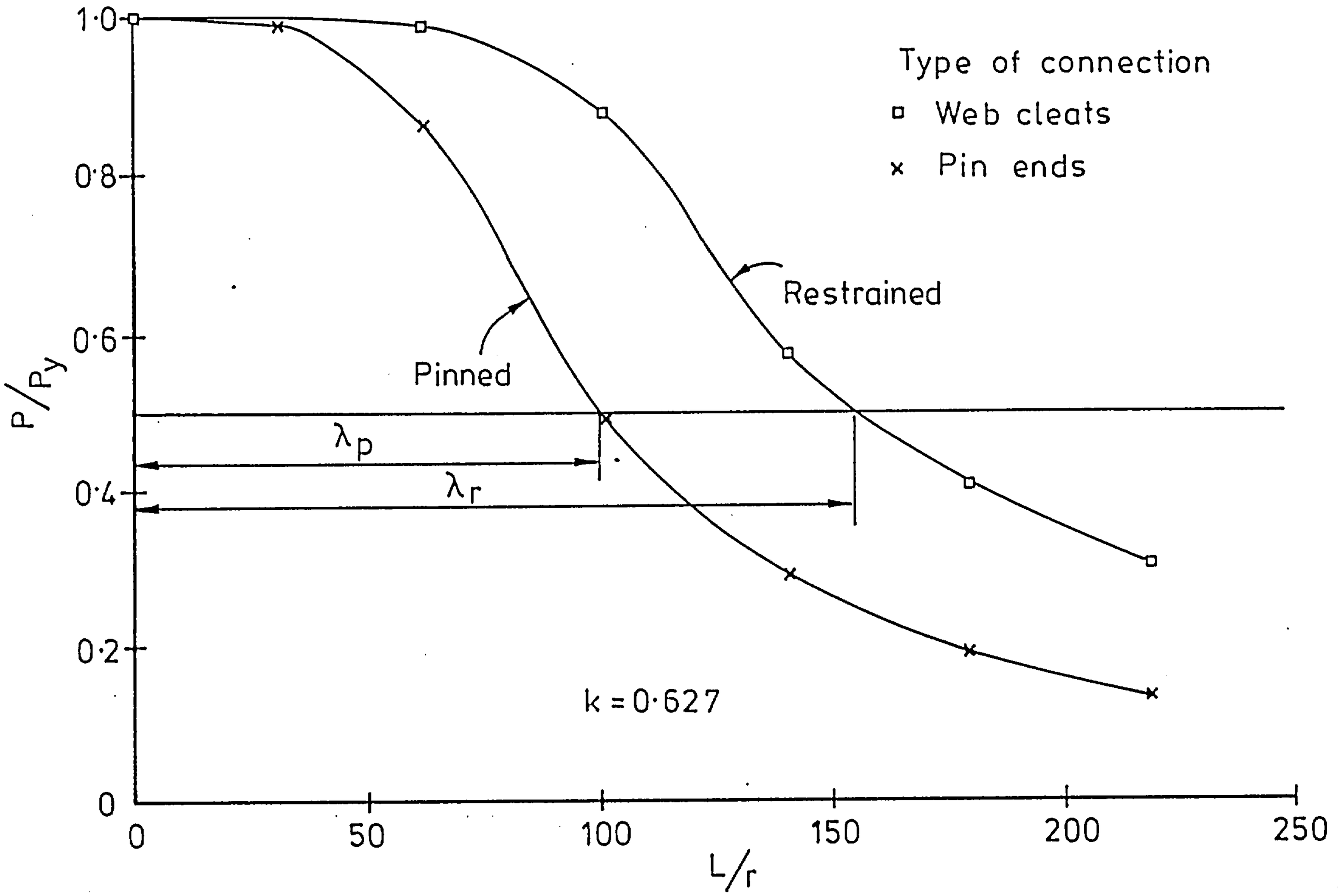

FIG. B·1 ULTIMATE STRENGTH CURVES FOR AN ISOLATED COLUMN

Table-B.1: Calculation of Effective Length Factor Using Column Strength Curves

$\frac{P_u}{P_y}$	λ_p	λ_r	k
0.30	139.0	219.4	0.633
0.35	127.7	202.1	0.632
0.40	117.7	183.5	0.641
0.45	109.0	168.9	0.646
0.50	101.1	156.3	0.647
0.55	95.7	146.3	0.655
0.60	90.4	137.6	0.657
0.65	85.1	131.6	0.646
0.70	80.5	125.0	0.644
0.75	75.8	119.7	0.633
0.80	71.1	113.7	0.626
0.85	62.5	107.7	0.580
0.90	55.9	76.7	0.579
0.95	46.5	82.4	0.565

REFERENCES

1. British Standards Institute, "BS5950; Part I: The Use of Structural Steel in Buildings", London, 1985.

2. American Institute of Steel Construction, "Manual of Steel Construction", 8th Edition, Chicago, U.S.A., 1978.

3. Canadian Standards Association, "Standard S16.1, Steel Structures for Buildings- Limit States Design", Ottawa, Canada, 1974.

4. Standards Association of Australia, "A.S.1250, Steel Structures", Sydney, Australia, 1975.

5. Jones,S.W., "Semi-Rigid Connections and Their Influence on Steel Column Behaviour", Ph.D. Thesis, Department of Civil and Structural Engineering, University of Sheffield, Sheffield, U.K., 1980.

6. Lui,E.M. and Chen,W.F. "Frame Analysis with Panel Zone Deformations", Report No. CE-STR-85-19, School of Civil Engineering, Purdue University, West Lafayette, Indiana, U.S.A, 1985.

7. Becker,R. "Panel Zone Effect on the Strength and Stiffness of Steel Rigid Frames", American Institute of Steel Construction, Engineering Journal, 1st Quarter, 1975, pp. 19-29.

8. Timoshenko,S.P. and Gere,J.M. "Theory of Elastic Stability", McGraw-Hill, 2nd Edition, New York, U.S.A., 1961.

9. Case,J. and Chilver,A.H., "Strength of Materials and Structures", Edward Arnold, 2nd Edition, London, 1971.

10. Bleich,F. "Buckling Strength of Metal Structures", McGraw-Hill, New York, U.S.A., 1952.

11. Narayanan,R., Ed., "Steel Framed Structures; Stability and Strength", Elsevier Applied Science Publishers, New York, 1985.

12. Steel Structures Research Committee, Second Report, Department of

Scientific and Industrial Research, H.M.S.O., London, U.K, 1934.

13. Frye,M.J. and Morris,G.A., "Analysis of Flexibly Connected Steel Frames", Canadian Journal of Civil Engineering, Vol.2, No.3, September 1975, pp.280-291.

14. Razzaq,Z. and Chang,J.G., "Partially Restrained Imperfect Columns", Proc. Conference on Joints in Structural Steelwork, Pentech Press Ltd., Teesside, England, April 1984.

15. Suggimoto,H. and Chen,W.F., "Small End Restraint Effect on Strength of H-Columns", Journal of Structural Division, Proc. A.S.C.E., Vol. 108, No. ST3, March 1982, pp. 661-681.

16. Chen,W.F. and Atsuta,T., "Theory of Beam-Columns", Volume 1, McGraw-Hill, 1976.

17. Vinnakotta,S., "Planar Strength of Restrained Beam Columns", Journal of Structural Division, Proc. A.S.C.E., Vol. 108, No. ST11, November 1982, pp. 2496-2516.

18. Coates,R.C., Coutie,M.G. and Kong,F.K., "Structural Analysis", 2nd edition, Reinhold (U.K.) Company Ltd., Berkshire, England, 1984.

19. Kirby,P.A. and Nethercot,D.A., "Design for Structural Stability", Crosby Lockwood Staples, Granada Publishing, London, 1979.

20. Vinnakotta,S., "Design of Columns as Part of Frames- Some Remarks", (Private Communications), 1983.

21. Vinnakotta,S., "Design of Columns in Planar Frames- A Few Comments", National Conference on Tall Buildings, 22-24 January 1973, New Delhi, India.

22. Cross,H., "Analysis of Continuous Frames by Distributing Fixed End Moments", Proc. A.S.C.E., Vol. 56, No. 5, 1930, pp. 919-928.

23. Zienkiewicz,O.C., "The Finite Element Method", McGraw-Hill, 3rd edition, London, 1977.

24. Bathe,K.J. and Wilson,E.L., "Numerical Methods in Finite Element Analysis", Prentice-Hall, Englewood Cliffs, 1976.

25. Rao,S.S., "The Finite Element Method in Engineering", Pergamon Press, Oxford,1982.

26. Anderson ,D., Bijlaard,F.S.K., Nethercot,D.A. and Zandonini,R., "Analysis and Design of Steel Frames with Semi-Rigid Connections", I.A.B.S.E. Survey, 1987 (to be Published).

27. Corradi,L. and Poggi,C., "A Refined Finite Element Model for the Analysis of Elastic-Plastic Frames", International Journal for Numerical Methods in Engineering, Vol. 20, No. 12, December 1984, pp. 2155-2174.

28. El-Zanaty,M. and Murray,D., "Finite Element Programs for Frame Analysis", Structural Engineering Report No. 83, April 1980, Civil Engineering Department, University of Alberta, Canada.

29. Johnston,B. and Mount,E.H., "Analysis of Building Frames with Semi-Rigid Connections", Tranc. A.S.C.E., Vol. 107, 1942, pp. 993-1019.

30. Rathburn,J.C., "Elastic Properties of Riveted Connections", Trans. A.S.C.E., Vol. 101, 1936, pp. 524-563.

31. Simitses,G.J. and Vlahinos,S.A. "Stability Analysis of a Semi-Rigidly Connected Simple Frames", Journal of Constructional Steel Research, Vol. 2, No. 3, September 1982, pp. 29-32.

32. Anderson,D. and Lok,T.S., "Elastic Analysis of Semi-Rigid Steel Frames", Research Report No. CE/17, University of Warwick, January 1985.

33. Livesley,R.K. "The Application of sn Electronic Digital Computer to Some Problems of Structural Analysis", Structural Engineer, Vol. 34, No. 1, January 1956, pp. 1-12

34. Chen,W.F. and Lui,E.M., "Effect of Joint Flexibility on the Behaviour of Steel Frames", Report No. CE-STR-85-22, School of Civil Engineering, Purdue University, West Lafayette, Indiana, U.S.A., 1985.

35. Lui,E.M., "Effect of Connection Flexibility and Panel Zone Deformation on the Behaviour of Plane Steel Frames", Ph.D. Thesis, School of Civil Engineering, Purdue University, West Lafayette, Indiana, 1985.

36. Cosenza,E., De Luca,A. and Faella,C., "Non-Linear Behaviour of Framed Structures with Semi-Rigid Joints", Construzioni Metalliche, No. 4, 1984, pp. 199-211.

37. Poggi,C. and Zandonini,R., "Behaviour and Strength of Steel Frames with Semi-Rigid Connections", Session on Connection Flexibility and Steel Frames, A.S.C.E. Convention, Detroit, October 1985.

38. English,G.W. and Adams,P.F., "Experiments on Laterally Loaded Steel Beam-Columns", Journal of Structural Division, Proc. A.S.C.E., Vol. 99, No. ST7, July 1978, pp. 1457-1470.

39. Aoki,T. and Fukumoto,Y., "Experiments of End-Restrained Steel Welded H-Columns", Third International Colloquium on Stability of Metal Structures, Paris, 16-17 November 1983, pp. 71-76.

40. Bergquist,D.J., "Tests on Columns Restrained by Beams with Simple Connections", Report No. 1, Department of Civil Engineering, The University of Texas at Austin, Austin, Texas, U.S.A., January 1977.

41. Lay,M.G. and Galambos,T.V., "The Experimental Behaviour of Restrained Columns", Welding Research Council Bulletin No. 110, November 1965, pp. 17-37.

42. Gent,A.R. and Milner,H.R., "The Ultimate Load Capacity of

Elastically Restrained H-Columns Under Bi-Axial Bending", Proc. Institute of Civil Engineers, Vol. 41, December 1968, pp. 685-704.

43. Woods,R.H., Needham,F.H. and Smith,R.F., "Test of a Multi-Storey Rigid Steel Frame", The Structural Engineer, Vol. 46, No. 4, April 1968, pp 107-119.

44. Joint Committee's First Report, "Fully Rigid Multi-Storey Welded Steel Frames", The Institution of Structural Engineers and The Welding Institute, December 1964.

45. Smith,R.F. and Roberts,E.H., "Test of a Fully-Continuous Multi-Storey Frame of High Yield Steel ", The Structural Engineer, Vol. 49, No. 10, October 1971, pp. 451-466.

46. Joint Committee's Second Report, "Fully Rigid Multi-Storey Welded Steel Frames", The Institution of Structural Engineers and The Welding Institute, May 1971.

47. Davison,J.B., Kirby,P.A. and Nethercot,D.A., "Column Behaviour in PR Construction: Experimental Behaviour", A.S.C.E. Convention, New Orleans, September 1986, (to be published in Journal of Structural Engineering, A.S.C.E., 1987.

48. Davison,J.B., "Strength of Beam-Columns in Flexibly Connected Steel Frames" ,Ph.D Thesis, Department of Civil and Structural Engineering, University of Sheffield, (in preparation).

49. American Institute of Steel Construction, Manual of on for Steel Construction, "Load and Resistance Factor design", 1st Edition, Chicago, U.S.A., 1986.

50. Kirby,P.A., Davison,J.B., and Nethercot,D.A., "Large Scale Tests on Column Subassemblages and Frames", State of the Art Workshop, Connections Strength and Design of Steel Structures, E.N.S., Cachan, France, May 1987.

51. Nethercot,D.A., "Steel Beam to Column Connections- A Review of Test Data and Their Application to the Evaluation of Joint Behaviour on the Performance of Steel Frames", C.I.R.I.A. Report RP 338, London, 1984.

52. Goverdhan,A.V., "A Collection of Experimental Moment-Rotation Curves and Evaluation of Predicting Equations for Semi-Rigid Connections", Doctoral Dissertation, Vanderbilt University, Nashville, Tennessee, 1984.

53. Davison,J.B., Kirby,P.A. and Nethercot,D.A., "Rotational Stiffness Characteristics of Steel Beam to Column Connections", Journal of Constructional Steel Research, Vol.7, 1987 (in press).

54. Brebbia,C.A. and Connor,J.J., "Fundamentals of Finite Element Techniques for Structural Engineers", John Wiley, New York, U.S.A., 1974.

55. Hayes,J.G., "Numerical Methods for Curve and Surface Fitting", The Institute of Mathematics and its Applications, May/June, 1974, pp. 144-152.

56. Nethercot,D.A., "Residual Stresses and Their Influence upon the Lateral Buckling of Rolled Steel Beams", The Structural Engineer, Vol. 52, No. 3, March 1974, pp. 89-96.

57. Young,B.W., "Residual Stresses in Hot-Rolled Sections", Report CUED/C-Struct./TR.8, Department of Engineering, University of Cambridge, 1971.

58. Alpsten,G.A., "Thermal Residual Stresses in Hot-Rolled Steel Members", Report No. 337.3, Fritz Engineering Laboratory, University of Lehigh, December 1968.

59. Ersvik,O. and Alpsten,G., "Experimentell Undersokning av Knachallfastheter has Bredflansprofiler HE200A Ritade pa Olika

Satt", Stalbyggnadsinstitutet, Sweden, Report 19:3, December 1970. (in Swedish).

60. Fujita,Y. and Yoshida,K., "Compressive Strength of Columns with Initial Deflections", International Colloquium on Column Strength, Paris, France. 23-24 November 1972, pp. 108-120.

61. Przemeineiski,J.S., "Theory of Matrix Structural Analysis", McGraw-Hill, New York, U.S.A., 1968.

62. Kardestuncer,H., "Elementary Matrix Analysis of Structures", McGraw-Hill, New York, U.S.A., 1974.

63. Johnston,B. Ed., "Guide to Stability Design Criteria for Metal Structures", 3rd edition, Wiley-Interscience, New York, U.S.A., 1976.

64. English,G.W. and Adams,P.F., "Experiments on Laterally Loaded Steel Wide-Flange Beam Columns", Structural Engineering Report No. 33, Department of Civil Engineering, University of Alberta, Edmonton, Canada, 1972

65. Fukumoto,Y., Private Communications, 1985.

66. Lui,E.M. and Chen,F.W., "End Restraint and Column Design Using LRFD", A.I.S.C., Engineering Journal, 1st quarter, Vol. 21, No. 1, 1983, pp. 29-39.

67. Yura,J., "The Effective Length of Columns in Unbraced Frames", Engineering Journal, A.I.S.C., Vol. 8, No. 2., April 1971, pp. 37-42.

68. Bjorhovde,R., "Effect of End Restraint on Column Strength Practical Applications", A.I.S.C., Engineering Journal, Vol. 21, No. 1 , October 1984, pp. 1-13.